UNIVERSIDAD DE JAÉN

TESIS DOCTORAL

•

VALORIZATION OF AGRO-INDUSTRIAL WASTE IN SUSTAINABLE CERAMIC MATERIALS. TECHNICAL AND ENVIRONMENTAL ANALYSIS.

PRESENTADA POR:

Romina D. Farías

DIRIGIDA POR:

Tutora: **Prof. Carmen Martínez García**
Cotutora: **Prof. María Teresa Cotes Palomino**

Tutora Italiana: **Prof. Luisa Barbieri**
Cotutora Italiana: **Dra. Ing. Nora María Fernanda Andreola**

LINARES, 10 Abril 2018

SUMMARY [ENGLISH]

Increasingly tighter regulations regarding waste, the reduction of the non-renewable resources and its higher prices, the increasing demand for renewable energy sources and green chemicals, are pushing the manufacturing processes toward higher sustainability, to improve cost-effectiveness and meet customers demand, i.e., circular economy. Agro-industrial waste valorization is one of the current research areas that concerned a great deal of researchers over the past few years as a potential alternative of disposal for a wide range of waste/by-products in landfill sites.

Landfill, incineration and composting are common technologies for waste disposal. However, they are not satisfactory treating organic waste due to the liberation of methane gas to the atmosphere, unpleasant odour, natural land transformation, high energy consumption and slow reaction kinetics. In fact, research efforts have also been oriented on techniques capable of decomposing organic matter, but, no valuable product can be generated. For that reason, recent research has focused on its utilization as energy source mostly, and recovery matter in alternative uses (e.g., pore forming agents, fertilizer, herbicide removal, silica adsorbent).

This research is focused on the alternative uses of different local clay minerals through the valorization of waste/by-products available in the local agro-industry, as a replacement of primary resources to elaborate sustainable clay-based materials like lightweight aggregates (LWA_S) for drainage layer in green roofing ($LWAS_{GR}$) and agronomic use ($LWAS_{AP}$).

This investigation research was conducted and coordinated in two different locations: the University of Jaen, High Polytechnic School of Linares, Spain, coordinated by Prof. Carmen Martinez Garcia (Tutor) and Prof. Teresa Cotes Palomino (Cotutor) form the Department of Chemical, Environmental and Material Engineering and research group TEP 222, and the University of Modena and Reggio Emilia, Department of Engineering "Enzo Ferrari" (DIEF), Italy, coordinated by Prof. Luisa Barbieri (Tutor) and Dr. Eng. Fernanda Andreola (Cotutor) and with the collaboration of Prof. Isabella Lancelotti.

The waste and by-products used as a partial substitute of natural resources (clay minerals) have been studied to determine both their aptitudes as porous agents, saving energy consumption in the sintering process, improved LWA_S insulation capacity, and capabilities as potential fertilizers for agronomic purposes. As a pore-forming agent, bagasse (BB), diatomaceous earth (DE), and sludge from wastewater treatment plant (BS) from brewery industry were chosen, meat-bone

meal (MBM) and corn cob (CC) was used to reduce sintering temperatures (200-400°C less). Cattle-bone ashes (CBA) and fertilizer glass (FG) were added to the material in order to confer it a fertilizer capacity due to their phosphorus (P) and potassium (K) content. Raw materials were characterized to determine their physical and chemical characteristics, as follows: total content of C-H-N-S (elemental analysis), chemical and mineralogical composition (X-ray fluorescence, XRF and X-ray diffractometry, XRD), thermal behavior (thermogravimetric analysis, TGA-DTA-DSC), loss of ignition (LOI), higher heating value (HHV).

Diverse types of clays minerals from different locations were blended. White, black, yellow and red ES clays were provided for Arcillas Bailen S.L., from a clay-pit in Bailen, Jaen Province, Spain, and red IT clay was provided by Escavazioni Industriali Baroni s.r.l., from a clay-pit from Roncobotto, Modena province, Italy.

For the production of LWA_S for drainage layer in green roofs ($LWAS_{GR}$), three types of clay in equal parts, black, yellow and red ES (BYRC), were mixed with a different percentage (0, 2, 4, 6, 8, 10, 12.5 and 15wt%) of brewery residues, previously dried and ground sludge from wastewater treatment plant (BS), bagasse (BB) and diatomaceous earth (DE). Before sintering, the samples were preheated into the furnace at temperatures near 200°C for 24 h. Once the furnace had reached the temperature (900, 950 or 1000°C), the samples were introduced, staying in the furnace at the required temperature for one hour, after which was turned off, and the samples were cool through natural convection.

To produce LWA_S for agronomic proposes were used two different clay based mixtures WBC (30% white and 70% black ES clays) and RC (100% red IT clay) and mixed following two different steps. In the first step, WBC clay-based mixture (30% white and 70% black clays) was used with 0, 5, 10, and 15wt% of brewery wastewater treatment plant (BS), meat-bone meal (MBM) and corn cob (CC) and sintered at 900 and 1000°C for one hour. In the second step, WBC clay-based mixture and red IT clay-based mixture (RC) were mixed with 15wt% of BS, as a pore-forming agent; moreover, 10wt% cattle-bone ashes (CBA) in comparison of 10wt% of fertilizer glass were added to the material for conferring it a fertilizer capacity due to their phosphorus (P) and potassium (K) content, and sintered at 1000°C for one hour. The fertilizer glass (FG) was obtained by mixing 40wt% of cattle-bone ashes as P intake; 42wt% of Glassy Sand® (GS) as parent glass; 18wt% of potassium carbonate, as K intake. The fertilizer glass mix was subjected to melting at 1450°C for 2 hours and cast in water in order to obtain grains ready to use.

Technological parameters were determined following standards for each sustainable material: bulk and real density, total porosity, water absorption capacity, pH, electrical conductivity, pore size distribution, leaching test were determined to evaluate different technical, chemical and physical aspects of the two materials. Besides, with the aim of studying the mineralogical and microstructural characteristics X-Ray Powder Diffraction, Scanning Electron Microscopy (SEM-EDS) techniques, were performed.

Carbon Footprint (CFP) is part of the Life Cycle Analysis (LCA), a method by which the environmental externalities generated by a system are based on the contribution of Greenhouse Gases (GHG). CFP is the simplified version of the LCA, in which instead of considering several impact categories, only the Global Warming is considered. It was included in the CFP the processes of raw material extraction, and the sintering process of the samples considered the most relevant regarding energy consumption and environmental impact generation. In this research was perform the modelling of the CFP conducted with Simapro® software, PRé Consultants, according to ISO standards.

The different clay minerals and waste/by-products have the potential for high-quality manufacturing products, such as LWA_S for green roof drainage layer and agronomic purposes, generating improvements in the technical characteristics of the material like water absorption, insulation capacity, and controlled fertilizing capacity, representing savings in natural and primary resources and energy consumption, as well as an alternative to landfill disposal.

Wastes used as a pore-forming agent can be efficiently used as an improver of its lighter and insulator structure capacity linked to water absorption capacity. Brewery residues present suitable candidates for the development of sustainable materials for green roofs ($LWAS_{GR}$). For $LWAS_{GR}$, the best results were obtained using bagasse (BB) in percentages of 10-15wt%, sintered at 1000°C.

For the $LWAS_{AP}$ the best result was obtain using 15wt% of brewery sludge (BS) as pore-forming for the two clay base-mixtures (WBC and RC), sintered for 1 h at 1000°C.

The leaching test results show the capacity of controlled nutrient release for LWAS for agronomic purposes, in water and citric acidic medium. As phosphorus intake, sample RC_{CBA} shows the best results, and as potassium intake, best results were archived with WBFG. The addition of FG favours the long-term release (21 days) of K and P.

This test also revealed for the two materials ($LWAS_{GR}$ y $LWAS_{AP}$), that according to standards, are non-harmful to the environment.

Saving on primary resources and energy (reduction of sintering temperature ΔT=100-300°C), generates an improvement in the CFP analysis, reducing the environmental impact in average of 21.00% for LWA_S for green roofs production in comparison with LWA_S without waste (BYRC), being the samples with bagasse 15wt% (BB_{15}) the ones with the best results. For LWA_S for agronomic porpoises ($LWAS_{AP}$), the reduction of the CFP is 20.00% for WB_{CBA} and RC_{CBA}. In the case of samples with FG addition the CFP increase of 11.00%, due to the energy that requires the fertilizing glass thermal treatment.

SUMMARY [ESPAÑOL]

Las regulaciones cada vez más estrictas sobre residuos, el agotamiento de los recursos no renovables y sus precios cada vez más altos, la creciente demanda de fuentes de energía renovables y químicos verdes, están empujando a los procesos de fabricación hacia una mayor sostenibilidad, para mejorar la rentabilidad y satisfacer la demanda de los clientes, es decir, economía circular. La valorización de los residuos agroindustriales es una de las áreas actuales de investigación que preocupan a una gran cantidad de investigadores en los últimos años como una alternativa potencial de eliminación de una amplia gama de residuos/sub-productos en vertederos.

El vertido, la incineración y el compostaje son tecnologías comunes para la eliminación de desechos. Sin embargo, no son adecuadas para el tratamiento de residuos orgánicos debido a la liberación a la atmosfera de gas metano, olores desagradables, transformación del paisaje natural, alto consumo de energía y lentas reacciones cinéticas. De hecho, los esfuerzos de investigación se han orientado hacia técnicas capaces de descomponer la materia orgánica, sin generar ningún producto valioso. Por esa razón, investigaciones recientes se han centrado principalmente en su utilización como fuente de energía y en su valorización como insumos en otros procesos productivos (por ejemplo, agentes formadores de poros, fertilizantes, eliminación de herbicidas o adsorbente de sílice).

Esta investigación se centra en los usos alternativos de diferentes minerales de arcillas locales a través de la valorización de residuos/sub-productos disponibles en la industria local, como sustitutos de recursos primarios para la elaboración de materiales sostenibles basados en arcilla como agregados ligeros de arcilla (LWA_S) para capa de drenaje de techos verdes ($LWAS_{GR}$) y uso agrícola ($LWAS_{AP}$).

La investigación se realizó y coordinó en dos ubicaciones diferentes: la Universidad de Jaén, Escuela Superior Politécnica de Linares, España, coordinada por la Prof. Carmen Martínez García y la Prof. Teresa Cotes Palomino del Departamento de Ingeniería Química, Ambiental y de Materiales del grupo de investigación TEP 222, y la Universidad de Módena y Reggio Emilia, Departamento de Ingeniería "Enzo Ferrari" (DIEF), Italia, coordinado por la Prof. Luisa Barbieri y la Dra. Ing. Fernanda Andreola, con la colaboración de la Prof. Isabella Lancelotti.

Los desechos y sub-productos usados como un sustituto parcial de los recursos naturales (minerales arcillosos) han sido estudiados para determinar sus aptitudes como agentes

formadores de porosidad, ahorro de consumo de energía en el proceso de sinterización, mejorado de la capacidad aislamiento térmico y su capacidad para proveer capacidades de liberación de fertilizantes en forma controlada para su uso en agricultura. Como agente formador de poros, se utilizó el bagazo (BB), tierra de diatomeas (DE) y lodos de la planta de depuradora (BS), harina de carne y huesos (MBM), y mazorca de maíz (CC) para reducir temperaturas de sinterización (200-400^{o}C), en comparación con los áridos comerciales. Se añadieron cenizas de huesos (CBA) y vidrio fertilizante (FG) al material para conferirle una capacidad fertilizante debido a su contenido de fósforo (P) y potasio (K). Las materias primas se caracterizaron físicas y químicamente: contenido total de C-H-N-S (análisis elemental), composición química y mineralógica (fluorescencia de rayos X, XRF y difractometría de rayos X, XRD), comportamiento térmico (análisis termogravimétrico, TGA-DTA-DSC), pérdida por ignición (LOI) y capacidad calorífica (HHV).

Se mezclaron diversos tipos de minerales de arcillas procedentes de diferentes lugares. Arcilla blanca, negra, amarilla y roja ES fueron suministradas por Arcillas Bailen S.L., procedentes de Bailen provincia de Jaén, España. La arcilla roja IT fue suministrada por Escavazioni Industriali Baroni s.r.l., de una cava ubicada en Roncobotto, provincia de Módena, Italia.

Para la producción de LWA_S como capa de drenaje en techos verdes ($LWAS_{GR}$), se mezclaron tres tipos de arcilla en partes iguales, negra, amarilla y roja ES (BYRC), con un porcentaje diferente (0, 2, 4, 6, 8, 10, 12,5 y 15wt%) de residuos de la industria cervecera, lodos de depuradora (BS), bagazo (BB) y tierra de diatomeas (DE). Antes de la sinterización, las muestras se precalentaron en el horno a temperaturas cercanas a los 200^{o}C durante 24 horas. Una vez que el horno había alcanzado la temperatura (900, 950 o 1000^{o}C), las muestras se introdujeron, permaneciendo en el horno a la temperatura requerida durante una hora, después de lo cual se desconectó, y las muestras se enfriaron por convección natural.

Para la elaboración de LWA_S para usos agrícolas ($LWAS_{AP}$) se usaron dos mezclas diferentes de arcilla WBC (30% de arcilla blanca y 70% de arcilla negra ES) y RC (100% de arcilla roja IT) y se mezclaron siguiendo dos pasos diferentes. En el primer paso, se usó la mezcla de arcilla WBC (30% arcilla blanca y 70% de arcilla negra ES) con 0, 5, 10 y 15wt% de lodos de depuradora (BS), harina de carne y hueso (MBM), y mazorca de maíz (CC), sinterizado a 900 y 1000^{o}C durante una hora. En función de los resultados obtenidos en el primer paso, en el segundo paso, la mezcla WBC y la mezcla de arcilla roja italiana IT (RC) se mezclaron con 15wt% de BS, como agente formador de poros; además, se añadieron al material 10wt% de cenizas de hueso (CBA) en comparación con 10wt% de vidrio fertilizante, para conferirle una capacidad de fertilizante

debido a su contenido de fósforo (P) y potasio (K). Las muestras se sinterizaron a 1000ºC durante una hora. El vidrio fertilizante (FG) se obtuvo mezclando 40wt% de cenizas de hueso, como aporte de P; 42wt% de Glassy Sand® (GS) como vidrio principal; 18wt% de carbonato de potasio, como aporte de K. La mezcla de vidrio fertilizante se fundió a 1450 ° C durante 2 horas.

Los parámetros tecnológicos se determinaron siguiendo los estándares para cada material: densidad aparente y real, porosidad total, capacidad de absorción de agua, pH, conductividad eléctrica, tamaño de poro, prueba de lixiviación para evaluar diferentes aspectos técnicos, aspectos químicos y físicos de los dos materiales. Además, con el objetivo de estudiar las características mineralógicas y microestructurales se realizaron técnicas de difracción de Rayos X en polvo y escáner microscópico (SEM-EDS).

La huella de carbono (CFP) es parte del análisis del ciclo de vida (LCA), un método mediante el cual las externalidades ambientales generadas por un sistema se basan en la contribución de los gases de efecto invernadero (GEI). CFP es la versión simplificada de LCA, en la que, en lugar de considerar varias categorías de impacto, solo se considera el calentamiento global. Se incluyeron en la CFP los procesos de extracción de materia prima y el proceso de sinterización de las muestras consideradas más relevantes en cuanto al consumo de energía y a la generación de impacto ambiental. La modelización de la CFP se llevó a cabo mediante el uso del software Simapro®, PRé Consultants, de acuerdo con las normas ISO.

Los diferentes minerales arcillosos y residuos/sub-productos presentan potencialidades para la fabricación de productos de alta calidad, como LWA_S para capas de drenaje en techos verdes y usos agrícolas, generando mejoras en las características técnicas del material como absorción de agua, capacidad de aislamiento y capacidad de liberación controlada de fertilizantes, que representa el ahorro en recursos naturales y el consumo de energía, así como una alternativa a la eliminación en vertederos.

Los desechos/sub-productos usados como agente formador de poros contribuyen al descenso de la densidad, generando un material más ligero, mejorando la capacidad de aislamiento térmico del material. Los residuos de la industria de cerveza son adecuados para el desarrollo de materiales sostenibles para su uso como material de drenaje en la construcción de techos verdes ($LWAS_{GR}$).

En el caso de los $LWAS_{GR}$, los mejores resultados se obtuvieron utilizando bagazo (BB) en porcentajes de 10-15wt%, sinterizados a 1000ºC).

Para el $LWAS_{AP}$ el mejor resultado se obtuvo usando un 15wt% del lodo de depuradora (BS) como agente formador de poros con las dos mezclas de arcilla (WBC y RC) sinterizadas durante una hora a 1000ºC.

Los resultados de la prueba de lixiviación muestran la capacidad de liberación controlada de nutrientes para LWA_S con fines agrícolas, en medio ácido y acuoso. Como el aporte de fósforo, RC_{CBA} muestran los mejores resultados, y como aporte de potasio, los mejores resultados se obtuvieron con la mezcla WBC_{FG}. La adición de vidrio favorece la liberación a largo plazo (21 días) de K y P.

Las pruebas de lixiviación llevadas a cabo a los dos materiales ($LWAS_{GR}$ y $LWAS_{AP}$) demuestran que los dos materiales según los estándares no son dañinos para el medio ambiente.

El ahorro en recursos y energía (reducción de la temperatura de sinterización ΔT = 100-300ºC), genera una mejora en el análisis CFP, reduciendo el impacto ambiental en un promedio del 20-30% para la producción de LWA_S en comparación con LWA_S sin residuos, siendo las muestras con bagazo 15wt% (BB_{15}), los que obtuvieron los mejores resultados; y para los $LWAS_{GR}$, fueron con 15wt% de lodos de depuradora (BS) y 10wt% de cenizas de hueso (CBA) para las dos mezclas base de arcilla (WB_{CBA} y RC_{CBA})para $LWAS_{AP}$.

SUMMARY [ITALIANO]

Le normative sempre più severe in materia di rifiuti, la riduzione delle risorse non rinnovabili e i prezzi più elevati, la crescente domanda di fonti energetiche rinnovabili e prodotti chimici verdi sono tutti fattori che stanno spingendo i processi produttivi verso una maggiore sostenibilità, per migliorare l'efficacia dei costi e soddisfare la domanda dei clienti, ovvero si sta andando verso il concetto di economia circolare. La valorizzazione dei rifiuti agroindustriali è una delle attuali aree di ricerca che sta interessando una grande moltitudine di ricercatori da alcuni anni a questa parte come potenziale alternativa al conferimento in discarica di una vasta gamma di rifiuti/sottoprodotti.

Discarica, incenerimento e compostaggio sono tecnologie comuni per lo smaltimento dei rifiuti, tuttavia non sono soddisfacenti nel trattamento dei rifiuti organici a causa della liberazione di gas metano nell'atmosfera, odore sgradevole, trasformazione naturale del terreno, elevato consumo di energia e cinetica di reazione lenta. In effetti, gli sforzi della ricerca sono stati orientati anche su tecniche in grado di decomporre la materia organica, ma non è possibile generare alcun prodotto valido. Per questo motivo, la recente ricerca si è concentrata per lo più sull'utilizzo dei rifiuti organici come fonte di energia, e materia di recupero in usi alternativi (ad esempio, agenti di formazione di pori, fertilizzante, rimozione di erbicidi, adsorbente a base di silice).

Questa ricerca si incentra sugli usi alternativi di argille locali diversi minerali argillosi attraverso la valorizzazione di rifiuti/sottoprodotti dell'industria agroalimentare locale, in sostituzione di materie prime naturali per realizzare materiali sostenibili a base di argilla come aggregati leggeri (LWA_S) per lo strato drenante di coperture verdi ($LWAS_{GR}$) e per uso agronomico ($LWAS_{AP}$).

Questa attività di ricerca è si è sviluppata in due diversi centri di ricerca: l'Università di Jaen, High Polytechnic School di Linares, in Spagna, sotto il coordinamento dalle prof.sse Carmen Martinez Garcia e Teresa Cotes Palomino dal Dipartimento di Ingegneria Chimica, Ambientale e dei Materiali e gruppo di ricerca TEP 222, e l'Università di Modena e Reggio Emilia, Dipartimento di Ingegneria "Enzo Ferrari" (DIEF), Italia, sotto il coordinamento dalla Prof. Luisa Barbieri con la collaborazione dell'Ing. Fernanda Andreola e della Prof.ssa Isabella Lancelotti.

I rifiuti e i sottoprodotti usati come sostituti parziali delle risorse naturali (minerali argillosi) sono stati studiati per determinare sia le loro attitudini come agenti porizzanti, il risparmio di consumo energetico nel processo di sinterizzazione, il miglioramento della capacità di

isolamento negli aggregati leggeri, sia come potenziali fertilizzanti per scopi agronomici. Come agenti di formazione dei pori sono stati individuati bagassa (BB), terra di diatomee (DE) e fango proveniente dall'impianto di trattamento delle acque reflue (BS) dell'industria birraria, invece per ridurre le temperature di sinterizzazione (circa 200-400 °C in meno) farina di ossa di animali (MBM) e pannocchia di mais. Cenere di farina animale (CBA) e un vetro fertilizzante (FG) sono stati aggiunti al materiale al fine di conferire una capacità fertilizzante grazie al loro contenuto di fosforo (P) e potassio (K). Le materie prime sono state caratterizzate per determinare le loro caratteristiche fisiche e chimiche, come segue: contenuto totale di CHNS (analisi elementare), composizione chimica e mineralogica (fluorescenza a raggi X, XRF e diffrattometria a raggi X, XRD), comportamento termico (analisi termogravimetrica, TGA-DTA-DSC), perdita in peso (LOI), potere calorifico superiore (HHV).

Sono stati miscelati diversi tipi di minerali argillosi provenienti da luoghi diversi. Argille spagnole bianca, nera, gialla e rossa fornite da Arcillas Bailen SL, una cava di argilla a Bailen, provincia di Jaen, in Spagna, e un’argilla rossa italiana fornita da Escavazioni Industriali Baroni srl, Roncobotto, provincia di Modena, Italia.

Per la produzione di aggregati leggeri (LWA_S) per lo strato di drenaggio nei tetti verdi (LWASGR), tre tipi di argilla in parti uguali, nera, gialla e rossa spagnole(BYRC), sono stati mescolati con una differente percentuale (0, 2, 4, 6, 8, 10, 12.5 e 15% in peso) dei residui del birrificio, preventivamente essiccati e dei fanghi macinati provenienti dall'impianto di trattamento delle acque reflue (BS), della bagassa (BB) e della farina di diatomee (DE). Prima della sinterizzazione, i campioni sono stati preriscaldati in forno a 200°C per 24 ore. Una volta raggiunta la temperatura di trattamento termico vero e proprio (900, 950 o 1000°C), i campioni sono stati introdotti, mantenuti in isoterma per un'ora, dopo di che il forno è stato spento e a seguito di un raffreddamento naturale, i campioni sono poi stati estratti.

Per produrre gli aggregati leggeri (LWA_S) per gli scopi agronomici di cui sopra, sono state utilizzate due diverse miscele di cui una a base di due argille spagnole WBC (30% bianca e 70% nera) e l’altra di sola argilla italiana RC (100% rossa) e miscelate seguendo due diversi passaggi. Nella prima fase è stata utilizzata la miscela a base delle due argille spagnole WBC (30% di bianca e 70% di nera) additivata con 0, 5, 10 e 15% in peso di fango da impianto di trattamento delle acque reflue di birrificio (BS), farina di ossa di carne (MBM) e pannocchia (CC), che poi è stata sinterizzata a 900 e 1000°C per un'ora. Nella seconda fase, sia la miscela a base delle due argille spagnole WBC che quella costituita da sola argilla rossa italiana RC sono state additivate del 15% in peso di fango da birrifico, come agente di formazione dei pori; inoltre il 10% in peso di cenere

di ossa (CBA) o il 10% in peso di vetro fertilizzante (FG) è stato aggiunto al materiale per conferirgli capacità fertilizzante grazie al contenuto di fosforo (P) e potassio (K) e il tutto sinterizzato a 1000°C per un'ora. Il vetro fertilizzante (FG) è stato ottenuto mescolando 40% in peso delle ceneri di ossa di animali per apportare P, 42% in peso di Glassy Sand® (GS) come vetro madre, 18% in peso di carbonato di potassio, come apportatore di K La miscela di vetro fertilizzante è stata sottoposta a fusione a 1450°C per 2 ore e frittata in acqua per ottenere un granulato pronto all'uso.

I materiali ottenuti sono stati caratterizzati attraverso diversi parametri tecnologici in base agli standard commerciali: massa e densità apparente ed assoluta, porosità totale, capacità di assorbimento dell'acqua, pH, conduttività elettrica, distribuzione delle dimensioni dei pori, test di rilascio lisciviazione. Inoltre, al fine di studiare le caratteristiche mineralogiche e microstrutturali, sono state eseguite analisi in diffrazione a raggi X di polveri e microscopia elettronica a scansione(SEM-EDS).

Carbon Footprint (CFP) fa parte del Life Cycle Analysis (LCA), un metodo mediante il quale gli impatti ambientali generati da un sistema vengono considerati soltanto dal contributo dei gas a effetto serra (GHG). CFP è la versione semplificata della LCA, in cui invece di considerare diverse categorie di impatto, viene preso in considerazione solo il riscaldamento globale. Nella CFP sono stati inclusi i processi di estrazione delle materie prime e di sinterizzazione dei campioni considerati i più rilevanti per quanto riguarda il consumo di energia e la generazione di impatto ambientale. In questa ricerca è stata eseguita la modellazione della CFP condotta con il software Simapro®, PRé Consultants, secondo gli standard ISO.

E' stato verificato che i diversi minerali argillosi e i rifiuti/sottoprodotti agro sono potenzialmente utilizzabili per la produzione di materiali di alta qualità, quali aggregati leggeri per lo strato di drenaggio dei tetti verdi e altri per scopi agronomici per es con proprietà fertilizzanti, generando miglioramenti nelle caratteristiche tecniche del materiale come l'assorbimento d'acqua, la capacità di isolamento e la capacità di rilascio di nutrienti controllata nel tempo, sottolineando così la possibilità di risparmio in risorse naturali e primarie e il consumo di energia, nonché un'alternativa allo smaltimento in discarica.

I rifiuti utilizzati come agenti di formazione dei pori possono essere efficacemente utilizzati ottenendo miglioramento nelle proprietà dell'alleggerimento e dell'isolamento grazie alla capacità di assorbimento dell'acqua. I residui dei birrifici appaiono dei candidati idonei per lo sviluppo di materiali sostenibili per lo strato di drenaggio per tetti verdi ($LWAS_{GR}$). Per i tetti

verdi, i risultati migliori sono stati ottenuti utilizzando la bagassa (BB) in percentuali del 10-15% in peso, sinterizzando per 1 ora a 1000°C.

Per $LWAS_{AP}$ il risultato migliore è stato ottenuto per $WBBS_{15}$ e $RCBS_{15}$ con il 15% di fango di birrificio come porizzante con temperatura di processo di 1000°C per 1 ora.

I risultati del test di lisciviazione su $LWAS_{AP}$ hanno mostrato la capacità di rilascio controllato di nutrienti per LWA_S a fini agronomici. In merito al rilascio di fosforo, i campioni RC_{CBA} mostrano i migliori risultati e, in merito al rilascio di potassio, i migliori risultati sono stati raggiunti con WB_{FG}. L'aggiunta di vetro favorisce il rilascio a lungo termine (21 giorni) di K e P.

Questo test mostra anche che i due materiali ($LWAS_{GR}$ e $LWAS_{AP}$) secondo gli standard sono materiali non nocivi per l'ambiente.

Risparmio sulle risorse primarie ed energia (riduzione della temperatura di sinterizzazione ΔT = 100-300°C), genera un miglioramento nell'analisi della CFP, riducendo l'impatto ambientale in media del 30% per la produzione di LWA_S contenenti rifiuti rispetto a LWA_S senza rifiuti, essendo i campioni con bagassa 15% in peso quelli con i migliori risultati per $LWAS_{GR}$ e WB_{CBA}/RC_{CBA} per $LWAS_{AP}$.

ACKNOWLEDGMENTS/AGRADECIMIEINTOS/RINGRAZIAMENTI

To Angel, my family, Spanish and Argentine, my tutors/co-tutors, Prof. Carmen Martínez García, Prof. Luisa Barbieri, Prof. Teresa Cotes Palomino, Dr. Eng. Nora Maria Fernanda Andreola. To TEP 222, Prof. Isabella Lancellotti. To Elena, Vittorio, Tin Ming, Pablo, Araceli and Myriam. To the University of Jaen, Higher Polytechnic School of Linares and to the University of Modena and Reggio Emilia for this opportunity.

ABBREVIATIONS

LWA_S. Lightweight aggregates

$LWAS_{GR}$. Lightweight aggregates for green roofs

- BYRC. Black, yellow and Red ES (Spanish) clay in equal parts (clay base mixture)
- BS_X (2, 4, 6, 8, 10, 12.5, 15wt%)
- BB_X (2, 4, 6, 8, 10, 12.5, 15wt%)
- DE_X (2, 4, 6, 8, 10, 12.5, 15wt%)

$LWAS_{AP}$. Lightweight aggregates for agronomic porpoises

- WBC. White (30wt%) and Black (70wt%) clay (clay base mixture)
- RC. Red IT clay (Italian) (clay base mixture)
- $WBBS_{15}$. 85wt% WBC and 15wt% BS
- WB_{FG}. 85wt% WBC, 15wt% BS and 10wt% of fertilizer glass (GS)
- $WB_{CBA.}$ 85wt% WBC, 15wt% BS and 10wt% of cattle bone ash (CBA)
- $RCBS_{15}$. 85wt% RC and 15wt% BS
- RC_{FG}. 85wt% RC, 15wt% BS and 10wt% of fertilizer glass (GS)
- RC_{CBA}. 85wt% RC, 15wt% BS and 10wt% of cattle bone ash (CBA)

TN. Technical Nutrient

CE. Circular Economy

BS. Sludge from wastewater treatment

BB. Bagasse

DE. Diatomaceous earth

MBM. Meat-bone meal

CC. Corn cob

CBA. Cattle-bone meal ashes

GS. Glassy sand®

FG. Fertilizer glass

OMC. Organic matter content

LOI. Loss of ignition

LCA. Life cycle assessment

CFP. Carbon Footprint

Kg CO_2 eq. kg of carbon dioxide equivalent

GHG. Greenhouse gas

GWP. Global warming potential

LCI. Life cycle inventory

ISO. International Organization for Standardization

INDEX

A. State of Art 1

A.1. Introduction 1

A.2. Technical nutrient (TN) and Circular economy (CE) 2

A.3. Eco-labelling and Sustainable products 5

A.4. Life Cycle Assessment 8

A.4.1. Carbon Footprint 11

A.5. Agro-food and Recycling Industry. Waste management 15

A.5.1. Brewery industry 15

A.5.1.1. Bagasse 16

A.5.1.2. Diatomaceous earth 17

A.5.1.3. Sludge 17

A.5.2. Meat products industry 19

A.5.3. Cereal production 20

A.5.4. Glass manufacturing/recovery 21

A.6. Clay Minerals 21

A.6.1. Spanish clay minerals 25

A.6.2. Italian clay minerals 26

A.7. Ceramic industry 28

A.7.1. Ceramic products and Environmental externalities 28

A.7.2. Overview in the substitution of alternative raw materials 30

A.8. LWA_S industrial process and uses. 33

A.8.1. LWA_S and waste valorization 37

A.8.1.1. Chemical composition and bloating behavior 43

A.8.2. LWA_S and their use in agriculture 45

A.8.3. LWA_S for green roofs 46

A.8.4. LWA_S and Controlled realized fertilizers 49

B. Purpose and Scope 52

C. Materials and experimental methods 58

C.1. Raw materials characterization 58

C.1.1. Elemental analysis (C, H, O, N, S determination) 58

C.1.2. Carbonates determination. Calcimetry 58

C.1.3. X-Ray Fluorescence (XRF) 59

C.1.4. Loss of ignition (LOI) 60
C.1.5. Organic matter content determination 60
C.1.6. X-ray Powder Diffraction (XRD) 61
C.1.7. Thermogravimetry TG/TGA/DTG and Differential thermal analysis DTA/DSC 62
C.1.8. Calorific power determination (Calorimetry) 64
C.1.9. Particle size distribution analysis 65
C.1.10. Thermo-mechanical dilatometry analysis 65
C.2. LWA_S Characterization 66
C.2.1. Technical parameters. Density, porosity and water absorption. 67
C.2.2. pH 68
C.2.3. Electrical conductivity 69
C.2.4. Scanning electron microscopy (SEM) and Dispersive X-ray Spectrometry (EDS) 69
C.2.5. Porosity characterization 71
C.2.5.1. Mercury intrusion porosimetry (MIP) 71
C.2.5.2. Adsorption and desorption isotherms - BET theory 73
C.2.5.3. Comparison of the two techniques 75
C.2.6. Leaching Test and Inductively Coupled Plasma Mass Spectrometry (ICP-MS) 75
C.2.7. Insulation capacity 79
C.3. Carbon Footprint (CFP) calculation 79
C.3.1. System description and Functional unit 80
C.3.2. Life Cycle Inventory 80
C.3.2.1. LWA_S for green roofs 82
C.3.2.2. LWA_S for agronomic porpoises 82
C.3.3. Assumption and Cutting 83
C.3.4. Life Cycle Impact Assessment Methodology 84
D. Results and Discussion 86
D.1. Clays minerals 86
D.1.1. Reception condition 86
D.1.2. Clays minerals characterization 86
D.1.2.1. Chemical analyses: Elemental, FRX, LOI, and Carbonates determination (calcimetry) 86
D.1.2.2. Mineralogical analysis: X-ray powder diffraction (XRD) 89
D.1.2.3. Thermogravimetric analyses (TG-DTA-DSC) 92
D.1.2.4. Particle size distribution analysis (Granulometric) 98

D.1.2.5. Clay-based mixtures thermal behavior analysis 101
D.1.2.5.1. Clay-based mixtures theoretical chemical composition 101
D.1.2.5.2. Thermogravimetric analyses (TG-DTA-DSC) 102
D.1.2.5.3. Thermo-mechanical dilatometry analysis 104
D.2. Waste/by-products/technical nutrients 107
D.2.1. Reception condition 107
D.2.2. Waste/by-products characterization. 110
D.2.2.1. Organic waste/by-products. 110
D.2.2.1.1. Chemical (Elemental, FRX, LOI), calorimetry, calcimetry and organic matter determination. 110
D.2.2.1.2. Mineralogical analysis: X-ray powder diffraction (XRD) 112
D.2.2.1.3. Thermogravimetric analyses 115
D.2.2.2. Inorganic Waste/By-products. 118
D.2.2.3. Fertilizer glass (FG) preparation and characterization 121
D.3. Sample preparation 123
D.3.1. LWA_S for drainage layer in green roofs ($LWAS_{GR}$) 123
D.3.2. LWA_S for agronomic purposes ($LWAS_{AP}$) 124
D.4. LWA_S chemical composition and bloating behavior 127
D.5. LWA_S characterization 130
D.5.1. $LWAS_{GR}$. Green roofs drainage layer. 130
D.5.1.1. Technical parameters. Density, porosity and water absorption determination. 130
D.5.1.2. Mercury intrusion porosimetry (MIP) 135
D.5.1.3. Microstructure and chemical analysis (SEM-EDS) on external surface 138
D.5.1.4. Leaching test 141
D.5.1.5. Insulating properties 142
D.5.1.6. Carbon footprint calculation (CFP) 144
D.5.2. LWA_S for agronomic purposes. $LWAS_{AP}$ 145
D.5.2.1. Technological properties. First stage. 145
D.5.2.2. Technological properties. Second stage. 148
D.5.2.3. LWA_S X-ray powder diffraction (XRD) 152
D.5.2.4. Mercury intrusion porosimetry (MIP) 153
D.5.2.4.1. WB clay-mix samples. 154
D.5.2.4.2. RC clay-mix samples 157
D.5.2.5. Microstructure and chemical analysis (SEM-EDS) external surface. 160

D.5.2.5.1. WB clay-mix samples. 160
D.5.2.5.2. RC clay-mix samples 163
D.5.2.6. Leaching test 167
D.5.2.6.1. Test in water: 30 minutes. 168
D.5.2.6.2. Citric Acid Test: 30 minutes. 169
D.5.2.6.3. Citric Acid Test: 21 days. 172
D.5.2.7. Insulation capacity 174
D.5.2.8. Carbon Footprint calculation (CFP) 175
E. Conclusions 177
F. Future research lines 181
Bibliography 182

A. STATE OF ART

A.1. INTRODUCTION

Climate change, energy crisis, resource scarcity, and pollution are significant issues humankind will be facing in future years. Sustainable development has become a priority for the world's policymakers since humanity's impact on the environment has been dramatically accelerated in the past century with fast increasing population and the concomitant sharp decrease of ultimate natural resources. Finding alternatives and more sustainable ways to live, to pass on to future generations are one of these critical messages relates to waste generation and pollution. Diverse types of waste (e.g., agricultural, food, industrial) is produced day by day in vast quantities, causing a substantial problem in its management and disposal. A widespread feeling of "environment in danger" has been present everywhere in our society in recent years, which, however, has not yet crystallized in the general awareness. Various valorization techniques are currently developed and producing products and services meeting industrial and client's demands. Many methods could achieve sustainable development, methods that could not only improve waste management but could also lead to the production of industrially relevant and sustainable chemicals, materials, and fuels, e.g., valuable end-products from waste (Arancon et al., 2013).

At a global scale, climate change is a serious international concern and the extraction, processing, and use of natural resources contributes directly to climate change through the burning of fossil fuels, while the disposal of materials in landfills contributes through emissions of greenhouse gases. Valorisation of waste and their transformation in technical nutrients by recovering in the form of material and energy resources can contribute to the resource efficiency and GHG mitigation efforts (Goedkoop et al., 2009; Turner et al., 2016).

Landfill, incineration and composting are common, mature technologies for waste disposal. However, they are not satisfactory to treating organic waste due to the generation of toxic methane gas and lousy odor, high energy consumption, and slow reaction kinetics. In fact, research efforts have also been oriented on effective technologies to decompose organic waste. However, no valuable product is generated from the decomposition process. Instead of disposing and decomposing food waste, recent research has focused on its utilization as an energy source (e.g., for bioethanol and biodiesel production). Organic waste is also used to produce organic chemicals via bio-refinery or white biotechnology (e.g., succinic acid and bio-plastics) (Arancon et al., 2013).

The waste valorization and productive sector are under increasing pressure to improve its environmental performance. In the European Union (EU), members are legally obliged to adopt and implement regional policy instruments to meet the environmental objectives and targets outlined in a broad international legal framework. The EU Waste Framework Directive establishes the "waste hierarchy," a five-step priority order of waste management comprising, in descending order of priority, prevention, preparation for reuse, recycling, another recovery (e.g., energy from waste), and disposal (EC, 2008). The Landfill Directive sets a target for member states to reduce the amount of biodegradable municipal recollection solid waste to landfill in a 35% by 2016 (EC, 1999). A target of achieving 50% recycling household waste materials (paper, glass, metals, and plastics) is established in the Packaging and Packaging Waste Directive (EC, 1994). Moreover, at a broader level, the EU is committed to reducing its GHG emissions by at least 20% and 40% of 1990 levels by 2020 and 2030 (EC, 2015), respectively. Managing resources to maximize environmental sustainability and contribute towards the achievement of national targets set by the EU entails crucial strategic and investment decisions by local waste managers, who are simultaneously tasked with maintaining a reliable and economical waste removal service to residents under increasing budgetary pressures. To reduce the burden on local waste managers and promote environmentally sustainable practices, there is a need for reliable waste policies that guide and enable effective local decisions and actions.

This overall, includes all productive and energy production processes, including, construction materials. At the world level, civil works and building construction consume 60% of the raw materials extracted from the lithosphere. From this volume, the building represents 40%, in other words, 24% of these global extractions. In Europe, the mineral extractions per capita intended for building amount to 4.8 tonnes per inhabitant per year, which is 64 times the average weight of a person, highlighting the need to work towards dematerialization in building (Zabalza Bribián et al., 2011).

The mining and minerals industry faces some of the most challenging sustainability encounters of any industrial sector. To secure its continued "social-license" to work, the industry must respond to these challenges by engaging its many different stakeholders and addressing their sustainability concerns, through the use of alternative materials (technical nutrients), in response to the concept of circular economy. The industry must also be able to measure and assess its sustainability performance and to demonstrate continuous improvements over long-term (Azapagic, 2004).

A.2. TECHNICAL NUTRIENT (TN) AND CIRCULAR ECONOMY (CE)

Due to the exponential generation of waste, there is a clear need to incorporate waste from other processes into the production systems, through valorization as raw materials to close the cycle. Waste valorization is the process related to converting waste materials into technical nutrients, e.g., more useful products. Such concept has already existed, related to waste management, in the present times with renewed significance due to the fast depletion and scarcity of natural and primary resources, the increased waste generation and landfilling technique worldwide, generating the need for more sustainable and cost-efficient waste management protocols (Nzihou, 2010).

The circular economy concept is based on the materials and products design that facilitate the disassembly and reuse, with the primary purpose of waste valorization as raw materials, technological nutrients. This process is based mainly on eco-design, with the primary objective of closing the life cycle, emulating the biological processes. Technical nutrients (TN) are designed to be recovered and reused, in replacement of natural and primary resources, within the closed-loop cycle of sustainable manufacturing processes.

The linear economy model 'take, make, dispose of' relies on large quantities of cheap, easily accessible materials and energy, without limits. The circular economy (CE) is an attractive and viable alternative that businesses are already exploring, being restorative and regenerative by design and aims to keep products, components, and materials at their highest utility and value along the cycle, emulating biological cycles. It enables key policy objectives such as generating economic growth, creating jobs and reducing environmental impacts, including carbon emissions (Ellen MacArthur Foundation, 2015).

In a more evolved concept, the technical nutrients are the links of the circular chain, circular economy, closely related to energy efficiency, pollution reduction and the sustainability of limited resources, which creates the need for a system of interconnection of the different that crosses all productive processes, is the research and innovation the central axis of this concept.

The European Community (EC) legislation and Horizon 2020 program, is aligned with the concept of zero-waste generation, mining the valorization of 100% of the waste generated by the production process/energy use. In this sense, EC has made substantial progress in waste valorization, as raw materials and promoting sustainable ways of waste management. However, performance varies considerably between the Member States. Almost the 20% of member countries have already efficiently reduced the landfilling waste treatment, reducing it from 90%

to less than 5% in the past 20 years. The EC still generate about five tons of waste per person/year, more than a third is recycled efficiently (European Commission, 2014).

It is estimated, that more efficient use of resources along the entire value chain reduces the need for input of virgin materials, meaning savings for European industry in the order of € 630 million a year and potentially to raise the GDP (Gross Domestic Product) up to 11% (Innova Europe, 2012). This fact reduces costs by inverting the economic chain, allowing to suppress landfills cost through the valorization, from waste to raw material, reducing the input of virgin raw materials.

According to the Ellen MacArthur Foundation (2012, p.7), "A circular economy is an industrial system that is restorative or regenerative by intention and design. It replaces the 'end-of-life' concept with restoration, shifts towards the use of renewable energy, eliminate the use of toxic chemicals, which impair reuse, and aims for the elimination of waste through the superior design of materials, products, systems, and, within this, business models".

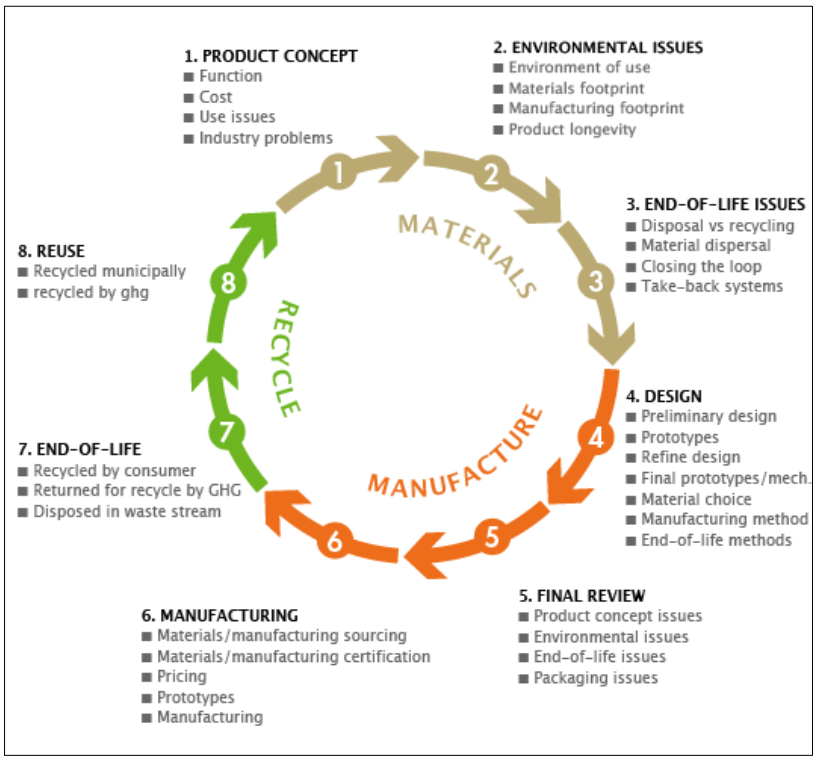

Image A.2.1. Design Cycle (Ditto Hangers, 2018).

The Circular Economy concept is based on few simple principles. First, CE aims to 'design out' waste. Waste does not exist because the products are designed and optimized for a cycle of disassembly and reuse (Image A.2.1). Secondly, circularity introduces a strict differentiation

between consumable and durable components. Thirdly, the energy required to fuel the cycle should be renewable by nature, again to decrease resource dependence and increase system resilience. For technical nutrients (TN), the CE largely replaces the concept of a consumer with that of a user, e.g., new contract between businesses and their customers based on product performance (The Ellen MacArthur Foundation, 2012).

In other terms, the production of recycled material that renters further life cycles represent a potential credit for avoiding the production of an equivalent quantity of natural and primary resources. The system that recycles the waste into a valuable product is credited with the environmental burdens of the corresponding primary production but is charged with energy and ancillary materials used in the recycling process, currently called system expansion.

A.3. ECO-LABELLING AND SUSTAINABLE PRODUCTS

The ultimate goal of Eco-design is to improve product's environmental performances (eco-products). Reason and motivation for a company to develop eco-products is to increase the market share and to enhance the corporate image, as a corporate business strategy.

As a result, the environmental aspects of the product have to be communicated to the customers and relevant stakeholders. Environmental labeling can put forth a significant impact on the market if the environmental awareness of the consumer is high. The certification processes generate a state of trust that provides information about a part or all, of the life cycle of the product to the consumer, depending on the certification procedure, i.e., depending on what the company wants to communicate about of specific product. This generates a responsible consumption, where the client decides what the impact action is through the consumption of a product/service.

The development of the environmental product declarations (EPD_S) has become a significant application of a life cycle assessment (LCA). The EPD_S consists of a series of impact category indicator results. Nowadays, three types of environmental communication are available: Type I, II, and III.

- Type I. Environmental labeling. The "classic" eco-labeling schemes, which award a mark or a logo based on the fulfillment of a set of criteria's.
- Type II. Self-declared environmental claims. Claims which were made by manufacturers and businesses, and could be seen as being of "self-declared".

- Type III. Environmental declarations. It is considered a formalized set of environmental data describing the environmental aspects of a product.

Table A.3.1. Summary of the different types of environmental communications.

	Type I	Type II	Type III
Life cycle analysis	No	No	Yes
Third party verification	Yes	No	It does not require, but it increases credibility
The eco-label communicates…	Environmental benefit	Environmental attribute	Environmental declaration
ISO standard	ISO 14024:2018	ISO 14021:2016	ISO 14025:2007 and ISO 21930:2017

Type I, Environmental labeling (ISO-14024:2018, 2018) states that product should meet environmental criteria based on life cycle considerations, i.e., the product must demonstrate environmental superiority over competing products that attend the same function throughout its entire lifecycle. Products meeting the specific values imposed by Type I program's criteria can obtain the label. However, only 20 to 30% of the products in any product category are awarded labels, due to the selectivity principle (Wimmer W., Züst R., 2004). Some of the best known Eco-labelling programs include the Blue Angel in Germany, Nordic Swan in the Nordic countries, Environmental Mark in Japan and Korea and Environmental Choice in Canada, and EU flower in the EU, among others (Image A.3.1).

Image A.3.1. Eco-labeling programs. Blue Angel, Nordic Swan, Environmental Choice, and EU flower respectably.

Type II, declaration according to the ISO 14021 standard (ISO-14021:2016, 2016), consist of an environmental claim or "self-declaration" by the manufacturer about the ecological characteristics of the product itself, single environmental attribute e.g., the recycled content, recyclability or biodegradability of the product, the absence of substances harmful to the environment, non-toxic or natural finishing treatment (Image A.3.2).

Image A.3.2. Symbols of recyclability or biodegradability of a product.

Type III, is the actual environmental product declaration (EPD) (Image A.3.3), for which ISO 14025 provides the guidelines (ISO-14025:2006, 2006). ISO 21930 complements ISO 14025 by providing the principles, specifications and requirements to develop an EPD for construction products and services, construction elements and integrated technical systems used in any type of construction works (ISO-21930:2017, 2017).

These guidelines are not specific enough to make EPD. Instead, the standard describes a procedure to make more specific product category rules. Without such rules, one cannot produce an EPD (M. Goedkoop, M. Oele, J. Leijting, T. Ponsioen, 2013).

Image A.3.3. Symbols of environmental product declaration (EPD)

The construction activities are of the industrial processes with an environmental impact, since the massive consumption of natural resources. At the same time, the need to deepen in the generation or rehabilitation of buildings with specific adaptations to each geographical location, concerning to thermal insulation, acoustics, associated with the generalized rising prices and costs of energy production to the necessary conversion from non-renewable to renewable energy sources, mainly solar and wind.

Over the past two decades, EURIMA (European Manufacturers Insulation Association) studied the development of thermal insulation standards in European new buildings, highlighting the most significant potential for energy savings in some northern Countries. However, they indicate that the primary efforts should focus on Southern Europe and most populated Countries: if Swedish insulating standards were employed in States such as Belgium, Spain, and Italy, energy savings would reach up to 90%. Is also estimated that in Europe savings could be higher than 50% (European Insulation Manufacturers Association (EURIMA), 2011; Proietti et al., 2013).

The regulations developed in the field of the sustainability construction works, RPC 305/2011 EU European Building Products Regulations, replacing Directive DPC 28/106, links environmental product declarations with sustainability assessment.

Following the European guidelines and regulated by ISO standards, some of the most relevant eco-label systems are:

- The Environmental Declarations of Construction Products® (EDC_P), is a type of certification provide quantitative information on the different environmental impacts that can be caused by a construction product throughout its life cycle. There are specific eco-labels for construction materials such as the EDC_P® System. The EDC_P® Certification is an eco-labeling system of EPD (Environmental Product Declaration) of the pioneering construction in Spain.
- AENOR (Spanish Association for Standardization and Certification), is another program manager through which it can obtain the Environmental Declaration of Construction Product.
- DGNB eco-label is an environmental certification system of German origin, applicable to buildings, which provides a life cycle assessment of the building based on information from the EDC_P of each material/product/service that constitutes said building.

A.4. LIFE CYCLE ASSESSMENT

The life cycle assessment (LCA) is an environmental management tool to achieve the eco-efficiency, highlight and quantify the potential environmental aspects and impacts throughout the life cycle of a product/process/activity, from the acquisition of raw materials, through life cycle "from the cradle to the grave", providing the guidelines for raw materials selection in the development of green materials (Bories et al., 2016; Kumbhar et al., 2014) and for further eco-label certifications (Zabalza Bribián et al., 2011).

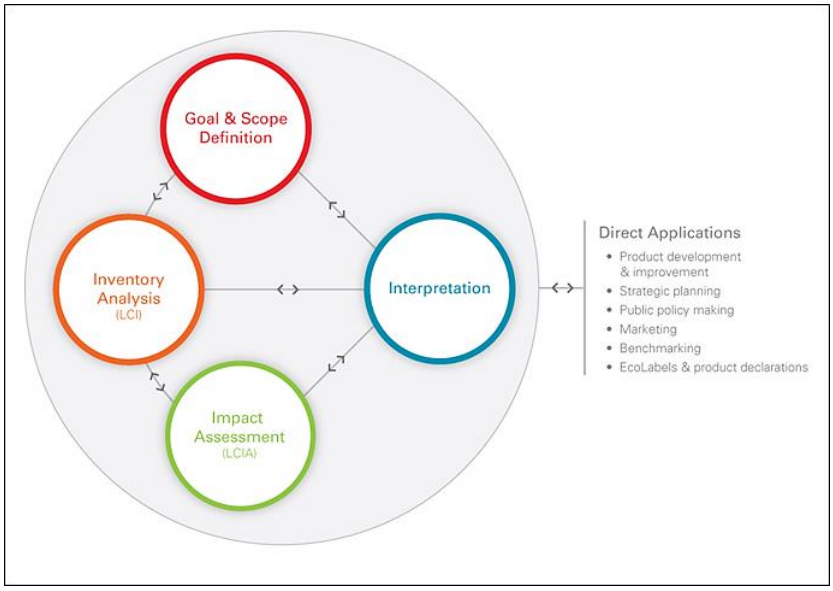

Image A.4.1. LCA study four main areas (LCANZ, 2015).

The assessment includes all the activities, processes, by-products connected to the system analyzed, including raw material processing, production, maintenance, recycling, and disposal "end of life". ISO 14040, considers the principles and framework for a life cycle assessment, while ISO 14044 specifies the requirements and guidelines for carrying out an LCA study (UNE-EN-ISO-14040, 2006; UNE-EN-ISO-14044, 2006). LCA study is divided into four main areas according to ISO standards (Image A.4.1):

Goal and scope definition. Defining the goal includes determining the reason for carrying out the LCA study, the intended audience, and the application while defining the scope involves setting the system boundaries and the level of detail, e.g., limits of the system, level of detail of the analysis are outlined, the functional unit used in the analysis and data sources description. The functional unit is understood as the unit to which LCA study data are referred.

Inventory, the definition of inputs and outputs. This phase includes data collection and calculation procedures to identify and quantify all adverse environmental effects, associated with the functional unit, including emissions of pollutant gases, water effluents, solid waste, consumption of natural resources, noise, radiations, odors, and every environmental release incurred throughout the life cycle processes (Image A.4.2).

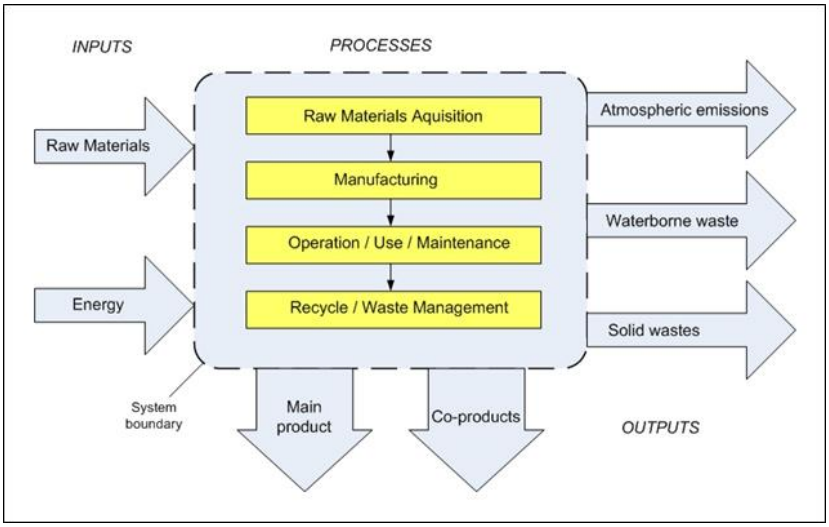

Image A.4.2. The main stages and typical inflows and outflows considered in lifecycle assessment (Ditto Hangers, 2018).

Impact assessment. Method, quantitative, and qualitative process to characterize and assess the effects of the environmental loadings identified in the inventory component. Once the inventory is modeled, we can know and evaluate the magnitude and significance of the potential environmental impacts of a system. To do this, one must select a set of environmental variables, or "impact categories", depending on what one wants to analyze.

The impact assessment phase has two mandatory steps: classification and characterization. Classification of the LCI results involves dividing the LCI results into impact categories, e.g. global warming, acidification, and human toxicity. In characterization, the potential impact of each emission or resource use is estimated, using specific scientific factors.

Life Cycle Interpretation. In this last step, the results of an LCI and LCIA are summarised and discussed to provide the basis for conclusions, recommendations, and decision-making, depending on the goal and scope previously defined.

There is a wide range of tools to conduct an LCA or for the development of the different phases, applications and particular fields in the industry. Only a few free tools are available. Some main characteristics of the tools are included, too, indicating, e.g., the operating language, industrial sector and whether the tool is free or commercial (Lehtinen et al., 2011).

Various LCA databases are attached to the LCA tools, and some can be used separately. There are both freely available and commercial databases. The software-database libraries are composed of data compiled for the software-developer and with others research centers like

Ecoinvent which is developed by the Swiss Center of the same name, all associated with recognized research centers around the world, providing information of productive processes, energy consumption, waste management, extractive activities.

A.4.1. CARBON FOOTPRINT

Carbon Footprint (CFP) is a part of the LCA, a method by which the environmental externalities generated by a system are based on the contribution of Greenhouse Gases (GHG), emitted by direct or indirect effects. CFP is the simplified version of the LCA, in which instead of considering several impact categories, only the Global Warming is considered. ISO 14064-1,2,3 determines the standards for the calculation of the CFP (UNE-EN-ISO-14064-1:2006, 2015; UNE-EN-ISO-14064-2:2006, 2015; UNE-EN-ISO-14064-3:2006, 2015).

The CFP is measured in kilograms of CO_2 equivalents (kg CO_2-eq), based on the analysis of greenhouse emissions, direct or indirect effects on climate change, emitted throughout the life cycle of a product. Even doesn't provide information about the entire environmental impact of product/service, its results are easy to understand and directly connected to the study of global warming potential.

Each greenhouse gas (GHG) has a different global warming potential (GWP), related to their persists for a different time-length in the atmosphere. The three main greenhouse gases and their 100-year global warming potential (GWP) compared to carbon dioxide are:

- 1 x CO_2. Burning fossil fuels (coal, natural gas, and oil), solid waste, wood, and also as a result of specific chemical reactions (e.g., cement manufacturing). Part of it is absorbed by plants as part of the biological carbon cycle.
- 25 x methane (CH_4), i.e., releasing 1 kg of CH_4 into the atmosphere is about equivalent to releasing 25 kg of CO_2. Methane is emitted in the production and transport of coal, natural gas, and oil; livestock and other agricultural practices and by the organic waste degradation in landfills.
- 298 x nitrous oxide (N_2O), i.e., releasing 1 kg of N_2O into the atmosphere is about equivalent to releasing 298 kg of CO_2. N_2O is emitted during agricultural and industrial activities, as well as during combustion of fossil fuels and solid waste.
- Water vapor is not considered to be a cause of global warming because it does not persist in the atmosphere for more than a few days.

There are other greenhouse gases which have far higher global warming potential (GWP) but are much less prevalent. These are sulfur hexafluoride (SF_6), hydrofluorocarbons (HFC_S), and perfluorocarbons (PFC_S). There exist a wide variety of uses for those GHG´s, but they have been most commonly used as refrigerants and for fire suppression. Many of these compounds also have a depleting effect on ozone in the upper atmosphere.

The Table A.4.1.1 shows the 100-year global warming potential for greenhouse gases reported by the United Nations Framework Convention on Climate Change (UNFCCC). The column on the right shows the multiplication factor that the chemical would warm the earth over in a 100 year period, compared to CO_2. The table shows that a release on 1.00 kg of C_2F_6 is equivalent to 12200.00 kg or 12.20 tonnes of CO_2 (IPCC, 2007).

Greenhouse Gas	Formula	100-year GWP
Carbon dioxide	CO_2	1.00
Methane	CH_4	25.00
Nitrous oxide	N_2O	298.00
Sulfur hexafluoride	SF_6	22800.00
Hydrofluorocarbon-23	CHF_3	14800.00
Hydrofluorocarbon-32	CH_2F_2	675.00
Perfluoromethane	CF_4	7390.00
Perfluoroethane	C_2F_6	12200.00
Perfluoropropane	C_3F_8	8830.00
Perfluorobutane	C_4F_{10}	8860.00
Perfluorocyclobutane	c-C_4F_8	10300.00
Perfluoropentane	C_5F_{12}	13300.00
Perfluorohexane	C_6F_{14}	9300.00

Table A.4.1.1. The GWP values (IPCC, 2007).

The consumption of earth-based materials such as clay in the production of ceramic materials results in a resources depletion, environmental degradation, and energy consumption. The extraction of the clays causes a degradation of the landscape and an alteration of the soil surface. Among the most significant environmental impacts is the substantial modification of the topography of the area, surface layers due to erosion and lack of vegetation, soil sterility, emissions of particulate matter to the atmosphere due to the blasting of the surface layer and biomass. In contrast, the ceramic industry presents a high potential for waste valorization (Proietti et al., 2013).

It is the extraction activities of clay material, drying, and sintering of the ceramic samples, are the processes with more externalities regarding environmental impact, all related to non-removable energy source input (fossil fuels).

Although fossil fuels are continually being formed via natural processes, they are considered to be non-renewable resources, taking millions of years to form, and the known viable reserves are being depleted.

Carbon dioxide is responsible for the half of the Earth's greenhouse effect warming. Methane, which is increased by escaping natural gas, contributes 18%, and nitrogen oxides, which are products of fossil fuel burning, account for 6%. This is estimated to cause 20% of the greenhouse effect (Bernard L. Cohen, 2008).

It is estimated that emissions are forecast to reach around 37.00 billion tons of CO_2 from fossil fuel burning and industrial activity in 2017. Global carbon dioxide emissions from fossil fuel burning and industrial uses are projected to rise by up to 2 percent in 2017, as well as to rise again in 2018. It is estimated that natural processes, can only absorb half of that amount of carbon dioxide emitted (EIA, 2007).

Despite the global economic growth, total emissions held level from 2014 to 2016 at about 36 billion tons per year, stoking hope among many climate change advocates that emissions had reached an all-time high point and would subsequently begin to decline. However, that was not to be, the new analysis suggests (Image A.4.1).

Glen Peters, one of the study's co-authors and a researcher at the Center for International Climate Research in Oslo, said: "the 2017 number would be a record high for emissions from fossil fuel burning and industrial uses (such as cement), although carbon emissions from deforestation and land-use changes were higher in 2015".

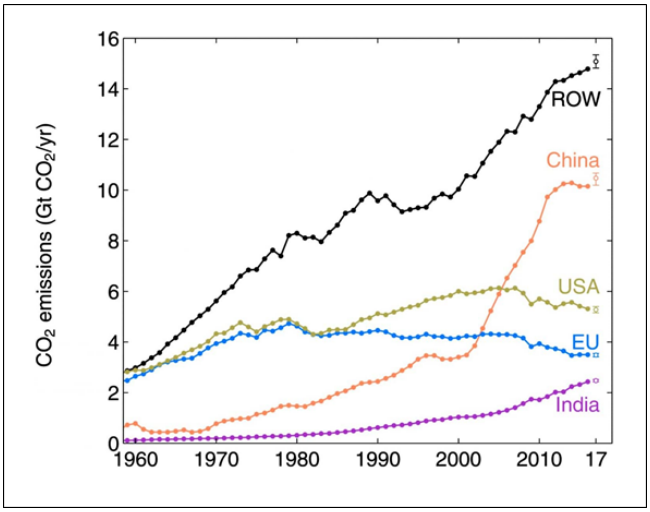

Image A.4.1.1. Carbon dioxide emissions from fossil fuel use since 1960 for China, the United States, the European Union, India, and the Rest of the World (ROW) (Global Carbon Project and CDIAC) (C. Mooney, 2017).

All in all, the finding is bad news for global climate policy. The Paris agreement, now supported by every nation except for the United States, aims to limit the warming of the planet to "well below" 2.00°C above pre-industrial levels and to try to hold warming to 1.50°C (C. Mooney, 2017). However, this requires emissions not just to stay flat but to go down.

The potential environmental effect in ceramic materials production (Kumbhar et al., 2014; Pappu et al., 2007) and database inventory development (Haddad et al., 2013), as well as waste valorisation in the ceramic matrix (Bories et al., 2016; Zabalza Bribián et al., 2011). CFP also was conducted to the compared evaluation of aggregate production from recycled waste materials and virgin sources by LCA (Hossain et al., 2016). The potential environmental effect of waste valorization throw the development of ceramic materials compared with its commercial ones has already been studied (Proietti et al., 2013; Simion et al., 2013).

Hence the importance of saving virgin raw materials and energy consumption such as clays due to the partial replacement of technical nutrients available in nearby industrial areas.

Based on the concept of the circular economy, this research is focused on evaluation of environmental indicators as global warming, in terms of Carbon Footprint calculation in the development of sustainable LWA_S, with the addition of agro-industrial waste to reduce sintering temperature, energy consumption in the sintering process by organic matter combustion, and virgin raw material inputs.

A.5. AGRO-FOOD AND RECYCLING INDUSTRY. WASTE MANAGEMENT

The agro-food industry must continue to adapt to society's changing habits and preferences. Some of the most critical issues for the industry are differentiating products by quality and origin (enhanced traceability and an indication of origin), healthy and functional foodstuffs, eco-friendly products, new consumer family types (immigrants, single person households) and food as a cultural issue. In the same line is essential to highlight that this sector is also facing the imperative need for continuous development of environmental strategies to reduce the impact of production and waste generation.

The agro-food industry can be defined as the sector which includes all operations related to processing, preserving, preparing and packaging agricultural and food products carried out in industrial production units.

The Gross Value Added (GVA) of agro-food industry in Spain in 2010 was about 20.500 million, approximately 15.70% of the total GVA of Spanish industry, and had a turnover of €94.580 billion, representing 18% of the whole industrial production in Spain. More specific, The cereal production in the period from July 1, 2016, to June 30, 2017 (i.e., wheat, corn, barley, rye, oats, sorghum), was 23,252.1 tons (MAPAMA-España, 2017).

Agriculture is one of Italy's key economic sectors, accounting for around 2.3% of Gross domestic product (GDP). Italy's agriculture is typical of the northern and southern division found within the European Union. The northern part of Italy produces grains, soybeans, meat, and dairy products, while the south specializes in fruits, vegetables, olive oil, wine, and durum wheat. Italy has an extensive, diversified industrial economy with roughly the same total and per capita output as France and the United Kingdom. Italian industries, including the food-processing sector, rely on the imports of raw materials. Italy is one of the largest agricultural producers and food processors in the European Union (EU)(Export, 2017).

A.5.1. BREWERY INDUSTRY

In the food industry, the sector of brewing in Europe had produced 395 million hectolitres in 2015 (Brewers of Europe, 2016). Beer is the fifth beverage most consumed worldwide, exceeded by tea, carbonated drinks, milk, and coffee. The brewing industry has an ancient tradition processing but still a dynamic sector open to new developments (Fillaudeau et al., 2006).

Beer is the beverage resulting from the fermentation of yeasts and the wort from barley malt (alone or mixed with sugar-soluble starches by enzymatic digestion) after cooking and flavored with hops. The malt is obtained by the germination, drying, and toasting of the barley.

During production, beer alternately goes through three chemical and biochemical reactions (mashing, boiling, fermentation, and maturation) and three solid-liquid separations (wort separation, wort clarification, and rough beer clarification. Consequently, water consumption, wastewater and solid-liquid separation constitute real economic opportunities for improvements in brewing (Fillaudeau et al., 2006).

Breweries sector is very concerned about the techniques used and its continues improvements, regarding product quality and cost-effectiveness. In the same line, the objective of developing technologies and alternatives for minimizing/valorizing waste for the reduction of the problems derived from its management/final disposal of waste/by-products produced in massive quantities, mainly diatomaceous earth, water treatment plant sludge, bagasse, and yeast.

Most of the solid residues generated are organic (bagasse, yeast and sewage sludge), which can be considered as by-products valorized by another industrial process (human nutrition, animal feed, pharmaceutic) or for agricultural use as organic fertilizer. Given the commercial value of the solid waste generated in the brewery process and the very high BOD charge, is placed in different storage systems and not treated in the wastewater treatment plant.

A.5.1.1. BAGASSE

Bagasse represents the 80% of the malt volume, generates approximately 20.00 kg/hl of beer produces. While the yeast produced during fermentation is four times higher than that initially introduced. Both residues should be considered as by-products since they have value as raw material for other industrial activities (animal feed, pharmaceutical industry, human food). However, their value as a by-product depends on characteristics such as their humidity or freshness, for this the brewery must have facilities to ensure adequate storage. Leachates generated during storage must be collected and sent to the water treatment plant. As a reference, the energy consumption necessary to reduce the humidity of bagasse from 60% (moisture obtained after its mechanical pressing) to 15% is 15-20 MJ/hl of beer (AINIA, 1996).

Bagasse has been commonly recycling in diverse ways, like its use an adsorbent for metal effluent decontamination (O'Connell et al., 2008). It also may be used for plants or mushrooms substrates by composting (Sánchez, 2010; Silva et al., 2009). Another more complex treatment

is extracting which produces sustainable wood adhesives (de Barros Filho et al., 2011) and multi-component adsorption of cadmium and zinc (Mohan and Singh, 2002). However, the most common alternative use involves its usage as sustainable fuel based on its high calorific power (HHV). Also, was studied as a pore forming agent for clay bricks formulation (Bories et al., 2014; Eliche-Quesada et al., 2011; Martínez et al., 2012), obtaining materials with better characteristics of thermal insulation and mechanical resistance. For the formulation of LWA_S also was investigated there use as a pore-forming agent and as a bloating precursor, due to there high silica content, present good results in the formulation of sustainable LWA_S, with improved insulation capacity (Farias et al., 2017b).

A.5.1.2. DIATOMACEOUS EARTH

The clarification process consists of removing the solids from the beer by centrifugation that allows removing up to 99% of the yeast. Subsequently, the beer is forced to go through diatomaceous earth filter. The consumption of diatomaceous earth is approximately between 0.1-0.3 Kg/Hl of brewed beer.

Exhaust diatomaceous earth has some characteristics that make their management difficult (inert calcareous matrix with a high content of organic solids and high humidity). The first action should be the reduction of moisture content to avoid the production of discharges (leakages) and odors, to facilitate their management. This residue is considered as non-hazardous waste, EWC 02-03-01 (sludges from washing, cleaning, peeling, centrifuging and separation. Wastes from fruit, vegetables, cereals, edible oils, cocoa, coffee, tea and tobacco preparation and processing; conserve production; yeast and yeast extract production, molasses preparation and fermentation).

This residue was studied as removal of herbicide paraquat from an aqueous solution (Tsai et al., 2005), silica adsorbent (Tsai et al., 2004). Furthermore, was investigated its use as a pore-forming agent in ceramic bricks (R J Galán-Arboledas et al., 2013) to improve insolating (thermal and acoustic) related to lighter materials. Exhaust diatomaceous earth represents a reliable source of silica and aluminum, to decrease carbonates content, remarkable characteristics for sustainable LWA_S formulation (Farias et al., 2017b), improving insulation capacity.

A.5.1.3. SLUDGE

Disposal of sludges from wastewater treatment plants is a serious global environmental matter. Subsequently, there are several alternatives for its management: landfill disposal, application in

contaminated soil, incineration (energy use), biogas generation, and valorization as raw material, technical nutrient. In any case, these management solutions must be adapted to the corresponding regional or local legislation.

This waste is generated in the biological treatment system, as a consequence of the high organic load presented by the brewery's water during production, to reduce the values of COD, BOD_5 and solids in suspension up to values that allow its discharge. Biological systems consist of causing the development of microorganisms capable of digest the organic matter present (generally higher than 60%) in the water by oxidization or reduction and transformed into new microorganisms that are removed by decantation or flotation. The system performs sludge purges, and it follows the stages of concentration and dehydration, to be later removed by a certified waste-operator.

The sludge also has relatively complicated management in some cases. Its most straightforward use is composting and subsequent use as fertilizer or agricultural amendment provided that it not present concentrations of heavy metals above the legislated limit values.

The following implementation of wastewater treatment plants increases the quantities of sludge requiring disposal. From an annual production of 5,5 million tons in 1992, the EU is heading towards nearly 9.00 million tons by the end of 2005 (European Commission, n.d.). The Directive 86/278/EEC encourages the use of sludge in agriculture, regulating its use due to prevent harmful effects on soil, vegetation, animals, and man. Treated sludge is defined as having undergone "biological, chemical or heat treatment, long-term storage or any other appropriate process so as significantly to reduce its fermentability and the health hazards resulting from its use."

For this reason, it was already studied the behavior of wastewater treatment plant sludge within the ceramic matrix as a pore-forming agent, for structural ceramics (Eliche-Quesada et al., 2011; Kizinievič et al., 2013). The use of sludge in LWA_S, has been deeply studied, due to the thermal treatment to which the arids are subjected, allowing the destruction/inertization of this type of waste with very good results insulation capacity and lighter materials (low bulk density), sewage sludge ash (Cheeseman and Virdi, 2005), sewage sludge (Franus et al., 2016; Gunning et al., 2009), washing aggregate sludge (González-Corrochano et al., 2012), sludge form brewing industry for LWA_S for agronomic aplications (Farias et al., 2017a) and to denveloup a sustenible material for its use as a derenage layer in green roofs (Farias et al., 2017b).

The wastewater treatment plant use in this research is classified as non-hazardous waste, EWC 02-07-05 (Wastes from the production of alcoholic/non-alcoholic beverages (except coffee, tea, and cocoa), sludge's from on-site effluent treatment).

A.5.2. MEAT PRODUCTS INDUSTRY

The production of meat and meat-products in Spain raise in 2014 5,759.00 transcend tonnes (bovine, pigs, sheep, goats, and poultry). Italy, in the same period 3,306.00 transcend tonnes (EUROSTAT, 2015).

The meat industry is made up of animal slaughterhouses (for beef, pork, lamb or similar), industrial companies that produce, prepare and package fresh, refrigerated and frozen meat and companies that produce meat-based products (sausages, pâtés, hams, etc.), generating a considerable quantity and variety of wastes and by-products (Barcelonactiva, 2013).

Regulation (EC) N^{o} 178/2002 (Regulation (EC) N^{o} 178/2002, 2002) constitutes the latest European legislation on food safety. Animal by-products are defined as the entire bodies or parts of bodies or products of animal origin not intended for human consumption. The animal by-product, including meat-bone meals, are classified into three categories: category 1 and 2 represent materials with high risk, and category three classify as low risk. Category 1: all body parts, of animals suspected of being infected with a transmissible spongiform encephalopathy (TSE), including the products derived from animals that have absorbed forbidden substances or substances dangerous for the environment. Category 2: manure and digestive tract content; products of animal origin containing residues of veterinary drugs and contaminants in concentrations that exceed the Community limits, products of animal origin, that are imported from third countries, fail to comply with the Community veterinary requirements, that have not been slaughtered for human consumption. Category 3: parts of slaughtered animals which are fit for human consumption but are not intended for human consumption for commercial reasons; parts of slaughtered animals which are rejected as unfit for human consumption but are not affected by any sign of a communicable disease; blood obtained from animals declared fit for human consumption. Animal by-products derived from the production of products intended for human consumption, including degreased bones and greaves (Cargill et al., 2004).

Materials belonging to category 3 can be directly disposed of as waste by incineration in an approved incineration installation, also used as raw material for pet food production, and processed by a specific method in an approved processing plant, for its utilization as biogas source by composting. While for materials belonging to category 1 and 2 the safest alternative

is the thermal treatment that ensures to destroy potential bovine spongiform encephalopathy (BSE) pathogens in high-temperature processes.

The meat-bone meal (MBM) and cattle bone ashes (CBA), used in this research are residues belonging to category 3. Nowadays, MBM in some cases is disposed of as a waste due to the severely limited technological options for its use and recovery, also related to the demand for this type of by-product. The only possible alternative is the thermal treatment which ensures to destroy potential BSE pathogens in high-temperature processes (Deydier et al., 2005).

MBM is an easily flammable fuel due to its high calorific power. The energy recovery from Incineration of MBM is seen as useful by the cement industry because the thermal process where cement clinker is burnt has right conditions for complete combustion, and at the same time, substitute primary fossil fuels have environmental and economic advantages (Conesa et al., 2003).

In this sense, this type of waste was investigated to the obtainment of active glasses (Barbieri et al., 2014), to development of glass-ceramics (Cicek et al., 2014), soil applications (Mondini et al., 2008), as a fertilizer (Jeng et al., 2006), as a pore-forming agent and in LWA_S for agronomic porpoises (Farias et al., 2017a).

CBA is a by-product derived from the calcination of cattle bone fragments derivate form the processing and production of meat products. Several authors studied the cattle bone ashes (CBA) as porous hydroxyapatite source for bio-ceramics development (Champion, 2013; Joschek et al., 2000; Khoo et al., 2015), as fertilizing agent for cultivated soils (Mondini et al., 2008; Ylivainio et al., 2008) and active glass production (Barbieri et al., 2014).

MBM and CBA could be used as raw materials for animal feeding or disposed of as waste, classify as EWC 02-02-02 (animal-tissue waste. Wastes from the preparation and processing of meat, fish and other foods of animal origin), depending on the market for that waste.

A.5.3. CEREAL PRODUCTION

Corn is one of the most consumed cereals in the world. In the EU 60,279.00, MT (megatons) was produced in 2016, in fourth place after the United States, China, and Brazil (IndexMundi, 2016).

In 2016 Italy amounts production of grain maize and corn cob mix was 6,840.00 thousand tonnes and for Spain 4,070.00 thousand tonnes being Italia in the fife place followed by Spain on the European least of production (EUROSTAT, 2017).

Corn cob, is the central core of ear maize, is the part of the ear on which the kernels grow. When harvesting the corn, the corn cob may be collected as part of the ear or could also leave as part of the corn stover in the field.

The corn cob has many applications for its high calorific value, high liquid absorption capacity, wear resistance, discrete abrasiveness, and high elasticity, and has been studied as a building material for its insulating properties and for lightweight concrete for non-structural applications (Pinto et al., 2012, 2011), as an alternative fuels (Allesina et al., 2015), as adsorbent for sequestering heavy metal ions (Sud et al., 2008), lightweight concrete for non-structural applications (Pinto et al., 2012), thermal insulation material (Pinto et al., 2011), as a pore-forming agent to developed sustainable ceramic bricks (Njeumen Nkayem et al., 2016), and in LWA_S for agronomic porpoises (Farias et al., 2017a).

A.5.4. GLASS MANUFACTURING/RECOVERY

Latest industry data, published by the European Container Glass Federation (FEVE), show that the EU28 average recycling rate for glass packaging hits the 73% mark for the first time in 2015. Over 25 billion glass containers continue to be recycled in a closed loop making glass a model of the circular economy. Sweden, Belgium, Luxembourg, Austria, and Germany continue to be the best performers. Italy, the Netherlands, and Malta improved in previous years. However, it is Eastern Europe that is catching up as the industry begins to address the glass recycling challenges in these countries. The increased recycling efforts make Europe the continent with the highest glass recycling rates in the world (European Container Glass Federation., 2015).

The glass material used in the research, Glassy Sand® (GS) is a claimed glass derived from the secondary treatment of glass cullet from municipal recollection. It is not classified as a waste; it is a commercial product. Specific treatments are performed on the starting glass cullet to obtain very low impurities (<0.068%), hence the fraction non-suitable for glassworks is submitted to a successive treatment to obtain two ends of waste: GS, with characteristics for glassworks and ceramics sand, usually used in ceramic industry.

A.6. CLAY MINERALS

Clay minerals have a high-water absorption capacity, due to the negatively charged clay particles, attract the positive dipole of the water molecule which may expand the double clay lattice structure substantially (Earthlok, n.d.). The presence of unbalanced electrical charges of clay grains on the surface, with positive and negatively charged ions, attracting the oppositely

charged ions, are capable of dissolving plant nutrients (allow cation exchange, therefore nutrients mobility).

Clay minerals also can draw water molecules. This attraction surface phenomenon is called adsorption, different from absorption due to the ions and water is not attracted inside the clay grains (Oakton, n.d.).

They are found most often in shales, the most common type of sedimentary rock, in cool, dry, humid or temperate climates, clay minerals are relatively stable and an essential component of soil.

One of the main characteristics of clay minerals is that when are mixed with an appropriate amount of water provide the material a deformation capacity (plasticity) under the action of external pressure and retain the shape after the applied force is removed (J. K. Mitchell, 1993).

The development of X-ray diffraction techniques and the subsequent improvement of microscopic and thermal procedures allowed to establish that clays are composed of few groups of crystalline minerals types and related to the SiO_2 ratio.

Clay minerals are phyllosilicates layer that usually formed as products of chemical weathering of other silicate minerals at the earth's surface. Composed mostly of hydrous-layer silicates of aluminum, occasionally containing magnesium (Mg), iron (Fe) potassium (K) and calcium (Ca). The hydrated aluminum silicates with a reticulated and layered structure (formula of type $xAl_2O_3 \cdot ySiO_2 \cdot zH_2O$) which are divided into various classes, each characterized by its reticular structure. In the clays, there are also hydrated oxides such as hydrated silica ($SiO_2 \cdot nH_2O$), hydrated alumina ($Al_2O_3 \cdot nH_2O$) and ferric oxide hydrate ($Fe_2O_3 \cdot nH_2O$). All these compounds confer the plasticity properties (Italiana, 1993).

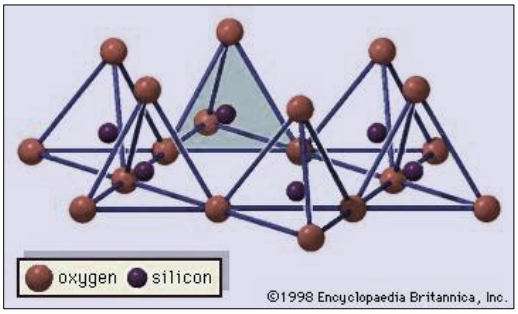

Figure A.5.1. Single silica tetrahedron (shaded) and the sheet structure of silica tetrahedrons arranged in a hexagonal network (Source: Encyclopædia Britannica, Inc.)

The structure at the base of these minerals is the tetrahedron, formed by a silicon atom surrounded by four oxygen atoms (Figure A.5.1). The tetrahedra are connected in hexagonal rings that together form the tetrahedral sheet. Another layer usually has as a structural motif of the octahedra formed by cations of aluminum or magnesium in the center, surrounded by hydroxide ions (OH). Also, the octahedra are connected to each other in hexagonal rings that together form the octahedral sheet (Figure A.5.2). From the superimposition of tetrahedral and octahedral layers, the "package" is obtained, which can repeat an indefinite number of times. The plasticity increases together with the water content; once a certain limit has been overcome, the mixture becomes fluid and flows due to its weight alone. During the firing phase, the plasticity properties are gradually lost as the temperature rises, around 600/700°C, beyond these values there is the decomposition of the hydrated silicates (deoxydrilation).

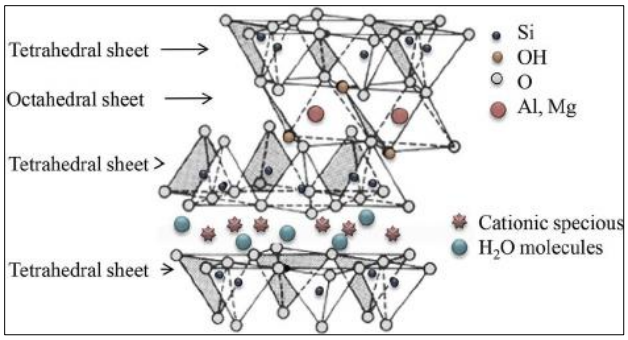

Figure A.5.2. Clay mineral and two tetrahedral between one octahedral sheet (Ghadiri et al., 2015).

The industrial applications of clays lie in their physical-chemical properties. These properties derived, mainly from:

- The small particle size (less than 2.00 µm).
- The laminar morphology (phyllosilicates).
- Isomorphic substitutions, the appearance of charges in the sheets and the presence of weakly bound cations in the interlaminar space.

As a consequence of these factors, they have a high active surface area, with unsaturated bonds. For this reason, they can interact with very diverse substances, especially polar compounds, so they have plastic behavior in clay-water mixtures with a high solid/liquid ratio with swelling behavior.

On the other hand, the charge in the sheets is compensated with the entrance in the interlaminar space of cations weakly bound and with variable state of hydration, which can be easily exchanged by contacting the clay with a saturated solution with other cations. This property is known as cation exchange capacity and is also the basis of many industrial applications.

The absorption capacity is directly related to the specific surface and porosity, related to two types of processes: absorption (physical processes such as retention by capillarity) and adsorption (when there is a chemical interaction between the adsorbent, clay, and adsorbed liquid or gas, adsorbate).

The hydration and dehydration of the interlaminar space are characteristic properties, whose importance is crucial in the different industrial uses. Although hydration and dehydration occur regardless of the type of cation exchange, the degree of hydration is linked to the nature of the interlaminar cation and the loading of the sheet. The absorption of water in the interlaminar space results in the separation of the sheets resulting in swelling. This process depends on the balance between the cation-sheet electrostatic attraction and the hydration energy of the cation.

The clays are eminently plastic. This property is because the water forms a coating on the sheet particles, producing a lubricating effect that facilitates the sliding of some particles over others when an effort is exerted on them. The high plasticity of the clays is a consequence, of its laminar morphology, extremely small particle size (high surface area) and high swelling capacity.

Ceramic pastes are usually composed of three types of raw materials: plastics, antiplastic (or degreasing) and flux. The plastic component is always clay. Clays are constituted mostly by quartz, which acts as a refractory material, and potassium feldspar, as a flux material, since it is transformed into the glass when the ceramic mixture is subject to high temperature, joining the refractory components (García Romero and Suárez Barrios, 2004).

The red clays, according to their flux capacity, can be classified as flux and refractory. The fluxes can be subdivided concerning their content carbonates content. Those with low carbonate content are usually used in single firing pavements, while those with medium and high contents are used in single firing porous coatings. Red refractory clays are often used in the manufacture of extruded pavements.

Nowadays, commercial clay minerals, use as industrial raw material, are among the most important mineral resources, both for the volume exploited and the production value. 90% of the production is dedicated, preferably to the manufacture of construction materials and aggregates. Only 10% is dedicated to other industrial uses (i.e., paper making, rubber, paints, absorbents, bleaches, demolition sands, chemical and pharmaceutical products, agriculture).

During the sintering stage, various transformations occur and are interesting to analyze the general behavior of clays, to understand its technical parameters. This changes can be summarized as it follows (Mattone and Storia, n.d.):

- Loss of residual free water and that absorbed on particles (up to 200°C).
- Oxidation of organic matter, crystalline bound rupture, and formation of a mixture of silica (SiO_2) and alumina (Al_2O_3) (around 700°C).
- Decarbonisation of limestone ($CaCO_3 \rightarrow CaO + CO_2$) and formation of a silica and alumina compound called at 800-900°C.
- Formation of a liquid phase that favors the formation of Mullite (between 900 and 1100°C). Over 1400°C there is an excessive reduction in viscosity of the liquid phase with a consequent breaking of the piece under the influence of its weight.

The clay minerals used in this research poses different characteristics derivated from own origin and extraction. Below are described the characteristics and origin of them.

A.6.1. SPANISH CLAY MINERALS

Black, white, yellow and red ES clay are four of the five clay minerals used in this research provided for Arcillas Bailen S.L., Jaen Province, Spain.

The ceramic industry of Bailén is based, fundamentally, on the manufacture of bricks and perforated blocks. The ceramic cluster in Bailen (Jaen) produces around 20% of Spanish national production of structural ceramics. As it was described before, the raw materials used by ceramic industry in Bailen has traditionally used four types of clay, usually consist of mixtures of carbonates clays (white, yellow and black) from the marine sediments from Neogene, that filled the Guadalquivir Basin and Triassic red clays from de Iberian Massif (Figure A.5.1.1) (R J Galán-Arboledas et al., 2013).

The main components of these shales are illite, kaolinite, quartz, and feldspars, with lesser amounts of chlorite, pyrophyllite, paragonite and chlorite/vermiculite mixed-layers. The

materials contain high amounts of alumina (17-21 %) and iron oxide over a wide range (1.33-9.21 %). The grain-size analysis shows that more than 90% is <20 μm. Most of these materials are only potentially suitable for shaping by pressing, due to the low plasticity related to the high quartz and feldspar content (Vázquez, 2004; Vázquez et al., 2003).

These clay mixtures are in general only adequate for the production of red porous ceramics for masonry (Gonzalez et al., 1998). In this research is intended to give this clay mineral other alternative uses in the development of sustainable materials.

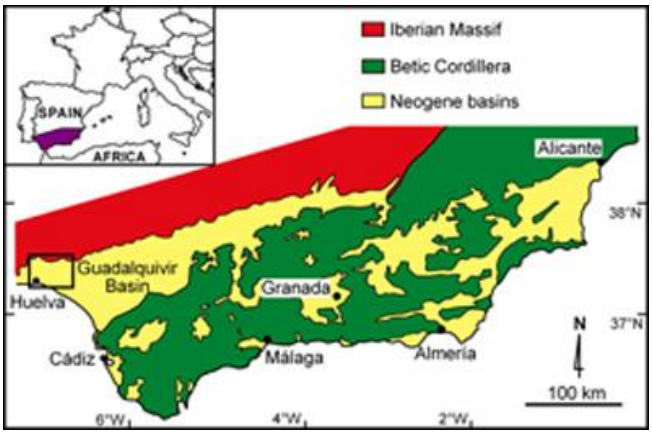

Figure A.5.1.1. Location of Guadalquivir basin (south of Spain) (Perez, 2014).

The white and red ES clays do not have an application by themselves since the plasticity values of these clays are outside the maximum limits recommended for extrusion forming.

A.6.2. ITALIAN CLAY MINERALS

Sassuolo area (northern Italy) is the most extensive tile making district in the world, which has practically served over the past years as an industrial scale laboratory for assessing the technological properties of clays and their suitability for the production of wall and floor tiles. Overall, approximately 2 million ton/year of clay materials are used in colored bodies: marly clays for wall tiles (majolica, 'birapida', 'monoporosa') and red shales for both floor tiles (glazed red stoneware) and wall tiles ('monoporosa') (Dondi, 1999).

The red clay IT used for the alternative development of LWA_S for agronomic purposes, comes from the extractive pole Nº20 "Roncobotto - Le Salde" of Samone under the municipal district of Zocca (MO), corresponding to the geological formation Eocene-Miocene Epi-Ligurian sequences (Figure A.5.2.1.(4)).

The surface of the quarry measures 1,075,000.00 m^3, which corresponds to a total theoretical volume of material equal to 4,000,000.00 m^3 of which 1,500,000.00 m^3 of clay material were assessed in 2000.

From a geological point of view, the clayey area is due to the formation of the Varicolor Clays, created in the Apennine chain in the sedimentary succession called Epiligure, set up starting from the Middle Eocene on the already tectonized Ligurian units (Zanzucchi, 1975).

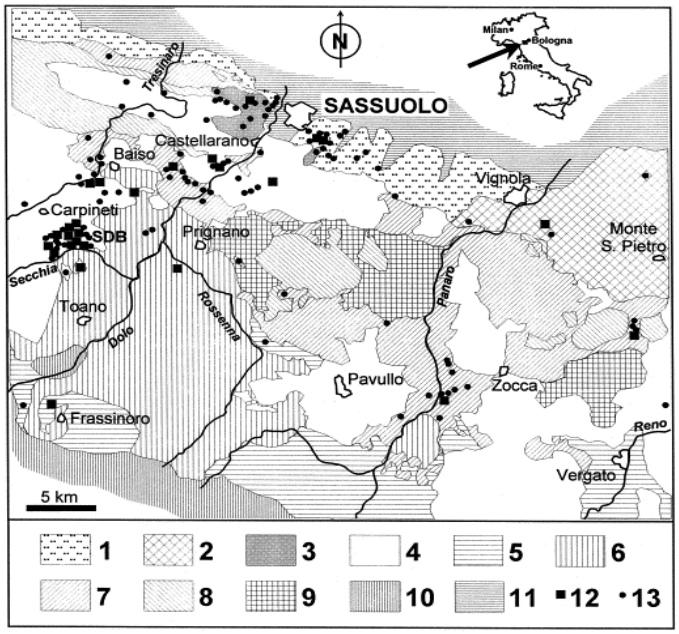

Figure A.5.2.1. Geological map of the northern Apennines around the Sassuolo Ceramic District. Apenninic margin (Pliocene-Pleistocene) Fm (1), Marano Fm (2) and Rio del Petrolio Fm (3). Eocene-Miocene Epi-Ligurian sequences (4). Ligurian units (Cretaceous-Eocene) (5), Monghidoro Unit and Val Rossenna melange (6), Basal Complex Ligurid II (7), Cassio Unit (8), Coscogno tectonic melange (9). Tuscan Nappe (10). Quaternary continental deposits (11). Quarries: active (12) and abandoned (13). SDB: Secchia-Dorgola Basin (Dondi, 1999).

Red IT clay was extracted and provided by "Escavazioni Industriali Baroni s.p.a.", supplier of the Modenese ceramic pole (Campani, 1999). Provides clay and raw materials for use in ceramics, clay for bricks manufacturing and clay suitable for use in the landfill or any other type of processing where the clays can be used.

Figure A.5.2.1. (a) Clay-pit Roncobotto - Le Salde and (b) Red clay (Samone) (Baroni, n.d.).

A.7. CERAMIC INDUSTRY

In 2012, the total waste generated in the EU-28 by all economic activities and households was 2,514 million tons, where 33% corresponds to the construction activity (Eurostat, n.d.), being one of the leading productive activities that more natural and primary raw materials consumed.

The ceramic industry includes the following industrial branches: construction ceramics: bricks, roof tiles, stoneware tiles, floor tiles and refractory materials; fine ceramics: products of pottery, earthenware, fine stoneware, porcelain, electro porcelain and sanitary ware; and technical ceramics.

The first two constitute traditional ceramics, and these products are prepared with virgin raw materials, which can be according to their function, plastic or non-plastic. The first ones are mostly clays. Clay is sediment formed by very fine particles (>50% is <2.00 µm), which when is mixed with water become a plastic material easy to mold, which consolidates by the application of heat. Another feature is that they mostly contain phyllosilicates with a very fine grain size less than 2.00 µm. It also contains associated minerals such as quartz, feldspars, calcite, pyrite, as well as specific associated non-crystalline phases, which may or may not provide plasticity, like organic matter (Galán and Aparicio, 2005).

Within the group of technical ceramic materials, is find light aggregates (LWA_S), which, unlike their counterparts, have a relative density of or less than sand, gravel, and crushed stone.

A.7.1. CERAMIC PRODUCTS AND ENVIRONMENTAL EXTERNALITIES

From the environmental point of view, the extraction of clays causes a deterioration of the landscape and an alteration of the soil surface. The exploitation is carried out in the open, using conventional mechanical means. The conditions of the clay material to be removed varies from one clay pit to another, but, generally, in most of them are less than 15.00 m deep (García

Romero and Suárez Barrios, 2004). Among the most significant environmental impacts is a substantial modification of the topography of the extraction and adjacent areas, erosion of the surface layers due to lack of vegetation and morphological change of the stratum, soil sterility, emissions of particulate material into the atmosphere, by blasting of the stratum surface and biomass.

The factors that control in a decisive way the emissions in the elaboration of ceramic materials are:

- The concentration of the polluting elements in the raw material, i.e., the risk of contamination will be higher for higher contents of fluorine, chlorine, and sulfur in the raw materials.
- The quantity of these elements transferred during the industrial thermal treatment. This factor is conditioned by the mineralogical composition, temperature and residence time and type of fuel.

The ceramic raw materials firing implied the destruction of a large number of minerals phases and the formation of new ones with higher mechanical resistance. In this process, the release of volatile elements and compounds can occur, like fluorine (F), chlorine (Cl), boron (B), lead (Pb), bromine (Br), nitrogen oxides (NO_X), and oxides of sulfur (SO_X), among others. In general, is related to the mineralogical phases formations influenced by the preparation of raw material, drying, and sintering processes. Also, these aspects are controlled by the type of ceramic product that is manufactured, e.g., bricks, tiles, porcelain, toilets, refractories (González et al., 1998).

The Cl contents in raw materials are related to the soluble salts percentages (especially balite) and minerals in the clay. The S contents are conditioned by the presence of pyrite, gypsum and organic matter. The sintering conditions and the type of fuel used influence the percentage of SOX emission and S content of the finished products.

The studies developed in Italy, have allowed obtaining reliable results, showing a relationship between the F contents and the different geological formations, from the raw materials used in the brick industry. The concentrations vary between 500.00 and 1250.00 ppm (0.05-0.125%) with an average value of 860.00 ppm (B. Fabbri, 1995).

In Spain, in Bailen area, Triassic materials have F contents between 800.00-1000.00 ppm, while those of the Miocene 500.00 and 1200.00 ppm, closely related to the percentage in illite.

Miocene materials and its F content, are also influenced by apatite content (fluorapatite). The analysis of these data reveals the fluctuation of the concentration of F in the raw materials used in the different ceramics industries.

The raw materials used in Bailen have very variable percentages of S within the same formation, with concentrations ranging between 80.00 and 2360.00 ppm. The content of S in the tertiary clays are very low in the order of 60.00 ppm (A.Vieira, C. Gomes, F. Rocha, 1996; F. Rocha, A. Vieira, 1997).

Regarding Cl content, data from Italy have extreme values between 10.00 and 1000.00 ppm; its average distribution is 95.00 ppm. The lowest concentrations correspond to the Oligocene, Flolocene and Pleistocene clays, and the highest to the Pilocenas clays.

The S content in Italian clays varies widely, reaching up to 6000.00 ppm, being more abundant the clays with low S content, depending on the geological ages. The clays of the Holocene and Pleistocene are those that present lower contents in S and those of the Pliocene that have higher percentages.

A.7.2. OVERVIEW IN THE SUBSTITUTION OF ALTERNATIVE RAW MATERIALS

Among construction materials, traditional clay-based materials are heterogeneous products that can accommodate waste or by-products without significant modifications to the production process or the final products' properties (Dondi et al., 1997). The ceramic industry is familiarized with the introduction of other materials to the ceramic matrix. Defatting or non-plastic raw material is defined as the material that is included in the ceramic mixture that does not provide plasticity. These raw materials are used to optimize the dimensional changes that take place during the sintering process, as well as to improve the shrinkage of drying, since they usually increase the pore size and, therefore, the permeability of the material, facilitating drying and degassing during preheating. The degreasers commonly used by the structural ceramic sector are materials such as quartz, feldspars, granite rocks, sands, reprocessed material from fired clay (chamotte), granulated slag, ground shells (Vicente et al., 2012).

The energy saving associated with the addition of degreasers to a ceramic paste lies in the inert nature of these, in most cases, not requiring energy consumption for drying and sintering (Vicente et al., 2012).

The extend research focuses on the development of clay−waste mixtures to obtain sustainable ceramic materials, have shown benefits, describe as it follows:

- Savings of natural and primary resources (recovery matter in alternative uses).
- Environmental impact reduction (e.g., landfills disposal, unpleasant odor, natural land transformation).
- Saving energy consumption by alternative fuels valorization.
- Positive effects on the process, improved final product quality, and reduced cost of the final product due to the use of a waste additive in the process.
- Reduced amounts of waste to incineration or landfill treatment.

All these reasons are valid justifications to explore the possibilities of using waste materials beneficially. There are, however, limitations as to what is possible, for a variety of reasons. For example, use of waste is limited by the unacceptable release of inorganic or organic contaminants in the production processes, use and in its recycling or end-of-life stage (Alonso-Santurde et al., 2010).

In particular ceramic industry presents manufacture processes especially suitable for waste valorization, as much if it is an energy recovery as a material recovery of waste itself. A review of main experiences in waste valorization into ceramics allows identifying two groups of waste: organic ones or biomass and those having an inorganic nature (Dondi et al., 1997; S. Raut et al., 2011).

Organic wastes release their calorific value during the combustion produced in the firing process to manufacture ceramics, giving rise to lower energetic costs during manufacturing but to stricter control of gas emissions. Also, this combustion produces a porous microstructure in the fired ceramic products (Rajput et al., 2012; S. P. Raut et al., 2011), diminishing their density and likely improving their ability for thermal insulation (de la Casa et al., 2009; García-Ten et al., 2005; Martínez et al., 2012; Monteiro et al., 2008).

On the other hand, inorganic waste mostly formed by SiO_2 - Al_2O_3 - CaO and usually, some other minor metallic oxides, show a composition similar to the ceramic raw materials. Therefore, these wastes can constitute the matrix of ceramic materials due to the formation of crystalline phases or to verification during the firing process and, inertization of wastes. The valorization of these inorganic waste allows raw materials be saving and, sometimes, lower energy consumption to obtain optimized material properties (R J Galán-Arboledas et al., 2013).

In this sense, the ceramic industry presents manufacturing processes and equipment that makes the incorporation of waste, technological nutrients, especially feasible, generating a modernization in the supply of products for a growing market of sustainable products and eco-labeling processes.

Cement and ceramics are the materials best suited for achieving the inertization and neutralization of the waste by encapsulating it in the matrix (Couto D.M., Ringuedé A., Silva R.F., Labrincha J.A., 2003; Eliche-Quesada et al., 2011). In this way the waste ceases to be a problem for the environment and, in some cases, even this ratio gives manufactured materials with superior performance than their commercial counterpart (S. P. Raut et al., 2011).

Ceramics materials are extendedly studied as an alternative valorization of hazardous and non-hazardous waste and by-products for the production of sustainable construction materials to improve building energy savings (Sadineni et al., 2011), due to the need of finding innovative ways in substitution of landfill disposal. The study and recovery of these wastes is a challenge and an alternative that represents a future course of action. Therefore, it is considered that the ceramic industry has a structure to absorb this waste, without most changing its industrial process, without causing additional costs. This temperature renders many tips of wastes and at the same time contributes to the fuel requirements to heat the kiln (Bjorklund and Finnveden, 2005; Blengini and Garbarino, 2010; ESCSI, 2007).

The incorporation of residues from the industrial origin in the ceramic matrix for the production of structural ceramics has been well studied. In the case of waste that has hazard pollutants, since it is a thermal treatment system allows confinement within the ceramic structure, like urban sewage sludge (Cusidó et al., 2003; Cusidó and Cremades, 2012; Cusidó and Soriano, 2011; Eliche-Quesada et al., 2011; Martínez-García et al., 2012), ash from biomass incinerator (Andreola et al., 2008; Bories et al., 2014; Garc et al., 2013; Salvo et al., 2015), recycled glass (Cicek et al., 2014; Ducman and Mladenovic, 2002).

The incorporation of agro-food wastes for the elaboration of structural ceramic materials also extendedly studied for its calorific power as an energy source and in the ceramic matrix as a pore-forming agent. Like paper sludge or paper waste (Cusidó and Cremades, 2012; González-Corrochano et al., 2009), urban sewage sludge spent (Cusidó et al., 2003), coffee grounds (Eliche-Quesada et al., 2011; Muñoz Velasco et al., 2015), corn cob (Njeumen Nkayem et al., 2016), vine shoot (Velasco et al., 2015), olive oil pommes (Cotes-Palomino, M.T.; Martínez-García, C.; Iglesias-Godino, F.J.; Eliche-Quesada, D.; Pérez-Latorre, F.J.; Calero de Hoces, F.M.;

Corpas-Iglesias, 2016; Ronda et al., 2015), spent diatomaceous earth (Galán-Arboledas et al., 2017; Martínez-García et al., 2015), recycle paper mill residue and rice husk ash (Chiang et al., 2009; Raut et al., 2013), cotton waste (Rajput et al., 2012), grapes and cherries seeds (Barbieri et al., 2013).

The result obtained by these investigations conclude that the addition of organic material favors the decrease in the bulk density, using the increased porosity, related to the oxidation of the organic matter, and the improvement of thermal conductivity, related to the insulation capacity of the new material.

The environmental benefit of the association of clays minerals and organic waste for the preparation of ceramic materials is manifested in the energy input by the calorific power from combustion. Also, represent an alternative with better environmental benefits in the stabilization/inserting within the internal structure of the ceramic through the valorization of waste.

A.8. LWA_S INDUSTRIAL PROCESS AND USES.

Most materials are to some extent porous: indeed, it is quite difficult to find or prepare a genuinely non-porous solid. It is well known that physical properties (density, thermal conductivity, and mechanical strength), dependent all of the pore structure of a solid and the control of porosity is of great industrial importance (Rouquerol et al., 1994).

LWA_S are stone-like end materials, suitable for their use in a wide range of concrete products and geotechnical applications. Aggregates can be categorizing according to its source, unit weight, and size. According to its source, aggregates can be classified as it follows (Caffo, 2008):

Natural aggregates. (i) Consists in rock fragments that can be used in their natural state, or after mechanical processing. (ii) Natural aggregate deposits (pit-run gravel). (iii) Natural gravel usually dug or dredged from a pit, river, lake, or seabed.

Crushed rock aggregates. (i) Crushed aggregate, quarried or excavated stone that has been crushed and separated to require particle size. (ii) The particles of crushed aggregate are wholly crushed (proper compaction and load-bearing properties). (iii) Crushed stone, particularly suitable for use in streets, roads and other areas exposed to traffic.

Recycled Aggregates. Recycled aggregate derived from construction and demolition waste. Applications of recycled aggregates without any processing include: bulk fills, bank protection,

base or fill for drainage structure, road construction, noise barriers, and embankments. In contrast, applications of new concrete with recycled aggregates includes pavements, shoulders, median barriers, sidewalks, curbs and gutters, bridge foundations, concrete base and bituminous concrete (pavements).

Artificial aggregates. Produced from clays mixtures, artificial cinders, foamed slag, expanded shales and slate, manufactured mostly to reduce dead loads and improve fire ratings of concrete in numerous construction projects; lightweight concrete masonry approximately 20.00% lighter, easier to install and transport; geotechnical applications, lightweight backfill reduces the loads on poor subsoils, thus minimizing settlement, behind retaining walls exerts lateral pressures in comparison with sand, stone or clay backfill, e.g., bridge abutments, fill for road construction, segmental retaining walls and lightweight fill for building structures; to produce lightweight soils for rooftop gardens and cultivation suppliers.

Natural raw materials suitable for manufacturing lightweight mineral granules are pumice, perlite, vermiculite, expandable clay, and slate. The raw materials, except pumice, first undergo different conditioning processes to bring them into the desired initial stage (Mueller et al., 2008).

Artificial LWA_S has a unit weight ranging between 0.67 and 2.10 g/cm^3, showing properties of high porosity, low bulk density, high water absorption, low compressive strength, and low elastic modulus (Huang et al., 2007).

When the thermal treatment of LWA_S is performed, the clay material receives a thermal shock that caused the sintering of the grains and changes in their physical properties like density and porosity, reducing the production costs (Bettzieche, H., Schops, W., Hohmann, 2000).

The high-temperature heating treatment (1100-1400^{o}C for 50-70 minutes) occur in the rotary kiln, where ceramic material receives a thermal shock, causing the formation of a hard vitrified layer on the surface. This occurs before the ceramization of the internal structure, preventing the gases and vapors (usually CO_2, CO, H_2O, O_2 or SO_2, among others) from the decomposition of organic matter and some mineral phases, run out. In this way the vitrification of the external skin will prevent the gases to escape, forcing the material to swell (pyroclastic behavior) generating the characteristic porous structure (Toth and Csaky, 1989). The aggregate can increase approximately five times its original size.

In other words, the cellular structure of the particles is developed by the heating of specific raw materials above the glass transition temperature. Where the gases generated by combustion cause the material to deform and expand, plastic behavior, which allows the expansion of the material permanently because once it is removed, the thermal load is not fully recovered, resulting in an LWA_S.

The organic fraction present in the clay minerals which is subjected to a pyrolysis process, derived from the heating and degradation of organic matter in the absence of oxygen. In these circumstances, the organic fraction it transforms partially to a gas phase. A part of the gases and vapors are retained inside the structure, which helps to inflate the material, the remaining gases go out to the kiln. In the interior, a carbon fraction (coke) of black color remains.

The LWA_S contain a relatively uniform system of pores having a size range of 5.00 to 300.00 µm, wrapped in a resistant glass cover, which depends on the thermal cycle to which it has been subjected.

This external porous structure is readily permeable, which saturates within the first few hours of moisture exposure. However, the internal porous structure saturates much more slowly. The latter will depend on the type of internal porosity, the relationship between the interconnected or non-interconnected porosity, and for this reason may not saturate after a long time of immersion (Styron, 1988). The porous structure (open and close porosity) is one of the determining factors which influences the chemical and physical reactivity interface with gases and fluids (Rouquerol et al., 1994), as well as the pH and the electrical conductivity, which for the LWA_S are assumed to be inert.

In a simplified version, the manufacturing process of LWA_S has the same steps that the structural ceramics, with the substantial difference in the processes of shaped (conformation) and thermal treatment that occur in a pelletizers and a rotary furnace respectively (Image A.7.1).

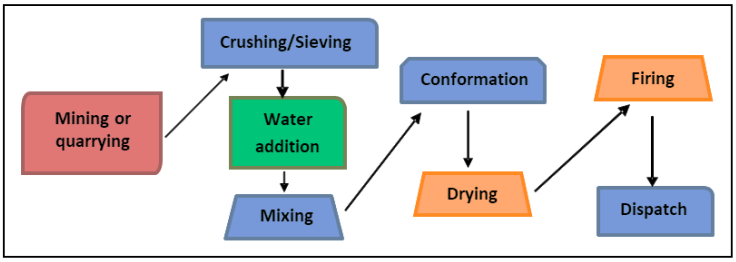

Image A.7.1. Process flow diagram for lightweight aggregate manufacturing.

Depending on the design of the rotary furnace, it has a certain degree of inclination of 3.00-6.00% of the horizontal plane. This favors the advance of the material through the furnace and the generation of high temperatures in the middle zone. The rotation speed will depend on the inclination degree but will be in the order of 1.50-2.50 rpm, corresponding to a tangential velocity of 0.30-0.90 m/sec (U.C. Cubaud, 1968).

The inclination facilitates the material loading and the output of the gas emissions (upper part of the furnace). By rotating it, the material descends to reach the combustion zone where temperatures of 1100-1400ºC can be achieved. The LWA_S exit through the lower region of the furnace where the flame is generated, using the combustion of the gas or fuel.

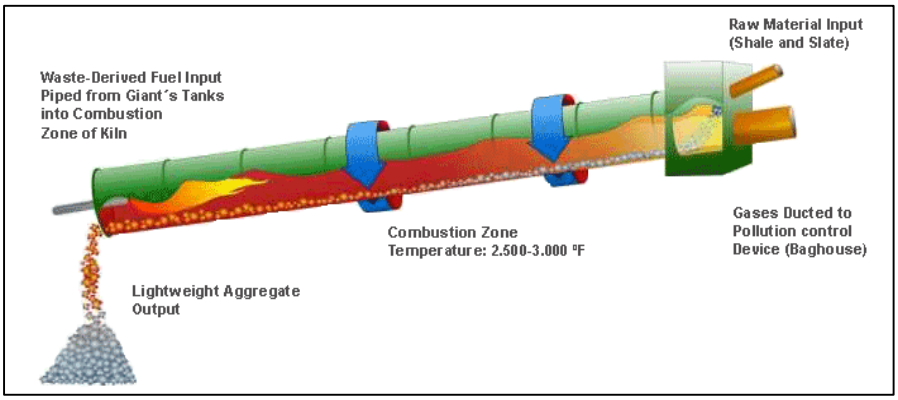

Image A.7.2. Rotary kiln for LWA_S production (Valderrivas, n.d.).

Regarding emissions from the production of lightweight aggregate consist primarily of particulate matter (PM), during clay extraction, processing (powder) and emitted by the rotary kilns, clinker coolers, crushing, screening, and material transfer and stockpiling operations. Pollutants emitted in the combustion carried out in rotary kilns include sulfur oxides (SO_X), nitrogen oxides (NO_X), carbon monoxide (CO), carbon dioxide (CO_2), and VOC's. Chromium (Cr), lead (Pb), and chlorides (Cl^-) also are emitted from the kilns. Other metals, including aluminum (Al), copper (Co), manganese (Mn), vanadium (V), and zinc (Zn), are emitted in trace amounts (Fallis, 2013). This fact mainly depends on the fossil fuels used by the furnace (coke, fuel oil, natural gas, propane, kerosene), the temperature of the thermal treatment and the raw materials used (Fallis, 2013).

Once the thermal treatment process is finished, the material is screened to obtain the desired granulometry according to the product specifications and its application.

LWA_S present a great diversity of applications. In the construction industry, it is widely used in the production of lightweight concrete, blocks and prefabricated elements (panels, partitions, bricks and light tiles) with a bulk density of less than 1200.00 kg/m³. In turn, it is used in for structural foundations, retaining walls. This material can reduce the pressure by 75.00% compared to conventional materials. Increases the stability of the land while reducing settlements and deformation, as it favors the drainage of surface and groundwater.

This material is also used in water treatment facilities for filtration, purification in municipal wastewater, drinking water, as well as in other filtering processes.

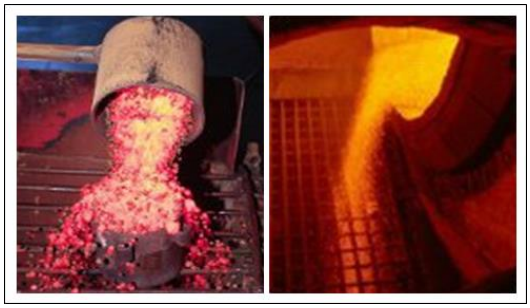

Image A.7.3. LWA_S discharge from the rotary kiln (Weber Saint-Gobain, n.d.).

A.8.1. LWA_S AND WASTE VALORIZATION

LWA_S have been attracting in the last decade a renovated attention driven by the increasing demand for lightweight structural materials (primarily concrete) and envelope materials with improved thermal, thermo-hygrometric and acoustic performances (Vašina et al., 2006), like lightweight mortars and external thermal insulation systems (Dondi et al., 2016; Elsharief et al., 2005).

Such interest is further fed by the growing concern on sustainability, which is addressing many studies on the use of urban and industrial wastes and by-products as possible technical nutrients for the development of LWA_S. The number of papers on this matter overpassed 150, and the publication rate has been increased from 1 to 2 papers per year in the 1990`s to the annual from 15.00-20.00 papers of the latest years (Dondi et al., 2016). Related to a wide range of waste and by-products were used as a replacement of clay minerals for sustainable LWA_S. Represent an alternative use as pore-forming for a full range of waste and by-products to produce sustainable materials (agro-food industry, municipal solid wastes, sediments from water treatment plants and dredging mud, residues from coal power plants, mining and quarrying, mineral transformation and metallurgical industry). Also, landfill disposal costs

continue to increase, also the costs of extracting natural raw materials provided from increasingly distant sites.

From thermal destruction, the process is similar. The gaseous compounds are wholly oxidized and leaving the ceramic matrix as CO_2 and H_2O, releasing their calorific power (exothermic reaction) during the combustion in the firing process, reducing energy inputs. On the other hand, inorganic waste shows a composition of clay minerals. Therefore, these wastes can constitute the matrix of ceramic materials due to the formation of new crystalline phases during the firing process and, inertization of wastes.

Producing LWA_S with less sintering temperatures (50-500^oC) (Arioz et al., 2008; Cultrone et al., 2004), means the possibility of producing materials with less environmental impact, reducing the emission of greenhouse gases to the atmosphere, boosting the local economy by offering innovative and eco-label materials.

LWA_S have been attracting in the last decade a renovated attention driven by the increasing demand for lightweight structural materials and envelope materials with improved thermal, thermo-hygrometric and acoustic performances (Hassanpour et al., 2012). The research based on the introduction of different waste in the ceramic matrix for the production of LWA_S present an extensive range of characteristics and results. As well as studies related to LWA_S base on the collection and recycling of construction and demolition waste (C&DW) (Blengini and Garbarino, 2010)

Furthermore, the reduction on the sintering temperature associated to the use of pore forming agents, was already widely investigated, reducing the sintering temperatures in batwing 50-400^oC (Farias et al., 2017a, 2017b; Martínez-García et al., 2015) in comparison with commercial LWA_S, also augmented by a cold-bonding (Gunning et al., 2009).

As a consequence, waste materials exhibit in most cases a different technological behavior, particularly a peculiar expansion behavior, respect to the present industrial batches utilized to produce LWA_S (Aineto, 2006; González-Corrochano et al., 2014). Thus, the use of wastes may impose substantial adjustments to the manufacturing process to get the desired technical performance of LWA_S. These changes mainly concern the shaping and firing processes, because of the different plasticity and thermal behavior of unconventional raw materials (González-Corrochano et al., 2014, 2012; Kaz'mina, 2010; Kim et al., 2010; Korat et al., 2013; Pinto et al., 2005; Zorić et al., 2012). From the environmental point of view, the total or partial change of virgin raw materials such as clays for waste destined to landfills or incineration, without

discussion is positive for the environment. From the life cycle analysis perspective, these sustainable materials can present certain environmental disadvantages in the sintering process, through the emission of gases into the atmosphere and during its use, generating leaching that can contain hazardous pollutants.

In general in combustion processes of solids, two important steps are present (Conesa et al., 2003):

- Pyrolysis stage, in which the solid feed undergoes reactions to yield volatiles (gases and tars) and a solid char fraction.
- Combustion stage, in which the char undergoes heterogeneous reactions to yield gaseous products and an inert residue (ash). Pyrolysis and combustion stages may be sequential or contemporary, depending on the feature of the process considered.

Great care should be taken when by using recycled materials to manufacture LWA_S because with different leachability of toxic elements present in the waste materials. Chemicals and physical properties must study to prevent potential risk to the environment due to the mobility of the trace toxic compounds. For that reasons, is essential to provide information on the chemical composition distribution and the potential mobility of metal present in the waste/technical nutrient to be valorized. Such analysis can contribute to a better understanding of whether the recycled LWA_S, which contains toxic elements, poses any harmful effect on the environment (Chang et al., 2007).

For example, in the case of the sewage sludge from municipal wastewater treatment plant, the study over the leachability of toxic elements is largely studied. If sludge's contain quantities of pollutants exceeding certain limits, dangerous leaching can be produced (Mahzuz et al., 2009). The resulting ceramic materials could lead to contamination levels of heavy metals. Hence their use should be carefully regulated from the environmental point of view (Iwata et al., 2004). In short, the parameters that most influence the inerting process, are, in order of importance (Cusidó and Cremades, 2012; Magalhães et al., 2004):

- Clay type
- Relative amount of sludge in the mixture
- Thermal treatment
- The state of agglomeration of the samples. The reaction between sludge and ceramic clays is the dominant mechanism of encapsulation of sludge's (in vitreous phase).

Table A.7.1.1. Literature review for different waste as raw materials for LWA_S manufacture.

Waste/Technical nutrients	Conclusions	Reference
Sewage sludge ash	The presence of larger pores is related to a decrease in the dry particle density values. When the LWA_S lacks the external layer, the water absorption values were dependent on the size and amount of each pore. The neo-formation of Ca-plagioclase and the consumption of quartz improved the compressive strength values.	(Donatello and Cheeseman, 2013)
Waste glass	Lightweight aggregate based on powdered waste glass was prepared by granulating the glass with an expansive agent at 880°C. Apparent density and water absorptions were 0.18 g/m^3 and 11.00 mass percentage, respectively.	(Ducman and Mladenovic, 2002)
Sewage sludge and waste glass powder	Waste glass improved sintering temperature, decreased water absorption and increased failure point loading and bulk density of aggregate. The addition of 30-50% of waste, bulk density lower than 2g/cm^3, water absorption lower than 10% and failure point loading as high as 892.00 N.	(Tuan et al., 2013)
Silica sludge, superfluous clay, waste glass, and residue from the polishing stone	With the addition to clay of polishing residue from granite-like rocks homogeneously porous granules with a density down to 0.42 g/cm^3 were obtained, whereas with the addition to waste silica sludge of polishing residue from granite-like rocks and waste glass with a foaming agent, densities from 0.57-0.82 g/cm^3 were obtained.	(Ducman and Mirtič, 2009)
Washing aggregate sludge, fly ash and spent motor oil	All mixtures showed bloating potential. The products obtained were lightweight aggregates (LWAs) by norm UNE-EN-13055-1. LWAs manufactured with 75%-25% and 50%-50% proportions of washing aggregate sludge: fly ash, heated at different temperatures and dwell times, were expanded LWA_S. They showed the lowest loose bulk density, the lowest dry and apparent particle density, the lowest water absorption, and the highest compressive strength.	(González-Corrochano et al., 2012)
Municipal solid waste incinerator fly ash	The results show that fly ash should be less than 30%. LWA_S with a specific gravity in the range of 0.88/1.69 g/cm^3 and crushing strength as high as 13.43 MPa can be produced. Compressive strengths ranged between 25 and 55 MPa.	(Hwang et al., 2012)
Sewage sludge and coal ash	The results indicated that using sewage sludge enhanced the pyrolysis/volatilization reaction due to its high organic matter content and decreased the bulk density and sintering temperature. Adding coal ash improved the sintering temperature while efficiently reducing the pore size and increasing the compressive strength of the product. Also, heavy metals were fixed inside products generated under these conditions, and the As, Pb, Cd, Cr, Ni, Cu, and Zn concentrations of the leachate were found to be within the limits of China's regulatory requirements.	(Wang et al., 2009; Zorić et al., 2012)

Fly ash	The LWA_S fired at 1150^oC were selected for the production of the light concrete by the following: the highest amount of pores less than 1 lm, the lowest value of interparticle porosity, excellent mechanical properties, and satisfactory value of thermal conductivity (k = 0.0872 W/mK). The aggregates of the above characteristics can provide excellent thermal properties of the structural concrete blocks.	(Zorić et al., 2012)
Stone cutting sludge, plastic wastes, and sepiolite	Three different wastes have been assessed in LWA_S production: granite and marble sludge (COR) as a major component, as well as sepiolite rejections (SEP) and polyethylene-hexene thermoplastics (P) as additives. SEP had great potential as a binder because just 10% of this was able to confer proper plasticity to extrude and shape deficient plasticity samples, such as COR. In general terms, an increase in temperature and time of firing involved greater sintering, which in turn was translated into higher shrinkage, density and compressive strength values, but less porosity and water absorption. Hence the LWAs fired at the lowest temperature and time of firing (1100^oC and 4 min) was the most lightweight.	(Moreno-Maroto et al., 2017a)
Carbon fibre and mineral wastes	Improvements in density and compressive strength, many these LWA_S have presented excellent properties to be used in concrete manufacturing. Furthermore, as FC seems to promote sintering conditions at lower temperatures and dwell times, savings in energy during firing would be another significant advantage. Also noteworthy are the cost savings in raw materials due to the use of wastes as components in the mixtures. This is the first time that carbon fibers are embedded within aggregates, opening a new means for waste utilization and the development of LWA_S for concrete.	(Moreno-Maroto et al., 2017b)
Industrial waste and carbon dioxide	The aggregates produced had a bulk density below 1000 kg/m3 and a high water absorption capacity. The energy intensive firing and sintering processes traditionally required to produce lightweight aggregates can now be augmented by a cold-bonding, low energy method that contributes to the reduction of greenhouse gases to the atmosphere	(Gunning et al., 2009)
Wastes of brewing industry (bagasse, sludge and diatomaceous earth)	The results demonstrate the possibility of using waste from the brewing industry, sludge, bagasse and diatomaceous earth in the production of expanded clay-based aggregates, and of using these aggregates for green roofs. The chemical composition, studied by X-ray diffraction, is appropriate for use in preparation of clay-based products. The organic content of the three wastes used benefits the samples produced as they have lower bulk densities and increased porosity. The results obtained from measuring porosity and thermal imaging reinforce the microstructure observed using SEM: addition of waste rises porosity, a phenomenon more evident in the bagasse. Lower percentages of bagasse increase closed porosity; as the micrographs show rounded and closed pores, high percentages (15%) indicate connected pores resulting in a more open structure with interconnected pores. Also, LCA results have confirmed that adding these wastes into clay body lead to decreasing the firing rejects. The oxidation of organic matter, produces energy savings in the furnace energy requirements, resulting in lower gas emissions to the environment, therefore economic savings.	(Farias et al., 2017b)

Sludge from brewing industry	This study investigated the properties of LWA_S produced with clay and sludge from the brewing industry and sintered at 950°C. The results show that adding brewing industry waste to LWA_S increases the water absorption and porosity of the samples prepared, making the LWA_S less dense and therefore more attractive for use as construction material. However, this increase in water absorption (46% in the samples fabricated with clay only) may have adverse effects when these construction materials are used since they would absorb water that could impede setting of the mortar. We conclude that using wastes in manufacturing LWA_S is a feasible option for principles of sustainable development. Waste from the brewery industry can provide environmental and economical used as a raw material due to higher heating value. The results enable to conclude that there is a linear relationship between the quantities of residue used and increased water absorption.	(Martínez-García et al., 2014)
Wastewater treatment plant, corn cob and meat-bone meal	From the results obtained it was determined that the LWA_S produced with this type of waste/by-product are suitable as substrate/soil for agricultural application. The mixtures $WBSB_{15}$ and $RCSB_{15}$ present physicochemical parameters suitable for their use in agricultural use purposes. The results indicate the potential for manufacturing high-quality, lightweight aggregates, using relatively simple processing. The energy saving, due to the combustion of organic matter inside the furnace and low-temperature sintering (200-400°C lower), reduces the environmental impact produced by the greenhouse gases released into the atmosphere, resulting in the production of sustainable materials. The LWA_S XRD analysis confirmed that the percentages of SB added to different clay mixtures are vaporized by the heat treatment at 1000°C, ensuring its correct treatment/disposal, without forming new crystalline phases in the material. The results showed that the three technological nutrients could be used efficiently as porosity forming agents for the elaboration of lightweight aggregates, representing a saving in the consumption of virgin raw materials and an alternative of the disposal in landfills.	(Farias et al., 2017a)
Paper-pulp	Incorporation of paper pulp sludge was successful as a raw material for lightweight expanded aggregates production. No alteration in the process or product characteristics was observed. The higher water content of the waste demands an initial close control of furnace operation. Monitoring of exhaust gases revealed that this could be a useful recycling procedure, mainly because of the high amount that can process.	(Pinto et al., 2005)
Rice husk ash	In this paper, the preparation of lightweight aggregate (LWA) from rice husk ash (RHA) obtained from a biomass power plant was studied. As-received and ground RHAs were mixed with sodium hydroxide solution (NaOH) and cured to get the hard sodium silicate paste. The samples were then crushed and heated to form LWA. The LWA was tested for acid and base solubility and disintegration in boiling water. The results showed that ground RHA-LWA gave better performances regarding expansion, solubility, and disintegration than the as-received RHA-LWA. However, the decay of LWA_S in boiling water was the main problem. It was found that the incorporation of 2-7% boric acid alleviated this issue and no sign of disintegration was observed. The density of LWA of 0.20-0.40 g/cm^3 was achieved.	(Chindaprasirt et al., 2009)

In the table, A.7.1.1 has listed a summary of the literature review for different waste as raw materials for LWA_S manufacture carried out.

A.8.1.1. CHEMICAL COMPOSITION AND BLOATING BEHAVIOR

Waste-based batches represent a new combination of chemical composition and processing conditions, bringing changes in the physical properties of LWA_S, i.e., water absorption, total porosity, bulk density, and mechanical strength. Along with the chemical composition, important variations may occur, i.e., vitreous phase, pore volume (Dondi et al., 2016; González-Corrochano et al., 2012, 2011).

The formulation of LWA_S can be designed, by plotting the chemical composition of raw materials/waste/by-products into the prediction schemes proposed by Riley (Riley, 1951) and or Cougny (Cougny, 1990), discriminate between ‘‘bloating” and ‘‘non-bloating” behaviour by locating the mixtures in a specific area in a ternary diagram:

- SiO_2-Al_2O_3- (Fe_2O3 + MgO + CaO + Na_2O+K_2O) (Riley, 1951).
- Al_2O_3-Fe_2O_3-(MgO + CaO + Na_2O+ K_2O) (Cougny, 1990).

Clays whose composition is located outside this area; according to Riley (Riley, 1951), they cannot expand thermally, although they can be mixed with additives that promote their expansion (Giraldo Cardenas and Garcia Escobar, 2006).

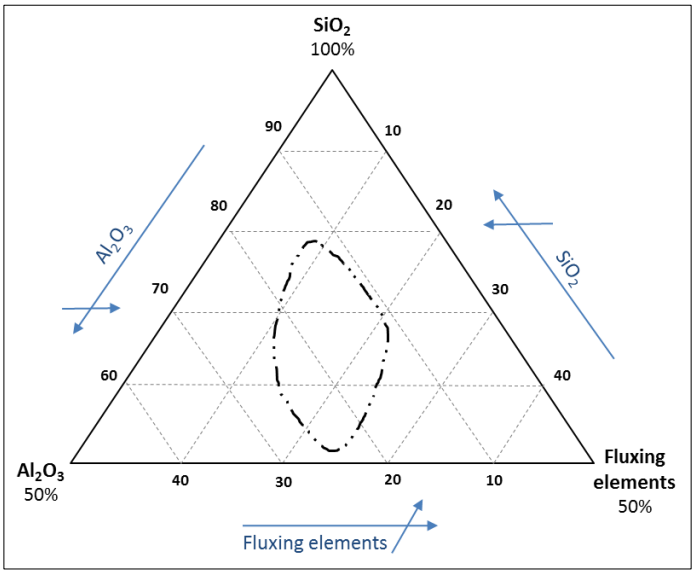

Figure A.7.1.1.1. Composition limits of bloating clays (Riley, 1951).

Although there are currently advanced mineral characterization techniques, simple chemical characterization remains a valid tool in the selection of the raw material/technical nutrients. According to M. Dondi (2017, p. 395): “The Riley’s field soon demonstrated less reliable than it initially seemed, as amendments were proposed already in the 1960s. Despite being known that the bulk chemical composition is not discriminant, as materials ‘‘that expand suitably, that expand inadequately, or that do not expand all fall in these same ranges”, the ‘‘chemical design” is still a popular procedure in the LWA_S batch formulation (Chen et al., 2012; de Gennaro et al., 2008; Dondi et al., 2016; Gonzalez-Corrochano, B.; Alonso-Azcarate, J.; Rodas, 2009; Hung and Hwang, 2007; Kavas et al., 2011; Kim, 2005; Liao and Huang, 2011; Quina et al., 2014; Tang et al., 2011; Wei et al., 2011)”.

However, this criterion is not unique, since it ignores two critical aspects of the phenomenon (Giraldo Cardenas and Garcia Escobar, 2006): the mineralogical composition. The materials that are inside the area defined by Riley correspond to products that can generate the necessary viscosity, but that do not have the possibility of producing gas realize, during thermal treatment. At the same time, does not consider the kinetic aspects of the process. In fact, the main problem lies in obtaining, simultaneously, the generation of the gases responsible for the expansion and partial melting of the surface of the LWA_S.

M. Dondi (“Lightweight aggregates from waste materials: Reappraisal of expansion behavior and prediction schemes for bloating”), purpose an overview of the composition and properties of LWA_S produced from wastes and other unconventional raw materials, aiming to adjust and redefine the expansion behaviour to assess whether the current prediction schemes are suitable for waste-clay minerals for LWA_S formulation. M. Dondi (Dondi et al., 2016) sustains that the waste materials can contain significant amounts of elements usually not considered (trace amounts). These components are P_2O_5, B_2O_3, and heavy metals (Ba, Cr, Mn, Pb, Sr, Zn), e.g., phosphorus is present in relevant quantities in sewage sludge’s (Chiou et al., 2006; Farias et al., 2017a; Mun, 2007) as well as in bagasse from beer production (Eliche-Quesada et al., 2011; Farias et al., 2017b; Martínez-García et al., 2015). Since P_2O_5, B_2O_3, and heavy metals can remarkably influence the technological behavior of LWA_S batches, the original Riley’s and Cougny’s parameters were modified to comprise these additional components:

- SiO_2-Al_2O_3- (Fe_2O3+MgO+CaO+Na_2O+K_2O+B_2O_3+P_2O_5) for (Riley, 1951).
- (Al_2O_3+TiO2)-(Fe_2O_3+CrO2+MnO+PbO+ZnO)-(MgO+CaO+Na_2O+K_2O+SrO+BaO) (Cougny, 1990).

A.8.2. LWA$_S$ AND THEIR USE IN AGRICULTURE

LWA$_S$ are extendedly use in agricultural applications as a growing medium (Molineux et al., 2009) or mixed with other growth media such as soil and peat to improve drainage systems as drainage layer, applicate for horticulture, ornamental crops, aquaponics (fish farming supplies the nutrients for plants grown with hydroponic systems), phyto-purification (wastewater treated using plant-based), hydroponic cultivation (plants, flowers and vegetables), green roofing (Bates et al., 2015; Molineux et al., 2009).

The aggregates become a reservoir for irrigating and controlled release water/fertilizers thereby reducing maintenance costs (management of storm-water and irrigation). Also, prevent soil compaction and provides thermal insulation, preventing overloads structures up to a 30%. Furthermore, it is used on the surface of the substrate to prevent the growth of weeds, improves water retention capacity during periods of drought (retain moisture in the soil), protects the soil from erosion and as well as isolation of roots during frost. The mixture in the soil prevents compaction and a lightening of the substrate (up to 10%) providing a higher oxygen level to promote plant growth. Are considered chemically inert and with neutral pH value, essential properties for all landscaping and horticulture applications. At the same time, its porous structure favors the proliferation of micro-organisms and provides favorable exchange spaces for the growth of plants.

Hydroponic cultivation means crops that grow without land use, substitute by water and nutrients (Image C.7.1). A crop of this type requires approximately 70% less water than traditional cultivation, with a faster rate of growth (about 50%), through the reduced of fertilizers use (Ecopneus, 2015). Hydroponic crops are applied not only on an industrial scale (crops without soil) but also in indoor and outdoor crops of domestic plants (ornamental, flower, fruit, horticultural, grass) and gardening in general.

Image C.7.2.1. LWA_S Hydroponic crops (Hydroponics, n.d.).

The LWA_S suitable for culture medium has a low apparent density of <1200.00 kg/m^3, a pH value in the range of 6.5-8 and electrical conductivity of <2.00 mS/cm (Enzo et al., 2001a; Martínez and Roca, 2011; Nye and Greenland, 1960).

The combination of readily accessible pores, difficult to access pores, providing the material with insulating properties, and the vesicular nature of the LWA_S, makes them such an environmentally useful material for its use as growing media.

This type of materials is suitable for the energetic rehabilitation of buildings through the installation vegetation walls or green roofs, to improve the insulation and generate energy savings in winter/summer, preventing excessive structural loads.

A.8.3. LWA_S FOR GREEN ROOFS

Green roofs involve growing vegetation on rooftops representing a tool that could help to mitigate the pollution effects. Green roofs have the potential to address several of the environmental problems associated with urbanization.

Green roofs partially replace the vegetation that was destroyed when the building was constructed related to the habitats lost at ground level. Green roofs can improve stormwater management, by runoff reduction (Carbone et al., 2014; Villarreal and Bengtsson, 2005), reduce the energy inputs to refrigerated/heated the building/house (Barrio, 1998; Getter et al., 2009), mitigate the urban heat island effect (Wong et al., 2003), help to increase the longevity of roofing membranes structure, reduce noise and air pollution by sequester carbon by means of the vegetation, increase urban biodiversity providing habitat for wildlife (birds and insects) and improve life quality (Berndtsson et al., 2009; Emilsson, T., Berndtsson, J.C., Mattsson, J.E., Rolf, 2007; Getter et al., 2007; Mentens et al., 2006; Rowe, 2011). It can also contribute to the mitigation of the effects of acid rain, studies have shown that rainwater is inertization by passing through the structure of a green roof (Vijayaraghavan et al., 2012). This is an important environmental benefit as compared to a situation where the acidic roof runoff is directly discharged to natural water recipients (Berndtsson et al., 2009).

Also representing a helpful tool, to building energy rehabilitation/transformation. Therefore, green roofs can be an essential element of the energy rehabilitation buildings programs promoted by the Administration with important environmental advantages, e.g., citizen health.

Image A.7.3.1. Thermal imaging. Green roof insulation capacity.

In the quest for the reduction of the "heat island effects" generated by cities, the easiest and most common approach is the replacement of the impermeable non-reflective surfaces such as tar and gravel roofs with vegetation (Image A.7.3.1). The installation of this systems presents an increase of structural load which can easily be reduced by employing expanded LWA_S as part of the growing medium and drainage layer, reducing structural load, as well as, controlled release of irrigating water (water storm management) and fertilizer. In this instance an aggregate with high water absorption is desirable. Germany is the leader regarding numbers of green roofs where they make extensive use of Liapor® and Leca® expanded clay aggregates as raw materials for the growing medium and also for the drainage layer. In horticultural mixtures, nowadays, it is common to use much lighter and ever more absorptive materials such as vermiculite and Styrofoam®. The combination of high water absorption (12.00 to 55.00%) and a relative particle density of 1.20 to 1.50 found in expanded aggregates that make them ideally suited for this use (Elías, 2012a, 2012b; J. P. Ries, 1996).

A green roof means a roof garden or living roof, vegetated roof assembly with engineered layers. The layer's system works together to create a suitable growing environment while maintaining the integrity of the roof structure and keeping the house dry and well insulated (thermal and acoustic). There are five mandatory green roof layers above the waterproof membrane:

- Plants. Restore nature, support biodiversity, keep the roof cool (insulation), and provide oxygen.
- Growing Medium. Creates a suitable growing environment in an extreme rooftop setting. The engineered mix is composed of a mixture of organic matter (plant nutrition) and aggregates materials (support structure and compactness prevention).
- Filter Cloth. Prevents the drains from becoming clogged with the growing media (organic material and soil).

- Drainage layer. Ensures the drainage of excess water preventing a waterlogged system or a significant increase in weight causing overload to the structure.

  At the same time, it acts as a reservoir of water available for plant roots. This is a porous material that in turn is the primary responsibility for acoustic and thermal insulation of the building/house.
- Root Barrier. Protects the roofing membrane from any root penetrations or organic material which could cause decay.

Optional layers include a membrane protection board, added insulation, a moisture retention layer, irrigation systems and erosion blankets. Green roofs can add anywhere from 9-45 kg/m^2 (or more) onto the total design load structure.

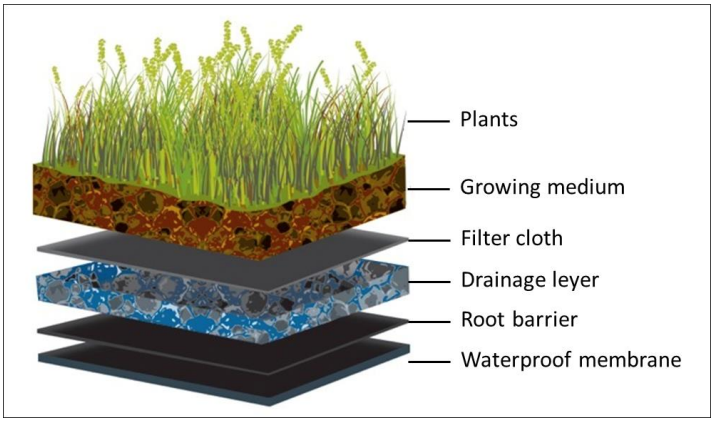

Image A.5.3.2. Green roof layers system.

Every green roof is different. The number of layers, depth of the system and therefore plants differ by multiple factors. Some of these may include roof's slope, height, sun exposure, wind exposure, weight load, design objectives and budget, climate and weather characteristics of the location.

Green roof systems could be classified as extensive, intensive and Semi-intensive systems. Extensive systems, consisting of a growing depth of 10.00 cm or less. Although this system can host a limited variety of plants, it is lightweight and usually requires less maintenance and water usage. Intensive systems are thicker and hence heavier, consisting of more than 20.00 cm. Depending on the weight allowance of the structure and slope, or if it was already calculated in the construction, some intensive systems can even grow medium tree size. Semi-intensive systems are in between the above depths (10.00-20.00 cm), making it suitable for growing a variety of grasses and wildflowers.

The energy consumption of the building sector represents 40% of the total of the European Union (EU), generating, also, appreciable CO_2 emissions. For the United Kingdom, e.g., it has been calculated that energy savings with green roofs can reach 45.00% in buildings without insulation and 13.00% in buildings with insulation.

The porous and light materials necessary for the installation of green roofs, both for the growing medium and for the drainage layer can be waste or by-products, as well as recycled ceramic materials or LWA_S made by the valorization of waste. This is a contemporary issue in the LWA_S research field. Thermal behavior of LWA_S is related to its thermal conductivity and density values which are influenced by the pore structure.

There are published experimental studies related to green roof agriculture (Avnimelech, 1986; Whittinghill et al., 2013; Whittinghill and Rowe, 2012) and the effect of recycled or sustainable materials in green roof substrates (Eksi et al., 2015; Nagase and Dunnett, 2011; Papafotiou et al., 2013; Rowe et al., 2006; Young et al., 2014). Also, substrate mix for extensive green roofs with crushed brick (Molineux et al., 2015; Vijayaraghavan and Raja, 2015) and LWA_S manufactured with brewery production wastes and by-products (Farias et al., 2017a).

In each case, it can be determined that the use of waste, as well as for the manufacture of materials, for use in the installation of green roofs, has good to very good results, in comparison with the commercial materials sold for that purpose. At the same time, sustainable materials are considered since waste finds another use, a technological nutrient, decreasing the environmental impact.

The adaptability of the waste materials or the materials made with waste obviously has to adapt perfectly to their use, mainly low density, inert material (pH and content of non-hazarded elements), high porosity (balance between open and closed porosity), a capacity of water retention and water release (storm-water management).

A.8.4. LWA_S AND CONTROLLED REALIZED FERTILIZERS

The control released fertilizers (CRF_S) are materials which gradually release their mineral nutrients, while at the same time providing proper nutrition to plants. Mineral fertilizers are some of the most important products of agricultural industry. While providing nutrients to crops, they increase their growth and at the same time play an important role in regulating pH system and the fertility of the soil.

If the delivered nutrients exceed the system capacity (crops) by capability, a decrease proses in its concentration is activated. These processes include both the physical processes (rinsing out, vaporization) and microbiological conversions (replacement, precipitation, hydrolysis).

In the production of mineral fertilizers, hazardous substances are released into the environment. These substances include sulfur oxides, nitric oxides, fluorine compounds and dust. At the same time, consumption of non-renewable sources should also be pointed out.

The task of paramount importance is to increase the effectiveness of nutrient absorption and to decrease the losses, at the same time to decrease the amount of fertilizers waste material produced by the industry.

Mineral constituent uptake (N, P, K) by plants in their vegetation cycle has a sigmoidal character (Shaviv and Mikkelsen, 1993). The use of CRFS ensures that those nutrients attend the crops requirements minimizing the losses between application and absorption by improved their effectiveness. Low effectiveness of nutrients, mostly nitrogen assimilation causes environmental problems due to soil microorganisms transform the exed nitrogen (left unused) in nitrates, a compound with high solubility and diffusion in water (Lubkowski and Grzmil, 2007). The inorganic ones were used to confer released capacity of main (K, P) and secondary nutrients (Ca, Mg, Na, S), for its use as a growing media.

The CRFs release their nutrients gradually during the whole vegetation season and consequently need to be applied once only, which significantly reduces both time and energy consumption.

Most studies quoted in the literature on the subject mention a system in which a granule of fertilizer is encapsulated, i.e., it is coated with an inert layer. After the fertilizer's application, water penetrates through a hydrophobic membrane into the inside of granule. Then, nutrients are dissolved, and the arising osmotic pressure leads to either a partial tearing off of the membrane or to its expansion, which allows ion transport through the coating into the soil (Kochba et al., 1990). A coating diffusion coefficient controls the rate of nutrients' release

A distinct category of the CRF_S are systems in which there is no physical barrier and in which the release rate decisive factor is either solubility/degradability of a given fertilizer. Such fertilizers include inorganic materials of low solubility (e.g., ammonium and metallic phosphates); and chemically or biologically degradable materials of low solubility (e.g., urea-formaldehyde condensates, oxamides, diurea).

From the technological point of view, the CRF_S can be divided into these in which the release is controlled by coating diffusion, coating erosion, chemical reaction, osmosis or swelling (Shaviv and Mikkelsen, 1993). The kinetics of nutrients' release is a process, which so far has not been entirely understood. Although the literature on the subject presents several kinetic equations describing the release rate, these equations mainly refer to the coating diffusion cases (Shaviv et al., 2003).

Despite the CRFs many advantages and the fact that they have been continuously developed, their use is still insufficient. It is estimated that the CRF_S constitute a mere 1.00% of the total amount of used fertilizers, due to the CRF_S high prices; they are from 2 to 8 times more expensive than the commonly used fertilizers (Lubkowski, 2014; Shaviv and Mikkelsen, 1993).

A preliminary study using waste to provide technical nutrients (P, K) in a controlled release fertilizer glass was performed by the Modena University research group (Barbieri et al., 2014).

B. PURPOSE AND SCOPE

Clays minerals were characterized through valorization of diverse organic/inorganic residues and by-products in the formulation of lightweight aggregates (LWA_S) with two different functions, drainage layer for green roofs and growing media with fertilizing capability.

The primary objectives of this research and the innovative scientific contribution, are related to the optimization of natural and primary resources (clays); energy saving (non-removable source) in clay minerals extraction and thermal treatment of the ceramic samples; the reduction of the environmental impact by decreasing the greenhouse gases emissions (GHG); propose an alternative disposal treatment to landfill; and offering innovative and sustainable materials, for industrial restructuring by boosting local economies.

This research is based on the circular economy concept, related to the zero waste generation by the valorization, process, and products re-engineering, emulating biological cycles. The use of waste/by-products generated in the local industry, from different production areas such as brewing production, meat products elaboration, corn harvesting, recycling of municipal collection glass were investigated and characterized as partial substitution of local clay minerals in the formulation of LWA_S. These productive activities are widely spread around the world, mainly in developed countries.

Therefore, it is considered that the research carried out, can be transposed to other geographic location, by the interconnection of different production processes to develop innovative and sustainable construction materials.

The three clay-base mixtures used in this research are are composed as follow:

The BYRC mixture, composed of equal parts by black, yellow and red ES clay, were provided for Arcillas Bailen S.L., Jaén, Spain. This composition is commonly used in the production of structural ceramics. Using BYRC clay-based mixture, it was intended to use a mix that the local ceramic industry was familiar with.

The WBC clay base-mixture composed of 30% white and 70% black clays, also from Bailen, is not a typical composition since white clay contains high carbonates content (XRF:20.00% of CaO), presenting problems during drying stage, so it is used in very small quantities in structural ceramics formulations. For this purpose and through collaboration with Arcillas Bailen S.L., it was proposed to work with white clay and valorize its use in other ceramic materials such as

LWA_S. High carbonates percentages are correlated to favorable bloating behavior in the production of porous and lighter ceramic structures.

The RC clay mix, composed by 100% Italian red clay (Red IT), comes from "Roncobotto - Le Salde" from Samone, Zocca district (MO), Italy, extracted and provided by Escavazioni Industriali Baroni s.r.l., it is used in the formulation of structural ceramics. This type of clay mineral offers interesting characteristics for sintering at lower temperatures (around 1000°C), related to significant oxides with melting properties content (vitrification capacity). To compare WBC clay mixture with local Italian clay with fewer carbonates content, RC was used to produce LWA_S for agricultural use.

The decisive factor on which waste/by-products used were chosen in this investigation was the proximity of the generation place where is the production of ceramic materials, following the concept of km 0, reducing transport distances, reducing environmental impact. At the same time, these residues represent an environmental problem since they are generated in massive quantities, landfilled treated. Another reason for choosing this agro-waste are their generated elevated quantities that can feed the ceramic production without issues.

The technical nutrients (TN) used were chosen according to different characteristics: i) pore-forming agent, allowing to lower sintering temperatures (100-200^{o}C), i.e., low bulk density ≤1200.00 kg/m^3 (UNE-EN13055-1, 2003), and high-water absorption and insulation capacity; ii) contribution of elements associated with the capacity of gas generation and vitrification to favour the swelling of the material, e.g., silicon, aluminium, sodium, carbonates, organic matter; iii) confer released capacity of main (K, P) and secondary nutrients (Ca, Mg, Na, S), for its use as a growing media.

The TN derivate from different production processes and provided for local industries. Three of the five organic residues characterized in this investigation comes from the beer production, Heineken S.A, located in the province of Jaen. Through collaboration with the brewery industry and their interest in the valorization of the massive quantities of waste generated, were used: sludge of the production wastewater treatment plant (BS), bagasse (spent grains of malt) (BB), and diatomaceous earth (yeast extraction in the clarification process of beer by filtration) (DE), they were used as a pore-forming agent in the elaboration of LWA_S. These residues were already investigated as a pore-forming agent for TEP 222 research group, in the application of structural ceramics (Eliche-Quesada et al., 2011; Galán-Arboledas et al., 2017; Martínez-García et al., 2014,

2012; Martínez et al., 2012) as well as in the elaboration of lightweight aggregates (Farias et al., 2017a, 2017b; Martínez-García et al., 2015).

The meat-bone meal (MBM) and the cattle-bone ashes (CBA) are by-products generated in the elaboration of meat products, one of the most widespread economic activities in Europe. These TN were provided by SAPI S.p.A, located in Castelnuovo Rangone, Province of Modena, Italy. Although they are by-products and not wastes, due to the European regulations increasingly restrictive concerning its use as raw material in other processes, the market for its valorization is very scarce, and mostly it is derived to landfill treatment.

Brewery sludge (BS), bagasse (BB), diatomaceous earth (DE), meat-bone meal (MBM) and Corn cob (CC) were used as a pore-forming agent, the cattle-bone ashes (CBA) was used as a nutrient contributor in the elaboration of LWA_S for agricultural use, due to its high phosphorus content.

The waste percentages used to formulate the batch and the sintering temperatures of the LWA_S were selected based on the investigations previously detailed by the two research groups, as well as a study of the existing bibliography; mainly the work carried out by M. Dondi, J. Gonzalez-Corrochano, C. R. Cheeseman, V. Ducman, O. Arioz. It sought the maximum percentage of pore-forming agent addition, valorizing the more significant amount of waste, without compromising the structure and durability of the material.

Glassy sand® (GS) was provided for Sasil s.p.a, located in Dosso, province of Biella, Italy. GS is a claimed glass derived from the secondary treatment of the recycling glass from the urban collection, not classified as waste; it is a commercial product with characteristics for its use in glassworks.

The fertilizer glass (FG) was obtained by mixing 40 wt% of cattle-bone ashes (CBA) as P intake; 42 wt% of Glassy sand® (GS) as parent glass and 18 wt% as K intake. The mix was subjected to melting at 1450°C for 2hours and cast in water. The percentages that constitute the formulation of the fertilizer glass (FG) were based on previous research work directed by Prof. Luisa Barbieri, related to the valorization of animal flour ash for active glasses (Barbieri et al., 2014).

Glassy sand® (GS), cattle-bone ashes (CBA), and fertilizer glass (FG) were previously characterized for the research group led by Prof. Luisa Barbieri, as support for lipase immobilization (Barbieri et al., 2016), cementitious composites (Bursi et al., 2017), as ASR performance of cement mortars (Saccani et al., 2017).

All technical nutrients were provided from the agro-food industry, except the Glassy sand® (GS). These alternative raw materials are classified as non-hazardous materials, free of heavy metals or pollutants that could represent a danger to the environment, allowing its use in green roofs or for agriculture. However, they have been tested to determine their harmlessness to the environment, according to European standards. As well as all the technical aspects related to its use and comparison with its commercial products with the same function.

Based on the initial description of the case study, the specific objectives of the research work are detailed as it follows:

TECHNOLOGICAL AIMS

By characterizing all the raw materials and technical nutrients used, regarding their chemical (XRF and elemental analysis), mineralogical (XRD) composition, thermal behavior (TGA/DTA/DSC) and bloating behaviors (Riley, 1951); to determine the potential of each mixture on its different applications.

At the same time, the technological characterization of the materials developed according to specific standards. The organic matter provided by the waste/technical nutrients by its oxidation, generates porous ceramic structures, making them lighter and with improved insulation properties. The use of pore-forming agents allows the reduction of the sintering temperature, generating a substantial reduction in energy input and economic saving. Highlighting that the elevated temperatures in the furnace destroy the waste during the thermal cycle.

Develop materials with potential for use in green roof construction, energy conversion of buildings, as well as materials as crop aids with fertilizer capacity.

ECONOMIC AIMS

The results that are expected will determine the energy and natural resources savings, producing economical savings, as well as the opportunity of producing innovative and sustainable materials to be eco-labeled, busting the local economy.

The costs optimization generates greater competitiveness for companies. As well as the diminution of the costs for the consumer, during the use of the new materials, with better performance as thermal/acoustic insulation, fertilizing capacity, producing eco-efficient materials, highlighting, the saving that implies the valorization of waste like raw materials,

incorporating them to the productive system, in contrast with landfill treatment. These economic benefits facilitate their adaptability in industrial production.

Another aspect considered is the easy introduction of these new technical nutrients in the production process to evaluate their possible industrialization, without generating additional costs and changes in the productive system.

ENVIRONMENTAL AIMS

The replacement of natural resources by waste allows an alternative treatment with less environmental impact. The energy recovery in the production process is linked to the energy contribution of the organic matter oxidation, decreasing the energy demand of the furnace and reducing the consumption of non-renewable energy (fossil fuels). Also, the geographic proximity of the places of generation and production allows a saving of fuel relative to transport and emissions.

It is intended to quantify and qualify the environmental average benefits regarding carbon equivalent, through the elaboration of Carbon Footprint (CFP). For this, it is proposed to use the data obtained in the investigations to perform a comparison, in environmental terms, of traditionally produced LWA_S (100% virgin clay material) and LWA_S produced with the addition of specific percentages of different residues locally generated. These environmental savings are related to the partial replacement of the clay by waste and energy saving using the exothermic reaction of the organic matter, impacting directly on greenhouse gases emissions (GHG), according to ISO standards.

The raw materials extraction and sintering processes are considered the most relevant regarding energy consumption and environmental impact generation.

STRATEGIC AIMS

Demonstrate the compatibility and traceability of this research work through the association of companies from different industrial sectors, which are developed in the same geographic location, for the saving of energy and raw materials, through investment in R&D (I+D+i).

Another aspect considered is the adaptability of these production changes in the industrial reality.

In turn, the possibility of environmental certification thus increasing the competitiveness of the product in the market, boosting the local economy.

C. MATERIALS AND EXPERIMENTAL METHODS

C.1. RAW MATERIALS CHARACTERIZATION

C.1.1. ELEMENTAL ANALYSIS (C, H, O, N, S DETERMINATION)

The technique is based on the complete and instantaneous sample oxidation by combustion in a pure oxygen atmosphere at approximately 1000°C. The different combustion products CO_2, H_2O; and N_2 are transported through the carrier gas (He) through a reduction tube and selectively separated into specific columns to be subsequently desorbed thermally. The sensors interpret each element: non-dispersive solid-state (IR) for carbon, hydrogen, and sulfur, differential thermo-conductivity (TCD) for nitrogen. The combustion furnace (resistance), reaches 1150°C and the combustion furnace (pyrolysis) for the analysis of oxygen; can reach a maximum of 1350°C. Finally, the gases pass separately through a thermal conductivity detector which provides a signal proportional to the concentration of each component of the mixture.

The total C, H, N and S content of clays minerals and waste/by-products were determined by the CHNS-O Thermo Finnigan Flash EA 1112 and LECO TruSpec micro CHNS elemental analyzers.

Image C.1.1.1. ECO TruSpec micro CHNS elemental analyzers.

C.1.2. CARBONATES DETERMINATION. CALCIMETRY

This method consists on the determination of the calcium carbonate content of the material, derivated from the volume of carbon dioxide (CO_2) released by the chemical reaction, between the sample, finely ground, and hydrochloric acid (HCl), according to the following reaction:

$$CaCO_3 + 2\ HCl \rightarrow CaCl_2 + CO_2\,(gas) + H_2O$$

The reaction between calcium carbonate and hydrochloric acid releases carbon dioxide, which allows calculating the volume of gas produced. Knowing that 1.00 mol of CO_2 is equal to 1.00 mol of $CaCO_3$, the calculations were made, and the percentage of carbonates determined.

For the calculation of $CaCO_3$ percentage of several materials, a method of volumetric measurement of the CO_2 gas produced by 1.00 g sample with 10.00 ml hydrochloric acid (2M) was used. In this research, the quantitative analysis of the calcareous fraction was determined using the Dietrich-Frühling calcimeter.

Taking into account the temperature and the atmospheric pressure at which the analysis was performed, these data are normalized to 0°C, 1.00 atm for CO_2.

With all data, the calculation was performed following this formula:

$$\% \text{ de } CaCO_3 = \frac{V_t (P_t - P_v) 273}{760 (273 + T)}$$

where,

- V_t: CO_2 volume generated by the reaction expressed in ml
- P_t: atmospheric pressure in mm Hg
- P_v: water vapor pressure at temperature T expressed in millimeter of Hg
- T: temperature at which the analysis was performed in °C

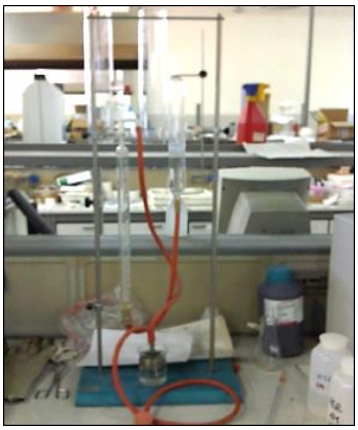

Image C.1.2.1. Dietrich-Frühling calcimeter.

C.1.3. X-RAY FLUORESCENCE (XRF)

X-ray fluorescence (XRF) is a quantitative and qualitative analytical tool that analyzes materials by the emission of X-rays that has been excited by bombarding with high-energy X-rays. When the elements of a specific sample are exposed to a high-intensity X-rays energy, sample emitted at energy levels unique to those elements. The source irradiates the sample by exciting the atoms and the detector measures the fluorescence radiation emitted. In other words, the elements are identified by the behavior of the atoms when they interact with radiation. This

radiation is incident on an analyzer crystal (with interatomic spacing d) that diffracts it at an angle (θ) dependent on its wavelength (λ) by the Bragg law (sin θ = nλ/2d).

A detector that can be move over a specific range of said angle measures the value of the radiation intensity at a given angle, therefore for a specific wavelength.

The incident photon promotes an electron to a state of increased energy, creating a gap (photoelectric effect). The gap is occupied by another electron, releasing energy through a fluorescence photon (Auger electron). The fluorescence radiation emitted by a chemical element has a characteristic spectrum and tabulated energies. That spectrum depended on energy levels and recognized all other elements.

The chemical composition of the raw materials was determined by X-ray Fluorescence (XRF) carried out with the following instruments:

- Philips Magix Pro (PW-2440) Philips, Amsterdam, The Netherlands.
- Bruker S8 TIGER endowed with the QUANT EXPRESS SPECTRA plus software.
- WDXRF model ARL ADVANT`XP, sequential house THERMO Fisher.

C.1.4. LOSS OF IGNITION (LOI)

Loss of ignition (LOI) is a test used in analytical chemistry, in the analysis of minerals, which consists of heating a sample to a specific temperature, until its mass stops changing. The ignition loss is reported as part of the elemental analysis.

The LOI value was determined by weighing an approximate amount of 1.00 g of the sample previously dried at 105°C for one hour. The sample was calcined for 2.00 hours at 1050°C for inorganic samples and 600°C for organic samples. These data are interpreted as the percentage of loss of carbon compounds associated with the organic matter content.

C.1.5. ORGANIC MATTER CONTENT DETERMINATION

For the quantification of the organic matter by calcination, was followed the method proposed by Navarro and Col. (1993), where 5.00 g of sample was weighed in 15.00 ml crucibles, placed in the stove for 24 hours at 105°C. The samples were allowed to cool (desiccator), weighed and set for 24 hours in a muffle furnace at 430°C, later they were transferred to a desiccator and after cooling the weight was recorded. Weight difference calculated organic matter content (OM%), according to $OM\% = [(M_2-M_3)/(M_2-M_1)]*100$

being:

- M_1: capsule weight
- M_2: capsule with the sample weight at 150°C
- M_3: capsule with the sample weight at 430°C

C.1.6. X-RAY POWDER DIFFRACTION (XRD)

For the characterization of raw materials and LWA_S developed in this research, X-ray diffraction analysis (XRD) was performed. XRD is one of the most important and widely used techniques in solid-state chemistry for the characterization, identification, and determination of crystal structures.

The samples were submitted to an X-ray beam, electromagnetic waves with a wavelength of 3-10 nm, produced by an X-ray tube under vacuum. This beam, colliding with the sample can interact in two ways: can be absorbed by the material, or it can be transmitted by varying the direction of wave propagation. The XRD technique analyzes the geometry and intensity of the electromagnetic waves dispersed by the atoms found in the several atomic planes.

For this research work was used the technique related to the diffraction of powders. Is the most widely used method in the study of crystalline phases of materials commonly used technique is Debye-Scherrer and Hull, known as "dust method." This method involves the use of a monochromatic X-ray beam which includes a substantial number of small, randomly oriented crystals so that it can admit that all possible orientations are taken and that all possible orientations are equally likely.

The advantage of this analysis is, by analyzing the peaks, to obtain the following information:

- The position of the peak determines the crystalline phase present.
- Peak intensity is the amount of phase index found in the sample.
- The width of the peaks identifies the size or deformation of the crystallites.

For the XRD analysis of the different types of clays, residues/by-products and LWA_S samples, the following measuring equipment were used:

Phillips PANalytical PW3710 Diffractometer. The slits of divergence and antidivergence were set at 1/4°, and Soller slits (incident and diffracted beam) of 0.04 rad were used. The measurements were performed from 5° to 80° for approximately one hour with a step size of 0.0167°. The tube worked at 45 kV, and 40 mA and the sample was rotated during the

measurement to increase the particle statistics; PANalytical's High Score Plus software has been used as an interpretation tool.

Bruker model D8 Advance Diffractometer. With anode Cu and Ni filter, with Kα radiation operating at 40.00 kV and 30.00 mA. Data were recorded in the range of 2θ between 5^{o} and 60^{o}, with a time interval of 0.019732' and 0.50" per step. The EVA software was used as an interpretation tool.

Siemens D5000 diffractometer (Siemens AG, Munich, Germany), Bragg-Brentano geometry (θ/2θ) and Kα1, two radiations and equipped with a graphite monochromator for the elimination of Cu (Kβ) radiation.

In this research and for the determination of the crystalline structures of the clays used the X-ray Powder Diffraction (XRD) was carried out on the samples without alteration, the clay fraction was not separated so they are in bulk and the powders were not oriented.

C.1.7. THERMOGRAVIMETRY TG/TGA/DTG AND DIFFERENTIAL THERMAL ANALYSIS DTA/DSC

Thermogravimetric analysis is based on the measurement of mass variation vs. physical or chemical changes of a substance as a function of temperature change. The result of this study is the thermogram or thermal decomposition curve, which shows the variation (or percentage) of mass as a function of time.

The thermal analysis allows determining properties like enthalpy, thermal capacity, mass changes and coefficient of heat expansion. Therefore, the analysis can provide information about the chemical and physical processes that take place, such as the temperature at which the thermal events occur, the thermal nature of the event, and whether it is an endothermic or exothermic process.

In this research, this analysis was carried out to characterize raw materials (clay materials and technical nutrients) and samples mixes, after and before thermal treatment. The thermogravimetry (TG/TGA/DTG) is related to the mass change in function of the temperature generated. Differential thermal analysis (DTA/DSC) is related to heat flux in function of the temperature generated.

Thermogravimetry (TG/TGA) is the primary thermoanalytical methods where the device is constructed around a micro-furnace connected to a super-sensitive micro-analytical balance.

The result is expressed in Δ mass vs. temperature. DTG is defined as the first derivative of the TG curve, while TG measures changes caused by mass loss.

Differential thermal analysis (DTA) is related to the temperature difference, which registers variations in the material where no mass-loss occur. The material under study and a reference (inert) are subjected to undergo on same thermal cycles. Any temperature difference between sample-reference is recorded (heating or cooling). The heat flow to the sample and the reference remain the same, rather than the temperature. If the event corresponds to an endothermic chemical reaction, sample temperature will lag behind the temperature of the reference; and when a reaction is an exothermic event, is the opposite.

Differential scanning calorimetry (DSC) recorded the electrical power (heat) needed to keep the sample analyzed and reference sample at the same temperature. By measuring the heat difference, this method allows them to study processes like decomposition, pyrolysis, ignition, phase changes, crystalline transition. Energy change (endothermic/exothermic) can be interpreted from the DTA/DSC curves by the integrating of peak area.

The reference (Inert) compound is needed for the measurement (it should not undergo any thermal changes and should not react with the pot material and thermocouple). It is typically aluminum oxide (Al_2O_3) or silicon carbide (SiC) for inorganic and silicone oil for organics materials.

The most commonly used thermocouples are chrome/alum and platinum/platinum-rhodium. The former provides a relatively high signal (about 4.00 mV at 100^{o}C) and linear with temperature. It can be used up to 800^{o}C (or 950^{o}C in an inert atmosphere). The second provides a much weaker signal (about 1.00 mV at 100^{o}C) but can be used up to 1500^{o}C.

For the TG-DTA-DSC analysis of the different types of clays, residues/by-products and LWA_S samples, the following measuring equipment were used:

Thermal Analyzer Mettler Toledo (TGA / DSC 1). Measures TG-DSC values simultaneously up to 10 µg. The module consists of an oven (HT1600) that works between RT-1600^{o}C and an ultra-microbalance (MX5) connected to a sensor of Pt-Rh (DSC HSS2). The balance is thermostated at 22^{o}C and protected by a continuous flow of N_2 of 20 ml/min. The thermobalance is coupled with a mass spectrometer of PFEIFFER VACUUM, (THERMOSTAR GSD320). The analyzes can be performed in air, O_2, and N_2 in crucibles of Pt and alumina of 30 and 70.00 µl. The software that controls the computer and evaluates the results is the STARe version 14.00 of the Mettler Toledo

STARe system. The equipment is coupled to a mass spectrometer is from Pfeiffer Vacuum model ThermoStar TM GSD 320. The tests were carried out in 70.00 µl Al_2O_3 crucibles in the temperature range 30-1100°C, with an O_2 flow of 80 ml/min, a heating rate of 10°C/min and 10 mg of sample.

Netzsch STA 429 Thermal Analyzer CD. Works in a temperature range from -160°C to 1400°C. It has a thermocouple for direct measurement of temperature in the sample/reference crucible. Resolution: 2.00 g (15,000 mg)/5.00 mg (25.00 mg).

Image C.1.7.1. Thermal Analyzer Mettler Toledo (TGA/DSC1).

C.1.8. CALORIFIC POWER DETERMINATION (CALORIMETRY)

Thus, the term calorific power, expressed regarding high heating value (HHV) and low heating value (LHV), expresses the amount of energy per mass unit that can be released by a chemical oxidation reaction. As measured in a bomb calorimeter represents the energy that can release the chemical bond between fuel and the oxidizer, liberated by the combustion. Carbon and hydrogen react with the oxygen to form the carbon dioxide (CO_2) and water (H_2O), including the energy (heat) liberated by the oxidation of other elements like sulfur.

Heats of combustion are measured by the heat obtained from the sample is likened to the heat obtained from the combustion of a similar amount of benzoic acid ($C_7H_6O_2$) were the calorific value is known. Pressurized with an excess of pure oxygen (30.00 atm) and containing a weighed mass of a sample (1.00-1.50 g) and water (1.00 ml), the vessel is submerged under a known volume of water (2.00 l). Through the ignition circuit connected to the "bomb," an electric ignition is produced. The heat flow crosses the stainless steel wall, thus raising the temperature of the steel bomb, its contents, and the surrounding water. The temperature change is then accurately measured with a thermometer.

Sometimes it is necessary to correct the value of calorific value since in some cases facilitators are used in which the means of ignition, the auxiliaries to the combustion intervene. By using stainless steel for the bomb, the reaction will occur with no volume change observed.

Image C.1.8.1. Thermal Analyzer Mettler Toledo (TGA/DSC1).

The HHV and LHV of the raw materials were determined by a Parr 1341 Plain Oxygen Bomb Calorimeter, following the UNE 32-006:1995 standard (UNE-32-006, 1995).

C.1.9. PARTICLE SIZE DISTRIBUTION ANALYSIS

Particle size analysis is an analytical procedure by which the distribution of sizes in a sample is measured and reported. Particle size analysis is an essential tool the characterization of a wide range of product performance factors.

Particle size analyzers variety from historical sieve to modern automated light scattering instruments. The most appropriate selection for a particular technique depends on factors like size range, nature of the sample, the information required, the analytical method, and sample throughput.

In this research, the granulometry of the five different clay minerals was analyzed by Mastersizer 2000 Ver. 5.22 (MAL101257), Malvern Instruments Ltd. Malvern, UK.

C.1.10. THERMO-MECHANICAL DILATOMETRY ANALYSIS

A Thermo-mechanical dilatometer is a precision instrument for the measurement of dimensional changes in the material, as a function of temperature. Dilatometry test a wide range of material including ceramics, glasses, metals, and polymers, as well as a wide variety of measurements like linear thermal expansion, the coefficient of thermal expansion, sintering temperature, shrinkage steps, phase transitions, density change, softening point and decomposition temperature, anisotropic behavior, and glass transition temperature.

The dilatometric analysis determines the dimensional changes, expansions, and contractions of the material due to the temperature and the reactions that occur inside it, which shows a volume change associated with it.

Traditional ceramics products are made of clay minerals, quartz, and feldspar. The technical properties of these products depend on physicochemical aspects of clays, their reaction kinetics during firing and ultimate microstructure development. Dilatometry is an unusual technique to study the densification behavior of ceramics. Differential coefficient of expansion (DCE) is the derivative of the percentage of linear change (PLC). DCE is taken as an indicator of phase development and other thermal reactions (Agrawal and Misra, 2014).

The theoretical firing curve can also be traced through the dilatometric curve (Abajo, 2000; Elias et al., 2007). The material to be tested is prepared and placed into the equipment furnace. One end of the sample is supported on a sensor, which is displaced with it, by thermal expansion or by an increase in length.

To carry out the dilatometric analysis of the three clay based mixtures used in the research, a DIL 402 C Dilatometer was used. The thermogram records the variation of the length as a function of temperature.

Image C.1.10.1. Dilatometer DIL 402 C and samples analyzed.

C.2. LWA_S CHARACTERIZATION

The drying processes of the raw materials/waste/by-products and LWA_S samples were carried out in the following stoves:

- PID System stove, model M120-VN Basic.

- Memmert Mod. 30-1060.

For the calcination of raw materials/waste/by-products samples and sintering prosses of the LWA_S, were carried out in the following furnace:

- Muffle furnace P-Selecta Mod. 2000366.
- Muffle furnace Lenton AWF13/12.

To determine the physical, chemical and structural properties of the materials developed in this research, the samples were submitted to different tests according to standards.

C.2.1. TECHNICAL PARAMETERS. DENSITY, POROSITY AND WATER ABSORPTION.

The density consists in the determination of haw close-packed the molecules of substances are, and how much the molecules weighs. The density is the ratio of the mass of a substance to the volume occupied by that mass.

Real density (RD), is defined as the mass of a particle divided by its volume, excluding open and closed pores. AD density is a constant value for a matter, i.e., the density of the solid material.

Bulk density (BD) is similar to the RD. Except that includes the volume of the solid material, open and closed pores, and the interparticle void, i.e., its value is lower than RD.

Particle density (PD), is similar to the RD. Except that includes the volume of the closed pores and excluding pores accessible to water (open porosity).

Water absorption capacity (WA%) is defined as the measurement of moisture capacity that a solid has when is wholly immersed in water for a specific time frame. This parameter is related to the open porosity and its interconnections.

Open porosity refers to the ratio of the fluid volume occupied by the continuous fluid phase (air, water, Hg) to the total volume of porous material.

Total porosity (TP%) is the sum of the closed and open porosity of a material determined by the relationship between its real density and its apparent density, using the following formula: TP% = [(AD - BD)/AD]*100.

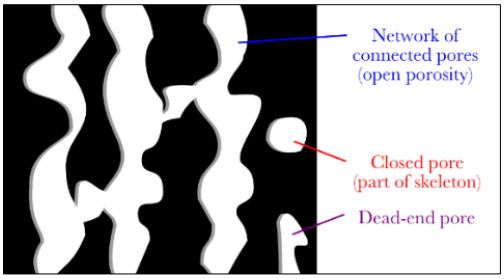

Image C.2.1.1. Porous types of porous materials

(http://apmr.matelys.com/Parameters/OpenPorosity.html)

Being an investigation carried out in two different universities and with different accesses to materials and equipment below are described the steps and standards followed for the determination of technical parameters of the LWA_S developed.

For the first stage in the development of LWA_S for agronomic porpuses, bulk density (BD) was determined by Envelope density analyzer Micromeritics Geo Pyc 1360 equipment and real density (AD), by pycnometer Accupyc TM II 1340 (Micromeritics, Norcross, GA, USA), Gas (He). Total porosity percentage (TP%), by means of the following formula: TP% = [(AD - BD)/AD]*100. Water absorption capacity (WA%) by two different test: immersion of samples in boiling water (100°C) for 6 hours (UNE-EN-772-7:1999, 1999) and immersion of the sample in water at room temperature for 24 hours (UNE-EN-772-21:2011, 2011).

$LWAS_{GR}$ and $LWAS_{AP}$ second step were submitted to the following procedures, to determine their technical characteristics. The particle density (PD) and water absorption (WA_{24}) were determined by the established procedure described by EN- ISO 1097-6 (annex C) (UNE-EN-1097-6, 2014), while bulk density (BD) and void percentage (VP%) were determined according to EN-ISO 1097-3 standards (UNE-EN-1097-3, 1999). Real density (RD) was calculated by pycnometer Accupyc TM II 1340 (Micromeritics) and total porosity (TP) using the following formula: TP%=[(1-BD)/RD]*100 (Bernhardt et al., 2013).

C.2.2. pH

The pH of a solution is a measure related to the molar concentration of hydrogen ions in the solution, using a measuring scale of 1-14, determines a measure of acidity (1-7) or basicity (7-14) of the solution, i.e., is approximately the negative of the logarithm in base 10 of the molar concentration, measured in units of moles per liter.

pH value has been measured to confirm inert nature of the materials suitable for a growth media. The registration of this parameter was made according to UNI-EN 13037: 2011, using a pH-meter Oakton CON 6 (UNE-EN-13037, 2012). For the determination of pH value, whole samples were weighed and stirred in a volume of distilled water in the ratio (solid/liquid 1:5). After one hour, the water has filtrated, and after calibration of the equipment, the data registered.

C.2.3. ELECTRICAL CONDUCTIVITY

The electrolytic conductivity in a liquid medium is related to the presence of salts in solution, whose dissociation generates positive and negative ions, which are responsible for transporting the electrical energy when the solution is subjected to an electric field. These ionic conductors are called electrolytes. The conductivity unit used in this research was micro siemens per centimeter (µmS/cm).

Conductivity is determined by connecting the electrolyte to a Wheatstone bridge. The diluted solutions follow laws of dependence on the concentration and additivity of ionic contributions of Kohlrausch.

Electrical conductivity value has been measured to confirm their counting as inert materials suitable as a growth media. The registration of this parameter was made according to UNE-EN 13038:2011, using a portable Oakton CON 6/TDS 6 (UNE-EN-13038, 2012). For the determination of EC, whole samples were weighed and stirred in a volume of distilled water in the ratio (solid/liquid 1:5). After one hour, the water has filtrated, and after calibration of the equipment, the data registered. For the EC values, the data measured were corrected by a dilution factor (1:5).

C.2.4. SCANNING ELECTRON MICROSCOPY (SEM) AND DISPERSIVE X-RAY SPECTROMETRY (EDS)

The backscattered electron images (SEM) display compositional data from different atomic number elements and their distribution. Dispersive X-ray Spectrometry (EDS) allows identifying those particular elements and their relative proportions in the sample (atomic %), i.e., qualitatively or semi-quantitatively determining chemical compositions.

SEM is based on the principle of optical microscopy in which the beam of light, is replaced by a high-energy electron beam, to generates a variety of signals from the surface of the sample. The sample must be conductive or to be covered with a layer of gold or carbon, which gives conductive properties.

The signals that derivates from electron-sample interactions reveal information about the sample the external morphology (texture), chemical composition, and crystalline structure. The data is collected over a selected area of the surface, and a 2-dimensional image is produced. Areas ranging from approximately 1.00 cm to 5.00 μm in width can be imaged in a scanning mode using SEM techniques, capable also, to performing analyses of selected point or areas on the sample by EDS technique.

When the beam reaches the surface of the sample, the following particles are mainly generated: backscattered electrons (1e) and secondary electrons (2e).

The operation consists on the acceleration of the electrons in an electric field, taking advantage of its undulatory behavior, carried out in the column of the microscope by using a difference of potential (1000-30000 volts). Electrons accelerated by a small voltage are used for susceptible samples, such as biological samples. The high voltages are used for metallic samples since these, in general, do not suffer damages like the biological ones and in this way, the shorter wavelength is used to provide better resolution imaging. The accelerated electrons came out of the barrel and focused so that the electron beam is as small as possible improving the resolution imaging.

When the beam hits the sample, many interactions occur between the electrons of the same beam and the atoms of the sample. On the other hand, the energy that the electrons lose when they "collide" with the sample can cause other electrons to be ejected (secondary electrons), and produce X-rays (Auger electrons). The most common is the one that detects secondary electrons, and it is with it that most of the images of scanning microscopes are made.

The macro-microstructural and elemental analysis of LWA_S for drainage layer in green roofs ($LWAS_{GR}$) were analyzed using a scanning electron microscope (SEM), with a high-resolution transmission electron microscope JEOL SM 840 (JEOL, Solutions for Innovation, Peabody, MA, USA).

The macro and microstructural and elemental analysis of LWA_S for agronomic proposes ($LWAS_{AP}$) and particulate matter (PM) emitted during the sintering process of the aggregates, were observed using SEM Quanta-200, coupled to a system for microanalysis X-EDS INCA-350, from Oxford Instruments.

Samples were pasted it with epoxy resin on an individual aluminum sample holder and metallization by sputter coating with a gold source (K550 Emitech).

Image C.2.4.1. Transmission electron microscope JEOL SM 840 and K550 Emitech.

C.2.5. POROSITY CHARACTERIZATION

It is known that physical properties such as density, thermal conductivity, and compression strength are all related to the pore structure of a solid. The control of porosity is of high industrial importance. Additionally, porosity is one of the factors which influence the chemical reactivity of solids and the physical interaction with the surroundings (Rouquerol et al., 1994).

C.2.5.1. MERCURY INTRUSION POROSIMETRY (MIP)

Mercury does not wet most substances and not penetrate pores by capillarity action. Entry into pore spaces requires applying external pressure in inverse preparation to opening size data. The required pressure is inversely proportional to the pore size, i.e., lower pressures are required to intrude Hg into large macropores, whereas much higher pressures are required to force Hg into small pores. Hg porosimetry analysis is the increasing intrusion of mercury into a porous structure under controlled pressures. No pore is penetrated by Hg unless a force is applied.

From the pressure versus intrusion data, the instrument generates volume and size distributions using the Washburn equation. At each surface interface, there is tension that acts tangentially to the interface. The surface tension acts like an elastic membrane contacting the surface until the surface forces are in equilibrium with the forces tending to increase the surface area of the interface. Liquid mercury has a high surface tension, i.e., molecular forces in its surface film tend to contact its volume into a form with least surface area: usually, its value is taken to be 485 dyne/cm. Mercury also exhibits a high contact angle against most solids.

If mercury is placed in contact with a pore opening, the surface tension of the mercury acts along the line of contact with the opening equal in length to the perimeter of the opening and creating a force-resisting entry (P.A. Webb, 1997).

When Hg is in contact with a pore opening of circular cross-section, the surface tension of Hg acts along the circle of contacts for a length equal to the perimeter of the circle.

Thus, the force with which Hg resists entering the pore is equal to $-\pi D\Upsilon\cos\Theta$, where D is the pore diameter, Υ the surface tension, and Θ the contact angle. Mercury contact angle with the most solids is 140^{o}. The externally applied force is the product of the pressure (P) and area (A) over which the pressure is applied. The negative sign enters because, for $\Theta > 90^{o}$, the term is intrinsically negative-signed. The force due to an externally applied pressure acts over the area of the circle of contact and is expressed mathematically by $\pi D^2P/4$, were P represent the applied pressure. At equilibrium the opposing forces are equal, thus:

$$-\pi D\Upsilon \cos\Theta = \frac{\pi D^2 P}{4}$$

alternatively, simplified:

$$D = \frac{-4\Upsilon \cos\Theta}{P} \qquad \text{(Washburn equation)}$$

Measuring the volume of mercury that intrudes into the sample, and each pressure changes, the volume of pores in the corresponding size type is known. The volume of mercury that enters the pores is measured by a mercury penetrometer (electrical capacitance dilatometer). It is a very sensitive apparatus and can detect a change in Hg volume of under 0.10 µl. The stem of the penetrometer is a capillary that acts as a reservoir for the analytical volume of Hg. The two conductors, Hg, and the metal plating are separated by glass, thus forming a coaxial capacitor. As pressure forces, Hg out of the capillary and into the sample, the Hg inside the capillary decreases and so is the capacitance. The decrease in capacitance, therefore, is proportional to the volume of Hg leaving the capillary with each change in pressure (Micromeritics, 1985).

The pore size distribution measurements were carried out by AutoPore IV Series (Automated Mercury Porosimeter), by Micrometrics (Norcross, GA, USA). Porosity was evaluated using the set-time equilibrium (10 s) mode between pressure limits of 345 kPa and 228 MPa. Under these operative conditions, it is possible to measure capillary pores raging (0.006–350 µm).

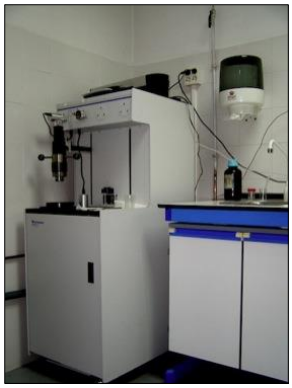

Image C.2.5.1. AutoPore IV Series Micrometrics
("http://www.scai.uma.es/servicios/aqcm/spo/spo.html," n.d.)

This technique has already been used by numerous investigations to characterize the porosity of porous materials such as lightweight aggregates (Bouguerra et al., 1998; Gallé, 2001; Henkensiefken et al., 2009; Kockal and Ozturan, 2011; Korat et al., 2013; Nguyen et al., 2014; Ramezanianpour and Malhotra, 1995).

C.2.5.2. ADSORPTION AND DESORPTION ISOTHERMS - BET THEORY

For an utterly non-porous material an adsorption isotherm, the curve raises speedily at low relative pressures, rises only discreetly at intermediate relative pressures, and quite rapidly as the relative pressure approaches unity. The retracing of the curve is produced in the reverse process due to the reduction of the relative pressure

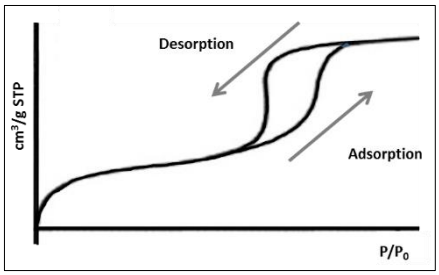

Figure C.2.5.2.1. Adsorption and desorption isotherm of a porous solid.

The initial rise in the curve is due to the absorbing molecules interacting first with the most active regions of the solid surface and then with the less active areas. As these areas are occupied, the curve diminishes.

By the midpoint of the curve, attachment of additional gas molecules on sites already occupied is occurring and other layers are forming. The gas-liquid change state due to the bulk

condensation of a liquid, producing the characteristic rise of the curve at the upper-right part of the graf (Figure C.2.5.2.1.). The information is located in the middle area of the curve showing a full loop, not retracing the absorption curve. The porous materials (mesoporous-macroporous) present this typical curve behavior, mining materials that have pores with openings form 2nm (20 Å) to 50 nm (500 Å). This characteristic porous structure is likely to have a wide range of size and shapes porosity, and also may be interconnected with one another.

In this research was used the calculation method called BJH (Barrett, Joyner, and Halenda), to calculate the surface area method (m^2/g), pore volume (cm^3/g) and pore size (Å). This mathematical approach derivate from the Kelvin equation involves hypothetical emptying of condensed adsorptive in the pores in a controlled way as the relative pressure (P/P0) decreased. This technique is equally applicable whether the adsorption branch of the isotherm downward from high-low pressure in the desorption branch. For BJH method the condition must be set arbitrarily where all pores are to be considered filled. Typically, this is taken to be at about 99.50% and relative pressure (P/P_0 = 0.995).

In this research, the adsorption and desorption isotherms with N_2 were determined, following the BJH method was calculated the characteristic distribution of mesoporosity for each sample. The BET theory named from the surnames of its originators, Brunauer, Emmett, and Teller, assumed that the active forces in the condensation of gases also are responsible for the binding energy of in multimolecular adsorption (P.A. Webb, 1997).

$$\frac{P}{Va\,(\mathrm{P_0} - P)} = \left(\frac{1}{Vm}\right)\left(\frac{P}{P_0}\right)$$

In this research, the analysis of the characteristic distribution of mesoporosity of the LWA_S for a drainage layer in green roofs ($LWAS_{GR}$) was made employing the ASAP 2020 Accelerated surface area and porosimetry System by Micromeritics (Norcross, GA, USA).

Image D.2.5.2.2. AutoPore IV Series Micrometrics
("http://www.scai.uma.es/servicios/aqcm/spo/spo.html," n.d.)

C.2.5.3. COMPARISON OF THE TWO TECHNIQUES

HG porosimetry and gas adsorption ostensibly measure the same properties; users frequently expect the pore size distributions to be similar.

Hg intrusion can be used to measure pore sizes down to about 3.5 nm, but this limit depends on the properties of the sample (compressibility), the upper limit is larger than the 25 µm. Hg intrusion does not give direct information about areas or morphologies. It is based on Laplace's equation for capillary pressure, and therefore theoretically gives only the size of the most significant entrance to a pore (P.A. Webb, 1997).

BET is a theory or method to determine surface areas; it will not give direct information about porosity. From N_2 adsorption at 77.00K (-196.15°C) could determine most of the parameters need when full isotherms are measured (from about 0 to about 1 p/p0, so more than the typical BET range). BJH theory could give pore size and area distributions, in a range from about 3 to 300 nm. Micropore sizes can be obtained from other theories (DR, DA, DFT among others) or other gasses (CO_2 at 273.00K/0°C). Gas adsorption methods will also not give direct information about bulk or apparent densities. Though gas pycnometry gives the skeletal density, and that is typically done at the start of a gas adsorption measurement (P.A. Webb, 1997).

C.2.6. LEACHING TEST AND INDUCTIVELY COUPLED PLASMA MASS SPECTROMETRY (ICP-MS)

The purpose of the ICP-mass analysis is to identify and quantify the chemical elements present in a sample by ionization and subsequent analysis by mass spectrometry. All the elements of interest can be determined by a single analysis (mass scanning) and, also, allows differentiating the different isotopes of the same element (multi-elemental isotope analysis). With this equipment, all elements except He, Ne, F, H, N, C, and O can be analyzed in a concentration range that depends on the element in question, from hundreds of ppm to even ppt in some cases.

The method measures element related to a specific light emitted by the element in the sample. Sample solutions are nebulized (gas), and the resultant aerosol is carried to the plasma torch where the spectrums of analyte-specific atomic-line emissions are produced. A diffraction grating disperses the spectrum, and the intensities of the individual emission lines are scrutinized by photomultiplier tubes. Background corrections are required to trace element

determination and are measured at wavelengths next to the analyte lines during analysis. The positions selected for background intensity measurement are determined by the spectrum adjacent to the analyte lines. These locations must be free of spectral interfering and must reflect the same change in background intensity as that happening at the analyte lines (Procedures et al., 2006).

The equipment used for the analysis the liquid samples (water/citric acid) from the LWA_S leaching test is an Agilent Model 7500a ICP-mass spectrometer. The control of the equipment, as well as the development of analytical methods for the acquisition and subsequent processing of data, is carried out using ChemStation software.

Image C.2.6.1. Agilent Model 7500a ICP-mass spectrometer.

The leaching test carried out for $LWAS_{GR}$ (LWA_S drainage layer of green roof) following standard DIN 38414-2, performed as it follows (DIN38414-2:1985-11, 1985):

The reagent was prepared by placing 5.70 ml of glacial acetic acid (CH_3COOH) and 64.3 ml of 1N sodium hydroxide (NaOH) and fill up to a one-liter volume with distilled water. Control of the pH range (4.93 +/- 0.05) was performed.

For the leachate determination test, at least 100 g of sample was taken, placed in a volumetric flask and covered entirely with the reagent. The sealing has then subjected to stirring at 60 rpm for 24 hours at room temperature (23 +/- 2^oC).

After 24 hours the extract was filtered, packed and brought to a pH less than 2. For its conservation, the specimens were placed under refrigeration at -4^oC. The samples were analyzed by ICP-mass spectrophotometry.

The leaching test carried out for $LWAS_{AP}$ (LWA_S agronomic purposes) was performed by following different standards depending on the media:

Test in water for 30 minutes was according to regulation CE N°2003/2003 (CE-2003/2003, 2003). The test was carried out as it follows: was pour 450.00 ml of demineralized water into a 500ml container; then placed the container on the mechanical agitator with a magnetic anchor at 300 rpm; weigh, with an approximation of 0.001 g. A sample quantity of 5.00 g with a granulometry lower than 500.00 µm was transferred it to the flask; after 30 minutes, the solution was filtered with a dry cellulose-filter. The liquid-solid ratio was 90 ml of water per gram of sample (5 g per 450 ml).

Test in Citric acid 2v/v% was perform following the provisions of Italian Legislative Decree N°75/2010 (Decree 75/2010, 2010), as it follows: was prepare, by pure crystallized citric acid, 120 ml of 2v/v% citric acid solution; place the beaker containing the solution on the magnetic stirrer at 30 rpm; weighted with an approximation of 0.0001g. A sample quantity of 1.00 g with a granulometry lower than 100.00 µm was transferred it to the flask; after 30 minutes/21 days filter the solution on dry cellulose paper filter. For the test carried out with powdered samples, the samples were pulverized with agate mill and sieve up to <100 µm. After the test, the liquids were filtered by Whatman 540 filter and then by cellulose membrane (<0.45 mm) to avoid solid suspended. Finally, the eluates separated were acidified using HNO_3 (c) to pH=2. The correction of pH was only performed in samples summited to test in water.

To analyze the control-release of different microelements and the influence of the porous material structure, the analysis was performed with the whole (WS) and powdered samples (granulometry <100 microns) (PS). 21 days allows determining the long-term release of nutrients and elements present in the sample. The use of citric acid 2%, simulates the acid conditions of a crop soil. At 20°C citric acid has a pH of 2.73.

In the test carried out with powdered samples, were pulverized with agate mill and sieve up to <100 µm.

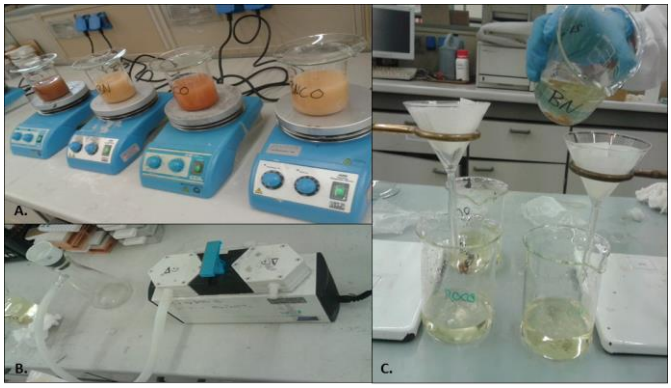

Image C.2.6.2. Stirring-bases and filtration process.

Since the initial quantities of the elements present in the Leaching samples test are very heterogeneous, it was necessary to analyze comparable quantities to obtain reliable conclusions, thus converting the ppm (mg/l) values into mg referring to the volume used for the medium (water or citric acid) by the proportion:

H_2O (ppm):(1000) = (X):(90 ml)

Citric Acid 2% (ppm):(1000) = (X):(120 ml)

The data thus converted, were used to calculate the percentage release of each element, relative to the initial arid, for all four different blends.

In Table C.2.6.1., sample weight and volumes used for tests were listed.

Table C.2.6.1. Test - weight and volumes samples used

H_2O 30' (WS)	Sample weight (g)	Vol. (ml)	pH	pH ICP
WB_{FG}	3.79	341.24	7.58	2.62
RC_{FG}	3.95	355.91	7.41	2.5
WB_{CBA}	3.05	275.25	7.67	2.74
RC_{CBA}	3.18	286.92	7.47	2.53

Citric AC. 30'(WS)	Sample weight (g)	Vol. (ml)	pH
WB_{FG}	2.07	249.12	2.53
RC_{FG}	1.91	229.99	2.44
WB_{CBA}	2.05	246.96	2.54
RC_{CBA}	2.05	246.99	2.48

Citric AC. 21 days (WS)	Sample weight (g)	Vol. (ml)	pH
WB_{FG}	2.06	247.58	3.40
RC_{FG}	2.07	249.19	3.04
WB_{CBA}	2.04	245.97	3.37
RC_{CBA}	1.96	236.28	3.07

Citric AC. 21 days (PS)	Sample weight (g)	Vol. (ml)	pH
WB_{FG}	2.19	245.73	3.20
RC_{FG}	2.22	247.11	3.01
WB_{CBA}	2.23	246.92	3.41
RC_{CBA}	2.01	239.91	3.10

An analysis of the fertilizer glass (FG) in water and citric acid 2% was carried out, following the precedents described above (Table C.2.6.2). These results were used for the calibration of the ICP analysis.

Table C.2.6.2. ICP analysis of FG in water and citric acid 2%

mg/l	**Na**	**Al**	**Si**	**P**	**K**	**Ca**	**Fe**	**Pb**
H_2O	3.34	0.19	17.9	2.26	3.89	4.49	0.07	<0.05
Citric acid 2%	329.00	25.77	88.00	484.00	412.00	487.00	3.89	0.20

Test samples were analyzed by Plasma Spectrometer (ICP-MS) technique. The ICP analysis provided the instrument reading for each element by calibration line drawn from the results. Using a standard solution which gives the X-Y axis calibration lines and equations to calculate the ppm values for each element.

C.2.7. INSULATION CAPACITY

To characterize another of the critical aspects of the material, the thermal insulation capacity between the aggregates without the addition of waste and those that were made with different waste percentages were compared.

For thermal imaging, the energy from the infrared portion of the electromagnetic spectrum is used, like digital cameras, creating images using the energy in the visible spectrum. All objects emit infrared energy, and the intensity depends on the temperature and various other factors like materials composition.

The apparent differences in temperature can be calculated by measuring the infrared energy emitted by an object and its surroundings, allow to detect issues with surface temperature variations, allowing to diagnose and document them.

Insulating properties for LWA_S were determined using the thermal imaging camera Fluke Ti-32 (Fluke, Everett, WA, USA), and Heat insulation/Heat conduction thermal house model 3.6.03-00 (Thermodynamics/PHYW, Germany). The procedures of the insulation capacity determination were according to standards (UNE-EN-12667:2002, 2002).

C.3. CARBON FOOTPRINT (CFP) CALCULATION

The calculation of the CFP is part of the LCA (UNE-EN-ISO-14040, 2006; UNE-EN-ISO-14044, 2006), a method by which the environmental externalities generated by a system are based on the contribution of Greenhouse Gases (GHG), emitted by direct or indirect effects. It is a simplified version of the LCA, in which instead of considering several impact categories, only the Global Warming is considered. ISO 14064 (UNE-EN-ISO-14064-1:2006, 2015; UNE-EN-ISO-14064-2:2006, 2015; UNE-EN-ISO-14064-3:2006, 2015) determines the standards for the calculation of the Carbon Footprint. For the modeling process was used the software Simapro 8 (Pré Consultants, 2006).

The aim of the CFP calculation is to compare the energy compensation and environmental performance between traditional production and LWA_S made with different percentages of

waste/by-product. The reduction in the consumption of earth-base materials (clay) and the reduction of the sintering temperature (ΔT= 300ºC), were compared.

C.3.1. SYSTEM DESCRIPTION AND FUNCTIONAL UNIT

The preliminary CFP analysis performed in this research includes the extraction of raw materials, transport to the university (were the LWA_S were produce) and the sintering process of the LWA_S (marked in Figure C.3.1.1 with a red dotted line). The other processes are assumed to be the same for all the aggregates, with or without technical nutrients (TN) addition. In this way, the analysis is simplified concentrating on the presses that represent the most environmental externalities due to energy imputes.

The functional unit (F.U.) was determined in 1.00 kg of LWA_S production. The tables referring to the production inventory (inputs-outputs) of each material are based on this functional unit.

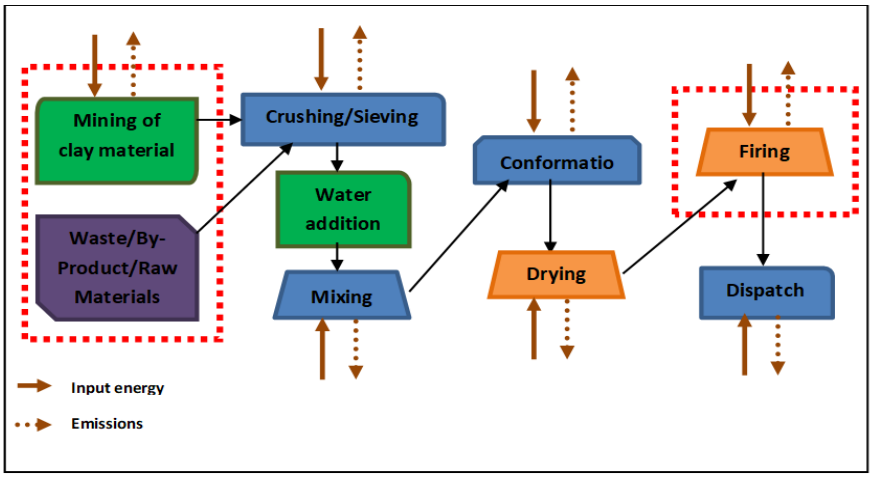

Figure C.3.1.1. LWA_S flow chart - Boundaries CFP analysis (in red).

The LWA_S for its use as a derange layer for green roofs ($LWAS_{GR}$) were produced in E.P.S. Linares, University of Jaen, Linares, Spain; and the LWA_S for agronomic porpoises ($LWAS_{AP}$) was produced in the Department of Engineering "Enzo Ferrari", University of Modena and Reggio Emilia, Modena, Italy. The sustainable material (clay and technical nutrients) were compared with the LWA_S without waste/by-products.

The results are expressed in kg of total equivalent carbon dioxide (Kg CO_2 eq.) emitted per kg of sintered aggregate within an hour.

C.3.2. LIFE CYCLE INVENTORY

The introduction of an organic compound within the mixture allows reducing the input energy to the system. The combustion of the organic substances, in fact, supports the heat treatment, making it less preponderant the external contribution regarding heat (Nzihou, 2010).

The data to elaborate the Life Cycle Inventory (LCI) of productive processes, inputs, and outputs, was obtained from the research group's investigation from both universities, biography study, field research, and database, also provided by the Simapro 8 modeling software.

LCA study was conducted with data collection of qualitative and quantitative parameters about raw material, allocations, type, and efficiency of fuel used in the rotary kiln. The data related to energy and material consumption in the kiln processes and gas emissions were collected from scientific group investigation as well through scientific publications. Source of data inventory can be seen in Table C.3.2.1.

Table C.3.2.1. Inventory analysis data collection souse.

Inputs/Outputs	**Source of data inventory**	
	Research data	**Secondary data**
Energy electric, Diesel, Pet-coke (solid fuel)	Field data collection, HHV calculations.	Ecoinvent 3, USLCI and EU & DK Input-Output Database libraries. (Alvarez, 2011; Biswas, 2014; Díaz Rubio and Del Río Merino, 2014; Dorado et al., 2003; González-Corrochano et al., 2009; Hwang et al., 2012)
Clay material collection	Field data collection, FRX, XRD composition.	Ecoinvent 3 database. (Barbieri et al., 2014; Cotes-Palomino, M.T.; Martínez-García, C.; Iglesias-Godino, F.J.; Eliche-Quesada, D.; Pérez-Latorre, F.J.; Calero de Hoces, F.M.; Corpas-Iglesias, 2016; Cotes-Palomino et al., 2016; Farias et al., 2017a, 2017b; R J Galán-Arboledas et al., 2013; Martínez-García et al., 2015, 2014; Ronda et al., 2015; Saccani et al., 2017)
Waste/by-products (BS, BB, DE, FG, CBA)	FRX, XRD composition, HHV determination.	(Bovea and Powell, 2016; Donatello and Cheeseman, 2013; Franus et al., 2016; Galitsky et al., 2003; Jeng et al., 2006; Kizinievič et al., 2013; Mueller et al., 2008; Ng and Martinez Hernandez, 2016; Nzihou, 2010; Tortosa Masiá et al., 2007)
Sintering process (Emissions to air/water/soil)	Field data collection	Ecoinvent 3, USLCI and EU & DK Input-Output Database libraries. (Cheeseman and Virdi, 2005; ESCSI, 2007; Fallis, 2013; Farias et al., 2017a, 2017b; R. J. Galán-Arboledas et al., 2013; González et al., 1998; Pinto et al., 2005)

By this assumption, for each process, it was necessary to calculate the high heating value (HHV) of each residue and considered a reduction regarding heat input.

C.3.2.1. LWA_S FOR GREEN ROOFS

Based on the data listed in Table C.3.2.1.1, the calculations of the CFP have been made through the use of the 2013 IPCC method. The samples without residue (BYRC), sintered at 1300°C, and the samples with 15wt% of waste (BS_{15}, BB_{15}, and DE_{15}) sintered at 1000°C, were compared.

The distances traveled by the raw materials/technical nutrients and clay minerals, were calculated from E.P.S. Linares, University of Jaen, Linares, Spain (Latitude: 38.085418/Length: -3.646555) to Heineken S.A. and Arcillas Bailen S.L. The data source was listed in Table C.3.2.1. (Inventory analysis data collection souse).

Table C.3.2.1.1. Data Inventory $LWAS_{GR}$.

		BYRC	**BS_{15}**	**BB_{15}**	**DE_{15}**
Raw materials/technical nutrients	Clay (kg)	1.00	0.85	0.85	0.85
	Sludge (Kg)	-	0.15	-	-
	Bagasse (kg)	-	-	0.15	-
	Diatomaceous earth (Kg)	-	-	-	0.15
	Water (kg)	-	-	-	-
Transport	Truck (km)	15.00	15.00/40.00	15.00/40.00	15.00/40.00
Energy	Extraction (KWh)	2.14	1.82	1.82	1.82
	Drying	-	-	-	-
	Ground	-	-	-	-
	Sieving	-	-	-	-
	Sintering (KWh)	1300°C	1000°C	1000°C	1000°C
		3.24	2.66	2.34	2.74

C.3.2.2. LWA_S FOR AGRONOMIC PORPOISES

Based on the data listed in Table C.3.2.2.1, the calculations of the CFP have been made through the use of the 2013 IPCC method. The samples without residue (WBC/RC), sintered at 1300°C, and the samples with 15wt% of BS and 10wt% of FG or CBA, sintered at 1000°C were compared.

Concerning the fertilizer glass formulation, the inputs related to the thermal treatment, carried out for 6.50 hrs., with a maximum of 1450°C during 2.00 hrs., has been taken into account. The energy expenses of the mixing of the components and the grinding-sieving of the glass have not been added.

For the $LWAS_{AP}$ the distances travelled by the raw materials/technical nutrients were calculated from Department of Engineering "Enzo Ferrari", the University of Modena and Reggio Emilia, Modena, Italy (Latitude: 44.645105/Length: 10.927927), to Sapi S.p.a. (CBA), Sasil S.p.a. (Glassy

Sand®) and Colorobbia Italia S.p.a. (potassium carbonate). The data source is listed in Table C.3.2.1 (Inventory analysis data collection souse).

Table C.3.2.2.1. Data Inventory $LWAS_{AP}$.

		WBC/RC	**WB_{FG}/RC_{FG}**	**WB_{CBA}/RC_{CBA}**
Raw materials/technical nutrients	Clay (kg)	1.00	0.75	0.75
	Sludge (Kg)	-	0.15	0.15
	Fertilizer glass (kg)	-	0.10	-
	Cattle-bone ash (Kg)	-	-	0.10
	Water (kg)	-	-	-
Transport (Km)	Truck	45.00	45.00/280.00/ 15.00/140.00	45.00/15.00
Fertilizer glass thermal treatment (1400ºC, for 6.00 h)	Cattle bone ash (40%), Glassy Sand® (42%), and 18% K_2CO_3 (KW/h)	-	3.12	-
Energy (kWh)	Extraction (KW/h)	2.14	1.82	1.82
	Drying	-	-	-
	Ground	-	-	-
	Sieving	-	-	-
	Sintering (KW/h)	1300ºC	1000ºC	1000ºC
		3.24	2.66	2.66

C.3.3. ASSUMPTION AND CUTTING

In this preliminary CFP calculation, the intermediary processes derived from the preparation of raw materials like crushing, sieving, mixing, water addition, pelletizing and drying methods were considered the same for all regarding energy inputs and environmental impact. Although the nature of the waste is different and may require higher energy consumption in the milling/crushing process. Water addition could also change, for mixtures with residues.

The calorific power released during the clay sintering is considered equal to all the mixtures used (BYRC, WBC, and RC). Although, it is believed that the mix with the highest calorific power is the WBC followed by the BYRC and finally the RC, conclusions derived from the chemical analyzes carried out and the LOI values, related to the organic matter and carbonates content.

The fertilizer glass manufacturing leads to an increment of the costs and energy consumption during production. For that reason, aggregates formulated with FG were compared to samples made with CBA, as an alternative raw material with low energy consumption.

Concerning the distances associated with the transport of raw materials/waste for the samples formulation, $LWAS_{GR}$ all inputs were generated/extracted in the province of Jaen. The $LWAS_{AP}$,

through collaboration between universities in different geographical locations, the mixtures of WBC clays and the pore-forming agent, brewery sludge (BS), come from Spain. The CFP calculation, it was determined that the transport distance of the WBC and RC clay-base mixture are the same. Concerning BS, the same transport distance of the clays has been applied, since this waste could be generated and provided by any of the brewing industries located in the province of Modena.

The efficiency of the rotary kiln energy efficiency associated with wall convection losses, door seal, was not taken into account.

C.3.4. Life Cycle Impact Assessment Methodology

Each method consists of different eco-indicators, which are numbers that represent the environmental impact of a product, the higher the indicator, greater the associated environmental impact will be.

The allocation of environmental loads to the different flows of a process (inputs and outputs) and the realization of the equal balance are performed by a methodology based on the use of a vector containing all the information about all possible types of contamination, in this case, pollutants related with GHG generation. Each product or process has a vector associated with all the information about the pollution generated throughout the life cycle. The choice of method depends on the categories of impact to be considered. The methodology used in this study is IPCC 2013, developed by the Intergovernmental Panel on Climate Change, since it is regarded as a single category of impact, global warming, to calculate the Carbon Footprint.

IPCC 2013 is the successor of the IPCC 2007 method, collects characterization factors for the direct global warming potential due to gas emissions to air expressed in kg of carbon dioxide equivalent (Kg CO_2 eq.). This method analyzes emissions of different pollutants that produce global warming, and it allows calculating the Global Warming Potential with a timeframe of 20 and 100 years.

Although the result of the CFP is expressed in Kg CO_2 eq, its result doesn't represent the single measure of CO_2 emitted, since it takes into account all the greenhouse gases that contribute to global warming, such as methane (CH_4), nitrous oxide (N_2O), hydrofluorocarbons (HFC), perfluorocarbons (PFC), sulfur hexafluoride (SF_6), nitrogen trifluoride, sulfur trifluoromethyl pentafluoride (NF_3), trifluoromethyl sulfur pentafluoride (SF_5CF_3) and halogenated ethers. This

methods, convert the individual results of each gas into Kg total CO_2 equivalents, in other words, the Global Warming Potential (GHP).

D. RESULTS AND DISCUSSION

D.1. CLAYS MINERALS

D.1.1. RECEPTION CONDITION

Through collaboration between the two research groups, different types of clays minerals were provided from two geographic locations. White, black, yellow and red ES clays were provided from a clay-pit in Bailen provided for Arcillas Bailen S.L., Jaen Province, Spain. The clay material was provided with 5-9% of moisture content.

The red IT clay comes from the extractive pole N°20 "Roncobotto - Le Salde" of Samone, Zocca district (MO), Italy, extracted and provided by Escavazioni Industriali Baroni s.r.l. The clay material was provided with 9-12% of moisture content.

D.1.2. CLAYS MINERALS CHARACTERIZATION

To produce the two different LWA_S applications ($LWAS_{GR}$ and $LWAS_{AP}$) were used diverse types of clays minerals: Black, Red ES, Yellow, White and Red IT clay (Image D.1.2.1).

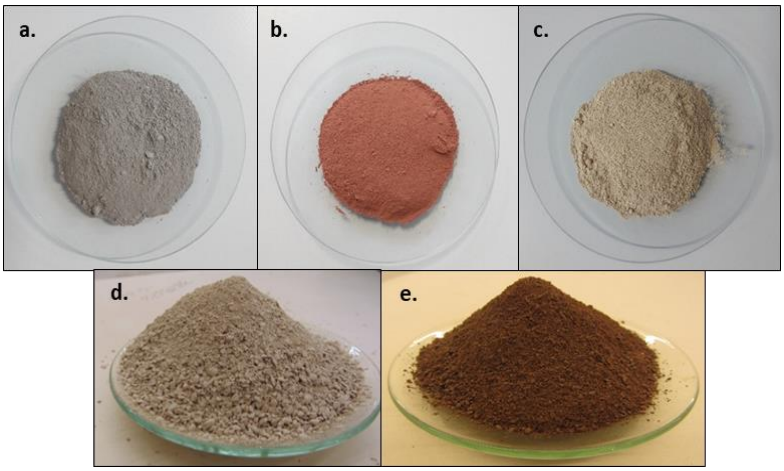

Image D.1.2.1. Clay minerals, a. Black clay, b. Red ES clay, c. Yellow clay, d. White clay and e. red IT clay.

D.1.2.1. CHEMICAL ANALYSES: ELEMENTAL, FRX, LOI, AND CARBONATES DETERMINATION (CALCIMETRY)

The elemental analysis (C-H-N-S content) of the clays minerals are shown in Table D.1.2.1.1. The carbon content, related to the organic matter (organic carbon) and $CaCO_3$ (inorganic) content,

being the white clay the one with the highest percentage 4.35% and red clays (ES and IT) the ones with the lowest. As for the values of nitrogen (N) and hydrogen (H), they remain quite the similar for all clays.

Table D.1.2.1.1. CNH-S analysis of clay minerals.

Clay Minerals	% N	% C	% H	% S
White	0.04	4.35	0.45	-
Black	0.05	3.33	0.35	0.73
Yellow	0.03	1.91	0.33	-
Red ES	0.04	1.05	0.47	-
Red IT	-	0.92	0.69	-

Clay base materials process produces many pollutants, mainly during clay extraction and processing (powder) and clay firing (F, Cl, SO_X, B, NO_X emission). In the case of F, Cl, and S, pollution depends on the concentration of such elements in the raw material (phyllo- sillicates, pyrite, gypsum, halite, apatite, carbonates), firing temperature, residence time in the kiln, and fuels type and combinations, and the type of kiln used.

The sulphur content, only registered for black clay (0.73%), can be related to pyrite, gypsum and organic matter existing in clay materials. The sintering conditions and the type of fuel, influence the gas emission and sulphur content of the finished products. In the Bailen area, the sintered materials contain more sulphur than the raw materials used, which indicates that they absorb sulphur from the fuels during thermal treatment. In all cases, are below the emission levels imposed by standards (González et al., 1998).

Concerning the N content, the concentrations for the five clays is very low or zero. The release of nitrogen compounds (NO_X) is closely related to the combustion of the fuels used by the furnace. Likewise, the concentrations of N in the raw materials must be controlled.

In table D.1.1.2, shows the results of the chemical analysis (XRF) of the clays used expressed in oxides percentages. From this data could be highlighted that the five different clays minerals present high contents of SiO_2, being the yellow clay the one with the highest value 60.40%, mostly from quartz and the rest from phyllosilicates. Concerning Al_2O_3 content, red ES is the one with the highest value 19.67%, followed by red IT 17.95%, main components of phyllosilicates minerals.

Table D.1.2.1.2. Chemical composition (XRF) of clays.

Oxides (%)	White	Black	Yellow	Red ES	Red IT
SiO_2	43,90	41,89	60,4	50,15	52,77
Al_2O_3	8,50	11,74	11,46	19,67	17,95
Fe_2O_3	3,30	4,06	4,02	8,21	7,89
MnO	0,10	0,04	0,03	0,12	0,19
MgO	2,10	1,94	1,39	3,57	3,88
CaO	20,00	15,64	8,73	2,80	2,57
Na_2O	0,20	0,27	0,38	0,02	0,66
K_2O	1,60	2,33	2,73	6,37	2,85
TiO_2	0,40	0,69	0,64	0,83	0,78
P_2O_5	0,10	0,15	0,10	0,20	-
SO_3	0,10	1,78	-	-	-
Others	-	6,24	0,58	0,20	0,56
LOI	19,90	13,23	9,54	7,86	9,90
Total	100,00	100,00	100,00	100,00	100,00

The alkaline compounds (CaO, Na_2O, and K_2O), are related to the melting capacity of clays, so their content determines the vitrification capacity and bloating behaviour of the ceramic material as a function of the sintering temperatures (Cubaud, J.C., Murat, 1969; R J Galán-Arboledas et al., 2013), conferring mechanical strength and durability. In this sense, it was observed that white and black clay have a high content of calcium oxide, 20.00%-15.64% respectively, while Red ES and Red IT have the lowest values 2.80%-2.57% respectively.

The high content of calcium oxide present in the white clay determined the proportion of the WBC clay mixture (30% of white and 70% of black), for the manufacture of the LWA_S for the agronomic purpose ($LWAS_{AP}$), due to the influence in the pH values of the manufactured materials (Farias et al., 2017a). The carbonates content was confirmed using H-D Calcimeter (Table D.1.1.3).

Table D.1.2.1.3. Carbonates content of clay minerals.

Clays Type	White	Black	Yellow	Red ES	Red IT
$CaCO_3$ (%)	34.39	16.65	9.90	5.70	4.96

The high contents of carbonates are related to materials with high porosity, presented problems in drying processes and resistance to higher temperatures (William D. Callister, 2007). The capacity to generate porosity is also related to the organic matter content in the clay minerals, and in this case, the white clay has the highest values of CaO and loss of ignition (LOI), 20.00% and 19.00% respectively (XRF). The carbonates content is again confirmed in the calcimetry results, 34.39% of $CaCO_3$ for white clay.

Concerning oxides with melting properties, red clays (IT and ES) have the highest content values of potassium, 2.85 and 6.37% respectively. Red IT clay presented the highest amount of sodium, 0.66%. These values are not related to porous ceramic materials.

The white and red (ES and IT) clays do not have an application by themselves since the plasticity values of these clays are outside the maximum, and minimum limits recommended for extrusion forming for structural ceramics (Vázquez, 2004; Vázquez et al., 2003).

The presence of iron (Fe) and titanium (Ti) is related to the chromospheres responsible for the red colouring of clays, red ES and red IT.

D.1.2.2. MINERALOGICAL ANALYSIS: X-RAY POWDER DIFFRACTION (XRD)

For the determination of the crystalline phases, each clay was analyzed by X-ray diffraction (XRD). In this kind of analysis is possible to determine the presence of plastic (clayed minerals) and non-plastic components (quartz, carbonates) in the clay minerals. From the study of XRD pattern, in which the presence of defined peaks corresponds to specific reticular distances, it is possible to identify the different crystalline phases.

The plastic fraction allows the processing of the clayed material (forming step, shaping step) and confers mechanical strength to the ceramic body. Roughly speaking, quartz in fine particle size (sand) contributes to fine-grained vitrification, and in a coarse grain form, to control the expansion behavior preventing breakage during sintering (Inert component, until approximately 1100^{o}C) (Murray, 2007). During cooling process, with high concentrations of quartz or/and large quartz grains size, it can generate many breakage problems, increasing porosity and lower its mechanical resistance, due to the appearance of cracks in ”grain edges” when differential contraction occurs between the quartz grains (shrinking due to the transformation of β-quartz in α-quartz during cooling) and the contraction of the ceramics matrix (Hortega-Huertas, 1996; Soto and Pérez Rodríguez, 1998).

The conditions, methodology, and description of X-Ray diffraction (XRD) analysis performed on clay samples are summarized in the section C.1.6. X-ray Powder Diffraction (XRD).

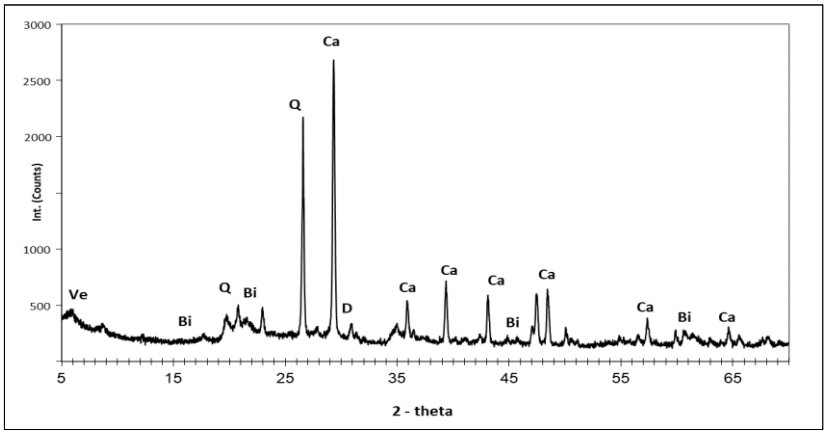

Figure D.1.2.2.1. White clay XRD. Calcite (Ca), quartz (Q), dolomite (Do) and biothite (Bi).

In Figure D.1.2.2.1, it is possible to observe the XRD analysis of white clay, where it was identified that the predominant phases correspond to calcite [$Ca(CO_3)$], (01-072-1214), and quartz [SiO_2], (01-079-1906), as it was expected in accordance with followed by dolomite [$CaMg(CO_3)_2$], (00-036-0426), and in lower quantities biothite [$K(Mg, Fe)_3AlSi_3O_{10}(OH, F)_2$], (96-900-0026).

In Figure D.1.2.2.2, it is possible to observe the XRD analysis of black clay, where the predominant phases corresponds to quartz [SiO_2], (00-046-1045) and calcite [$Ca(CO_3)$], (01-083-1762), with the presence of dolomite [$Ca,Mg(CO_3)_2$], (00-036-0426), lilite [$(K,H_3O)Al_2Si_3AlO_{10}(OH)_2$], (00-026-0911), a potassium silico-aluminate, and mica [K, Mg, Fe, Al, Si, O, H_2O], (00-002-0227).

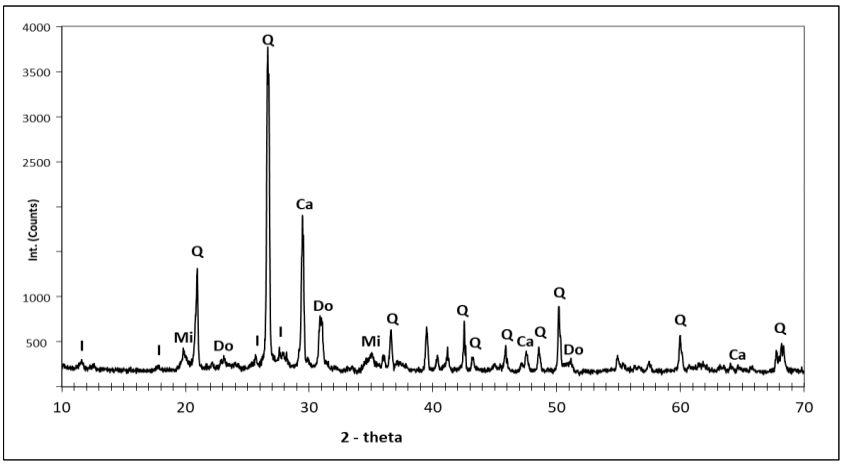

Figure D.1.2.2.2. Black clay XRD. Calcite (Ca), quartz (Q), mica (Mi), dolomite (Do) and illite (I).

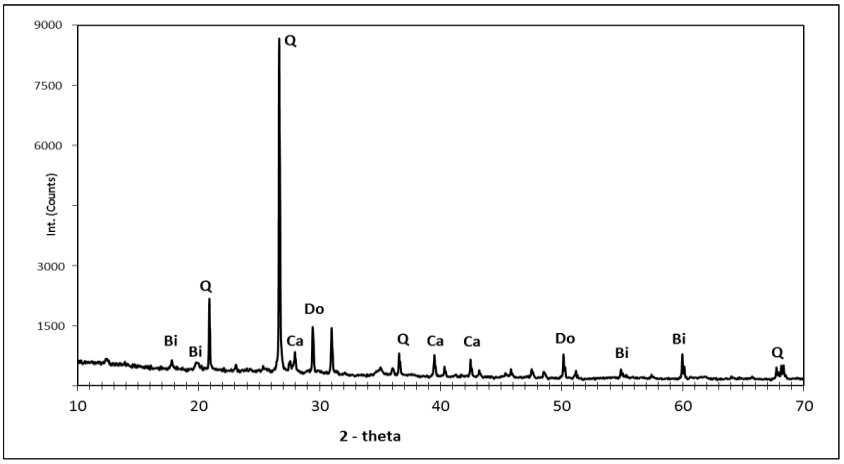

Figure D.1.2.2.3. Yellow clay XRD. Calcite (Ca), quartz (Q), dolomite (Do) and biothite (Bi).

In Figure D.1.2.2.3., it is possible to observe XRD pattern of Yellow clay, where the main phases are quartz [SiO_2], (01-079-1906) and calcite (01-072-1214), followed by dolomite (calcium carbonate and magnesium) [$(Ca,Mg)CO_3$], (00-036-0426), and biothite (96-900-0026).

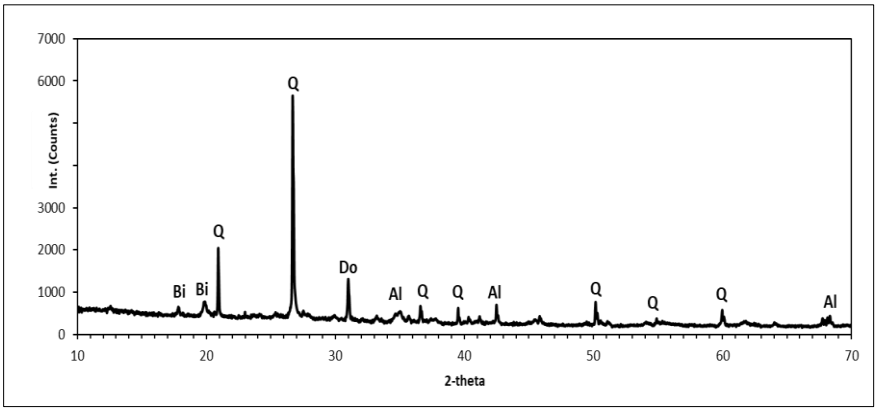

Figure D.1.2.2.4. Red ES clay XRD. Quartz (Q), biothite (Bi), dolomite (Do) and albite (Al).

In Figure D.1.2.2.4., it is possible to observe the XRD pattern of Red ES clay, where the predominant phase corresponds to quartz [SiO_2], (01-079-1906), followed by biothite [$K(Mg,Fe)_3AlSi_3O_{10}(OH,F)_2$], (96-900-0026), dolomite [$(Ca,Mg)CO_3$] (calcium carbonate and magnesium), and albite ($NaAlSi_3O_8$), (00-041-1480).

The Spanish clays minerals white, black and yellow, characterized by medium-high plasticity (phyllosilicates: smectite and illite), presenting some problems of drying (Neogene clays). By contrast, the Red ES clay (Triassic clay) contain few carbonates, with no calcite content, detected, providing low plasticity and right drying conditions (R J Galán-Arboledas et al., 2013).

The result of XRD analysis shows that white, black and yellow clays are characterized by the higher content in quartz and calcite, predominant phyllosilicates like illite, micas, smectite, and bentonite, in correlation with the chemical (XRF), mineralogical (XRD) and bibliography analysis performed.

In Figure D.1.2.2.5., it is possible to observe the XRD pattern of Red IT clay. The predominant phases corresponds to quartz [SiO_2], kaolinite [$Al_2Si_2O_5(OH)_4$], (01-078-1996), and muscovite [$KAl_2(AlSi_3O_{10})(F,OH)_2$]; with presence of calcium and magnesium (Dolomite [$(Ca, Mg)CO_3$]), and iron oxides (Hematite [Fe_2O_3]), (97-018-2848), according with chemical analysis Fe: 7.89% (XRF).

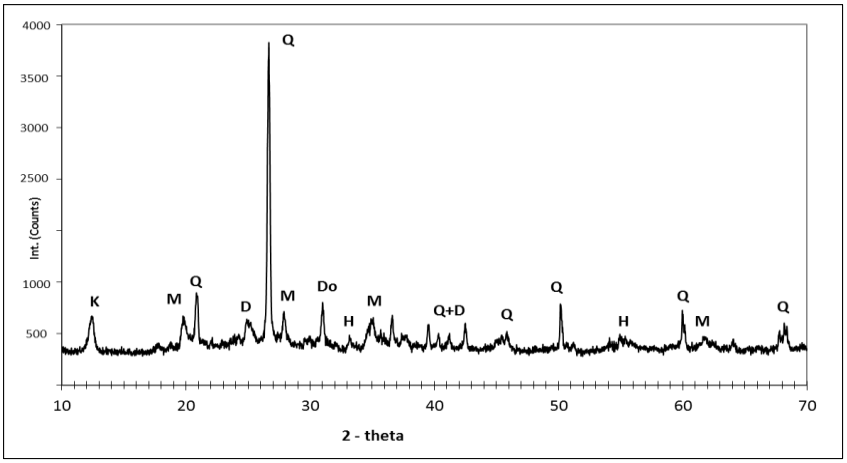

Figure D.1.2.2.5. Red IT clay XRD. Quartz (Q), dolomite (Do), kaolinite (K), hematite (H), and muscovite (M).

The two red clays (ES and IT) are very similar chemically, differing fundamentally very slightly in the content of silica, aluminum, and iron, with a significant difference in the content of potassium. Both presents, as predominant phases, quartz [SiO_2], and dolomite [$CaMg\ (CO_3)_2$]. The abundant iron content in the two red clays is reflected in the presence of biothite [$K(Mg,Fe)_3AlSi_3O_{10}(OH,F)_2$] in the red ES; hematite [Fe_2O_3], in the red IT clay.

After the analysis of all the diffraction patterns of the clays can be highlighted that they contain mainly quartz (Q) [SiO_2], calcite (C) [$CaCO_3$], biotite (Bi) (iron and aluminum phyllosilicate) and dolomite (D) [$CaMg\ (CO_3)_2$], in less proportion other phyllosilicates such as vermiculite, and plagioclase as albite (Al). The content of calcite, dolomite, pyrite, and hematite, during the thermal treatment, can produce gas at a sufficiently high temperature, and generate the expansion of the material (Riley, 1951).

D.1.2.3. THERMOGRAVIMETRIC ANALYSES (TG-DTA-DSC)

The more significant presence of calcium and magnesium carbonate in the clay influences the subsequent heat treatment since it decomposes producing the corresponding oxide with a CO_2 release. The CO_2 emission must be controlled to prevent it from happening abruptly (Aoubaa et al. 2016). This uncontrolled reaction can cause cracks or breaks in the structure of the material, with direct influence on mechanical strength and durability.

The conditions, methodology, and description of thermogravimetric analyses performed are summarized in the section C.1.7. (Thermogravimetry TG/DTA/DSC and Differential thermal analysis DTA/DSC).

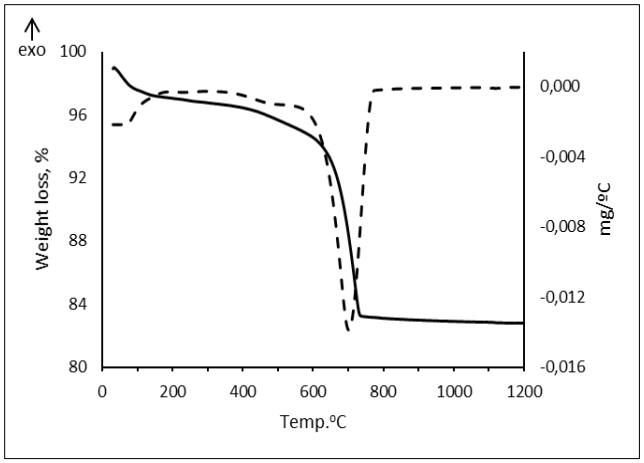

Figure D.1.2.3.1. White clay TG-DTG.

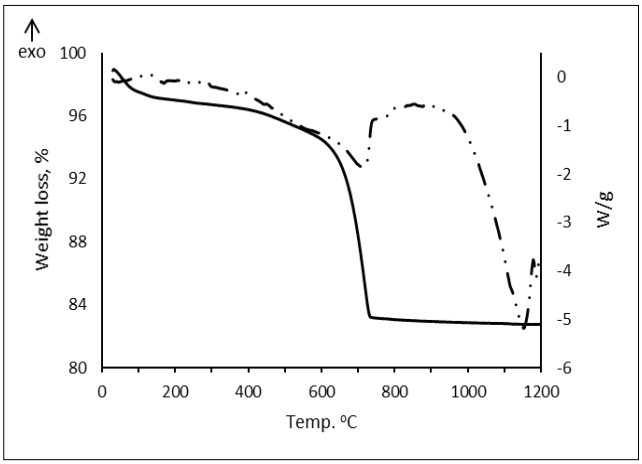

Figure D.1.2.3.2. White clay TG-DSC.

In figures D.1.2.3.1 and D.1.2.3.2, corresponding to TG-DTG-DSC analysis of white clay, were up to 200ºC the first endothermic pick appears with loss of mass and can be attributed to the loss

of moisture (free water adsorbed by the clay particles, around 100°C, and elimination of the water hydration of the interchangeable ion present in smectite structure, about 180°C.

From 200°C to 400°C, the DTG curve shows a relatively wide and slightly pronounced upward, exothermic band due to the combustion of the organic matter present in the clay mineral. From the 550°C the dehydroxylation of the clay mineral takes place, causing loss of mass, due to the loss of internal water, -OH groups, in the form of clay, an endothermic reaction. Between 700-800°C, takes place the decomposition of the carbonates, mainly calcium carbonate present in the sample, a significant mass loss of about 12%, endothermic phenomenon, by the high calcium oxide content revealed in the XRF analysis (20.00%) and calcimetry (34.39%). Over 800°C the TG curve is fundamentally flat, demonstrating the absence of additional weight loss. Weight loss, are in agreement with the loss of ignition (LOI) values related to the chemical analysis (XRF) (19.90%). The DSC curve shows an endothermic peak at 700-800°C relative to carbonates decomposition and an exothermic peak around 920°C, it is due to the formation of crystalline calcium phases, such as wollastonite, anorthite; neoformed by the reaction between CaO from the decomposition of the carbonates and the SiO_2 and AL_2O_3 from the decomposition of the structure of the clay minerals.

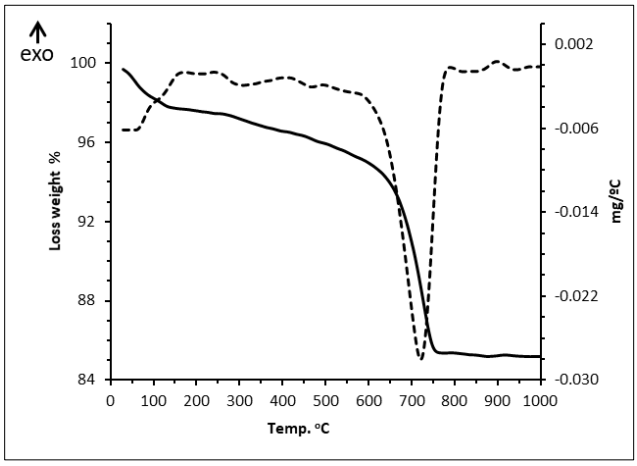

Figure D.1.2.3.3. Black clay TG-DTG.

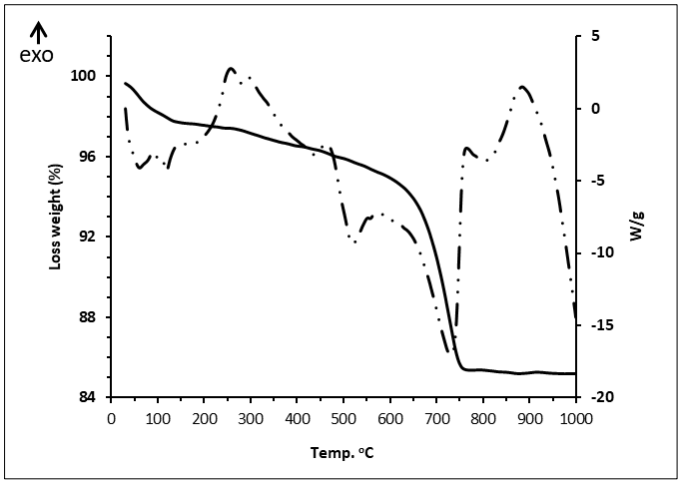

Figure D.1.2.3.4. Black clay TG-DSC.

In the TG-DTG-DSC of the black clay, figure D.1.2.3.3 and D.1.2.3.4 can be analyzed and observed that up to 200°C, two small endothermic peaks can be attributed to the loss of moisture. These two peaks are less pronounced compared with white clay, due to the black clay have less smectite content. Between 250-450°C, the oxidation of the organic matter begins to produce an exothermic peak. Up to 500°C the dehydroxilación (another endothermic peak corresponding to the elimination of water present in the phyllosilicates) of the clay mineral takes place and causes a loss of mass. A more massive loss of mass due to the decomposition of the carbonates which corresponds to 7%, in agreement with the calcium content found by XRF analysis (15.64%) and calcimetry (16.65%). The DTG curve shows two exothermic peaks at 800-850°C and 900-950°C relative to carbonates decomposition.

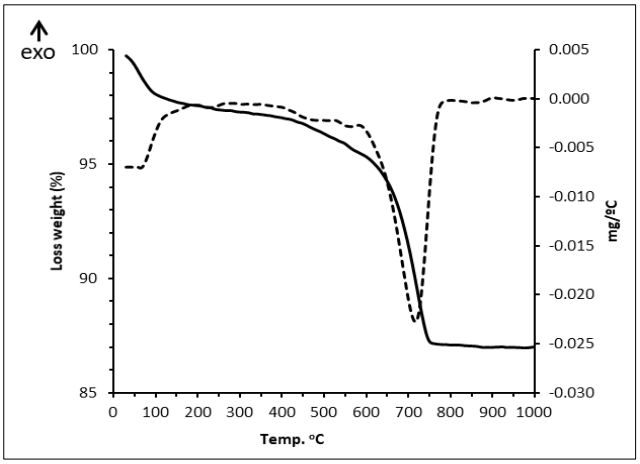

Figure D.1.2.3.5. Yellow clay TG-DTG.

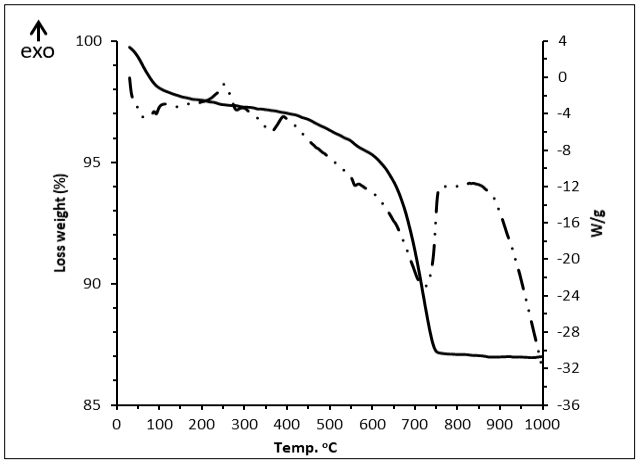

Figure D.1.2.3.6. Yellow clay TG-DSC.

In figures, D.1.2.3.5 and D.1.2.3.6 corresponding to yellow clay are evident: a loss of free water around 90ºC, endothermic event, the combustion of organic matter at 250ºC with a loss of weight, exothermic event, loss of water in the form of hydroxyl groups, dehydroxylation of clay (around 450ºC). Endothermic peak at 573ºC due to the allotropic transformation of quartz. It appears in the yellow clay because it has the highest silica content (60.40%-XRF) and in agreement with XRD analysis. Decomposition of carbonates around 700ºC, endothermic event and finally melting (about 1000ºC), endothermic event.

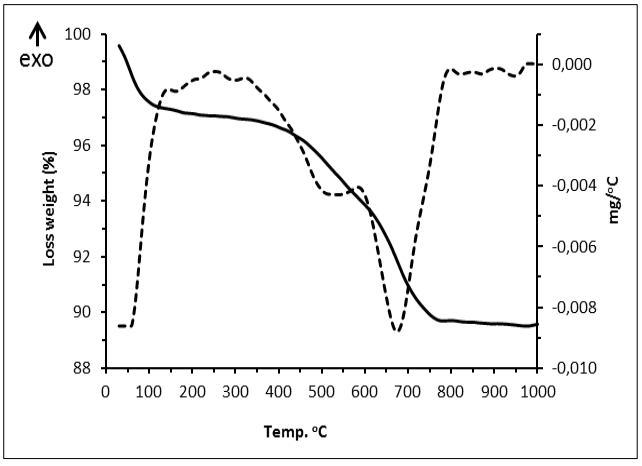

Figure D.1.2.3.7. Red ES clay TG-DTG.

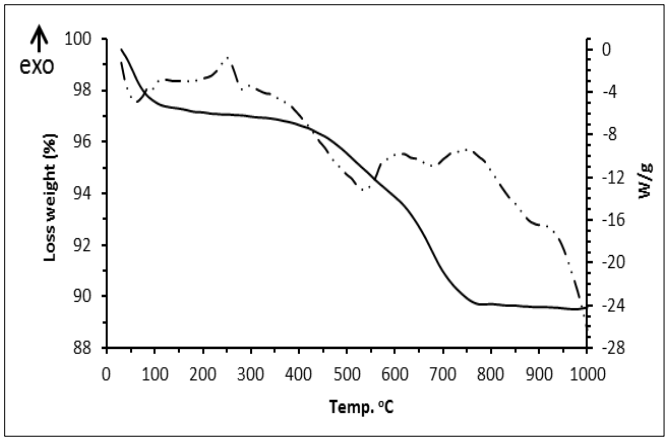

Figure D.1.2.3.8. Red ES clay TG-DSC.

In figures D.1.2.3.7 and D.1.2.3.8, corresponding to red ES clay are presents a loss of free water around 85°C, endothermic event, the combustion of organic matter between 200-300°C with a loss of weight, exothermic event, loss of water in the form of hydroxyl groups, dehydroxylation of clay (around 550°C). The decomposition of carbonates occurs around 650°C, exothermic event, red ES clays do not contain carbonates in the form of calcite, but dolomite (in agreement with XRD analysis), that is why the decomposition occurs at a previous temperature than in the other analyzed clays. Exothermic peak around 920°C, due to the formation of crystalline calcium phases.

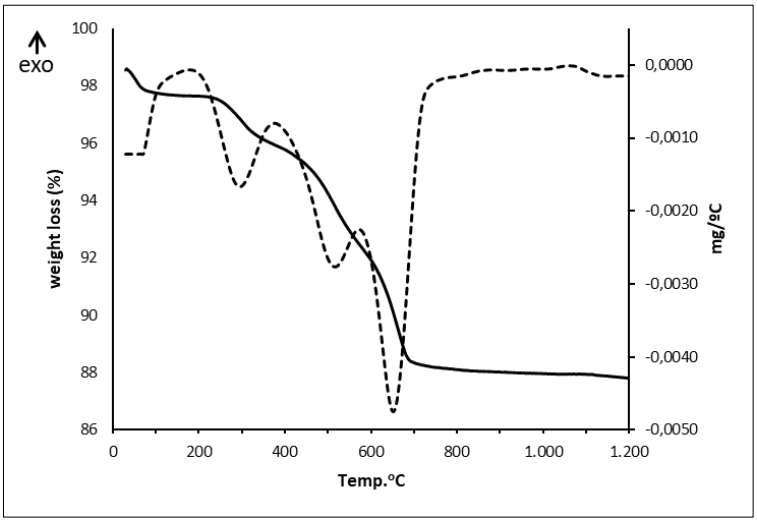

Figure D.1.2.3.9. TG-DTG Red IT.

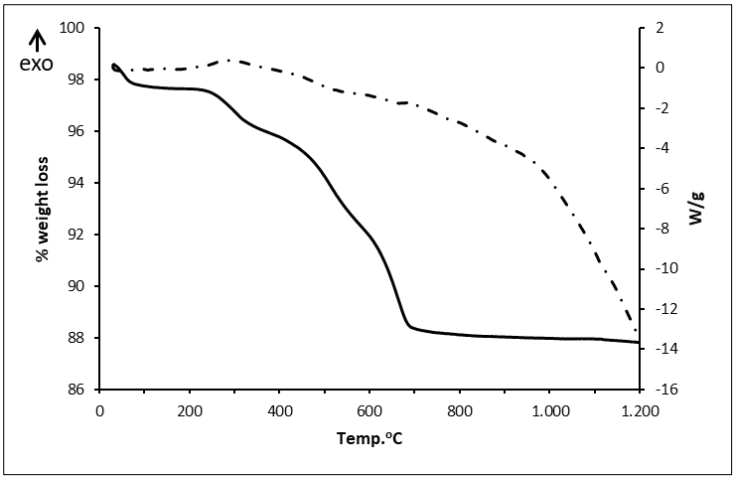

Figure D.1.2.3.10. Red IT TG-DSC.

In Figure D.1.2.3.9 and D.1.2.3.10, corresponding to red IT clay presents a loss of free water approximately 50ºC and 150°C (0.625%), endothermic event. Between 250-450°C the combustion of organic matter with a loss of weight of 1.70%, exothermic event, loss of interlayer water in the form of hydroxyl groups, dehydroxylation of clay (around 550ºC), endothermic event, with a loss of weight of 3.40%. Around 650ºC, the decomposition of the carbonates in calcium oxide and carbon dioxide provokes an endo-peak with a loss of weight around 4.40%, by XRF analysis with a CaO content of 2.57% and calcimetry (4.96%). Finally melting (around 1200ºC), endothermic event. Summarizing the weight losses (humidity, dehydroxylation and carbonate decomposition) agree with the LOI of 9.90% from XRF analysis.

D.1.2.4. PARTICLE SIZE DISTRIBUTION ANALYSIS (GRANULOMETRIC)

The particle size distribution is an index that indicates what sizes are present in what proportions (relative particle quantity as a percentage where the total amount of particles is 100 %) in the sample particle group to be measured.

Frequency distribution indicates the amounts of particles existing in respective particle size intervals after the range of target particle sizes are divided into separate intervals (%). Cumulative distribution (for particles passing the sieve) expresses the percentage of the amounts of particles of specific particle size or below. Alternatively, cumulative distribution (for particles remaining on the sieve) expresses the percentage of the amounts of particles of specific particle size or above.

After grinding process of the clay minerals, all were submitted to the same procedure of particles size measurement. The results of the particle size analysis, are presented as frequency

distributions or/and cumulative curves, figure D.1.2.4.1 - D.1.2.4.5. From the different graphs, it is possible to observe, the characteristic diameters D_{10}, D_{50}, D_{90} corresponding to the diameters below which is the 10%, 50%, and 90% respectively of the particle size distribution (continuous cumulative curve). The results were reported according to the equivalent spherical diameter (ESD), defined as the diameter of the sphere equal to the maximum particle size.

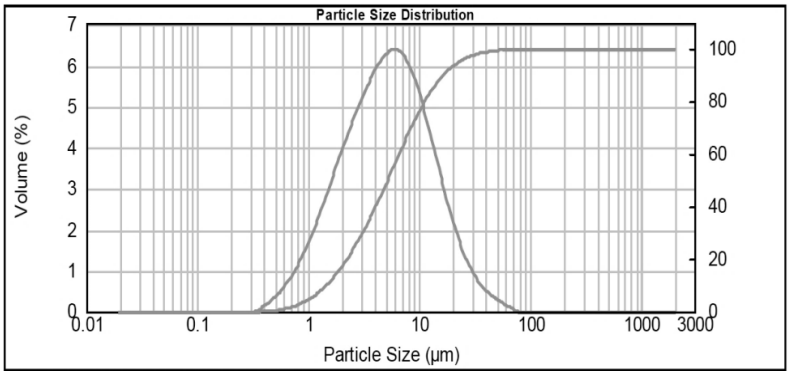

Figure D.1.2.4.1. Particle size distribution analysis of white clay.

In figure D.1.2.4.1, corresponding to white clay, it is evident a most likely uniform Gaussian distribution with a maximum of 6.5 µm. About the characteristic diameters, 10% powders have has a diameter lower than 1.80 µm, 50% lower than 5.00 µm, and 90% lower than 16.00 µm.

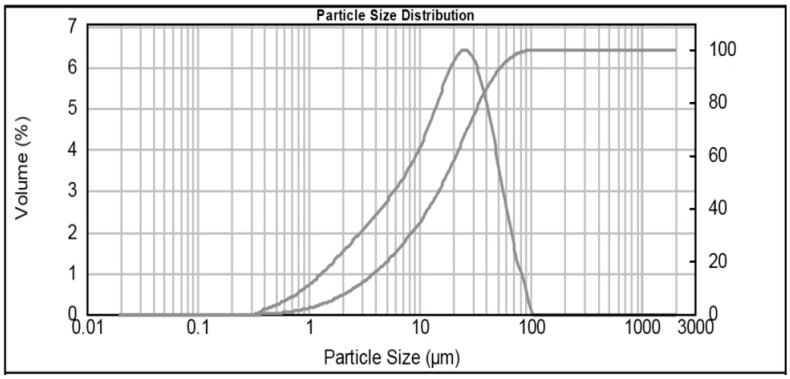

Figure D.1.2.4.2. Particle size distribution analysis of black clay.

In figure D.1.2.4.2, corresponding to black clay, it is evident a Gaussian distribution with a maximum of 6.40 µm. The characteristic diameters, 10% of the dust has a diameter lower than 1.80 µm, 50% lower than 18.00 µm, and 90% lower than 13.00 µm.

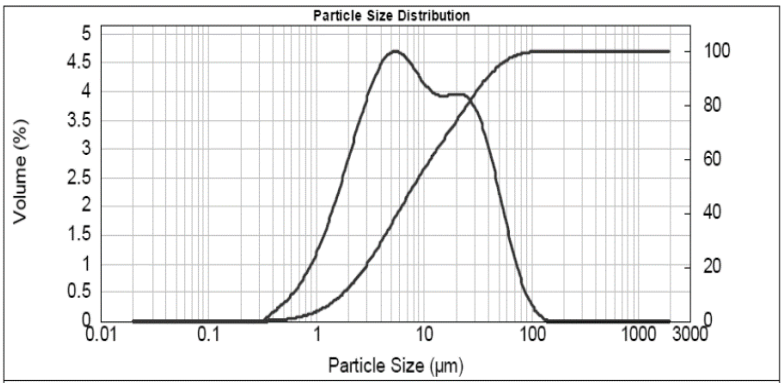

Figure D.1.2.4.3. Particle size distribution analysis of yellow clay.

In figure D.1.2.4.3, corresponding to yellow clay, it is evident a non-uniform Gaussian distribution with a maximum of 4.60 µm and with another pick at 4.00 µm. The characteristic diameters, 10% of the dust has a diameter lower than 1.90 µm, 50% lower than 8.30 µm, and 90% lower than 13.00 µm.

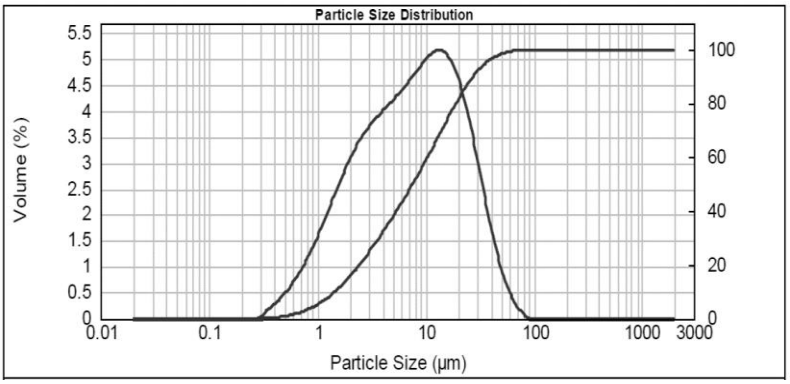

Figure D.1.2.4.4. Particle size distribution analysis of Red ES clay.

In figure D.1.2.4.4, corresponding to red ES, it is evident a Gaussian distribution with a maximum of 5.20 µm. The characteristic diameters, 10% of the dust has a diameter lower than 1.50 µm, 50% lower than 8.00 µm, and 90% lower than 11.00 µm.

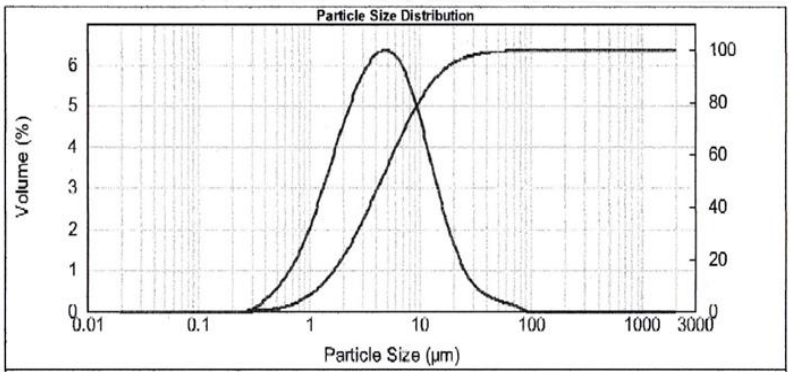

Figure D.1.2.4.5. Particle size distribution analysis of Red IT clay.

In figure D.1.2.4.5, corresponding to red IT clay, there is a uniform Gaussian distribution with a maximum of 6.50 µm. About the characteristic diameters, 10% of the powders have a diameter lower than 1.28 µm, 50% lower than 4.45 µm, and 90% lower than 14.29 µm.

D.1.2.5. CLAY-BASED MIXTURES THERMAL BEHAVIOR ANALYSIS

It was analyzed the three clay base mixtures used in this research for the formulation of LWA_S for drainage layer for green roofs and as growing media for agronomic purposes. As a reminder:

- **BYRC.** Black, yellow and red ES clay in equal parts, for the elaboration of LWA_S for drainage layer in green roofs ($LWAS_{GR}$).
- **WBC.** 30% white and 70% black clay, for the elaboration of LWA_S for agronomic purposes ($LWAS_{AP}$).
- **RC.** 100% red IT clay, for the elaboration of LWA_S for agronomic purposes ($LWAS_{AP}$).

D.1.2.5.1. CLAY-BASED MIXTURES THEORETICAL CHEMICAL COMPOSITION

In Table D.1.2.5.1, can see the theoretical chemical composition, calculated from the chemical analysis (FRX) listed in table D.1.2.1.2, and based on the different proportions of the clay mixtures used for the elaboration of the sustainable LWA_S ($LWAS_{GR}$ and $LWAS_{AP}$).

Table D.1.2.5.1.1. clay-base mixtures theoretical chemical composition.

Oxides (%)	BYRC	WB	RC
SiO_2	50.81	42.49	52.77
Al_2O_3	14.29	10.77	17.95
Fe_2O_3	5.43	3.83	7.89
MnO	0.06	0.06	0.19
MgO	2.30	1.99	3.88

CaO	9.06	16.95	2.57
Na_2O	0.22	0.25	0.66
K_2O	3.81	2.11	2.85
TiO_2	0.72	0.60	0.78
P_2O_5	0.15	0.14	-
SO_3	0.59	1.28	-
Others	2.34	4.37	0.56
LOI	10.21	15.23	9.90
Total	100.00	100.00	100.00

D.1.2.5.2. THERMOGRAVIMETRIC ANALYSES (TG-DTA-DSC)

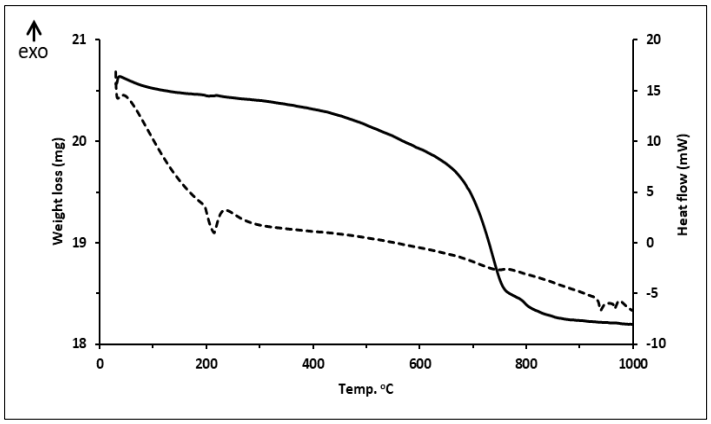

Figure D.1.2.5.2.1. TG-DSC clay based mixture for $LWAS_{GR}$ (BYRC)

The clay-based mixture named BYRC produces a small endothermic peak around 50°C that can be attributed to moisture loss, 2% weight loss (figure D.1.2.5.2.1). As temperature increases, weight loss increases. At 200°C, another major endothermic peak corresponds to the elimination of interlaminar water present in the phyllosilicate clays. As the temperature increases, begins the oxidation of organic matter, an exothermic peak appears. The dehydroxylation of the clay mixture occurs at 500°C, causing mass loss. Between 700-850°C decomposition of carbonate takes place, clays arise producing calcium oxide (CaO) and carbon dioxide (CO_2). Between 900-1000°C, peaks associated with the formation of calcium silicates.

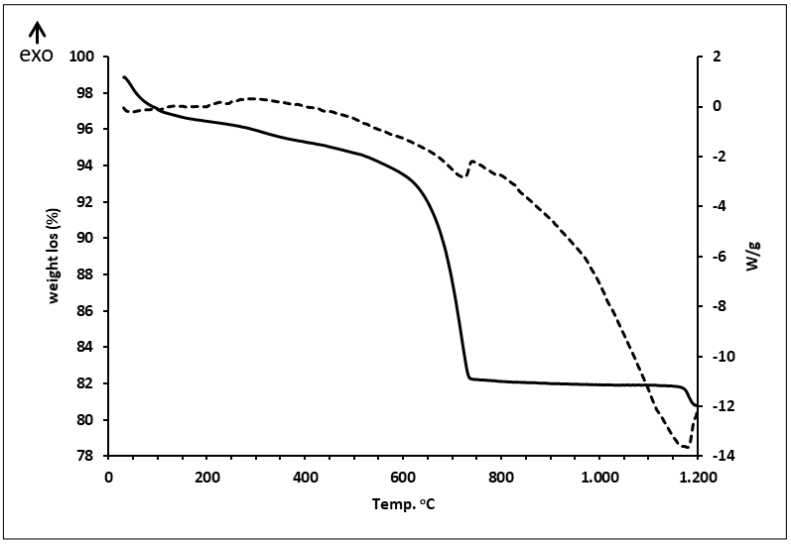

Figure D.1.2.5.2.2. TG-DSC of clay-based mixture for $LWAS_{AP}$ (WBC)

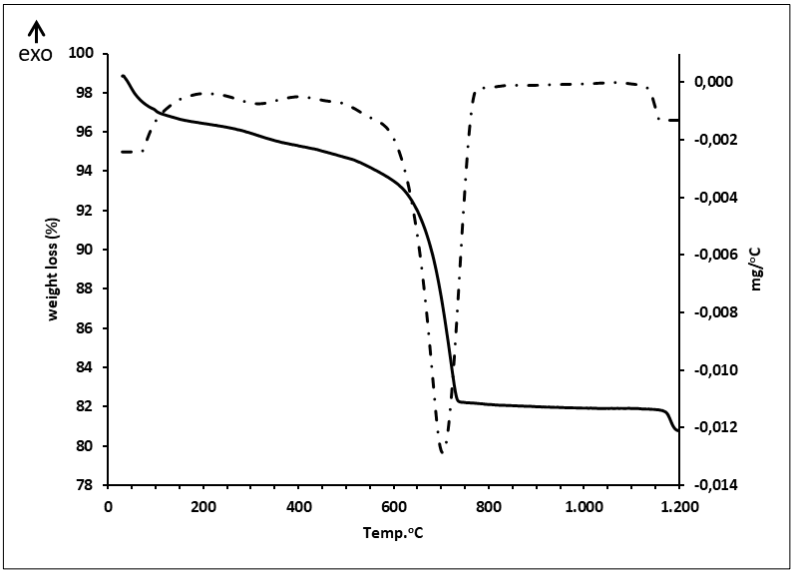

Figure D.1.2.5.2.3. TG-DTG of clay-based mixture for $LWAS_{AP}$ (WBC)

In the TG-DTG-DSC of the clay-based mixture WBC (30% white and 70% black clay), figure D.1.2.5.2.2 and D.1.2.5.2.3 can be analyzed and observed a small endothermic peak at approximately 50°C that can be attributed to the loss of moisture. As the temperature rises above 200°C, the oxidation of the organic matter begins to produce an exothermic peak. Up to 500°C the dehydroxilación (another endothermic peak corresponding to the elimination of the interlaminar water present in the phyllosilicates) of the clay mineral takes place and causes a loss of mass. A more massive loss of mass between 700-850°C is observed due to the decomposition of the carbonates. This peak is displaced to the right by the increase of the carbonates present in the white clay.

TG-DTA-DSC corresponding to RC clay based mixtures (100wt% red IT) was analyzed in D.1.3.1 (Clay minerals), figure D.1.2.3.9 and D.1.2.3.10.

D.1.2.5.3. THERMO-MECHANICAL DILATOMETRY ANALYSIS

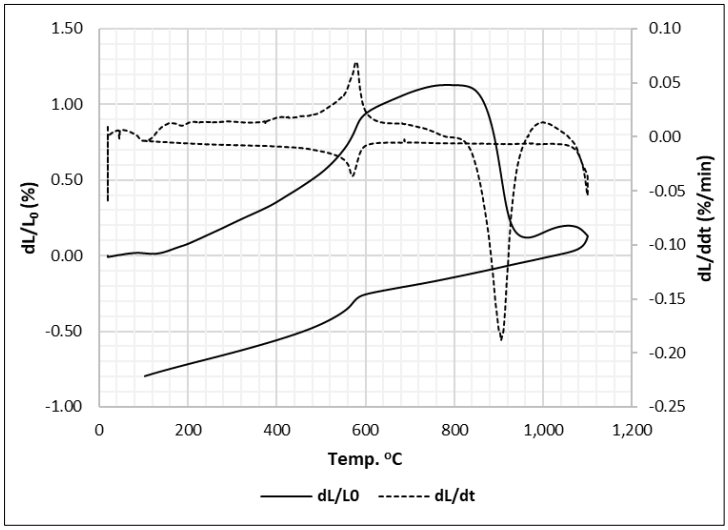

D.1.2.5.3.1. Dilatometry analysis of clay-base mixture for $LWAS_{GR}$ (BYRC)

The dilatometric analysis is shown in figure D.1.2.5.2.1 corresponding to BYRC clay-based mixture. Up to 550°C, there is a contraction between 150°C and 200°C due to the presence of smectite (R J Galán-Arboledas et al., 2013). The increase in the temperature range of 550-600°C is explained by the presence of free quartz (from quartz α to quartz β) and causes an expansion, confirmed by a peak in the values of the first derivative; also related to the loss of water chemically bound with clay minerals (deoxidrilation). From 600°C the expansion loses intensity reaching maximum value approximately at 800°C for this mixture, was maximum expansion value reached, due to the decomposition of carbonates, in correlation with TG-DTA in Figure D.1.2.5.1.1. The sintering process causes material contraction, reaching its maximum speed at 920°C. At 900°C, reactions between the clay material and the cations present in the clay occur, mainly the Ca2 (+) generated in the decomposition of the carbonates. This reaction produces a new expansion of the material, which is maintained up to 1050°C, from this temperature, the calcic phases begin to melt. During the cooling process, between the maximum test temperature, 1100 and 600°C, the cooling rate can be relatively fast, due to the low contraction behavior in a relatively pyro plastic state.

From this temperature, the cooling process up to the room temperature should be carried out at lower speeds, to accommodate the residual stresses caused by the quartz transformation

between 600-500°C, the cooling process up to the room temperature should be carried out at lower speeds to prevent cracks and the weakening of the material structure.

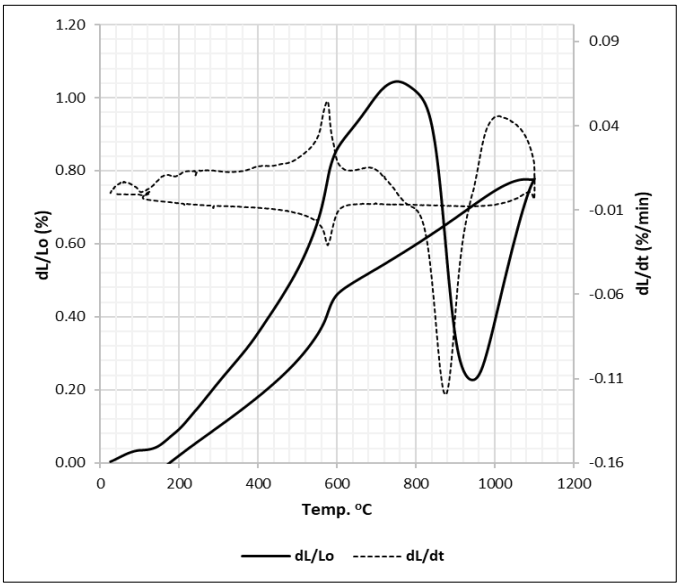

Figure D.1.2.5.3.2. Dilatometry analysis of clay-base mixture for $LWAS_{AP}$ (WBC)

The dilatometric analysis is shown in figure D.1.2.5.3.1 corresponding to WBC clay-based mixture. At 500°C, a continuous initial expansion takes place in which a higher intensity slope is observed through the derivative of the length concerning time (dL/dt).

The increase in the temperature range of 500-600°C is explained by the presence of free quartz, whose phase change occurs at 573°C (from quartz α to quartz β) and causes an expansion, confirmed by a peak in the values of the first derivative. From 600°C the expansion loses intensity reaching maximum value around 750°C for this mixture. This stabilization temperature of the expansion is lower when higher is the carbonate content of the clays, due to their decomposition. The maximum dilatation value can vary with the clay granulometry and the quartz content, i.e., higher quartz concentration, higher expansion; higher granulometry, the higher dilation. From this temperature, occurs a turning point of the curve expansion because of the beginning of the sintering of clay particles. The sintering process causes material contraction, reaching its maximum rate at 875°C. At 950°C, solid state reactions between the oxides free from the clay and the cations Ca^{2+} generated in the decomposition of the carbonates produce calcium silicate and silico-alluminates. This reaction produces a new expansion of the material. During the cooling process, between the maximum test temperature, 1100 and 600°C, the cooling rate can be relatively fast, due to the low contraction behavior in a relatively pyro plastic state, indicating that the material can be adapted to stresses derived from the cooling.

From this temperature, the cooling process up to the room temperature should be carried out at lower speeds, to accommodate the residual stresses caused by the quartz transformation between 600-500ºC.

The thermal decomposition of dolomite, $CaMg(C0_3)_2$, and calcite, $CaCO_3$, leads to the release of carbon dioxide, CO_2. In the case of dolomite, it is thought that the considerable dilatation observed can be explained by its decomposition in two stages, around 750°C and 900°C. These temperatures are low, and also Riley (Riley, 1951) has assumed that an intermediate compound that retains part of CO_2 would form, dissociating at higher temperatures. It has been shown that dolomite is an excellent agent of expansion, better than calcite (Cubaud, J.C., Murat, 1969).

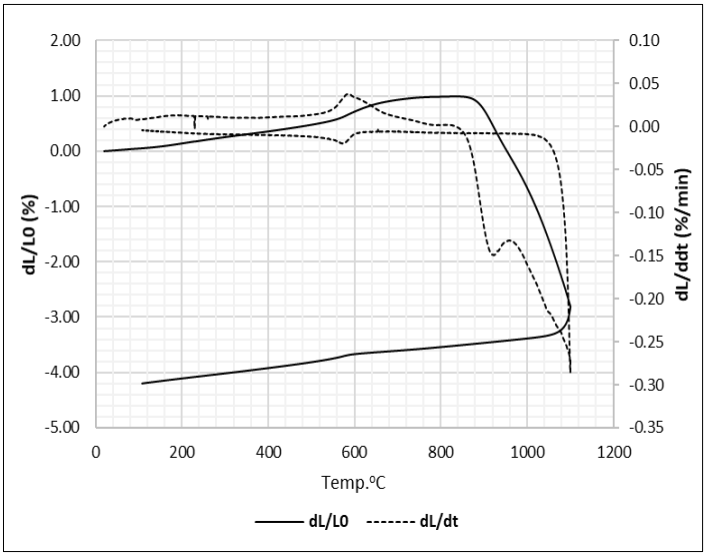

Figure D.1.2.5.3.3. Dilatometry analysis of clay-base mixture for $LWAS_{AP}$ (RC)

The red clay IT (RC) was found to be more thermally stable than the others two clay mixtures (BYRC and WBC), figure D.1.2.5.3.3. Almost up to 600ºC, a continuous expansion takes place in which a higher intensity slope is observed through the derivative of the length concerning time (dL/dt).

The increase in the temperature range of 550-600ºC is explained by the presence of free quartz (from quartz α to quartz β) causes an expansion, confirmed by a peak in the values of the first derivative; also related to the loss of water chemically bound with clay minerals (deoxidrilation). From 600ºC the expansion loses slightly its intensity reaching maximum value approximately at 850ºC. The sintering process causes material contraction, reaching its maximum speed at 900ºC. At 900ºC, reactions between the clay material and the cations present in the clay occur, mainly

the Ca2 (+) generated in the decomposition of the carbonates. This reaction produces a new expansion of the material, which is maintained up to 1100^{o}C.

The sintering process of the Italian red clay (red IT) is different to the mixtures formulated with Bailen clays. It presents a fluxing behavior, indicated by continuous contraction of material during thermal treatment, illitic behavior.

D.2. WASTE/BY-PRODUCTS/TECHNICAL NUTRIENTS

D.2.1. RECEPTION CONDITION

The residues derived from the production of beer and were provided by Heineken S.A., located in Jaen province.

The brewery sludge (BS) was delivered with a moisture content of 15-55%, classified as non-hazardous waste, EWC 02-07-05 (Wastes from the production of alcoholic and non-alcoholic beverages (except coffee, tea, and cocoa), sludges from on-site effluent treatment). The treatment plant only receives water effluents from the industrial processes, alimentary grade, not treating the other effluents coming from the secondary process related to de production of beer. It presents a consistency like mud and strong smell, due to the decomposition of organic matter. After drying, the material presented itself as hard stones, and it was subjected to grinding in a hammer mill.

Image D.2.1.1. Brewery sludge (BS).

Bagasse (BB) is the spent grains of malt, fibrous matter that remains in the filtration after maceration of the wort (must). This residue is stored and delivered with 40-60% moisture content approximately. Is considered as a non-hazardous waste, classify as EWC 02-03-05 (sludge from on-site effluent treatment. Wastes from fruit, vegetables, cereals, edible oils, cocoa, coffee, tea and tobacco preparation and processing; conserve production; yeast and yeast extract production, molasses preparation and fermentation).

Diatomaceous earth (DE) is a residue derived from clarification process in the beer filtration. This residue is stored and delivered with 100-200% moisture content. This residue is considered as non-hazardous waste, EWC 02-03-01 (sludge from washing, cleaning, peeling, centrifuging and separation. Wastes from fruit, vegetables, cereals, edible oils, cocoa, coffee, tea and tobacco preparation and processing; conserve production; yeast and yeast extract production, molasses preparation and fermentation).

Image D.2.1.2. Diatomaceous earth (DE).

Meat-bone meal (MBM) and cattle-bone ash (CBA) were provided by SAPI S.p.A, located in Castelnuovo Rangone, Italy. Related to the collection, disposal, and rendering service to the agro-food industry by processed animal proteins animal fats and used cooking oils. MBM is coarse-grained flour, without needing grinding proceed directly to the sieving, up to 1000 µm/1.00 mm grain sizes. A tiny number of tiny bones were retained in the sieve.

CBA is the residue of cattle bones faired for 2 hours at 900^{o}C. After thermal treatment, the CBA was ground with a ball mill and sieved up to 1000 µm/1.00 mm.

MBM and CBA could be used as raw materials for animal feeding or disposed of as waste, classify as EWC 02-02-02 (animal-tissue waste. Wastes from the preparation and processing of meat, fish and other foods of animal origin), depending on the market for that waste.

Image D.2.1.3. Right: meat-bone meal (MBM) and left: cattle-bone ash (CBA).

Corn cob used in this research was collected in the Emilia Romania Region, Italy. It is a woody residue with a fibrous heart, so its grinding has been done first with a ceramic mortar to reduce it in smaller pieces and then by using an electric coffee grinder.

Image D.4.2.1.4. Corn cob (CC) flour.

Glassy sand® (GS) was provided for Sasil s.p.a, located Brusnengo, Biella province, in the province of Biella, Italy. GS is a claimed glass derived from the secondary treatment, not classified as waste; it is a commercial product with characteristics for glassworks.

Image D.4.2.1.5. Glassy Sand®.

The potassium carbonate (K_2CO_3) used in the elaboration of the fertilizer glass (FG) is for industrial grade and was supplied by Colorobbia Italia s.p.a.

D.2.2. WASTE/BY-PRODUCTS CHARACTERIZATION.

D.2.2.1. ORGANIC WASTE/BY-PRODUCTS.

D.2.2.1.1. CHEMICAL (ELEMENTAL, FRX, LOI), CALORIMETRY, CALCIMETRY AND ORGANIC MATTER DETERMINATION.

Table D.2.2.1.1.1. CNH-S analysis of organic waste/by-products used.

Technical Nutrients	N%	C%	H%	S%
Brewery sludge (BS)	3.02	23.45	3.32	0.08
Brewery Bagasse (BB)	4.81	48.14	7.58	-
Meat-bone meal (MBM)	8.34	31.72	4.32	2.16
Corn cob (CC)	2.70	39.10	5.00	-

In table D.2.2.1.1.1, the elemental analysis is observed. The bagasse has the highest percentage of carbon (48.14%), follows by corn cob (39.10%) which is related to the organic nature of this residue. On the other hand, the carbon content of sludge from wastewater treatment plant, suggests an organic-inorganic chemical nature. These results are also related to de HHV and LHV in table D.2.2.1.1.2.

The presence of sulfur in the raw materials could lead during sintering proses, to be realized some compounds with environmental impact. Oxidation during the combustion process of this compound generates significant SO_2 and, to a lesser extent (less than 3%), SO_3. Although the rotary kiln has a highly reducing atmosphere, it is necessary to control the levels of this compound in the raw materials.

The amounts of carbon and hydrogen in the waste were determined by the calorific power obtained in the calorimetric analysis (Table D.2.2.1.1.2.). The heating value of a specific substance is the amount of heat released during the combustion of a specified amount of it. The energy value is a characteristic of each substance. It is measured in units of energy per unit of the substance (C.1.8. Calorific power determination).

The high hitting value (HHV) of corn cob and bagasse are similar to other alternative fuels, e.g., rice husk (Carter et al., 1982; Chiang et al., 2009; Chindaprasirt et al., 2009; Kadir and Ariffin, 2013) and sugarcane bagasse (Monteiro and Vieira, 2014; Zhang, 2013). These wastes could be used to save part of the fuel used in LWA_S manufacturing to fulfill the heating requirements.

D.2.2.1.1.2. Higher heating value (HHV, Kcal/Kg) and lower heating value (LHV, Kcal/Kg) determination.

Organic waste/by products	HHV (Kcal/Kg)	LHV (Kcal/Kg)
Brewery sludge	1243.52	1001.33
Bagasse	4766.03	4387.47
Meat-bone meal	3375.93	3148.48
Corn cob	4392.48	4129.23

In Table D.2.2.1.1.3, the chemical analysis (XRF) of the technical nutrients (agro-waste) is reported. BS and CBA show high amounts of calcium oxide (CaO), 26.45% and 53.89%, respectively (Table D.2.1.3). BS shows a high loss of ignition value (LOI) due to organic matter content flowed by MBM, suitable as a pore-forming agent, while CBA present a high P content, confirming their use as a nutrient source for fertilizer purposes. The results obtained from the XRF analysis show absence of toxic substances for possible agricultural use. In the case of MBM, the data show a high content of CaO and P_2O_5 and other oxides such as Na_2O, SiO_2, K_2O, and MgO.

Table D.2.2.1.1.3. Chemical composition (XRF) of organic waste/by-products.

Oxides	Brewery sludge ash	Bagasse ash	Meat-bone meal	Cattle bone-ash	Corn cob ash
Av.	**BS**	**BB**	**MBM**	**CBA**	**CC**
SiO_2	53.32	45.33	0.30	0.43	38.74
Al_2O_3	4.31	0.29	0.06	0.02	2.59
Fe_2O_3	2.42	0.97	0.24	0.01	1.48
MnO	0.04	0.13	-	-	0.84
MgO	1.00	4.60	0.23	1.11	2.32
CaO	26.45	6.30	21.75	53.89	1.92
Na_2O	1.43	0.24	0.54	1.40	0.63
K_2O	0.72	2.89	1.44	0.04	36.92
TiO_2	0.33	0.05	0.02	0.01	-
P_2O_5	8.59	25.29	8.02	41.24	7.31
ZrO_2	-	-	-	0.02	-
Cl	-	-	2.03	-	-
ZnO	-	-	0.07	-	-
Cr_2O_3	-	-	-	0.01	-
SrO	-	-	0.07	0.02	-
BaO	-	-	-	0.01	-
SO_3	-	-	1.86	0.05	-

PbO	-	-	-	-	-
LOI	1.39	2.82	63.39	1.74	1.25
Others	-	11.09	-	-	6.00
Total	100.00	100.00	100.00	100.00	100.00

The loss of ignition value (LOI) was determined by weighing an approximate amount of 1.00 g of the sample previously dried at 105°C for one hour. The samples were calcined for 2.00 hours at 1050°C (C.1.4. Loss of ignition (LOI)).

Brewery sludge (BS), bagasse (BB) and corn cob (CC) LOI values are 53.75%, 95.31% and 98.93% respectably. For chemical analysis, BS, BB and CC samples were submitted to thermal treatment at 600°C for 1 hour. The LOI value of their ashes is 1.39%, 2.82%, and 1.25% respectively. It can be noticed that the main oxide in BB and CC mineral ashes are silica and phosphorus and silica and potassium oxide respectively.

To determinate the carbonate content in BS, a calcimetry using H-D Calcimeter was performed (C.1.2. Carbonates determination), with a result of 25.24% of carbonates in the sample.

Table D.2.2.1.1.4. Organic matter content determination.

Organic waste/by-products	Organic matter content (%)
Brewery sludge (BS)	41.18
Bagasse (BB)	94.68
Meat-bone meal (MBM)	61.10
Corn cob (CC)	97.29

In Table D.2.2.1.1.4 shows the quantification of organic matter content (OMC) by calcination, carried out with the method proposed by Navarro and Col. (1993) (C.1.5. Organic matter content determination).

The high percentages of matter content are related to the organic carbon and its combustion, derivate, in the case of CC and BB to its cellulose content. For this reason, these residues are used as pore-forming agents in this research, since its combustion favours the generation of a porous matrix. During the sintering process, cellulose fibres burned and vacant holes that formed in their locations inside the clay matrix (Sutcu and Akkurt, 2009). Also, micro-pores occurred due to the decomposition of calcium carbonate. Calcium carbonate is used as pore forming agent in the manufacture of porous materials (Sutcu et al., 2014).

D.2.2.1.2. MINERALOGICAL ANALYSIS: X-RAY POWDER DIFFRACTION (XRD)

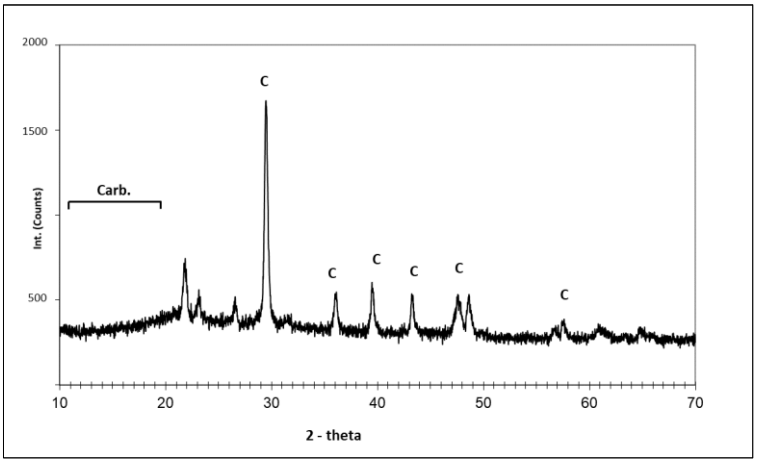

Figure D.2.2.1.2.1. XRD of brewery sludge (BS). Calcite (C) and carbon (Carb).

In figure D.2.2.1.2.1, corresponding to XRD of BS, it can be interpreted that the predominant crystalline phase corresponds to the calcite [$Ca(CO_3)$], (00-024-0027), related to the XRF analysis with CaO content of 26.45% and carbonates determination of 25.24% (calcimetry). The wideband (10-20°2Θ) indicate the presence of an amorphous phase, corresponding to the carbon present in the sample related to the organic matter. The peak near 22° (2Θ) might correspond to cellulose derivate from the malt (bagasse) use in the beer production.

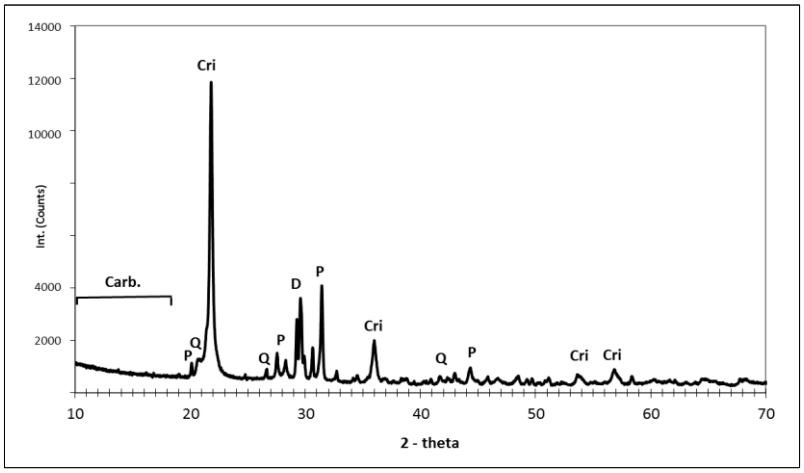

Figure D.2.2.1.2.2. XRD of bagasse (ash). Cristobalite (Cri), magnesium and calcium pyrophosphate (P), quartz (Q), diopside (D), carbon content (amorphous) (Carb.).

In figure D.2.2.1.2.2, can be observed the XRD pattern of bagasse (BB) ashes, the main crystalline phases are cristobalite (Cri) (SiO_2), (00-027-0605), derivate from its higher silica content (45.33%-XRF analysis); a magnesium and calcium pyrophosphate (P) (XRF-4.60 and 25.29% respectably), and quartz (Q) (00-89-8936), with the presence of diopside ($MgCaSi_2O_6$).

The bagasse ash shows a fibre-cell structure consisting mainly of isotropic silica in the form of cristobalite (Italiana, 1993).

The wideband between 10-20°2Θ, indicate the presence of amorphous phase, corresponding to the carbon present in the sample related to the organic matter remained in the sample after thermal treatment.

As can be seen in figure D.2.2.1.2.3, in the XRD of MBM were the predominant crystalline phase corresponds to hydroxylapatite [$Ca_{10}(OH)_2(PO_4)_6$], (00-001-1008). The non-crystalline phase, related to the organic carbon, make difficult to recognize other phases.

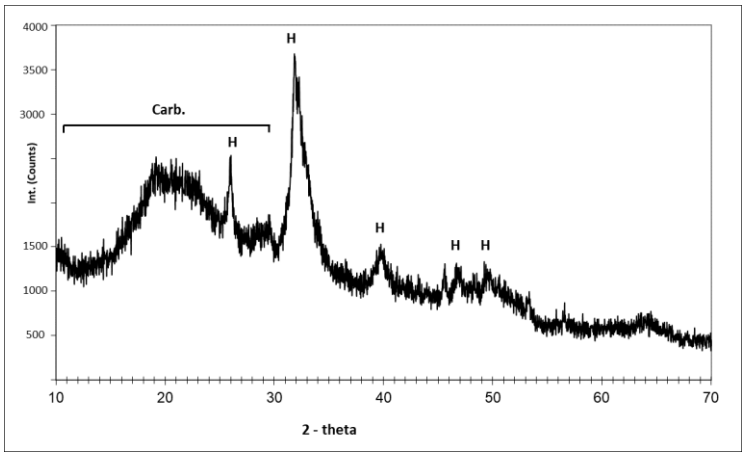

Figure D.2.2.1.2.3. XRD of MBM. Hydroxyapatite (H) and carbon content (Carb).

In figure D.2.2.1.2.4, corresponding to CBA XRD pattern, hydroxyapatite (H), (00-001-1008), is the primary crystalline phase (D. Pongkao et al., 1999; Tadic and Epple, 2004), the other phases present are calcite (C) [$CaCO_3$] and a calcium phosphate, magnesium and potassium (P) [$Ca_9MgK(PO_4)_7$] related to its high phosphorus and calcium content reviled in the chemical analysis, 41.24%, and 53.89% respectively. The presence of amorphous phase between 10^o-30^o 2 Θ, corresponding to the carbon relates to organic matter.

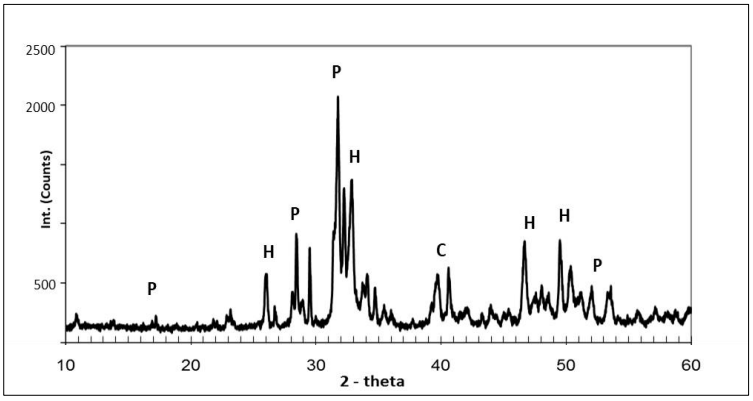

Figure D.2.2.1.2.4. XRD of cattle bone-ash (CBA).

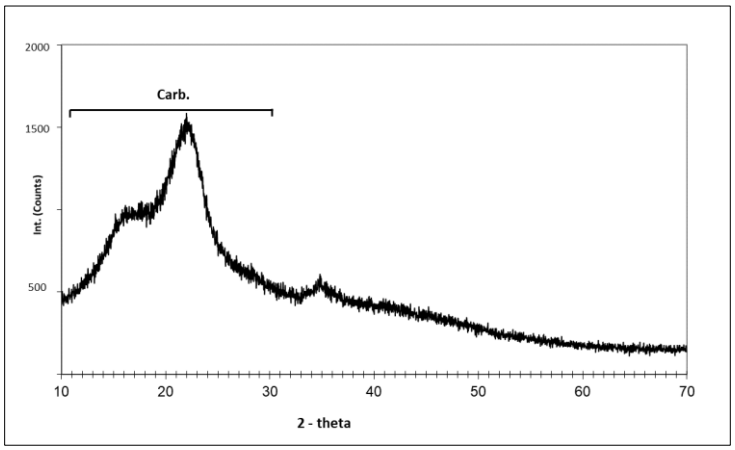

Figure D.2.2.1.2.5. XRD form corn cob (CC). Carbon content (Carb.)

In figure D.2.2.1.2.5, CC presented non-crystalline substances like 32.5%-45.6% cellulose; 39.8% of hemicelluloses and 6.7%-13.9% of lignin (Njeumen Nkayem et al., 2016).

D.2.2.1.3. THERMOGRAVIMETRIC ANALYSES

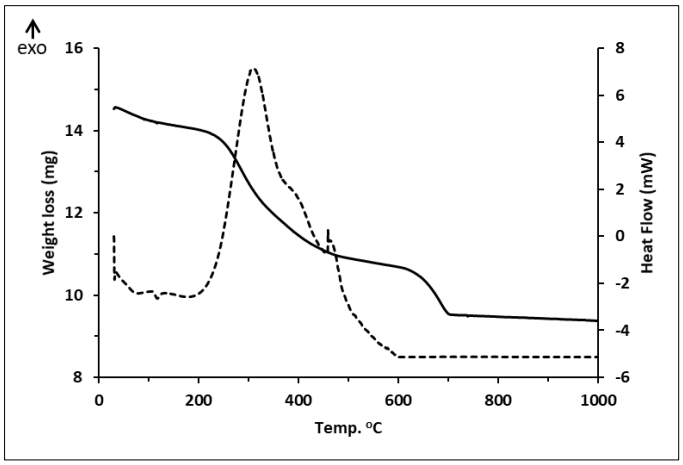

Figure D.2.2.1.3.1. TG-DTA of BS.

In Figure D.2.2.1.3.1, shows the TG-DTA analysis of brewery sludge (BS) where it is evident that up to 200°C, there is not a significant weight loss detected, the DTA curve indicates endothermic peak characteristic of loss of moisture. From 250°C to 700°C there are several exothermic reactions with particular relevance around 300°C, attributable to the combustion of the organic matter present. Between 600-700°C there is a new endothermic reaction, due to the decarbonization of the material, related to its high CaO content revealed in the XRF analysis (26.45%). Above 700°C there is a stable situation without further variations; the organic

substance is now wholly decomposed.

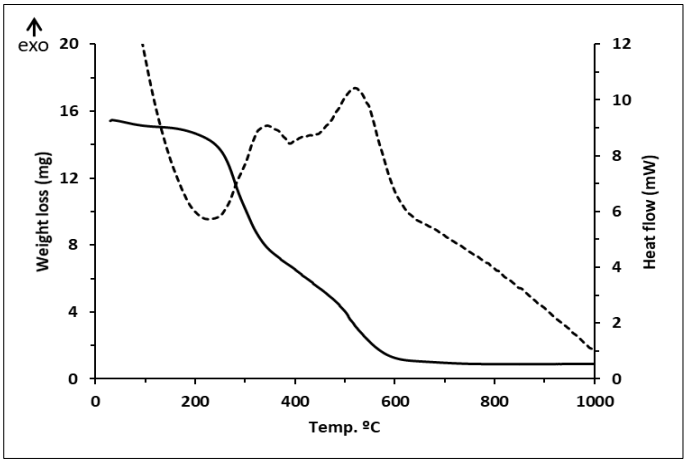

Figure D.2.2.1.3.2. TG-DTA of bagasse.

In TG-DTA curve form bagasse (Figure D.2.2.1.3.2) the first endothermic peak (100-200^{o}C) is related to the humidity evaporation. At 300 and 600^{o}C, two exothermic peaks can be observed associated with the significant weight loss that occurs due to combustion of the organic matter (organic matter content of 94.68%). The peak observed at approximately 570^{o}C can be attributed to the oxidation of the fixed carbon. Above 600°C, no significant events are observed.

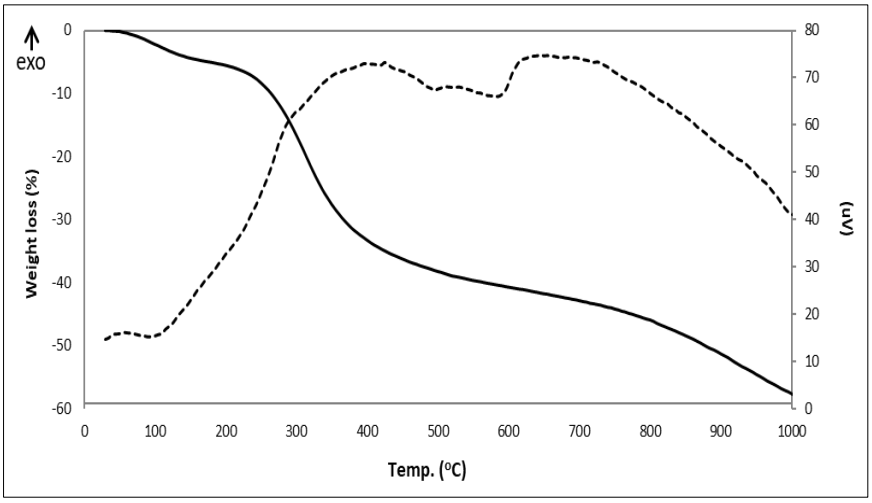

Figure D.2.2.1.3.3. TG-DTA of meat-bone meal (MBM).

In Figure D.2.2.1.3.3, MBM TG-DTA can be observed, that between 300 and 500^{o}C occur the most significant weight loss, approximately 50% (organic matter content of 61.10%), corresponding to the combustion of carbon.

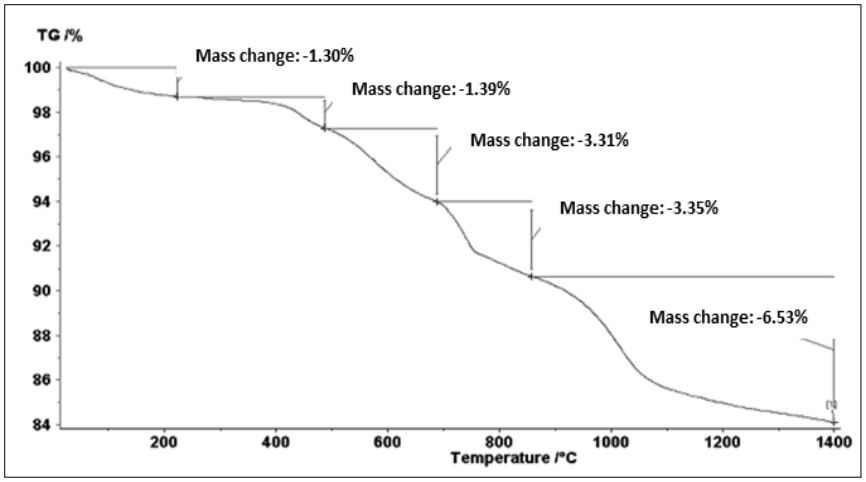

Figure D.2.2.1.3.4. TG of CBA (Lugari, 2011)

In Figure D.2.2.1.3.4 and D.2.2.1.3.5, it has analyzed the thermogravimetric behavior of CBA through TG-DSC curves. At 100°C, an endothermic event can be observed, corresponding to a loss of mass of 1.30% by the loss of moisture; at 450°C and 570°C two exothermic events, corresponding to a loss of mass of 1.40% and 3.35% respectively. These events are due to the oxidation of organic matter; at 750°C there is a further endothermic event, accompanied by a 3.00% weight loss due to the decomposition of calcium carbonate ($CaCO_3$) and the consequent formation of calcium oxide (CaO). At 1020°C there is a further endothermic event, which corresponds to a weight loss of 6-7%, probably due to the thermal decomposition of hydroxyapatite present in the sample; the sample is thermally stable until the maximum temperature reached (1400°C).

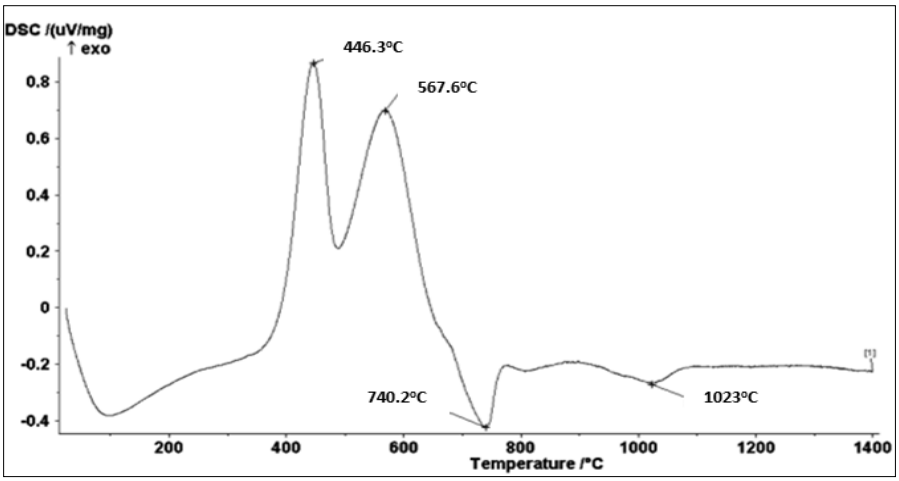

Figure D.2.2.1.3.5. DSC of CBA (Lugari, 2011).

To confirm with more certainty those exothermic events (450°C and 570°C) due to the combustion of organic matter, not related to the formation of new compounds were consulted previous studies performed from DIEF research group (UNIMORE) (Barbieri et al., 2014), were two samples were subjected to thermal treatment for 30 minutes at 420°C and 530°C.

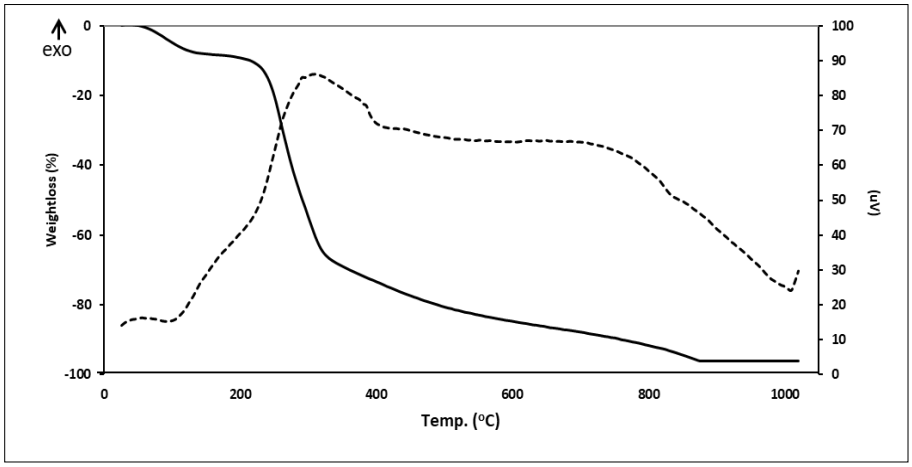

Figure D.2.2.1.3.6. TG-DTA of corn cob (CC).

In Figure D.2.2.1.3.6, it can be observed DTA-TG of CC (corn cob) and highlighted that between 200-400°C the more significant weight loss is seen, approximately 60%, corresponding to the combustion of the carbon related to de organic matter content, which is consistent with the characterization carried out (Elemental analysis, XRF, and HHV-LHV).

D.2.2.2. INORGANIC WASTE/BY-PRODUCTS.

The technical nutrients like diatomaceous earth (DE), Glassy sand® (GS) and potassium carbonate (K_2CO_3) were considered inorganic waste/by-products.

The elemental analysis of DE determines that the content of N is 1.11%, C is 6.46%, H is 0.87% and non S% content was found. Also, was determined the high and low heating value (HHV-LHV) in 594.36 and 548.24 Kcal/Kg respectively. DE can be considered that is an inorganic waste with a high saturation of organic matter due to the beer clarification (filtration) and yeast retention.

The quantification of organic matter content (OMC) by calcination, for DE, was 13.26%, carried out with the method proposed by Navarro and Col. (1993).

In table D.2.2.1. Can be seen the XRF analysis of the Diatomaceous earth (DE) ash, Glassy Sand® (GS), and potassium carbonate (K_2CO_3).

Table D.2.2.2.1. XRF analysis of inorganic technical nutrients (*Source: Sasil s.p.a.).

	Diatomaceous earth	**Glassy sand®**	**Potassium carbonate**
Oxide (%)	**DE ash**	**GS***	**K_2CO_3**
SiO_2	67.34	71.3	-
Al_2O_3	4.95	2.00	-
Fe_2O_3	0.66	0.37	0.02
MnO	-	-	-
MgO	0.11	2.23	-
CaO	0.43	10.00	0.05
Na_2O	1.20	12.68	0.46
K_2O	1.31	0.92	74.17
TiO_2	0.27	0.07	-
P_2O_5	0.35	-	-
ZrO_2	0.09	-	-
Cl	-	-	-
Cr_2O_3	-	-	-
PbO	-	0.04	-
LOI	0.04	0.17	25.30
Others	23.25	-	-
Total	100.00	99.78	100.00

The Glassy Sand® (GS) used in this research is a commercial product obtained from the claiming process of the cullet glass from collected waste. GS is a product elaborated for Sasil s.p.a, presents a moisture content of 5.00% and granulometry of 100 and 800 µm (Table D.2.2.2.2). The Sasil s.p.a provided the data for the XRF and granulometric analysis. The material is polluted with a low percentage of ceramics, metal, and plastic of the containers and bottles.

Table D.2.2.2.2. Glassy sand gravimetric analysis (Source: Sasil s.p.a.).

Sieve (mm)	**Weight (%)**
0.80 < x < 1.60	3.00
0.10 < x < 0.80	92.00
<0.10	5.00

The potassium carbonate (K_2CO_3) used in the composition of the fertilizer glass (FG) is for industrial grade and was supplied by Colorobbia®.

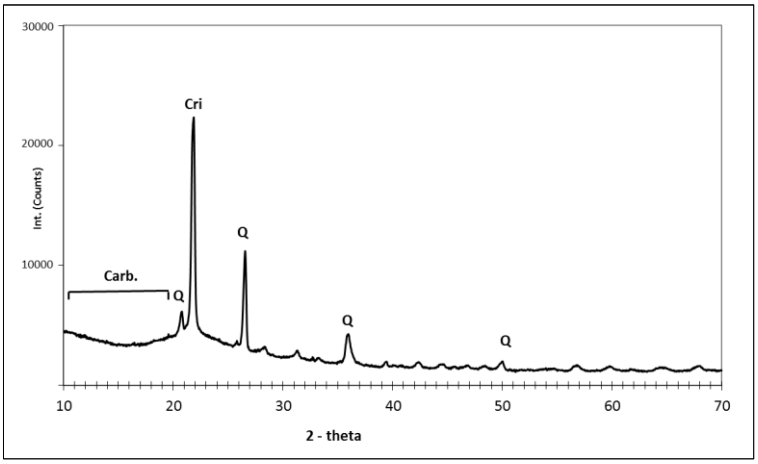

Figure D.2.2.2.1. XRD diatomaceous earth (DE). Cristobalite (Cri), quartz (Q), carbon (Carb.)

The predominant crystalline phases in the DE XRD analysis is cristobalite (Cri) [SiO_2] and quartz [SiO_2] (Q), in concordance with its high content of silicon oxide (XRF analysis 67.34%) (Figure D.2.2.2.1). The interval between 10°-20° 2Θ correspond to the organic matter present in the sample (amorphous carbon-crystalline structure) due to the organic matter (yeast) retain in the filtration process of beer (OMC: 13.26%), remained after thermal treatment.

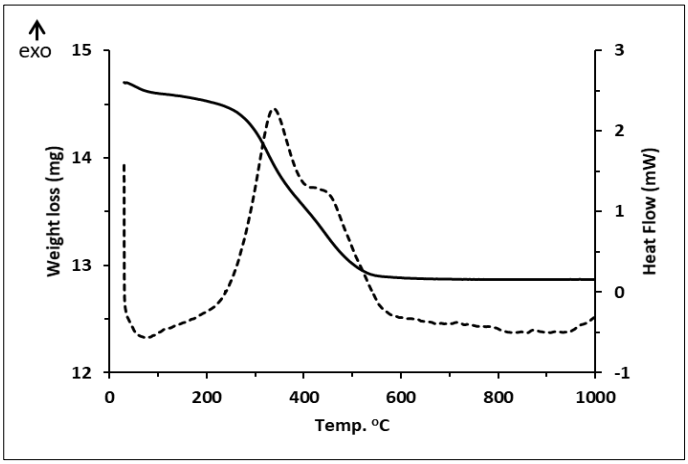

Figure D.2.2.2.2. TG-DTA of diatomaceous earth.

In figure D.2.2.2.2, corresponding to the TG-DTA analysis of DE, total weight loss is less pronounced, in comparison with the other technical nutrients, as it was expected from the results of the XRF analysis. At 150°C, another endothermic peak can be seen due to the loss of moisture content. Between 350-500°C can be observed an exothermic peak due to the loss of a small amount of organic matter (5-10%), representing a low energy input by the analysis carried out.

D.2.2.3. FERTILIZER GLASS (FG) PREPARATION AND CHARACTERIZATION

For the elaboration of lightweight aggregates for agronomic purposes ($LWAS_{AP}$), was used a fertilizer glass (FG), that was obtained by mixing cattle bone ash (40%), Glassy Sand® as a parent glass (42%), and 18% of potassium carbonate (K_2CO_3).

The proportions in the mixture of fertilizer glass were based on previous studies carried out by DIEF research group (UNIMORE). Different mixtures were studied to meet the mix with the best performance as fertilizer to the production of active glass (Barbieri et al., 2014; Lugari, 2011).

The glass blend was mixed for 2 hours and placed inside a refractory alumina silicate melting pot for the melting treatment in an electric furnace (Lenton EHF 1700). The thermal cycle for the glass fusion was listed in Table D.2.2.3.1.

Table D.2.2.3.1. Thermal cycle of glass manufacturing.

Stage	Temperature (°C)	Heat rate (°C/min)	Time (min)
Step 1	0 - 800	10°	80
Isotherm	800	-	20
Step 2	800 - 900	10°	10
Control	900	-	5
Step 3	900 - 1000	10°	20
Isotherm	1000	-	60
Step 4	1000 - 1300	10°	30
Isotherm	1300	-	30
Step 5	1300 - 1450	10°	15
Isotherm	1450		120
			Total = 6h 30’

To obtain the glass frit, the molten glass mass was poured into cold water, resulting in non-homogeneous grain size by the temperature contrast. The glass was ground up to 100 µm. The XRF analysis of the fertilizer glass (FG) can be seen in table D.2.2.3.2.

Table D.2.2.3.2. Chemical composition (XRF) of fertilizer glass (FG).

Oxide (%)	SiO_2	Al_2O_3	Fe_2O_3	MgO	CaO	Na_2O	K_2O	P_2O_5	PbO	Others	Total
FG	33.11	0.84	0.16	1.38	25.76	5.96	13.75	16.49	0.02	5.11	100.00

The fertilizer glass manufacturing leads to an increment on the costs and energy consumption during production, i.e., increasing environmental impacts. For that reason, aggregates

formulated with FG were compared to samples made with CBA, as an alternative raw material for low energy consumption.

Image D.2.2.3.2. Fertilizer Glass.

Figure D.2.2.3.2 shows the XRD analysis of the fertilizer glass, where N corresponds to sodium and calcium phosphate (specifically: $[Na_2Ca_2(PO_4)_{5/2}4CaO0.6Na_2OP_2O_5]$), corresponding to a new crystalline phase.

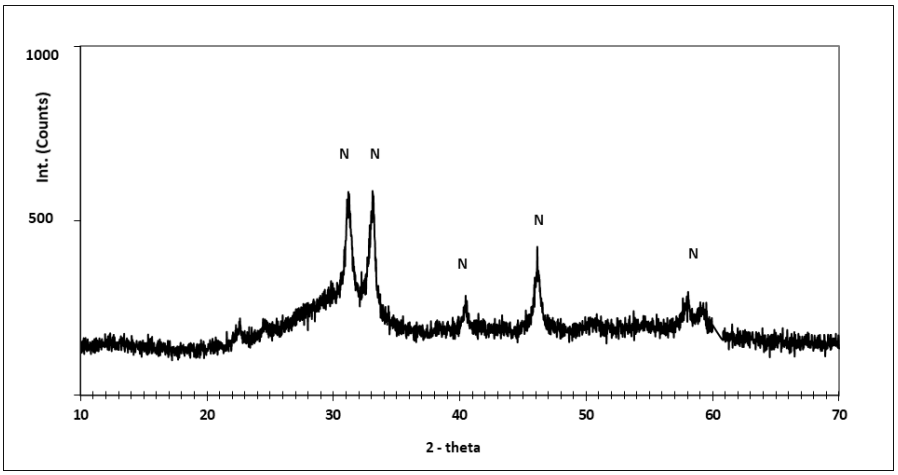

Figure D.2.2.3.2. XRD of Fertilizer glass (FG) (40-42-18).

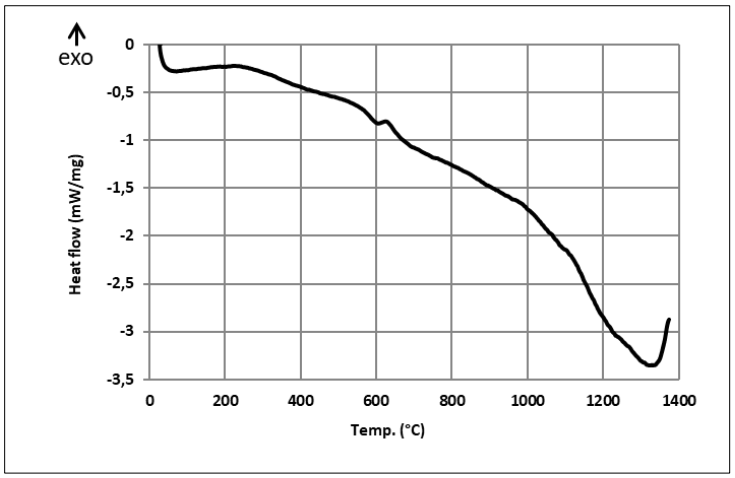

Figure D.2.2.3.3. TG of Fertilizer glass (40-42-18).

In figure D.2.2.3.3, it can be seen the TG analysis of the fertilizer glass, the curve has a regular slope, except for an endothermic event at approximately 620°C, due to a small crystallization event (Shelby, 2005).

D.3. SAMPLE PREPARATION

D.3.1. LWA_S FOR DRAINAGE LAYER IN GREEN ROOFS ($LWAS_{GR}$)

The clay minerals and waste/by-product after drying step, at 105°C for 24 hours to reduce the initial humidity, were mechanically subjected to grinding at different granulometry depending on each material, as it follows:

- Clay materials (Black, Yellow, and Red ES clay) were grinning in a hammer mill and mechanically save (Analysette 3 PRO) up to 500 µm/0.50 mm.
- Brewery sludge (BS), bagasse (BB), and diatomaceous earth (DE) were grinning in the hammer mill and sieved up to 1000 µm/1.00 mm grain sizes.

The clay base mixture for the samples preparation was composed of equal parts of the three types of clay: Black, yellow and red ES (BYRC). To determine the effect of the organic waste material on the clay-matrix, different amounts of bagasse (BB), wastewater treatment sludge (BS) and diatomaceous earth (DE) (0, 2, 4, 6, 8, 10, 12.5 and 15%) were added to the clay mixture (Table D.3.1.1). The appropriate quantities of pre-dry waste and clay were weighed and then mixed in a mortar. Water was added during this process to obtain the right plasticity for manually shaping.

Table D.3.1.1. LWA_S formulations batch (100.00 g).

	Black, Yellow, Red ES clay	Brewery sludge	Bagasse	Diatomaceous earth
Mix.(%)	**BYRC**	**BS**	**BB**	**DE**
BS_2	98.00	2.00	-	-
BS_4	96.00	4.00	-	-
BS_6	94.00	6.00	-	-
BS_8	92.00	8.00	-	-
BS_{10}	90.00	10.00	-	-
$BS_{12.5}$	87.50	12.50	-	-
BS_{15}	85.00	15.00	-	-
BB_2	98.00	-	2.00	-
BB_4	96.00	-	4.00	-

BB_6	94.00	-	6.00	-
BB_8	92.00	-	8.00	-
BB_{10}	90.00	-	10.00	-
$BB_{12.5}$	87.50	-	12.50	-
BB_{15}	85.00	-	15.00	-
DE_2	98.00	-	-	2.00
DE_4	96.00	-	-	4.00
DE_6	94.00	-	-	6.00
DE_8	92.00	-	-	8.00
DE_{10}	90.00	-	-	10.00
$DE_{12.5}$	87.50	-	-	12.50
DE_{15}	85.00	-	-	15.00

The samples were dried in a stove at 110ºC for 48 h to reduce their moisture content (Memmert Mod. 30-1060). The samples were preheated at 200ºC for 24 h to prevent fractures during the sintering process. After preheated treatment, samples were subjected to a firing process in a muffle furnace (P-Selecta Mod. 2000366). The furnace was set at the temperature required (900, 950 or 1000ºC), for one hour. Samples were allowed to cool through natural convection.

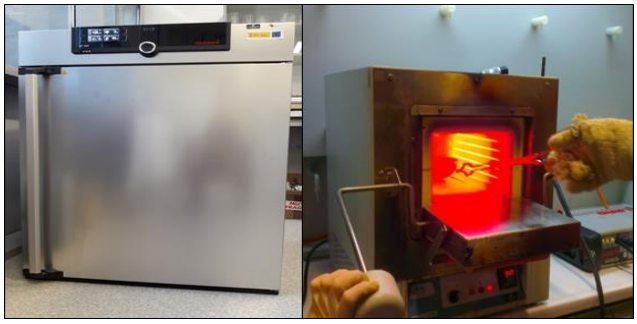

Image D.3.1.1. Stove (left) and muffle furnace (right).

The samples presented diameters between 15.25 -24.12 mm.

D.3.2. LWA$_S$ FOR AGRONOMIC PURPOSES (LWAS$_{AP}$)

The clay minerals and waste/by-product after drying step, at 105ºC for 24 hours to reduce the initial humidity, were mechanically subjected to grinding at different granulometry depending on each material, as it follows:

- Clay materials were grinned in a hammer mill and manually sieved to obtain 100 µm/0.1 mm grain sizes.
- Brewery sludge (BS), Meat-bone mail (MBM), corn cob (CC) cattle-bone ashes (CBA), were subjected to reduction of grain size, in a laboratory mill and were manually sieved

to obtain 1000 µm/1.00 mm grain sizes. The fertilizer glass (FG) was ground up to 100 µm/0.10 mm.

To produce $LWAS_{AP}$ two different clay-based mixtures were used: WBC (30wt% white-70wt% black clay) and RC (100wt% red clay). The characterization and optimization of the varied materials were carried out following two different steps:

In the first step was carried out the characteristics of the WBC clay-based mixture with the different wastes by mixing 0, 5, 10, 15wt% of BS, MBM and CC in substitution of clays, sintered at 900 and 1000°C for 1 hour. In Table D.3.2.1, the quantities are reported for the 100.00g mixture.

Table D.3.2.1. LWA_S formulations batch (100.00 g) (First stage).

	White clay	**Black clay**	**Brewery sludge**	**Meat-bone meal**	**Corn cob**
Mix.(%)	**-**	**-**	**BS**	**MBM**	**CC**
WBC	30.00	70.00	-	-	-
$WBBS_5$	28.50	66.50	5.00	-	-
$WBBS_{10}$	27.00	63.00	10.00	-	-
$WBBS_{15}$	25.50	59.50	15.00	-	-
$WBMBM_5$	28.50	66.50	-	5.00	-
$WBMBM_{10}$	27.00	63.00	-	10.00	-
$WBMBM_{15}$	25.50	59.50	-	15.00	-
$WBCC_5$	28.50	66.50	-	-	5.00
$WBCC_{10}$	27.00	63.00	-	-	10.00
$WBCC_{15}$	25.50	59.50	-	-	15.00

Based on the results of the first step, was decided to use BS 15wt% as pore-forming agent (Farias et al., 2017a) and introduce a different local clay mineral, Italian clay, red IT clay-based mixture (RC). At the same time, the addition of FG and CBA as potassium (K) and phosphorus (P) contribution, to conferred fertilizer capacity in substitution of clay. The mixtures were blended for the second step LWA_S samples as it follows (Table D.3.2.2):

- Samples without waste (WBC and RC),
- Samples containing 85wt% of WBC or RC and 15wt% BS ($WBBS_{15}$ and $RCBS_{15}$),
- Samples containing 85wt% of WBC or RC, 15wt% BS and 10wt% of fertilizer glass (FG) (WB_{FG} and RC_{FG}),
- Samples containing 85wt% of WBC or RC, 15wt% BS and 10wt% of cattle bone ash (CBA) (WB_{CBA} and RC_{CBA}).

Image D.3.2.1. $WBBS_{15}$ samples after the sintering process.

The materials were mixed and shaped manually into spherical specimens by the addition of water to obtain the adequate plasticity. Water was considered as a resource, and the amount used for each mixture was quantified.

The samples presented diameters between 11.96 -21.68 mm.

Table D.3.2.2. LWA_S formulations batch (100.00 g) (Second stage).

	White (30%)-Black (70%) clay	**Red IT (100%)**	**Brewery sludge**	**Cattle-bone ash**	**Fertilizer glass**
wt%	**WBC**	**RC**	**BS**	**CBA**	**FG**
WBC	100.00	-	-	-	-
$WBBS_{15}$	85.00	-	15.00	-	-
WB_{FG}	85.00	-	15.00	-	10.00
WB_{CBA}	85.00	-	15.00	10.00	-
RC	-	100.00	-	-	-
$RCBS_{15}$	-	85.00	15.00	-	-
RC_{FG}	-	85.00	15.00	-	10.00
RC_{CBA}	-	85.00	15.00	10.00	-

All the samples were dried in a stove (PID System, M120-VN Basic) at 105°C for 24 hours to eliminate their moisture content. Stove drying is done to avoid fractures in the material during the sintering process.

In all steps the sintering was carried out in a hot electric kiln (Lenton AWF13/12); the samples were placed directly at the corresponding sintering temperature (900 or 1000°C), for one hour. The samples were placed in small silico-aluminate containers, in each crucible were placed 3-4 samples. The samples were allowed to cool through natural convection.

Image D.3.2.2. LWA_S after sintering process (silico-aluminate container).

This type of heating treatment simulates the sintering process in the industrial rotary kiln. The material introduced into the furnace at high temperature receives a thermal shock that favors the formation of the characteristic porous structure and the vitrification of the surface layer, which confers durability to the material.

Weight loss percentages (WL%) data were obtained by the difference between the weight after drying stage and firing stage.

Image D.3.2.3. Furnace during sintering process and $LWAS_{AP}$.

D.4. LWA_S CHEMICAL COMPOSITION AND BLOATING BEHAVIOR

The chemical data of the ground mixtures (recalculated to 100%) were plotted on Fe_2O_3/Al_2O_3 vs. Σ(MgO, CaO, Na_2O, K_2O) diagram (Cougny, 1990; Dondi et al., 2016). By means of the theoretical calculation of the chemical compositions of each mixture developed in this investigation, they were placed in a binary diagram, in order to predict its blotting behaviour, i.e., it is expected that they produce a sufficient viscous phase to be able to trap a significant amount of gas, representing a useful technical nutrient source for LWA_S manufacturing (Dondi et al., 2016; Hung and Hwang, 2007).

Table D.4.1. $LWAS_{GR}$ theoretical chemical composition.

$LWAS_{GR}$	Fe_2O_3/Al_2O_3	Σ(MgO,CaO,Na_2O,K_2O)
BYRC	0.38	15.39

BS_2	0.39	15.52
BS_4	0.40	15.64
BS_6	0.41	15.77
BS_8	0.42	15.90
BS_{10}	0.43	16.03
$BS_{12.5}$	0.45	16.19
BS_{15}	0.47	16.35
BB_2	0.38	15.36
BB_4	0.38	15.33
BB_6	0.38	15.31
BB_8	0.39	15.28
BB_{10}	0.39	15.25
$BB_{12.5}$	0.39	15.22
BB_{15}	0.39	15.18
DE_2	0.38	15.14
DE_4	0.37	14.66
DE_6	0.37	14.65
DE_8	0.37	14.40
DE_{10}	0.37	14.15
$DE_{12.5}$	0.37	13.85
DE_{15}	0.37	13.54

In Table D.4.1, LWA_{GR} theoretical chemical composition was listed. In figure D.4.1, show the representation of raw materials composition in Cougny binary diagram (simplify version by M. Dondi (Dondi et al., 2016)), showing the bloating area, in dotted line. The different mixtures are located in the bloating area, mining the proper chemical features to expand during thermal treatment.

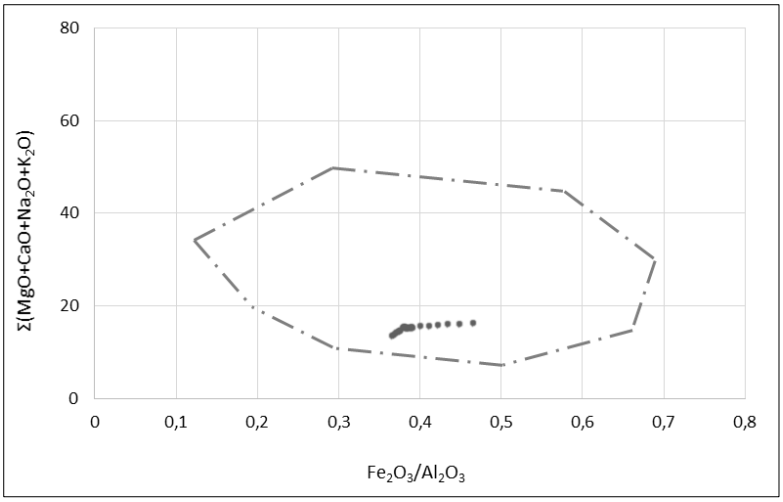

Figure D.4.1. Fe_2O_3/Al_2O_3- Σ(MgO,CaO,Na_2O,K_2O) diagram for $LWAS_{GR}$.

Table D.4.2. $LWAS_{AP}$ theoretical chemical composition.

$LWAS_{AP}$	**Fe_2O_3/Al_2O_3**	**Σ(MgO,CaO,Na_2O,K_2O)**
WBC	0.36	21.30
$WBBS_{15}$	0.47	21.40
WB_{FG}	0.46	25.75
WB_{CBA}	0.46	26.71
RC	0.44	9.96
$RCBS_{15}$	0.51	11.76
RC_{FG}	0.50	16.12
RC_{CBA}	0.50	11.43

In Table D.4.2, LWA_{GR} shows the theoretical chemical composition of the raw aggregate pellets before sintering. In figure D.4.2, show the representation of raw materials composition in Cougny binary diagram (simplify version by M. Dondi (Dondi et al., 2016)) showing the bloating area.

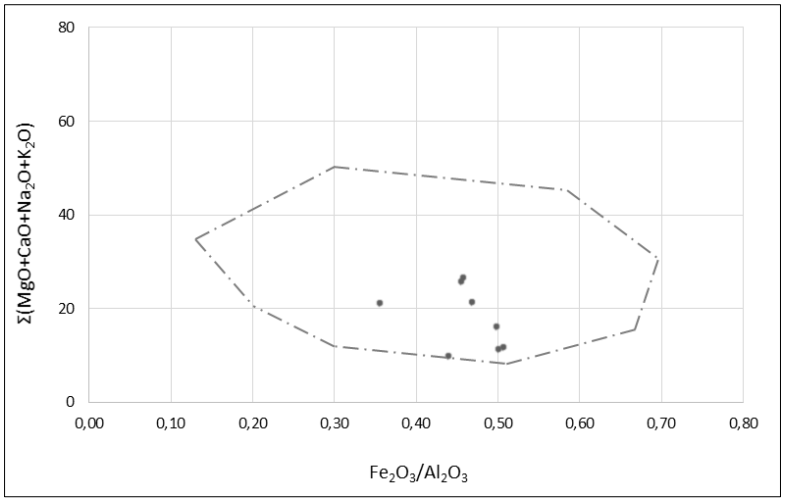

Figure D.4.2. Fe_2O_3/Al_2O_3- Σ(MgO+CaO+Na_2O+K_2O) diagram for $LWAS_{AP}$.

The mixtures of the two materials ($LWAS_{GR}$ and $LWAS_{AP}$) are in the bloating area. Therefore, can be considered that the combination of the different clay minerals and technical nutrients can be an important a reliable source of SiO_2, melting salts and organic matter to produce the sufficient gas and cause the swelling of the material.

D.5. LWA_S CHARACTERIZATION

D.5.1. $LWAS_{GR}$. GREEN ROOFS DRAINAGE LAYER.

D.5.1.1. TECHNICAL PARAMETERS. DENSITY, POROSITY AND WATER ABSORPTION DETERMINATION.

In table D.5.1.1.1 and figures D.5.1.1.1 - D.5.1.1.3 the loss of weight (WL%) during sintering process was reported, were BYRC correspond to the samples elaborated without waste (0wt%).

Table D.5.1.1.1. $LWAS_{GR}$ weight loss (WL%) during the sintering process, one hour.

	Brewery Sludge			**Bagasse**			**Diatomaceous earth**		
	BS			**BB**			**DE**		
LWA_S	900ºC	950ºC	1000ºC	900ºC	950ºC	1000ºC	900ºC	950ºC	1000ºC
0%	9.80	9.74	9.82	9.80	9.74	9.82	9.80	9.74	9.82
2%	12.00	12.06	12.14	9.64	10.70	10.69	10.32	10.37	10.41
4%	13.63	13.64	13.81	11.34	11.08	11.43	10.86	10.98	10.92
6%	14.84	14.86	15.11	10.69	10.95	11.13	10.95	10.98	10.91
8%	16.20	16.24	16.42	12.12	12.00	12.29	10.31	10.55	10.57
10%	18.14	18.20	18.35	10.67	13.45	13.47	10.56	10.66	10.73
12.5%	20.53	20.51	20.91	10.59	13.88	14.29	10.49	10.53	10.61
15%	22.42	22.55	22.77	14.18	14.26	14.49	10.73	10.57	10.74

Brewery sludge (BS) (Table D.5.1.1.1.) shows a media WL% of 11.12% (900ºC), 12% (950ºC) and 12.20% (1000ºC) related to its organic matter content (41.18%). The trend is slightly positive as a function of the waste addition % introduced.

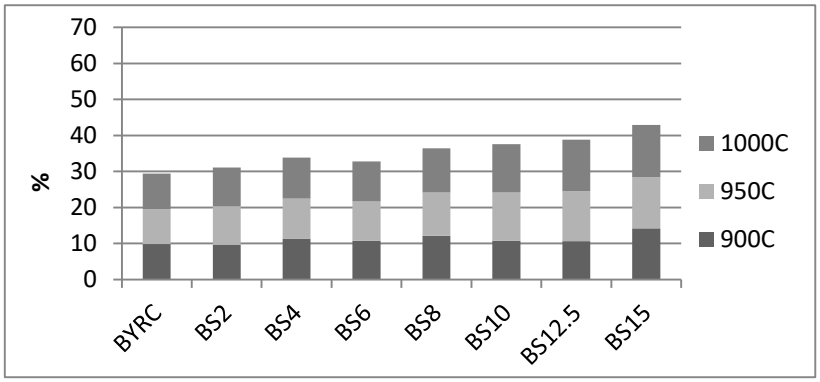

Figure D.5.1.1.1. BS samples weight-loss percentages after sintering for 1 hour.

As it was expected, the samples developed with bagasse (BB) reported the most significant weight loss % with a media valor of 16.08% at three temperatures (Table D.5.1.1.2) followed by BS with 11.77% and DE with 10.54%. There is a proportional relation between percentage of waste addition and WL%.

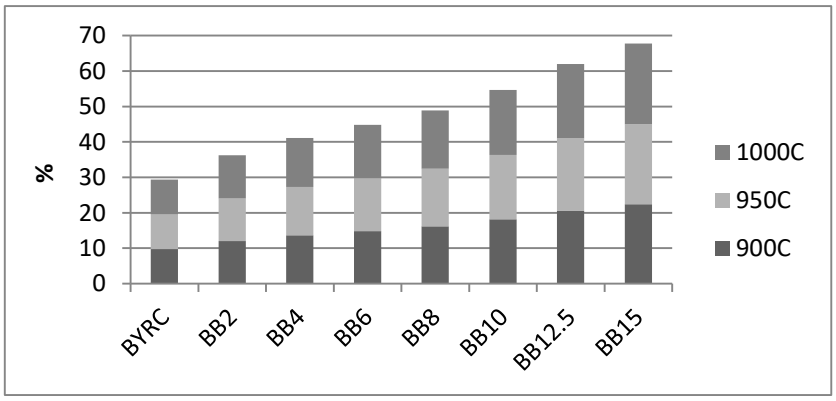

Figure D.5.1.1.2. BB samples weight-loss percentages after sintering for 1 hour.

Bagasse (BB) shows (Table D.5.1.1.2.) a media WL% of 15.94% (900ºC), 15.97% (950ºC) and 16.16% (1000ºC) related to its organic matter (OMC: 94.68%). There also is a relationship between waste addition % and WL%, less pronounced for BB.

Diatomaceous earth (DE) shows (Table D.5.1.1.3.) a media WL% of 10.50% (900ºC), 10.54% (950ºC) and 10.58% (1000ºC) related to its organic matter content (OMC: 13.26%) with an organic-inorganic nature.

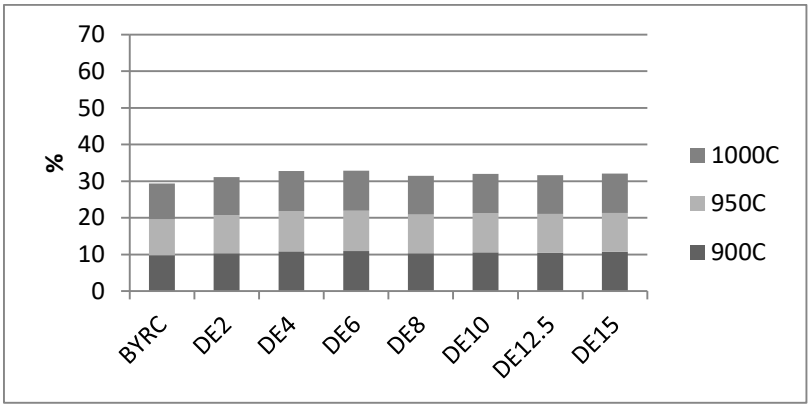

Figure D.5.1.1.3. DE samples weight percentages after sintering for 1 hour.

The weight loss, is related to the oxidation of the organic matter and with the decomposition of the carbonates, mainly coming, in this case, from the sludge (FRX: 26.46% calcium oxide) and the black clay (FRX: 15.64% calcium oxide). This can be verified by the thermogravimetric analysis of BYRC clay mixture and the waste used (BS, BB, and DE), in section D.1.2.5.1 and D.2.2.1.3, respectively.

LWA_S are granular materials with a loose bulk density (BD) less than 1.20 g/cm^3 or a particle density (PD) not exceeding 2.00 g/cm^3 (UNE-EN13055-1, 2003). The particle density (PD) and water absorption (WA_{24}) were determined by the established procedure described by EN- ISO 1097-6 (annex C) (UNE-EN-1097-6, 2014), while bulk density (BD) and void percentage (VP%) were determined according to EN-ISO 1097-3 standards (UNE-EN-1097-3, 1999). Real density (RD) was calculated by pycnometer Accupyc TM II 1340 (Micromeritics) and total porosity (TP) by means of the following formula: TP%=[(1-BD)/RD]*100 (Bernhardt et al., 2013). Procedure and equipment used were described in section C (C.2.1. Technical parameters. Density, porosity and water absorption).

Table D.5.1.1.2 and D.5.1.1.3 shows the results of the physical and technical parameters of $LWAS_{GR}$, sintered at three different temperatures, 900ºC, 950ºC and 1000ºC: water absorption (WA_{24}), particle density (PD), bulk density (BD), real density (RD), total porosity (TP%) and void (VP%).

From the data obtained, the results follow a tendency to decrease, in the case of PD, BD and RD, or to grow in the case of WA_{24}, OP, and VP with the addition of different percentages of waste and sintering temperature. In contrast, the BS samples present a hieratic tendency, which does not follow the same trend of the other mixtures (DE and BB).

Table D.5.1.1.2. $LWAS_{GR}$ water absorption, total porosity, and void percentage.

	Water Absorption (%)			Total Porosity (%)			Void (%)		
	WA_{24}			TP			VP		
	900ºC	950ºC	1000ºC	900ºC	950ºC	1000ºC	900ºC	950ºC	1000ºC
BYRC	18.11	18.24	18.94	40.08	42.64	47.64	49.25	55.56	68.26
BS_2	18.75	18.11	20.22	40.02	41.34	49.77	49.00	57.45	66.88
BS_4	19.99	20.83	21.34	40.27	43.97	49.72	49.23	58.66	70.57
BS_6	20.17	21.64	23.35	41.70	44.25	49.23	52.66	59.20	74.06
BS_8	23.14	24.74	25.72	46.21	47.36	51.49	57.47	67.95	81.53
BS_{10}	25.45	27.10	30.76	47.79	46.30	51.12	68.13	63.90	79.43
$BS_{12.5}$	20.98	24.90	32.32	46.42	47.10	50.01	64.34	65.96	74.71
BS_{15}	26.70	28.56	29.00	45.85	47.45	47.69	63.91	67.20	68.74
BB_2	20.86	21.75	22.19	41.25	44.66	45.48	55.85	60.89	63.43
BB_4	26.06	27.29	28.08	43.26	46.39	47.19	64.09	63.74	58.58
BB_6	29.63	31.13	32.26	43.73	45.89	46.64	58.99	52.63	64.52
BS_8	34.05	35.94	37.38	42.18	46.82	47.36	61.18	59.75	65.52
BB_{10}	35.60	36.01	39.72	44.29	47.96	51.46	65.22	68.03	78.72
$BB_{12.5}$	37.92	38.64	40.36	45.91	50.83	52.06	65.79	76.69	79.51
BB_{15}	38.64	41.69	45.32	48.47	52.89	55.07	69.44	70.54	80.45
DE_2	20.52	20.97	20.95	41.82	42.20	44.69	54.69	57.61	55.37
DE_4	23.76	24.30	24.39	42.38	45.60	47.78	55.03	63.77	63.64
DE_6	25.40	27.27	28.96	46.11	47.30	49.07	65.51	63.18	73.03
DE_8	28.26	29.80	30.89	46.47	48.67	50.61	66.06	71.35	77.14
DE_{10}	29.25	30.83	31.95	47.34	50.34	49.26	68.26	78.39	68.61
$DE_{12.5}$	29.69	31.09	32.02	47.89	52.93	49.12	69.00	85.79	67.80
DE_{15}	30.33	32.15	33.17	48.20	51.73	49.53	78.84	83.31	69.77

For expanded clay materials, high absorption values were linked to higher percentages of open porosity and lower bulk densities, in contrast with the structural ceramic materials.

Due to the addition of organic matter (waste), the high-water absorption values indicate higher open porosity, consistent with the WL% data presented in table 5.1.1.1. These results are related to low-density values characteristic for porous materials. The pore size distribution and median pore size were studied by Hg porosimetry (D.5.1.2. Mercury intrusion porosimetry (MIP)).

The decrease of bulk density and the increase of the porosity are directly related to mostly due to the oxidation of the organic matter and carbonates decomposition. The water absorption capacity depends on the open porosity and the morphology characteristics of the porous structure of LWA_S.

Table D.5.1.1.2. $LWAS_{GR}$ particle, bulk, and real density.

	Particle density (g/cm³)			Bulk density (g/cm³)			Real density (g/cm³)		
	PD			BD			RD		
	900ºC	950ºC	1000ºC	900ºC	950ºC	1000ºC	900ºC	950ºC	1000ºC
BYRC	3.00	2.94	2.85	2.01	1.89	1.69	3.35	3.29	3.23
BS_2	2.98	2.96	2.70	2.00	1.88	1.62	3.33	3.20	3.22
BS_4	2.91	2.84	2.69	1.95	1.79	1.58	3.26	3.19	3.14
BS_6	2.87	2.80	2.70	1.88	1.76	1.55	3.22	3.16	3.05
BS_8	2.74	2.70	2.61	1.74	1.61	1.44	3.23	3.06	2.97
BS_{10}	2.69	2.61	2.53	1.60	1.59	1.41	3.06	2.96	2.88
$BS_{12.5}$	2.61	2.55	2.45	1.59	1.54	1.40	2.97	2.90	2.80
BS_{15}	2.46	2.39	2.37	1.50	1.43	1.40	2.77	2.72	2.68
BB_2	2.93	2.88	2.86	1.88	1.79	1.75	3.20	3.23	3.21
BB_4	2.97	2.80	2.68	1.81	1.71	1.69	3.18	3.19	3.20
BB_6	2.83	2.61	2.55	1.78	1.71	1.55	3.11	3.16	2.90
BS_8	2.74	2.54	2.40	1.70	1.59	1.45	2.94	2.99	2.75
BB_{10}	2.66	2.47	2.32	1.61	1.47	1.30	2.89	2.82	2.68
$BB_{12.5}$	2.52	2.35	2.19	1.52	1.33	1.22	2.81	2.70	2.54
BB_{15}	2.44	2.20	2.04	1.44	1.29	1.10	2.79	2.55	2.39
DE_2	2.97	2.98	2.75	1.92	1.89	1.77	3.30	3.27	3.20
DE_4	2.93	2.90	2.70	1.89	1.77	1.65	3.28	3.25	3.16
DE_6	2.93	2.71	2.63	1.77	1.66	1.52	3.28	3.15	2.98
DE_8	2.84	2.64	2.48	1.71	1.54	1.40	3.19	3.00	2.83
DE_{10}	2.76	2.57	2.31	1.64	1.44	1.37	3.11	2.90	2.70
$DE_{12.5}$	2.62	2.45	2.22	1.55	1.32	1.32	2.97	2.80	2.60
DE_{15}	2.54	2.30	2.12	1.42	1.25	1.25	2.80	2.77	2.48

The organic matter, provided from the technical nutrients (BS, DE, and BB) was oxidized during thermal treatment, leading to an increase in the open porosity of the ceramic matrix. The decrease in the bulk density, related to the addition of waste and its organic matter quantity, from BYRC (clay mix without waste) to BS_{15}, sintered at the three different temperatures (900, 950 and 1000ºC) percent a maximum reduction of 510, 460 and 290 kg/m^3 respectively. For BYRC to BB_{15} 570, 600 and 590 kg/m^3; for BYRC to DE_{15} 590, 640 and 440 Kg/m^3. Otherwise, lower densities create lighter materials, preventing overload in the building structure.

Growing tendency of waste incorporation and temperatures proved the material with higher porosity providing insulating properties. Thermal imaging camera testing studied this property (D.5.1.5. Insulation properties).

Summarizing, the water absorption values are directly related to the increased amount of waste added, and the higher values were obtained for 15wt% BB, reaching 45.32% in the tree sintering

temperatures (900, 950 and 1000ºC). BB_{15} is a LWA_S according to standard, with a BD less than 1.20 g/m^3 (UNE-EN13055-1, 2003). Likewise, the BS_{15} and DE_{15} mixtures also present good results for their use in the construction of green roofs.

The capacity of absorbing water until saturated, reduce the water inputs by saving water, leaving moisture available to the plants and allowing the remaining water to drain. These aspects are related to the porous structure of the material, improving its insulation capacity, enabling to reduce evaporation.

D.5.1.2. MERCURY INTRUSION POROSIMETRY (MIP)

This analysis aims to study the characteristics of the porosity generated by the addition of organic and inorganic waste. The term "porosimetry" means the measurements of pore size distribution; Hg volume intrudes, apparent and skeletal density, and other porosity-related characteristics of the material (i.e., tortuosity, total pore area). This analysis provides essential data to understand the formation, structure, and potential use of many materials. The porosity of a ceramic material affects its physical and mechanical properties, i.e., its behavior in its surrounding environment (Micromeritics, 1985).

Bese on the results of the previous determinations, this study has been carried out on the samples with the addition of 15wt% of the three residues (Sludge, Bagasse and Diatomaceous earth) compared to the clay base mixture BYRC (black, yellow and red ES clay in equal parts), all sintered at 1000ºC for one houer.

In Image D.5.1.2.1, can be observed the characteristics of the porosity of BYRC clay-based mixture, is observed.

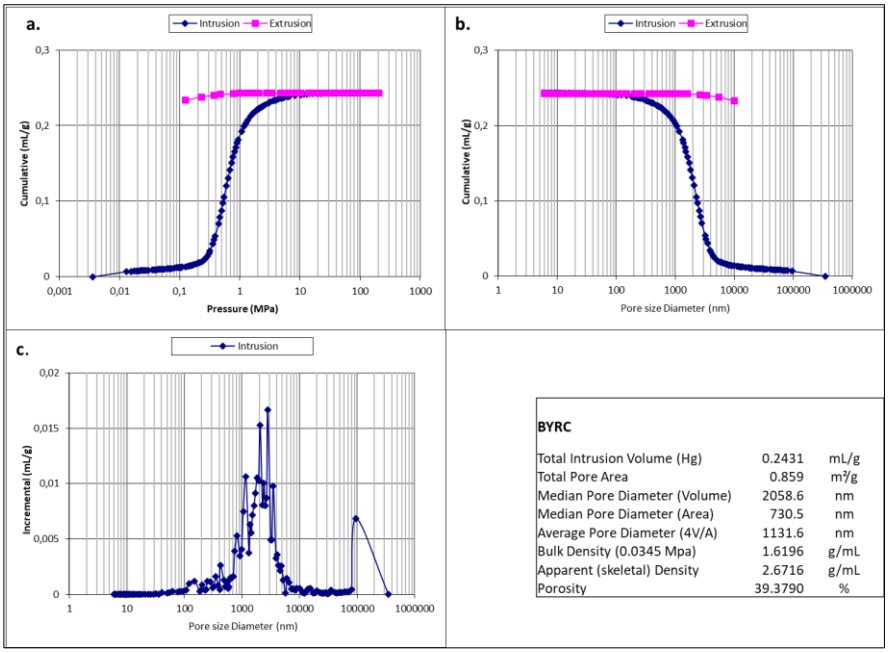

Image D.5.1.2.1. Porosimetry curves of BYRC sample. a) Cumulative intrusion volume vs. pressure; b) Cumulative intrusion volume vs. pore size diameter; c) pore size distribution.

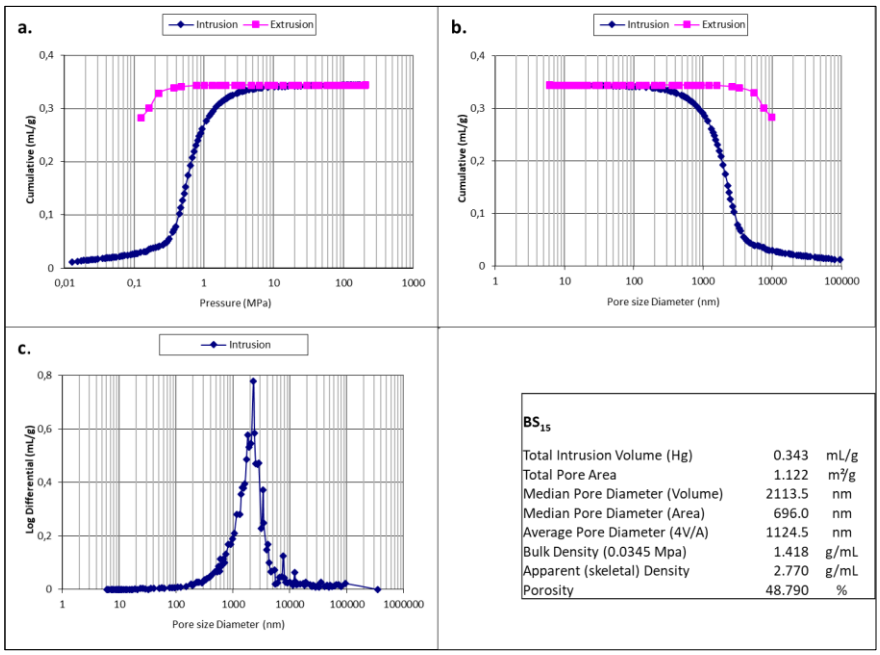

Image D.5.1.2.2. Porosimetry curves of BS_{15} sample. a) Cumulative intrusion volume vs. pressure; b) Cumulative intrusion volume vs. pore size diameter; c) pore size distribution.

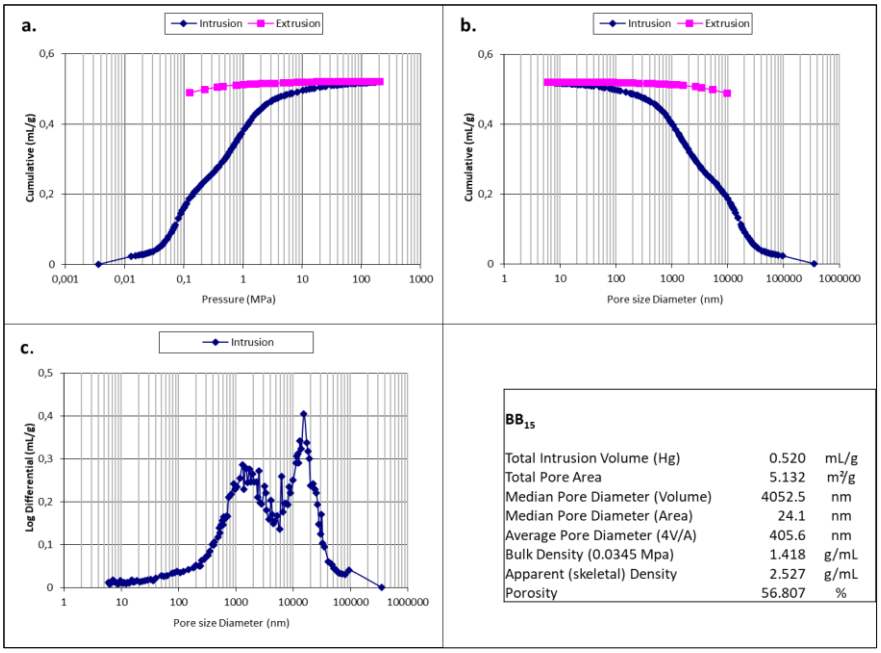

Image D.5.1.2.3. Porosimetry curves of BB_{15} sample. a) Cumulative intrusion volume vs. pressure; b) Cumulative intrusion volume vs. pore size diameter; c) pore size distribution.

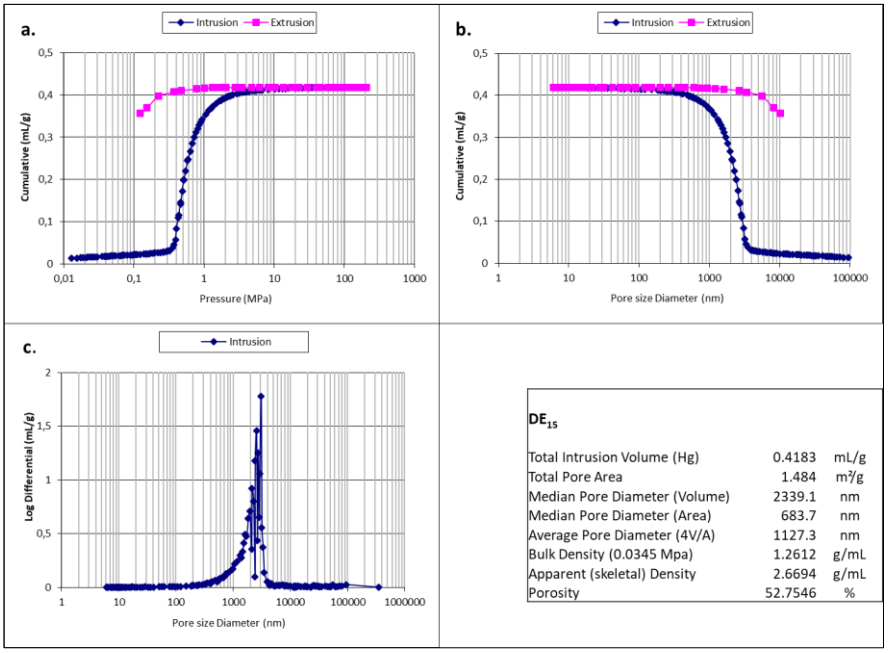

Image D.5.1.2.4. Porosimetry curves of DE_{15} sample. a) Cumulative intrusion volume vs. pressure; b) Cumulative intrusion volume vs. pore size diameter; c) pore size distribution.

The porosity of the clay-base mixture (BYRC), as was expected, has a lower porosity than the mixtures with the addition of residue. Likewise, BYRC has a high total porosity, due to the content of organic matter and carbonates of the clay mixture, mostly coming from the black

clay. In turn the porosity is very heterogeneous since the pore diameter is in a wide range 100-10000 nm/0.10-10 µm.

For the results obtained, confirmed that the addition of 15wt% BB generates the must porous structure in comparison with BS and DE addition. 15wt% BB it has a greater porosity, in quantity and size, related to the values of porosity 56.80%, bulk density 1.41 g/ml and total by area of 5.13 m^3/g. In turn the porosity is very heterogeneous since the pore diameter is in a wide range 100-100000 nm/0.10-100 µm. This is not only due to the content of organic matter (41.18% - Table D.2.1.4) contributed by BB, also to the contribution of silica (45.33% - XRF analysis) to the mixture.

Although DE has less amount of organic matter than BS, DE contributes a high SiO_3 value (67.34% - XRF analysis), allowing the reduction of carbonate contents in the mix, favouring the vitrification of the surface layer and capture the gases from compounds decomposition. (Barbieri et al., 2013; Ducman and Mladenovic, 2002). In any case, both BS_{15} and DE_{15} present interesting porosity values, being equally useful for their use as a drainage layer in green roofs.

D.5.1.3. MICROSTRUCTURE AND CHEMICAL ANALYSIS (SEM-EDS) ON EXTERNAL SURFACE

The morphological and chemical analysis of LWA_S surface was carried out by SEM-EDS technique. Base on the results, in section D.5.1.1, the aggregates with the addition of 15wt% of BS, BB, and DE waste, were analyzed and compared to the reference sample (100% clay (BYRC)), all sinteres at 1000°C.

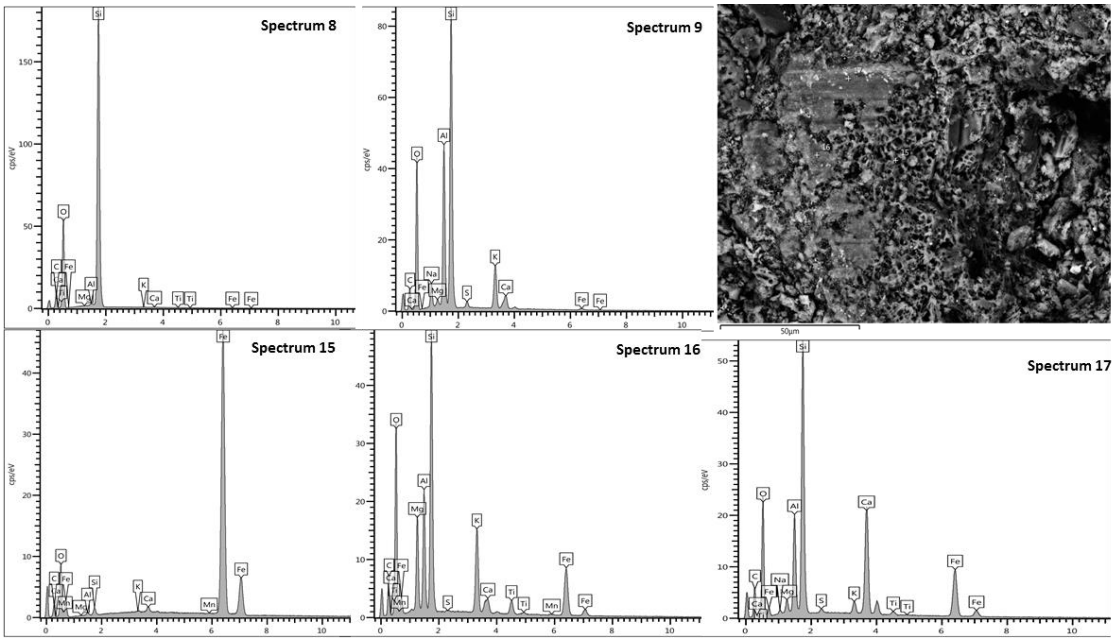

Figure D.5.1.3.1. SEM-EDS micrograph (1500x) BYRC $LAWS_{GR}$

In figure D.5.1.3.1 corresponding to BYRC, it is observed a high degree of sintering on the ceramic surface, with well-sintered grains. As a typical ceramic matrix, by EDS spectra it can observe a high concentration of Si (silicon), and Al (aluminum), low Fe (iron) content derivate mostly forms the red ES clay. You can also see the presence of Ca (calcium) derived from the three clays used, and Ti (titanium), mainly from red clay ES.

The ceramic structure looks compact. The open porosity is composed of very small pores (0.5-1.5 µm) and a dispersed bigger pores (50-100 µm).

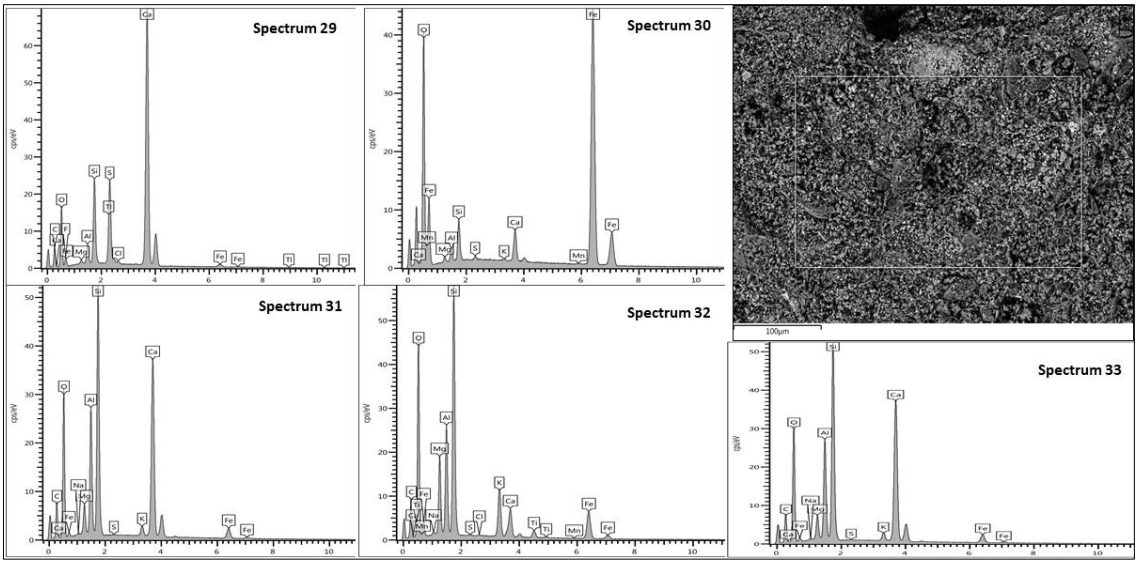

Figure D.5.1.3.2. SEM-EDS micrograph (1500x) BS_{15} $LAWS_{GR}$

In the case of BS_{15} (Figure D.5.1.3.2), a uniform and small size porosity were observed 1-5 µm. Some more sintered formations were observed that do not become compact as a grain. The light-colored and larger one's formations (Spectrum 29, 31, 32 and 33) are related to the high content of Ca (calcium) and Si, followed by Al and very little Fe. In turn, formations with high Fe and Al content were related to the red ES clay 8.21 and 19.67 % respectively, seen in the chemical analysis. The high content of Ca is related to the contribution of BS 15wt% (18.52% XRF analysis).

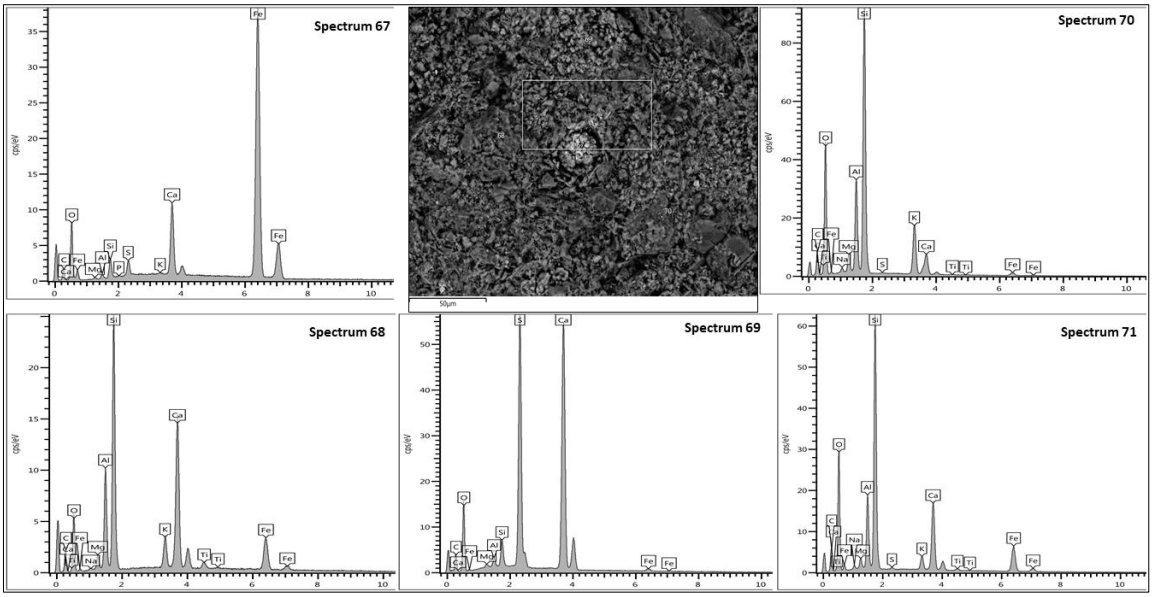

Figure D.5.1.3.3. SEM-EDS micrograph (1500x) BB_{15} $LAWS_{GR}$

For BB_{15} (Figure D.5.1.3.3), the porosity is less homogeneous than BS_{15}, with pores in the order of 2-15 µm. This fact may be due to granulometry and the fibrous nature of this waste. Grains with a high content of Si, Ca and a lower proportion of Fe was observed. The high contents of Si content contributed by the BB (45.33% XRF analysis).

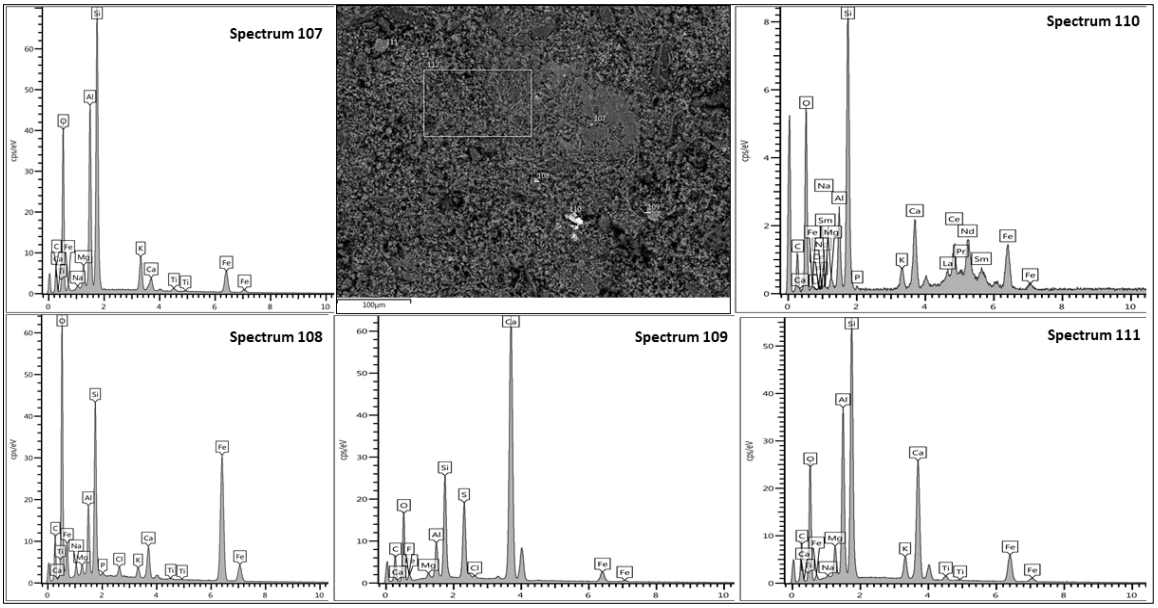

Figure D.5.1.3.4. SEM-EDS micrograph (1500x) DE_{15} $LAWS_{GR}$

For DE_{15} (Figure D.5.1.3.1), a more homogeneous porosity of the three wastes was observed, with a higher degree of compaction and sintering associated with the high amount of Si and Al. Over the surface, some light-colored grains were noted in the order of 10-15 µm with high Ca

contents. The high contents of Si are related to the high Si content contributed by the DE (67.34% XRF analysis).

While the analysis carried out in section D.5.1.2 (Hg intrusion porosimetry (MIP)) and scanning electron microscopy (SEM) can study the porosity of the material, the results of the two analyzes cannot be compared. For MIP sampling test, the LWA_S have to break into small pieces, thereby the data obtained are related mostly to the internal structure of the material, i.e., pore diameter and their interconnections (closed and open). On the other hand, with the SEM technique the external surface was observed, and with that can drown conclusions, e.g., ceramization state, porosity related to the capacity of water absorption (open porosity).

D.5.1.4. LEACHING TEST

The leaching test was carried out following standard DIN 38414-2, for $LWAS_{GR}$ BYRC, BS_{15}, BB_{15} and DE_{15} sintered at 1000°C (DIN38414-2:1985-11, 1985), being the ones that have the better results and introducing more amount of waste.

This test determines the hazardousness of the LWA_S leachates, suitable for determining the mobility of inorganic compounds present in liquids, solids, and multiphase residues. The samples were analyzed by ICP-mass spectrophotometry. Procedure and equipment used were described in section C (C.2.6. Leaching Test and Inductively Coupled Plasma Mass Spectrometry (ICP-MS)).

Table D.5.1.4.1. ICP results for $LWAS_{GR}$ (ppm-mg/l)

Ppm - mg/l	Cr	Ni	Cu	Zn	As	Se	Ag	Cd	Pb
BYRC	0.0221	0.0046	0.0220	0.0239	0.0120	0.0123	0.0021	0.0012	0.0017
BS_{15}	0.0293	0.0044	0.0215	0.0249	0.0117	0.0043	0.0024	0.0013	0.0016
BB_{15}	0.0305	0.0047	0.0238	0.0150	0.0152	0.0169	0.0030	0.0014	0.0040
DE_{15}	0.0151	0.0056	0.0252	0.0145	0.0128	0.0160	0.0031	0.0015	0.0034
2003/33/CE	<0.10	<0.12	<0.60	<1.20	<0.06	<0.04	-	<0.02	<0.15

Concentration value has been taken as a reference, concluding that measured elements are below the limits established by the European normative consulted (2003/33/CE, 2003).

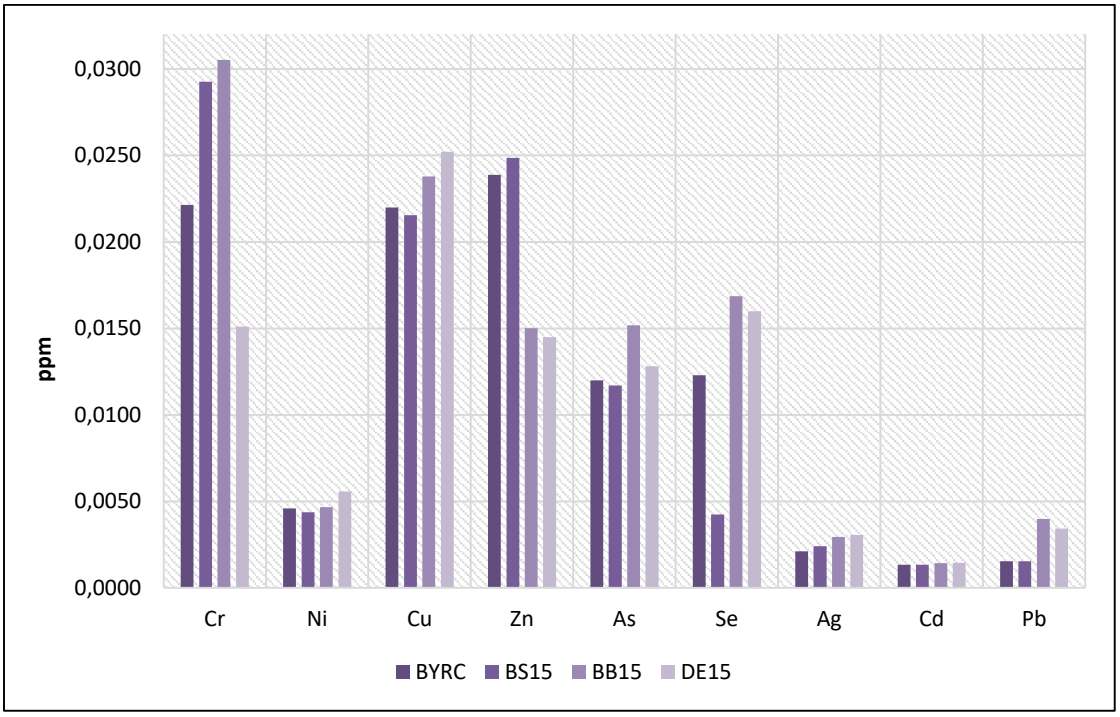

Figure D.5.1.4.1. ICP results for $LWAS_{GR}$ (ppm)

D.5.1.5. INSULATING PROPERTIES

The improvement of the insulation capacity in green roof installation, intel the reduction in the energy inputs to could/hit a building. The insulation capacity is related to the porous structure and low bulk density values. To analyze of the pores structure related to the insulation capacity of the LWA_S, was perform a test using a thermal imaging camera Fluke Ti-32 (Fluke, Everett, USA) and a Thermal house 3.6.03-00 (Thermodynamics, PHYW, Germany). Procedure and equipment used were described in section C (C.2.7. Insulation capacity).

The measurements were performed with the thermal camera, to take the images of infrared radiation emitted. The three $LWAS_{GR}$ BS_{15}, $BB_{15,}$ and DE_{15} (sintered at 1000°C) were compared with the aggregates without added waste (BYRC). For the measurements, the LWA_S for each mix was placed in a metal tray and located over the thermal house, according to standards (UNE-EN-12667:2002, 2002).

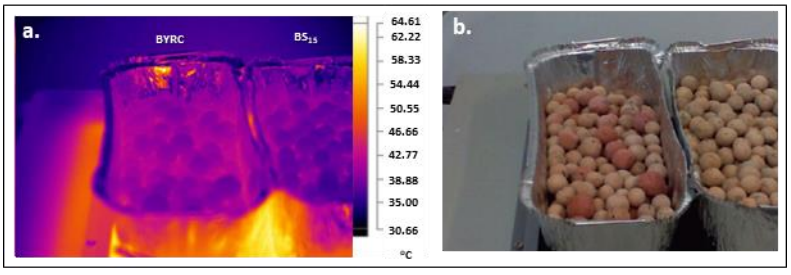

Image D.5.1.5.1. Comparison of thermal imaging of BYRC and BS_{15}. Infrared (a) and visible light imaging (b).

In image D.5.1.5.1, were analyzed the results of the thermographic camera test of BS_{15} in comparison with BYRC. From the thermal image (a), can be highlighted that the strong violet color is more evident in the right side of the image, related to BS_{15} by the temperature rate, sowed in Image D.5.1.5.2. The maximum temperature dropping occurs with BS_{15} in 1.56°C.

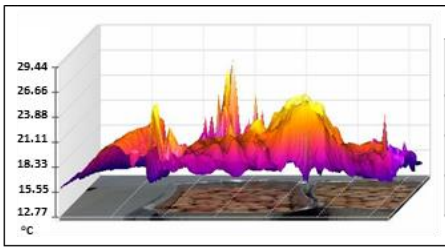

Temp. °C	BYRC	BS_{15}	Temp. dropping (°C)
Maximum	20.72	19.16	1.56
Average	17.11	16.27	0.84
Minimum	15.44	15.11	0.33

Image D.5.1.5.2. Image 3D-infrared and temperature rate of BYRC and BS_{15}.

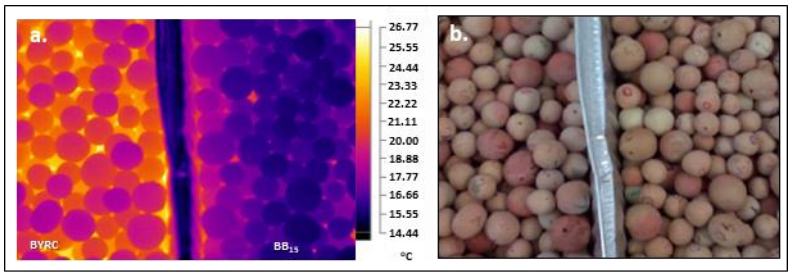

Image D.5.1.5.3. Comparison of thermal imaging of BYRC and BB_{15}. Infrared (a) and visible light imaging (b).

In Image D.5.1.5.4 from the thermal image (a), can be highlighted that the strong violet colour is more evident on the right side of the image, related to BB_{15} as it was expected and in accordance with the temperature rate, sowed in Image D.5.1.5.5, were the temperature dropping occurs with BB_{15} in 5.55°C, i.e., 26.27% maximum temperature reduction.

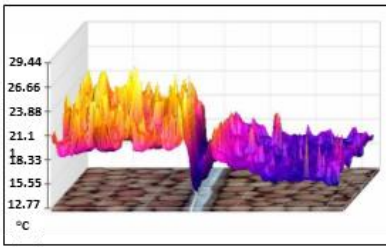

Temp. °C	BYRC	BB_{15}	Temp. dropping (°C)
Maximum	26.27	20.72	5.55
Average	20.33	16.27	4.06
Minimum	17.33	15	2.33

Image D.5.1.5.4. Image 3D-infrared and temperature rate of BYRC and BB_{15}.

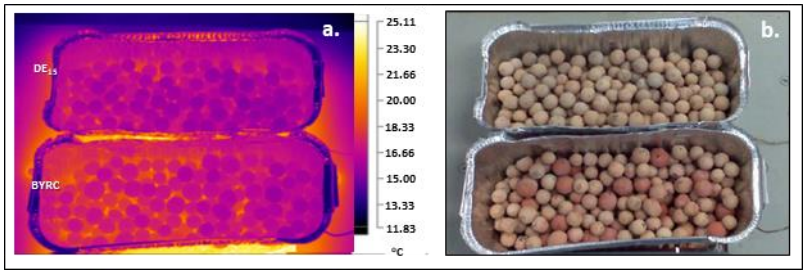

Image D.5.1.5.5. Comparison of thermal imaging of BYRC and DE_{15}. Infrared (a) and visible light imaging (b).

In image D.5.1.5.5, from the thermal image (a), can be highlighted that the strong violet and deep pink colours are more evident on the upper side of the image (DE_{15}) in accordance with the temperature rate, sowed in Image D.5.1.5.6, were the temperature dropping occurs with DE_{15} in almost 1.00°C, the lowest temperature reduction of the tree sustainable LWA_S.

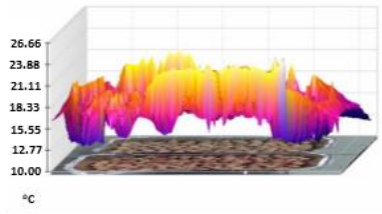

Temp.°C	BYRC	DE_{15}	Temp. dropping (°C)
Maximum	20.38	19.55	0.83
Average	17.27	16.33	0.94
Minimum	16.11	15.16	0.95

Image D.5.1.5.6. Image 3D-infrared and temperature rate of BYRC and DE_{15}.

The insulation capacity is related to the clause porosity (Elías, 2012b) and the water absorption capacity is related to open porosity. According to the weight loss and porosity percentages data in particular for BB_{15} reveal that higher organic content increased porosity and decreased bulk density, improving insulating properties. The improvement in this material characteristic generates a decrease in the energy consumption for heating/cooling the building. This aspect is also important for crops, increasing moisture retention by preventing evaporation.

D.5.1.6. CARBON FOOTPRINT CALCULATION (CFP)

Base on the inventory analysis displayed in sections C.3.2 (Life Cycle Inventory), C.3.2.1 (LWA_S for green roofs) and C.3.3 (Assumption and Cutting); and the application of IPCC 2013 GWP 20y as impact assessment methodology for global warming and Carbon Footprint calculation, the CFP calculation was carried out in comparison of $LWAS_{GR}$ with LWA_S without waste (BYRC). According with the research results, the aggregates suitable for use as a drainage layer in the installation of green roofs are BS_{15}, BB_{15} and DE_{15}.

Table D.5.1.6. CFP of LWA_S. BYRC, BS_{15}, BB_{15}, and DE_{15}. IPCC 2013 GWP 20y.

Unit	BYRC	BS_{15}	BB_{15}	DE_{15}
kg CO_2 eq.	4.78	3.82	3.21	4.12

The results show that 15% less extraction of virgin raw materials (clays) by replacing them with waste that acts as alternative fuels inside the furnace, reduces the demand for non-removable resources (electric energy, diesel, pet-coke). This affects directly to the gas emissions, associated with the greenhouse effect and global warming.

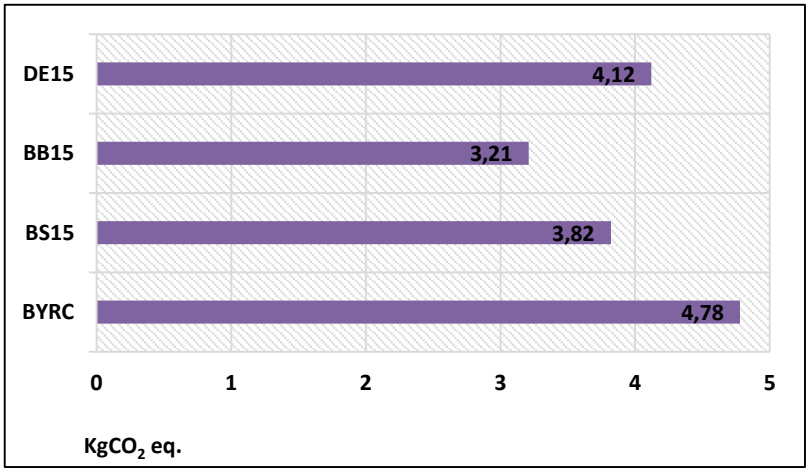

Figure D. 5.1.6.1. CFP of LWA_S, BYRC, BS_{15}, BB_{15}, and DE_{15}. IPCC 2013 GWP 20y.

The use of 15wt% of BS reduces about 20.00% the emissions of GHG, in turn, the addition of 15wt% of BB is reduced about 32.00% the GHG and finally 15wt% of DE, by about 13.00%. Mix that less $KgCO_2$ eq. emits is the BB_{15}, being the mixture with the more significant calorific contribution of the three.

D.5.2. LWA_S FOR AGRONOMIC PURPOSES. $LWAS_{AP}$

D.5.2.1. TECHNOLOGICAL PROPERTIES. FIRST STAGE.

Determination of proper percentage addition of organic matter to generate the porosity within the ceramic structure, one of the most important conditions required for the use of the material as a culture substrate.

To determine the optimal sintering temperatures and pore forming agent percentages, in the first stage were elaborated the samples with the WBC clay-base mixture clay with 0, 5, 10, 15% of BS (brewery sludge), MBM (meat-bone meal) and CC (corn cob), sintered at 900 and 1000°C, for one hour. The sustainable LWA_S developed were subject to the following tests: water

absorption capacity by immersion of samples in cold water for 24 hours (UNE-EN-772-21:2011, 2011) and in boiling water (100ºC) for 6 hours (UNE-EN-772-7:1999, 1999); bulk density (BD); real density (RD); total porosity percentage (TP%); pH value (UNE-EN-13037, 2012); electrical conductivity (EC) (UNE-EN-13038, 2012).

Table D.5.2.1.1. LWA_{AP} weight loss (%) after sintering for 1 hour at 900ºC/1000ºC.

LWA_S	**WBC**	**$WBBS_5$**	**$WBBS_{10}$**	**$WBBS_{15}$**	**$WBMBM_5$**	**$WBMBM_{10}$**	**$WBMBM_{15}$**	**$WBCC_5$**	**$WBCC_{10}$**	**$WBCC_{15}$**
900ºC	15.96	17.64	18.18	20.39	15.37	20.57	23.71	18.59	22.99	28.25
1000ºC	15.95	17.76	18.54	20.68	16.57	19.16	21.98	18.69	22.99	27.09

In table D.5.2.1.1, the weight loss (%) after sintering for 1 hour at 900ºC/1000ºC, are reported.

For the determination of the absorption capacity in cold water for 24 hours and water boiling water for 6 hours, in both cases, the samples were placed in glass vessels, as shown in figure D.7.2.1.1.A and B, wholly covered with distilled water. In the case of immersion in cold water, the samples stay in the distilled water for 24 hours. After this time the excess of surface water is removed with a damp cloth, and its weight is recorded.

The water absorption test by immersion in boiling water for 6 hours was carried out on heating-bases (or plate) (Figure D.5.2.1.1.B). The samples were left in the water to cool by convection. After this time the excess of surface water was removed with a damp cloth and weight.

Image D.5.2.1.1. Water absorption capacity test.

As can be seen in Image D.5.2.1.1.C, $WBCC_{15}$ samples sintered at the two temperatures (900-1000oC) showed a loss of material, during the test in boiling water for 6 hours, resulting in alteration of the measurements. These results are marked (*) in the result tables Table D.5.2.1.2 and D.5.2.1.3.

Employing the equipment described in section C (C.2.2. pH and C.2.3. Electrical conductivity), LWA_S were subjected to bulk and real density measurements, and the total porosity was calculated.

The results from the first Stage LWA_S the physicochemical properties like water absorption capacity in cold water (WAC%), water absorption capacity in boiling water (WAB%), bulk density (BD), total porosity (TP), pH and electrical conductivity (EC), at the two different sintering temperatures are listed in Table D.5.2.1.2 and Table D.5.2.1.3.

Table D.5.2.1.2. The first step LWA_S sintered at 900°C, physicochemical properties.

LWA_S/900°C	WAB (%)	BD (Kg/m^3)	TP (%)	pH	EC (mS/cm)
WBC	30.78	1470.00	20.40	12.34	7.32
$WBBB_5$	37.36	1340.00	41.20	11.64	3.83
$WBBS_{10}$	41.33	1260.00	49.81	11.44	3.40
$WBBS_{15}$	49.44	1180.00	55.73	10.56	3.92
$WBMBM_5$	40.00	1060.00	42.64	10.94	2.39
$WBMBM_{10}$	51.42	1050.00	53.92	11.96	6.37
$WBMBM_{15}$	37.18*	1000.00	62.79	10.91	4.04
$WBCC_5$	53.56	1120.00	49.08	11.81	5.23
$WBCC_{10}$	59.61*	950.00	57.22	11.25	3.89
$WBCC_{15}$	81.18*	820.00	69.06	11.08	3.87

In Table D.5.2.1.2., the case of aggregates sintered at 900°C, have shown satisfactory results, in particular, samples $WBCC_{15}$ with water absorption capacity (WA) of 81.18%, bulk density (BD) of 820.00 kg/m^3 and total porosity (TP) of 69.06%. Regarding chemical properties as pH and electrical conductivity (EC), the values measured 11.8, and 3.87 mS/cm respectively were high for use in soils. For that reason, the samples sintered at 900°C were considered unable for agriculture applications.

The LWA_S suitable for agricultural use would have specific physicochemical characteristics like water absorption capacity >40%, bulk density between 500.00-1200.00 kg/m^3, pH value in the range of 6.5-7.5 and electrical conductivity (EC) <2.00 mS/cm, as growing substrate conditions (Enzo et al., 2001b; Martínez and Roca, 2011). pH and conductivity have been measured to confirm their counting of inert materials suitable as a growth media.

Table D.5.2.1.3. The first step LWA_S sintered at 1000°C. Physicochemical properties.

LWA_S/1000°C	WA (%)	BD (Kg/m³)	TP (%)	pH	EC (mS/cm)
WBC	30.12	1490.00	20.13	11.30	3.42
$WBBS_5$	38.29	1310.00	52.90	9.65	0.94
$WBBS_{10}$	43.73	1240.00	55.85	7.26	1.26
$WBBS_{15}$	51.02	1120.00	60.15	7.50	1.48
$WBMBM_5$	36.55	1020.00	56.35	11.90	2.55
$WBMBM_{10}$	51.39	920.00	59.89	11.29	3.39
$WBMBM_{15}$	66.64*	960.00	64.73	10.22	1.98
$WBCC_5$	44.51	1120.00	58.13	11.28	3.35
$WBCC_{10}$	65.66*	1020.00	61.29	11.00	1.74
$WBCC_{15}$	76.08*	830.00	69.84	9.50	2.29

On the other hand, LWA_S sintered at 1000°C shown a decrease in pH value being inversely proportional to the percentage of waste/by-product introduced (Table D.5.2.1.3). This fact is due to the substitution of clays with a high content of alkaline and alkaline earth cations, i.e., carbonate.

Therefore, and based on the results of the first step, the following considerations were taken into account:

- Samples $WBBS_{10}$ and $WBBS_{15}$ present physicochemical parameters suitable for their use for agricultural purposes. The $WBBS_{15}$ composition shows better water absorption capacity.
- The pore-forming agent was set to 15wt% and 1000°C the sintering temperature.
- Brewery sludge (BS) was considered the waste with better adaptability. After draining presents a clay-like consistency, which makes it more suitable as an input in the production of LWA_S. The strong odor produced during the drying and sintering of the LAW_S can easily solve by storing a scrubber at the exhaust of the stove and oven.

$WBBS_{15}$ present physicochemical parameters that fall in range for their use as growth media. Also from a circular economy point of view was considered that these mixtures use a significant amount of waste generating substantial saving in the consumption of virgin raw materials and energy in the firing process.

D.5.2.2. TECHNOLOGICAL PROPERTIES. SECOND STAGE.

Therefore, and based on the results of the first step, in the second step it was considering working in the second step with local Italian clay, red clay (RC), with different properties and less

calcium carbonate content, to reduce pH value. At the same time, it presents a state of ceramization elevated at lower temperatures compared to the black and white clays, mainly due to the low content of carbonate (Farias et al., 2017a). Concerning the bloating behavior, red IT clay contains significant cuantities of oxides with melting properties content (vitrification capacity) related to the bloating capacity through the vitrification of the surface material during the thermal treatment.

At the same time, was added the fertilizer glass (FG) in comparison with CBA, based on previous research work related to in the final project elaborated by Alessandra Lugari and directed by Luisa Barbieri, related to the valorization of animal flour ash and Glassy sand® for active glasses (Barbieri et al., 2014). Those materials were added to confer fertilizing capacities to the LWA_S. GS, CBA, and FG was previously valorized for the research group led by Prof. Luisa Barbieri, as support for lipase immobilization (Barbieri et al., 2016), cementitious composites (Bursi et al., 2017), as ASR performance of cement mortars (Saccani et al., 2017).

For the production of LWA_S, two clay-based mixtures were used WB (30 wt% white-70 wt% black clay) and RC (100 wt% red clay). As a pore-forming agent 15wt% of brewery sludge (BS) was added to the mixture (Farias et al., 2017a). Cattle-bone ashes (CBA) and fertilizer glass (FG) 10wt%, were added to confer fertilizer capacity due to their phosphorus (P) and potassium (K) content.

The fertilizer glass (FG) was obtained by mixing 40 wt% of CBA as P intake; 42 wt% of GS as parent glass and 18 wt% as K intake (Barbieri et al., 2014). The mix was subjected to melting at 1450°C for 2hours and cast in water.

The samples were submitted to a sintering process at 1000°C for one hour. The formulation batch is reported as it follows:

- Clays without waste (WBC and RC),
- Clays containing 15 wt% BS ($WBBS_{15}$ and $RCBS_{15}$),
- Clays with 15wt% of BS in addition to 10wt% of glass (WB_{FG} and RC_{FG}),
- Clays with 15wt% of BS in addition to 10wt% of CBA (WB_{CBA} and RC_{CBA}).

Table D.5.2.2.1. LWA_S weight loss (WL%) after sintering.

LWA_S	**WBC**	**$WBBS_{15}$**	**WB_{FG}**	**WB_{CBA}**	**RC**	**$RCBS_{15}$**	**RC_{FG}**	**RC_{CBA}**
WL (%)	16.47	21.65	19.93	19.96	9.73	16.31	14.52	14.65

In table D.5.2.2.1, weight loss (WL%) from each sample expressed in percentage (%) was reported, after sintering at 1000°C for one hour.

LWA_S are granular materials with a loose bulk density (BD) less than 1.20 g/cm^3 or a particle density (PD) not exceeding 2.00 g/cm^3 (UNE-EN13055-1, 2003). The particle density (PD) and water absorption (WA_{24}) were determined by the established procedure described by EN-ISO 1097-6 (annex C) (UNE-EN-1097-6, 2014), while bulk density (BD) and void percentage (VP%) were determined according to EN-ISO 1097-3 standards (UNE-EN-1097-3, 1999). Real density (RD) was calculated by pycnometer Accupyc TM II 1340 (Micromeritics) and total porosity (TP) by means of the following formula: TP%=[(1-BD)/RD]*100 (Bernhardt et al., 2013).

Table D.5.2.2.2. LWA_S water absorption, total porosity, and void percentage.

	Water Absorption (%)	**Total Porosity (%)**	**Void percentage (%)**
	WA_{24}	**TP**	**VP**
WBC	29.26	33.21	41.09
$WBBS_{15}$	40.29	59.19	67.07
WB_{FG}	38.11	60.47	68.35
WB_{CBA}	39.86	71.18	79.06
RC	7.27	75.32	80.14
$RCBS_{15}$	19.01	49.61	57.49
RC_{FG}	16.99	59.39	60.31
RC_{CBA}	19.46	62.44	65.44

Tables D.5.2.2.2 and D.5.2.2.3 shows the results of technical properties of LWA_S sintered at 1000°C. Materials with connected or open pores tend to absorb water, in contrast, materials with isolated pores or a vitrified surface coating will absorb less water. The results demonstrated that the WA_{24} of sintered samples increases with the addition of 15wt% BS, depending on the clay mix used, 11.03% for WBC-$WBBS_{15}$ and 11.74% for RC-RBS_{15}. The decrease of WA% is observed with the addition of fertilizer glass (FG) in about 2.18% in $WBBS_{15}$-WB_{FG} and about 2.02% in RBS_{15}-RC_{CBA}. The addition of CBA generates an increase of WA_{24} of almost 2% for WB_{FG}-WB_{CBA} and RC_{FG}-RC_{CBA}.

If the values of WA_{24} and TP% are compared, it can be seen that the RC mixture has a very low water absorption capacity of 7.27%, in contrast to the very high TP (75.32%) and VP% (80.14%) value. This is related to the type of thermal treatment carried out in this research by placing the ceramic material directly at the sintering temperature (1000°C) for one hour, to promote the bloating of the ceramic material. Also, the thermal properties of red IT clay and its fluxing

capacity due to the content of oxides with melting features, associated with the low content of carbonates.

Table D.5.2.2.3. LWA_S particle, bulk, and real density.

	Particle density (g/cm^3)	Bulk density (g/cm^3)	Real density (g/cm^3)
	PD	**BD**	**RD**
WBC	1.92	1.34	2.63
$WBBS_{15}$	1.83	1.25	2.80
WB_{FG}	1.86	1.15	2.49
WB_{CBA}	1.80	0.72	2.34
RC	2.32	0.81	2.69
$RCBS_{15}$	2.19	1.34	2.29
RC_{FG}	2.14	1.19	2.30
RC_{CBA}	2.08	0.75	2.31

Can also be highlighted that the particle, bulk, and real density values tend to deceive as residue replaces the clay minerals in the formulation. This is more evident in the mixtures with the addition of FG since the parameters increase slightly.

Table D.5.2.2.4. LWA_S pH and electrical conductivity values.

Parameters	WBC	$WBBS_{15}$	WB_{FG}	WB_{CBA}	RC	$RCBS_{15}$	RC_{FG}	RC_{CBA}
pH	9.21	7.42	6.98	8.00	7.16	7.28	6.71	7.15
EC (mS/cm)	3.24	1.74	1.12	1.98	1.15	1.57	0.72	1.09

pH and EC values were within the ranges for use as additives or growing soils, except for WBC and WB_{CBA}, out of range for growing substrates.

Table D.5.2.2.5. Technical properties of commercial LWA_S.

	WA (%)	BD (kg/m^3)	TP (%)	pH	EC (mS/cm)
Leca Green®	37-40	600-800	65.00-76.00	7.00-8.00	2.20-4.00
Agrex®	22.80-27.30	270-550	-	-	-
Laterlite Agri®	0.30-0.38	-	-	6.00-7.00	-
Arexpan hydro®	-	-	-	7.00-8.00	-

Table D.5.2.2.5, shows the technical parameters of commercial LWA_S used as growing substrates in different applications like green roofs, hydroponic cultivation or pottery. It can be seen that the materials obtained are within the technical characteristics of these commercial materials.

The fertilizer glass manufacturing leads to an increment of the costs and energy consumption during production. For that reason, aggregates formulated with FG were compared to samples made with CBA, as an alternative raw material with low energy consumption.

D.5.2.3. LWAs X-RAY POWDER DIFFRACTION (XRD)

This study has been conducted to determine the new crystalline phases formed between the clay and technical nutrients that could favour the release of P and K, for their agronomic use. After thermal treatment (1000°C) a sample of each composition was submitted to XRD analysis.

In Figure D.5.2.3.1, is reported the spectra corresponding to WB clay-mix samples, WBC, WB_{15}, WB_{FG} and WB_{CBA}. The main peaks are related to quartz (Q) (01-085-0796) and Anorthite (A), ($CaAl_2Si_2O_8$), (00-041-1486). Moreover, a few carbonates are observed, remaining in the structure of the material after thermal treatment in the form of calcite ($CaCO_3$) associated with Akermanite [$Ca_2(Mg0.5Al0.5)(Si1.5Al0.5O_7)$], (01-079-2423) and Albite [(Na0.84Ca0.16) Al1.16Si2.84O_8], (01-076-0927). The addition of BS into the clays does not modify the mineralogy of the system: the characteristic peaks relative to the quartz (Q) remain but are reduced in intensity due to the replacement of clay. The presence of CBA introduces hydroxyapatite crystalline phase (P) [$Ca_5(PO_4)3OH$], (01-076-0694).

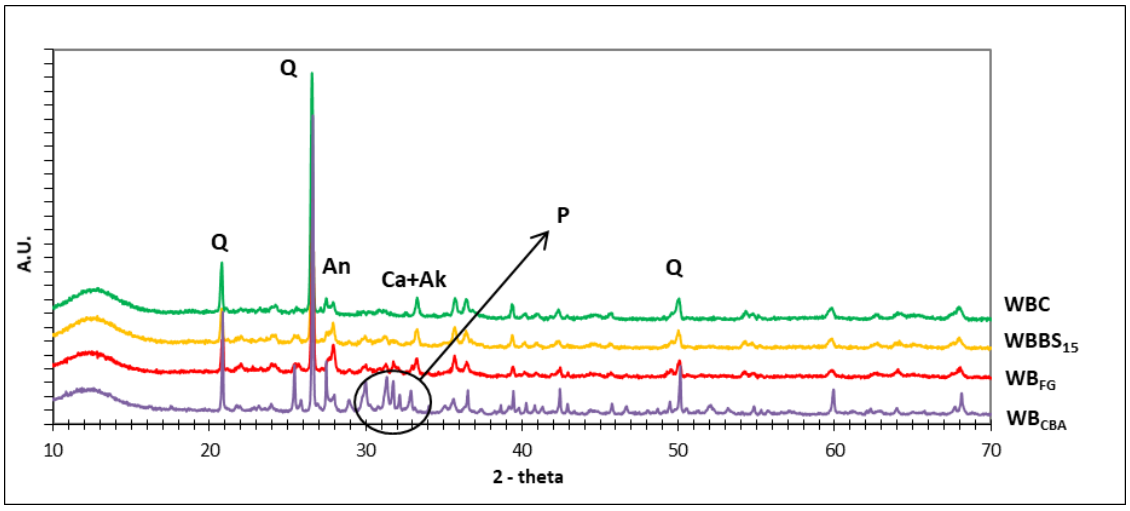

Figure D.5.2.3.1. XRD WB clay-mix samples. Quartz (Q), Anorthite (An), calcite (Ca), Akermanite (Ak) and hydroxyapatite (P).

In Figure D.5.2.3.2, corresponding to the RC clay-mix, the main peaks are related to quartz (Q), (01-085-0796), with the presence of Hematite (H), (Fe_2O_3), 01-073-0603, and Anorthite (An), ($CaAl_2Si_2O_8$), (00-041-1486). These phases remain when the other raw materials (BS and CBA)

are added to the clays: in particular Quartz and Hematite decrease, while Anorthite intensity increases. This last aspect is imputable to the presence of high amount of CaO in both BS and CBA that reacts with silicon oxide during the sintering step. The presence of CBA introduces hydroxyapatite crystalline phase (P) [$Ca_5(PO_4)3OH$], (01-076-0694).

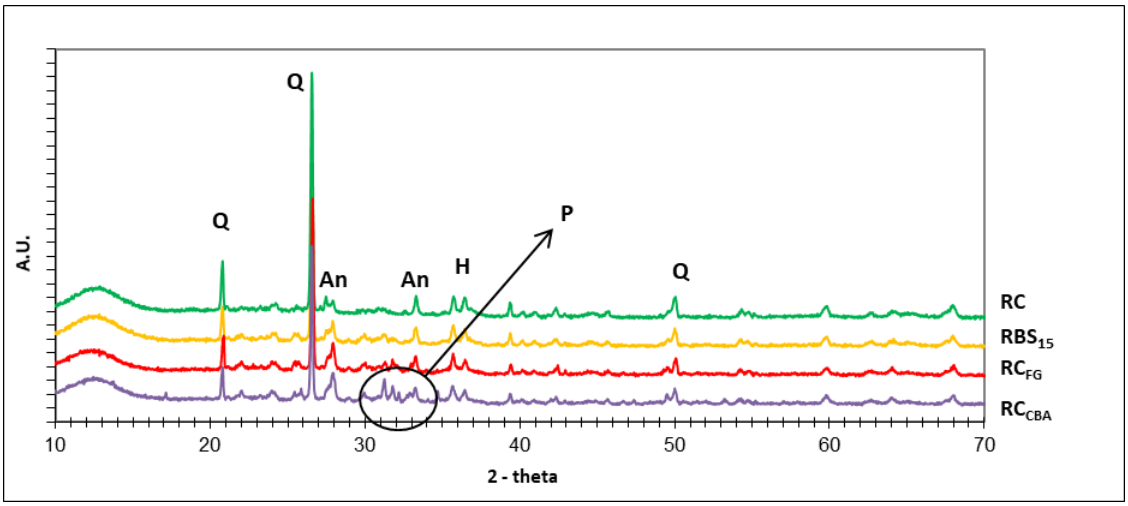

Figure D.7.2.3.2. XRD red Italian clay (RC) clay-mix samples. Quartz (Q), anorthite (An), hematite (H) and hydroxyapatite (P).

The presence of a crystalline phrase contenting phosphor (P), like hydroxyapatite, is important for the nutrition of the plants and the use of the LWA_S as a culture medium.

D.5.2.4. MERCURY INTRUSION POROSIMETRY (MIP)

This analysis aims to study the characteristics of the porosity generated by the addition of organic and inorganic waste. The term "porosimetry" means the measurements of pore size distribution, Hg volume intrudes, apparent and skeletal density, and other porosity-related characteristics of the material (i.e., tortuosity, total pore area). This analysis provides essential data to understand the formation, structure, and potential use of many materials. The porosity of a ceramic material affects its physical and mechanical properties, i.e., its behavior in its surrounding environment (Micromeritics, 1985). Procedure and instrumentation used were described in section C (C.2.5.1. Mercury intrusion porosimetry (MIP)).

Base on the results of the previous determinations, this study has been carried out on the samples without waste (WBC and RC), samples with the addition of 15wt% BS ($WBBS_{15}$ and $RCBS_{15}$), samples with the addition of 15wt% BS and 10wt% FG (WB_{FG} and RC_{FG}) and samples with the addition of 15wt% BS with 10wt% CBA (WB_{CBA} and RC_{CBA}), sintered at 1000°C.

D.5.2.4.1. WB CLAY-MIX SAMPLES.

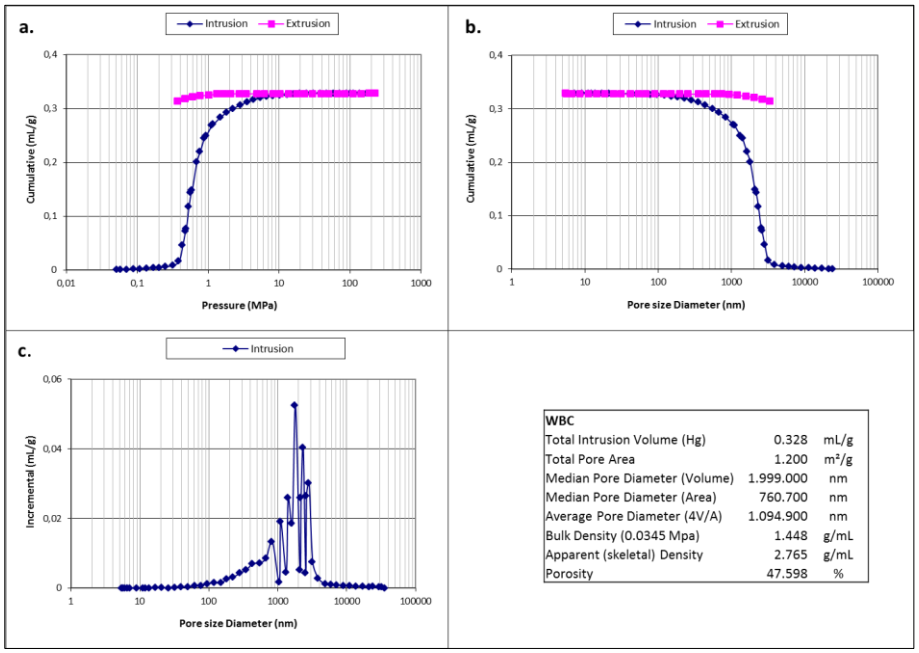

Image D.5.2.4.1.1. Porosimetry curves of WBC sample. a) Cumulative intrusion volume vs. pressure; b) Cumulative intrusion volume vs. pore size diameter; c) pore size distribution.

The comparison between the mixture with only clays (WBC) and the mixture with the addition of brewery sludge 15wt% ($WBBS_{15}$), confirmed the data obtained by picnometry, as expected. This difference is evident in average pore diameter (APD) values: of 1094.90 nm for WBC and 1273.00 nm for $WBBS_{15}$, as well as in the calculation of total porosity 47.59% and 54.78% respectively.

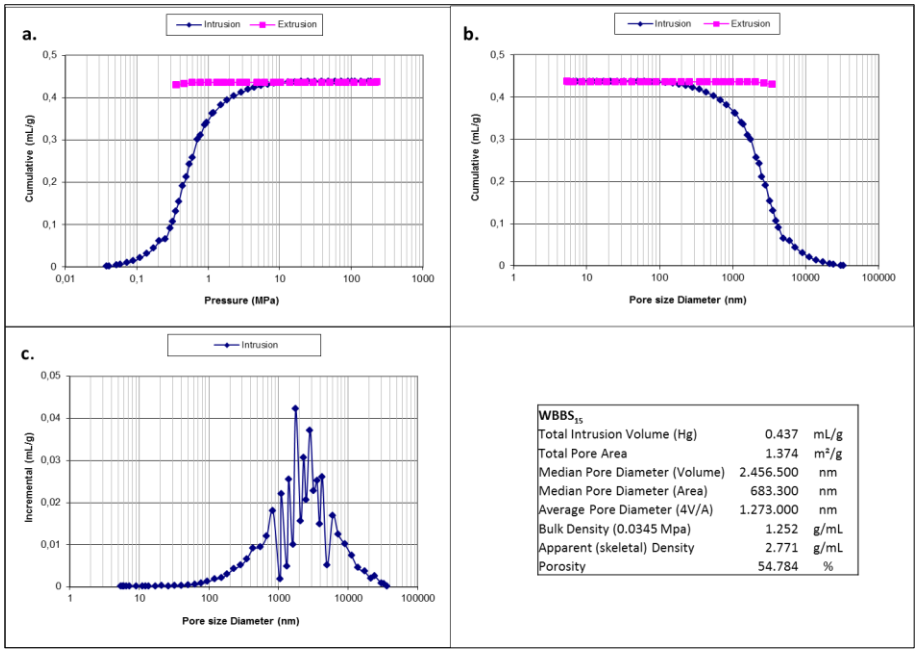

Image D.5.2.4.1.2. Porosimetry curves of $WBBS_{15}$ sample. a) Cumulative intrusion volume vs. pressure; b) Cumulative intrusion volume vs. pore size diameter; c) pore size distribution.

In the previous studies carried out, the water absorption capacity of the samples with the admission of FG (WB_{FG} and RC_{FG}), decreased by the addition of FG compared with $WBBS_{15}$ and $RCBS_{15}$. The absorption of water is related to the open porosity, in this analysis, all the porosity of the material is reported.

The total porosity value for WB_{FG} is 48.99%, reporting a decrease of 10,561% concerning $WBBS_{15}$. However, the parameters related to the size pores, WB_{FG} presents some larger pores, indicated by the average pore diameter value of 1339.90 nm/1.33 µm and 1273.00 nm/1.27 µm for $WBBS_{15}$.

For $RCBS_{15}$ it is observed that the different pore diameters, most of them in are in the range of between 700-1000 nm/0.7-1.00 µm (Image D.5.2.4.2.2.c), being the mixture with the largest number of pores and larger dimensions of all the blends made with WBC clay-mixture.

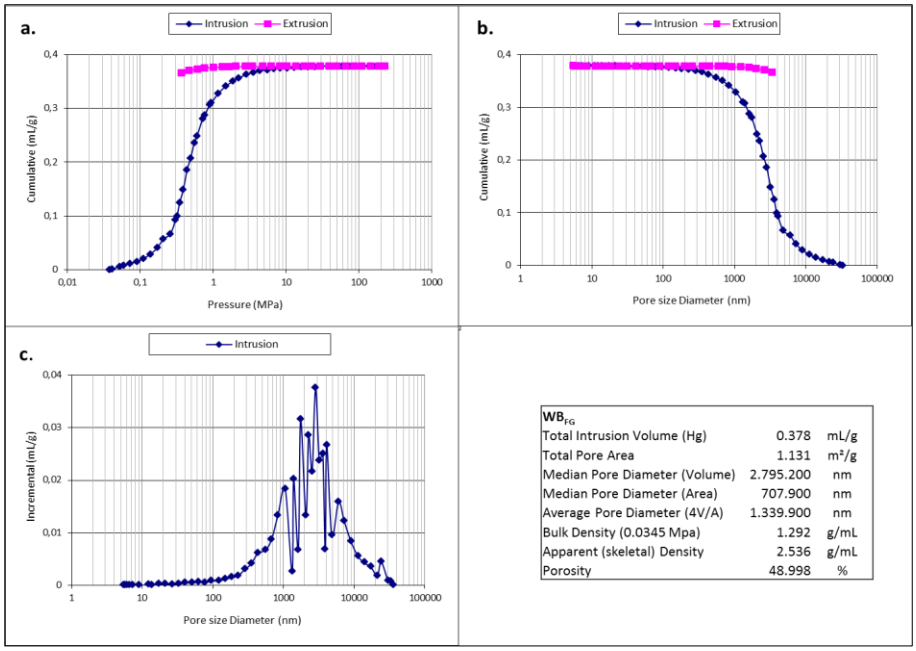

Image D.5.2.4.1.3. Porosimetry curves of WB_{FG} sample. a) Cumulative intrusion volume vs. pressure; b) Cumulative intrusion volume vs. pore size diameter; c) pore size distribution.

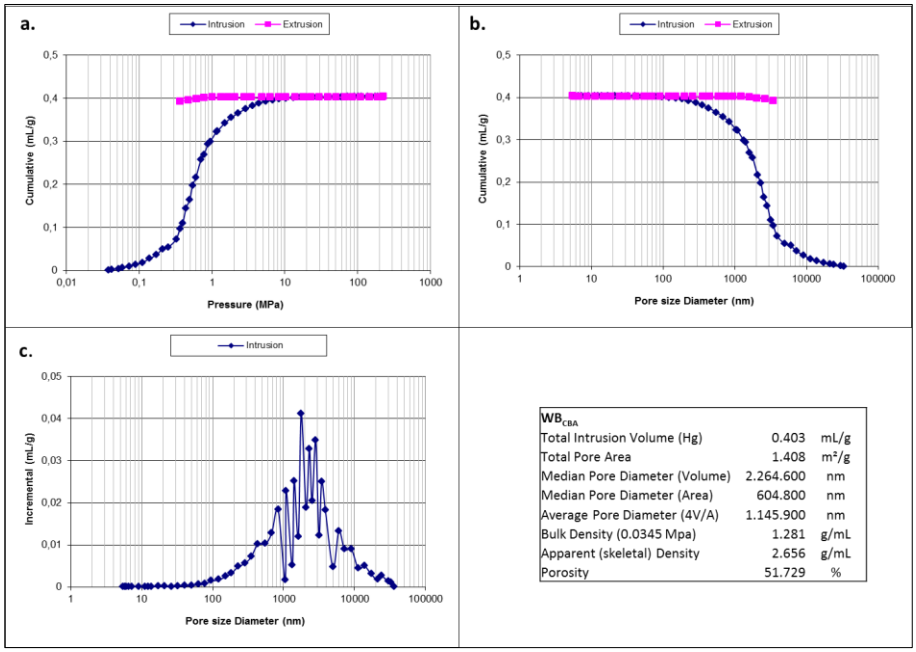

Image D.5.2.4.1.4. Porosimetry curves of WB_{CBA} sample. a) Cumulative intrusion volume vs. pressure; b) Cumulative intrusion volume vs. pore size diameter; c) pore size distribution.

By adding CBA, it also generates a decrease in the total porosity value 51.72% for WB_{CBA}, decreasing by 5.57% about $WBBS_{15}$ and increasing about WB_{FG} by 4.98%. Likewise, the volume

of average pore diameter (APD) is still higher for WB_{FG} (1339.90 nm/1.33 µ) than for WB_{CBA} (1145.90 nm/1.14 µm).

The differences between the two clay-base mixtures, WBC and RC, are very substantial. In previous studies, it has been confirmed that the high content of carbonates, among other reasons, generates a difference in the level of thermal reaction of the two mixtures. The WBC clay mixtures sintered less compared to RC mixture, at the same temperature (1000°C).

D.5.2.4.2. RC CLAY-MIX SAMPLES.

As seen in image D.5.2.4.2.1, the total porosity is the lowest of all the samples analyzed (22.15%), with a very low average pore diameter (233.60 nm). In the image D.5.2.4.5.c, can be highlighted that the main pores are from the same diameter, in the range 300-400 nm. The porosity value of WBC is double respect to RC porosity (47.59% -22.15%).

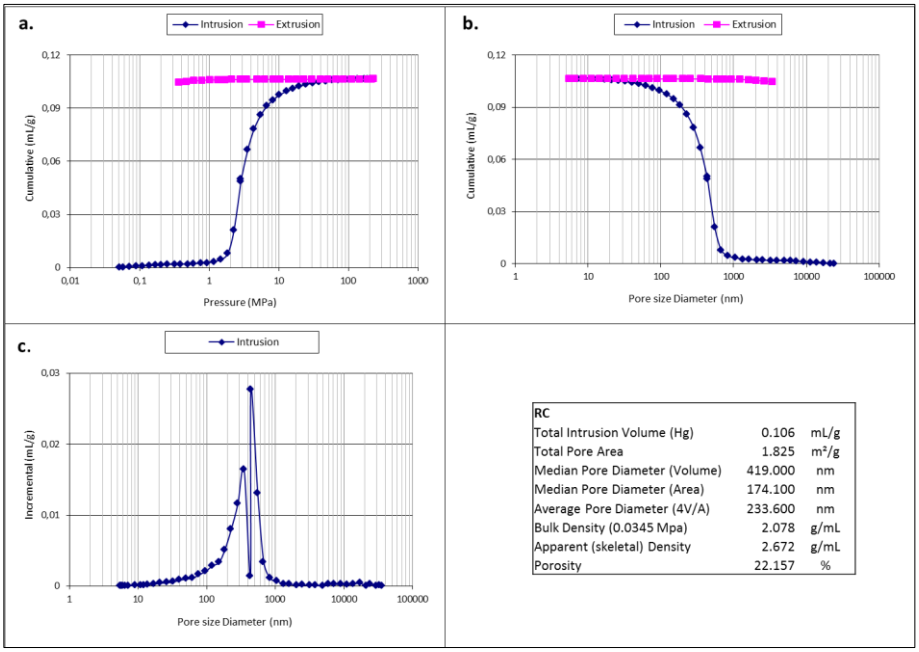

Image D.5.2.4.2.1. Porosimetry curves of RC sample. a) Cumulative intrusion volume vs. pressure; b) Cumulative intrusion volume vs. pore size diameter; c) pore size distribution.

For $RCBS_{15}$ (image D.5.2.4.2.2.c) shows that the different pore diameters, most of them in a range of between 700-1000 nm, being the mixture with the most substantial number of pores and largest dimensions of all the blends made with RC clay-mixture. As seen in the image D.5.2.4.2.2, the addition of 15wt% BS raises the porosity to 39.18%.

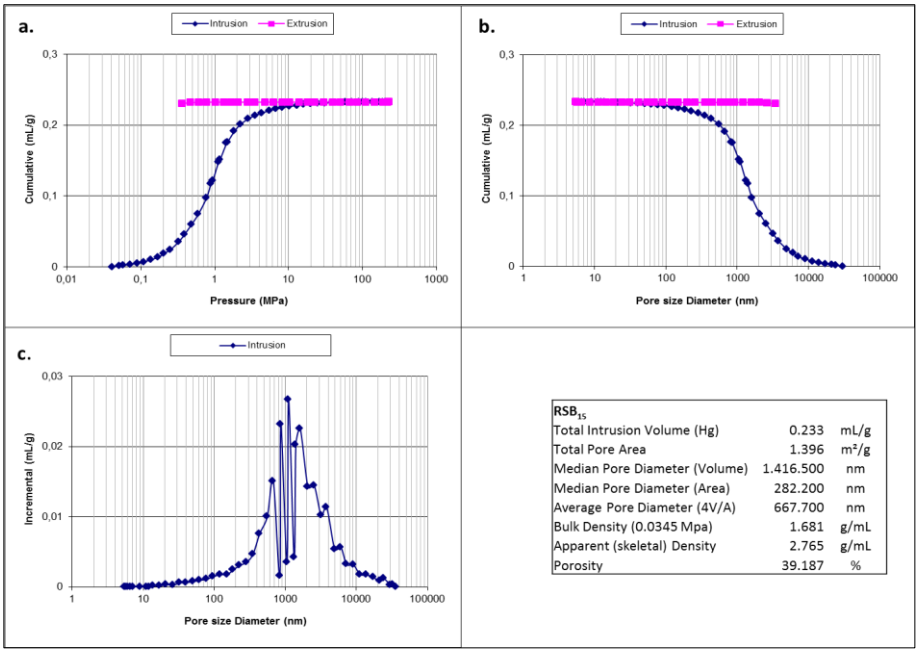

Image D.5.2.4.2.2. Porosimetry curves of $RCBS_{15}$ sample. a) Cumulative intrusion volume vs. pressure; b) Cumulative intrusion volume vs. pore size diameter; c) pore size distribution.

As it was previously observed, the addition of FG causes the descent of porosity in almost 10.00% also related to the water abortion capacity.

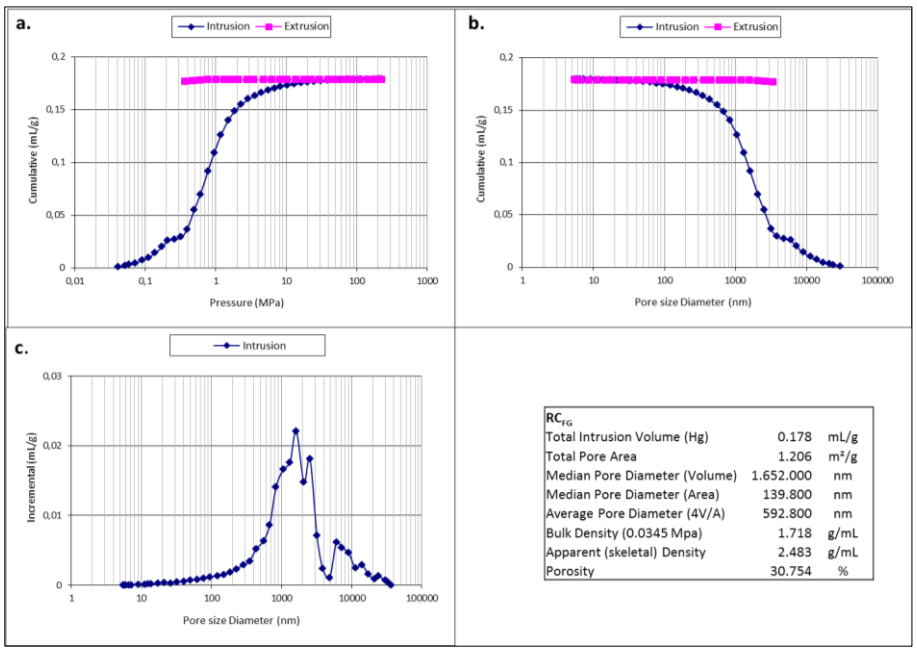

Image D.5.2.4.2.3. Porosimetry curves of RC_{FG} sample. a) Cumulative intrusion volume vs. pressure; b) Cumulative intrusion volume vs. pore size diameter; c) pore size distribution.

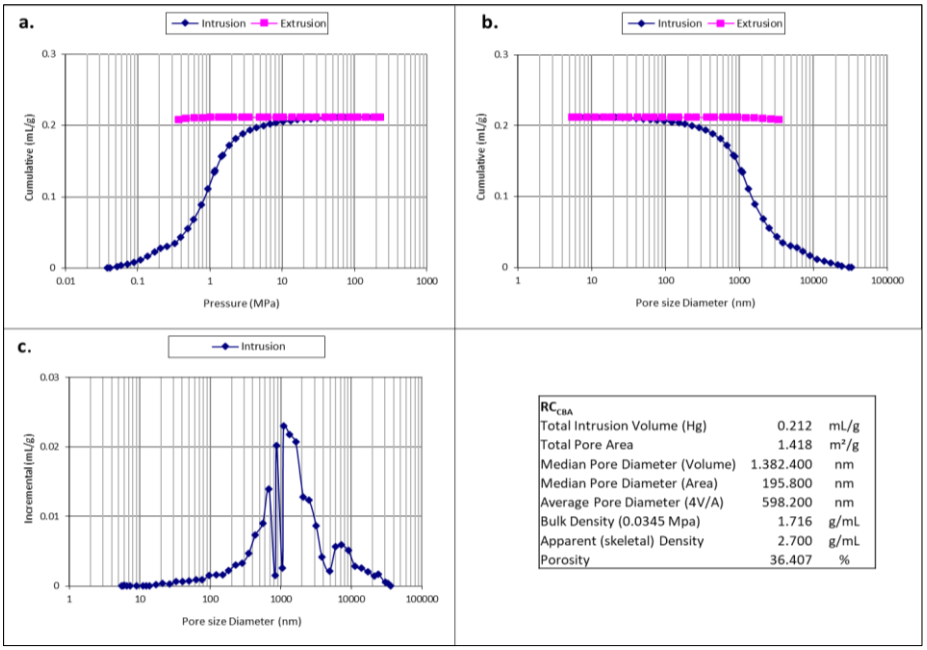

Image D.5.2.4.8. Porosimetry curves of RC_{CBA} sample. a) Cumulative intrusion volume vs. pressure; b) Cumulative intrusion volume vs. pore size diameter; c) pore size distribution.

In the porosity analysis of LWA_S, it confirms again the results obtained in the previous analyses carried out on the samples.

The vitrification capacity of the mixtures with FG generate the sealing of the superficial material layer, favouring the capacity of swelling generating larger pores, and lower water absorption capacity (Bui et al., 2013).

The values of apparent and bulk density as well as the values of porosity determined by this technique, do not coincide with the data obtained in tables D.5.2.2.2 and D.5.2.2.3. This is because the tests performed in section D.5.2.2 (Technological properties. Second stage) were performed on the whole samples, while the tests for Hg-MIP were performed on the broken samples in small pieces.

In the Table 7.5.2.4.1, shows data extracted from the results presented. Again it can be established that the addition of 15wt% of BS generates more porosity and with larger pore diameters. It can also be highlighted, and in correlation with the previous analyzes, that the red IT clay has a high ceramization, due to its melting components, so the surface layer is sealed and allows the material to expand generating a very porous ceramic matrix and with MPD very low (0.41 µm), in comparison to the WBC mixture (1.99 µm).

Table D.7.2.4.1. $LWAS_{GR}$ total intrusion volume (TIV), total pore area (TPA) and median pore diameter (MOD).

	WBC	**$WBBS_{15}$**	**WB_{FG}**	**WB_{CBA}**	**RC**	**$RCBS_{15}$**	**RC_{FG}**	**RC_{CBA}**
TIV-Hg (mL/g)	0.32	0.43	0.37	0.40	0.10	0.23	0.17	0.21
TPA (m^2/g)	1.20	1.37	1.13	1.40	1.82	1.39	1.20	1.41
MPD (Volume) (nm)	1990.00	2456.50	2795.20	2264.60	419.00	1416.50	1652.00	1382.40
MPD (Volume) (µm)	1.99	2.45	2.79	2.26	0.41	1.41	1.65	1.38

D.5.2.5. MICROSTRUCTURE AND CHEMICAL ANALYSIS (SEM-EDS) EXTERNAL SURFACE.

Using the scanning electron microscope (SEM) and energy dispersive spectroscopy (EDS), each $LWAS_{AP}$ were subject to microstructure analysis, regarding porosity, pore shape, superficial heterogeneity, and chemical composition. Proceed to the description of the results starting with the $LWAS_{AP}$ made with the 30% white-70% black clay (WBC), followed by the aggregates made with 100% red IT clay (RC). Particles showed different morphology and aggregation state depending on the sample.

D.5.2.5.1. WB CLAY-MIX SAMPLES.

Figure D.5.2.5.1.1 shows the microstructure of the WBC base mix. The porosity is concentrated on the grain edge and appears not complete sintering surface, not reacting to the thermal treatment (1000°C for one hour). The regular porosity can be linked to the organic matter and carbonates content in the clay material (LOI: white clay 19.90% and black clay 13.23%). The concentrations of silicon (21.29%) and calcium (7.91%) related to the quartz and calcite crystalline phases. Aluminium content (10.96%) linked to the vermiculite and biothite crystalline phases detected in XRD analysis (Image D.5.2.5.1.2).

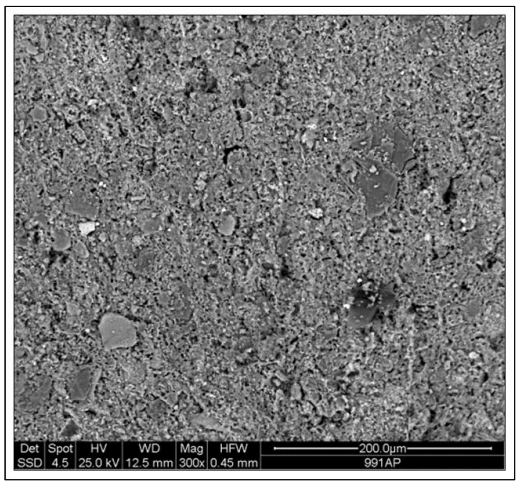

Image D.5.2.5.1.1. WBC - SEM image (300x) and EDS sample analysis.

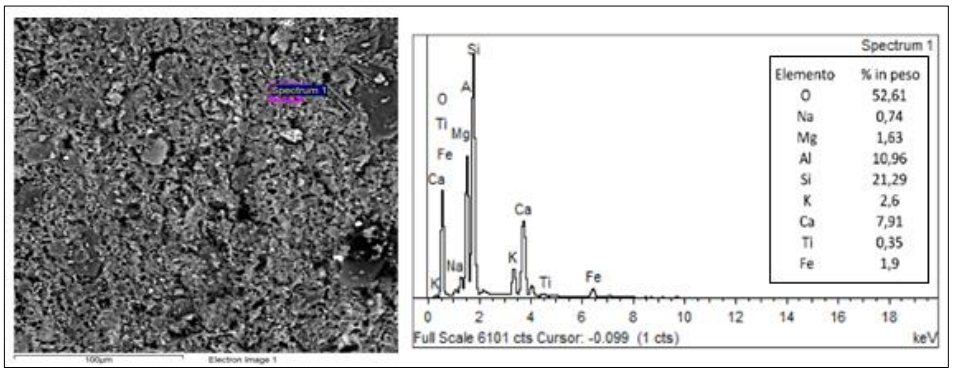

Image D.5.2.5.1.2. WBC - SEM image (600x) and EDS sample analysis.

The analysis of the $WBBS_{15}$ mixture (Image D.5.2.5.1.3), compared to the WBC mixture, shows more open porous structure, characterized by large inter-granular pores in the order of 1.00 µm/1000 nm, and well distributed. Elemental analysis (EDS) is similar to WBC sample, with the difference that some of the percentages change for the replacement of clay with 15wt% BS. This aspect is confirmed by the XRD analysis.

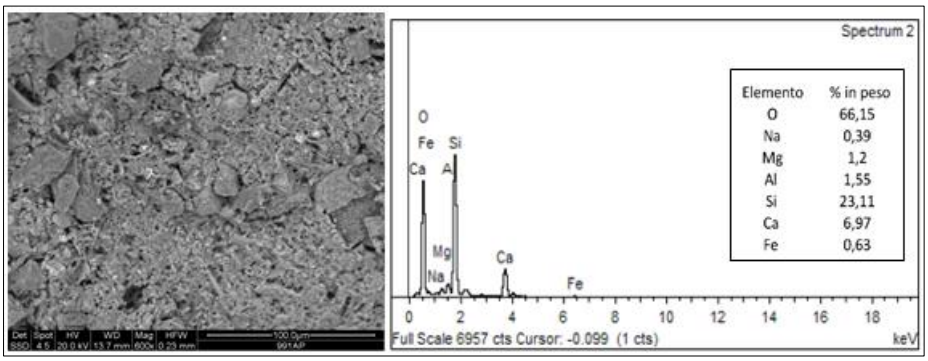

Image D.5.2.5.1.3. $WBBS_{15}$ - SEM image (600x) and EDS analysis.

The addition of fertilizer glass (FG), shows a minor sintering and more heterogeneity zones, characterized by different elements (Image D.5.2.5.1.4). There is sulphur (S) value of 6.83%, generated by sulfates present in white clay (XRF: 0.10%) and black clay (XRF: 1.78%), reported in the chemical characterization of raw materials. Low traces of K were found (0.75%).

Although the aggregate of 10wt% FG generates a higher level of surface sintering, in turn, the porosity and the interconnected porosity also decrease, since the addition of the FG to the mixture facilitates the vitrification of the ceramic surface (Image D.5.2.5.1.5).

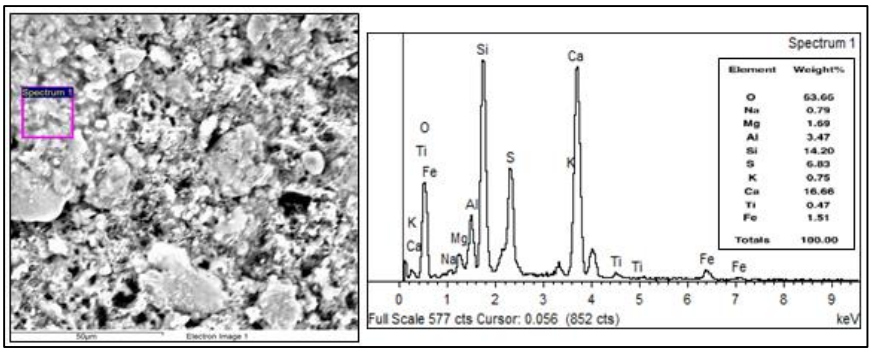

Image D.5.2.5.1.4. WB_{FG} - SEM image (1200x) and EDS sample analysis.

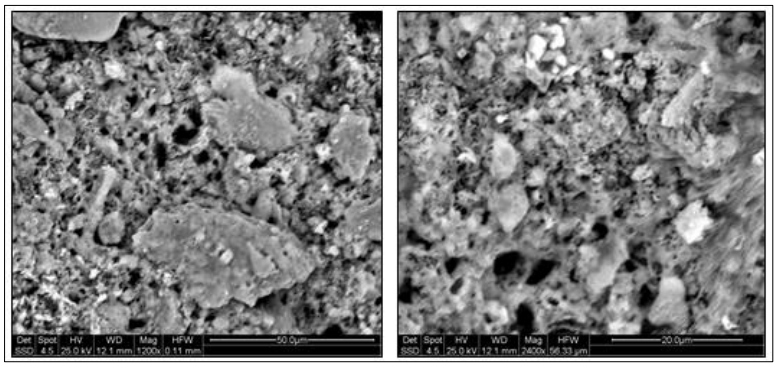

Image D.5.2.5.1.5. WB_{FG} - SEM image (1200x and 2400x)

In image D.5.2.5.1.6, corresponding to WB_{CBA} sample can be seen that some zones are rich in Ca (18.49%) related to clay materials (carbonates) and cattle bone ashes (CBA). Grain size between 5-20 µm presents substantial amounts of phosphorus (P) 9.14% and low potassium (K) concentration (0.61%). In contrast to Image D.7.2.5.7, higher concentrations of K were detected (3.59%) and no P.

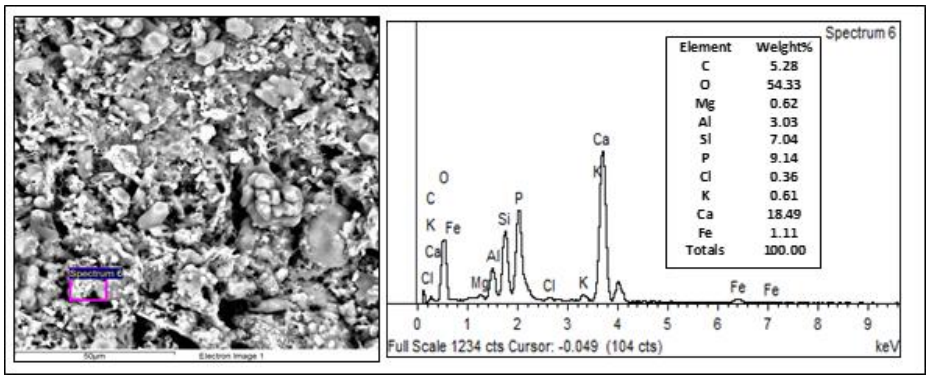

Image D.5.2.5.1.6. WB_{CBA} - SEM image (1200x) and EDS sample analysis.

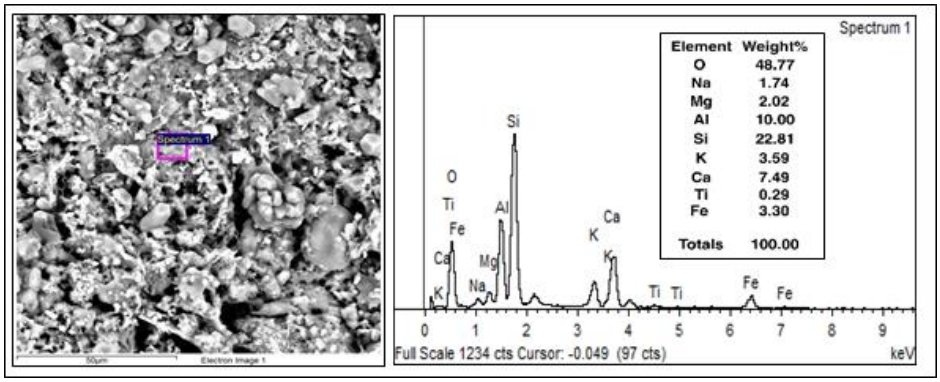

Image D.5.2.5.1.7. WB_{CBA} - SEM image (1200x) and EDS sample analysis.

The WB_{CBA} presents the less compact and sintered surface among the other samples (WBC, $WBBS_{15,}$ and WB_{FG}), being theoretically generated by the contribution of Ca from the clays minerals, BS and CBA, 18.52% and 53.89% respectively. Another interesting detail is shown in Image D.6.2.5.1.8, were the anorthite ($CaAl_2Si_2O_8$) plagioclase feldspar, and appears in a very distinctive crystalline form (red arrow).

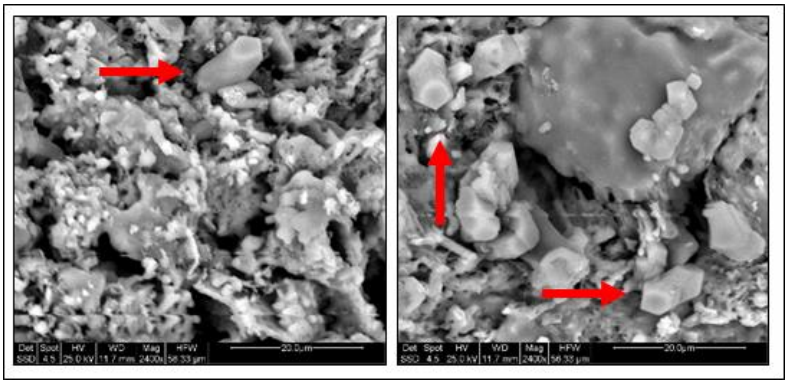

Image D.5.2.5.1.8. WB_{CBA} - SEM image (2400x)

D.5.2.5.2. RC CLAY-MIX SAMPLES

From RC mixture (100% red IT clay), can be highlighted the Fe (iron) concentration (6.41%) related to hematite detected in the XRD analysis. Iron is an element with high atomic weight, found mostly in the brightest areas of the material surface.

The significant concentrations are related to Si (17.76-25.59%), Al (10.63-8.21%) and Fe (8.49-3.24%), bound by silicon. Low quantities of calcium were found (1.50-1.41%) related to wollastonite ($CaSiO_3$), calcium meta-silicate (Image D.5.2.5.2.1). The figure shows a very compact surface with low open porosity, in the range of 0.50-1.00 µm/500-1000 nm, these findings are in agreement with water absorption capacity data reported above.

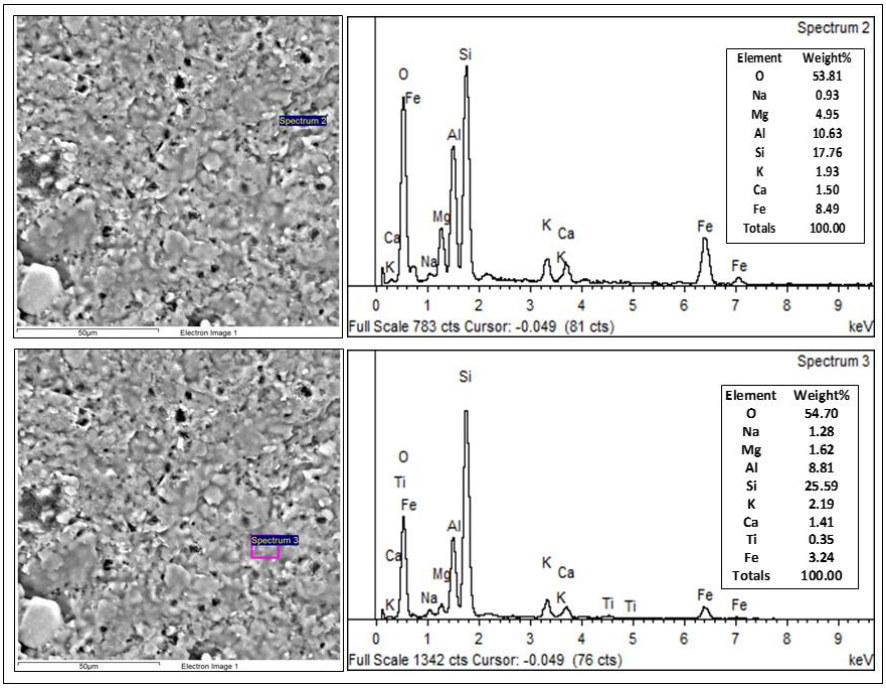

Image D.5.2.5.2.1. RC - SEM image (1200x) and EDS sample analysis.

Samples containing 15wt% of BS ($WBBS_{15}$) developed more porosity related to the oxidation of organic matter, with pores sizes in between 1-5 µm (Image D.7.2.5.1.2.2).

In Images D.5.2.5.2.1, the outer wall reveals a vetrified surface structure, and this is due to the thermal shock to which the aggregates were subjected.

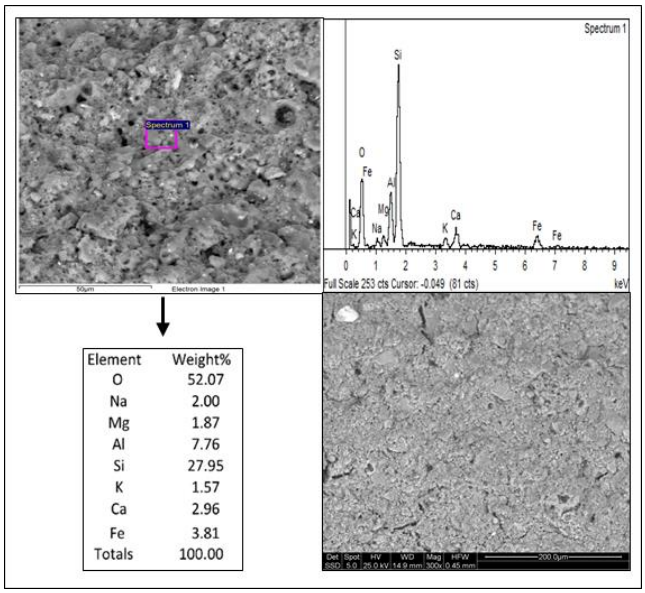

Image D.5.2.5.2.2. $RCBS_{15}$ - SEM image (300x/600x) and EDS sample analysis.

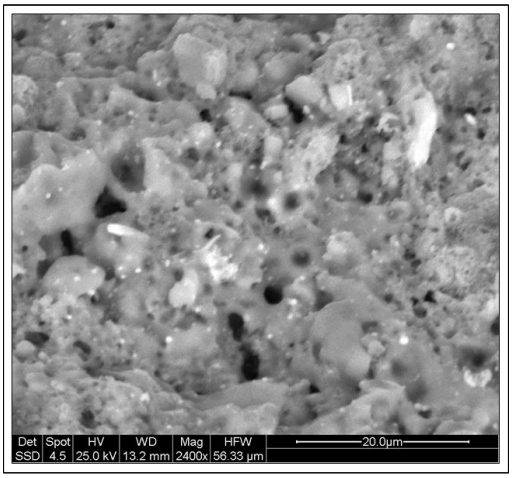

Image D.5.2.5.2.3. $RCBS_{15}$ - SEM image (2400x).

Image D.5.2.5.2.4, shows the sample with the addition of 15wt% BS and 10wt% FG (RC_{FG}), denoted fractures and inhomogeneities respect to the previous samples. It was observed that the micrographs at lower magnification (150x, 300x and 600x) same material did not react to the thermal treatment (1000°C for one hour).

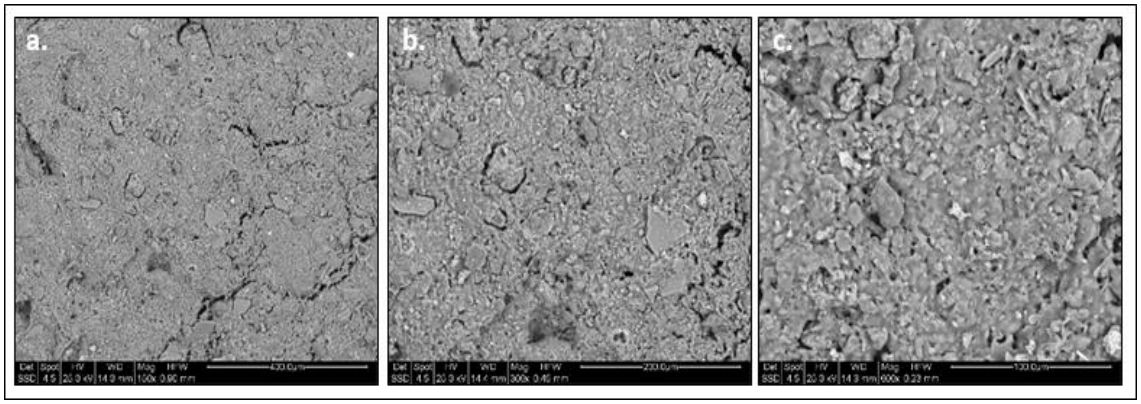

Image D.5.2.5.2.4. RC_{FG} - SEM image, a. 150x, b. 300x and c. 600x

The vitrified fraction contains mainly elements like Si (30.38%), Al 10.67% followed by Fe (5.51%) and K (4.48%) (Image D.5.2.5.2.5). The porous structure is less pronounced than in samples $RCBS_{15}$, influencing its water absorption capacity. By observing the images at higher magnification (1200/2400x), in the chemical analysis can be highlighted that the ceramic surface structure is mostly vitrified with high contents of Si (27.95%) related to de FG addition.

Analysing the white crystal in Image D.5.2.5.2.6 confirms the presence of orthoclase/feldspar [$KAlSi_3O_8$] by the presence of silica, aluminum, and potassium. In image 2400x zoom, the crystalline and spongy phases appear very distinct, with Mg (magnesium) concentrations

(8.55%) and iron (13.64%), indicative of the BS inorganic fraction remaining after the thermal treatment.

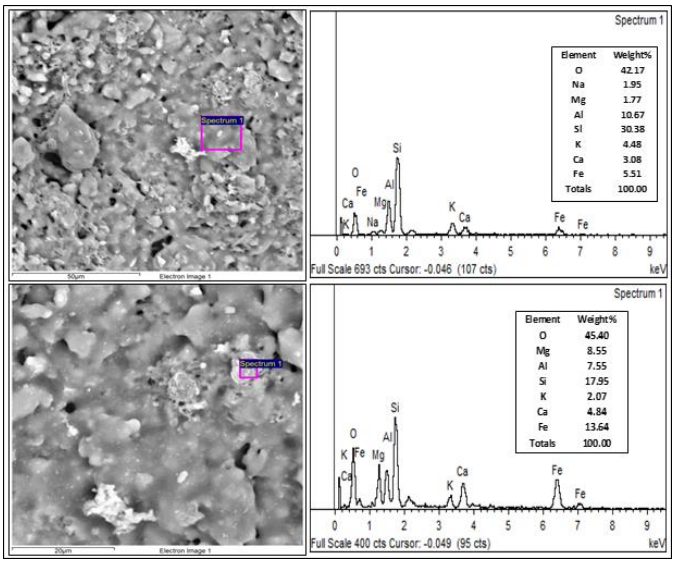

Image D.5.2.5.2.6. RC_{FG} - SEM image (1200/2400x) and EDS sample analysis.

In Image D.5.2.5.2.7, the sample with 15wt% BS and 10wt% CBA, reveals unevenness in the surface, slight superficial vitrification compared to the samples already analyzed. Silicon (22.79%), calcium (7.49%), are the most abundant elements; the P (3.13%) and K (1.82%) are high.

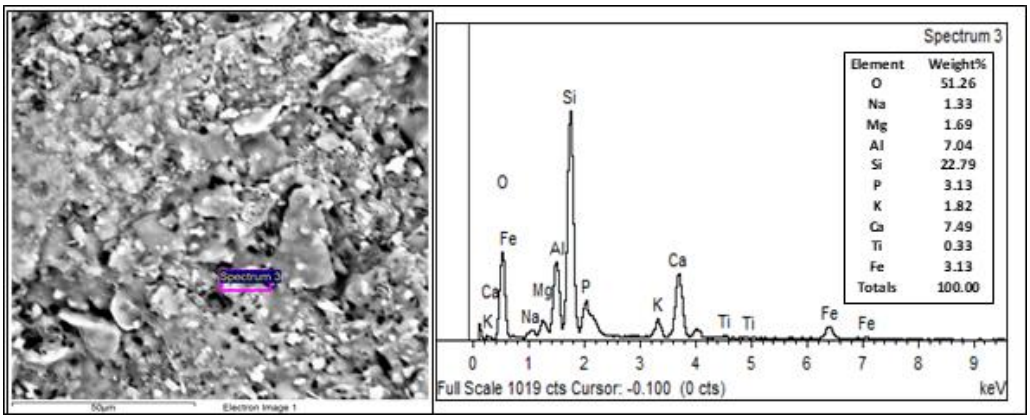

Image D.5.2.5.2.7. RC_{CBA} - SEM image (1200x) and EDS sample analysis.

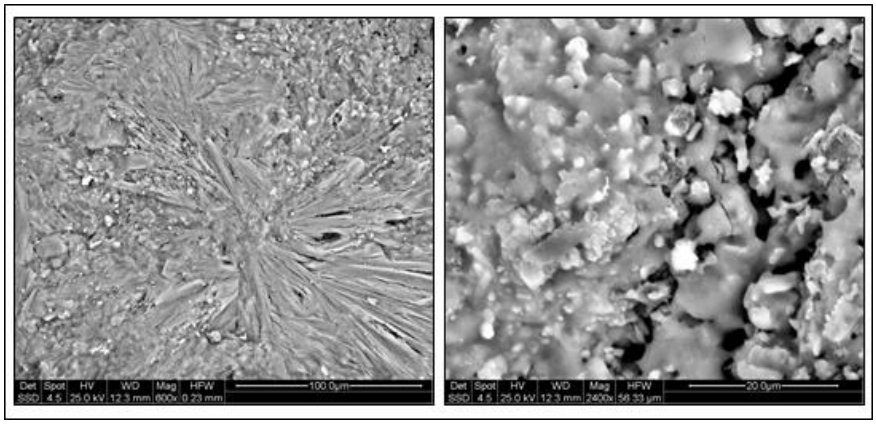

Image D.5.2.5.2.8. RC_{CBA} - SEM image (600x and 2400x)

As seen in the micrographs, the general tendency is that the porosity of the samples is related to the addition of the residues, this already be hypothesized by the water absorption test. Samples with the addition of FG are the exception (Bui et al., 2013). The addition of FG is related to the vitrification of the ceramic surface, conferring the material a lower water absorption capacity.

While the analysis carried out in section D.5.2.4 (Hg intrusion porosimetry - MIP) and scanning electron microscopy (SEM) can study the porosity of the material, the results of the two analyzes cannot be compared. For MIP sampling test, the LWA_S have to break into small pieces, thereby the data obtained are related mostly to the internal structure of the material, i.e., pore diameter and their interconnections. On the other hand, with the SEM-EDS technique the external surface was observed, and with that can drown conclusions, e.g., ceramization state, porosity related to the capacity of water absorption and chemical composition.

D.5.2.6. LEACHING TEST

The leaching test was performed in two different media, water (H_2O) and a solution of 2v/v%, citric acid ($C_6H_8O_7$), in two time frames (30 minutes and 21 days) to evaluate the nutrients release capacity for samples with 15wt% brewery sludge and 10wt% fertilizer glass (WB_{FG} and RC_{FG}) in comparison with samples with 15wt% BS and 10wt% CBA (WB_{CBA} and RC_{CBA}).

To analyze the control-release of different microelements and the influence of the porous material structure, the analysis was performed with the whole (WS) and powdered samples (granulometry <100 microns) (PS). 21 days allows determining the long-term release of nutrients and elements present in the sample. The use of citric acid 2%, simulates the acid conditions of a crop soil. At 20°C citric acid has a pH of 2.73.

Test in water for 30 minutes was according to regulation CE N°2003/2003 (CE-2003/2003, 2003). Test in Citric acid 2v/v% was perform following the provisions of Italian Legislative Decree N°75/2010 (Decree 75/2010, 2010).

Test samples were analyzed by Plasma Spectrometer (ICP-MS) technique. Procedure and equipment used were described in section C (C.2.6. Leaching Test and Inductively Coupled Plasma Mass Spectrometry (ICP-MS)).

D.5.2.6.1. TEST IN WATER: 30 MINUTES.

In this test, whole samples (WS) were analyzed. Table D.5.2.6.3 shows that aluminium (Al) is the most released element, the maximum value for WB_{CBA} (2.00%). Aluminium is related to anorthite ($CaAl_2Si_2O_8$) content, a potassium silico-aluminate detected with the XRD and microstructural analysis. Moreover, the high Al content is related to the silicoaluminate containers where the aggregates were sinterized. Phosphorus (P) presents low release values, 0.12% for WB_{CBA}, followed by RC_{FG} (0.06%).

Potassium (K) was released in larger quantities in WBC clay-base mixtures, WB_{CBA} nearly duplicated the percentage compared to WB_{FG} sample. In contrast, RC Italian clay aggregates RC_{CBA} and RC_{FG}, 0.11% and 0.07% respectively.

Table D.5.2.6.1.1. ICP results (ppm/%) H_2O test for 30 min., WS.

ppm	WB_{FG}	RC_{FG}	WB_{CBA}	RC_{CBA}
Na	0.5683	0.3623	0.5676	0.5337
Al	1.2406	1.9772	9.9888	1.9137
Si	0.2583	0.1781	1.8032	0.2068
P	0.0434	0.0540	0.2379	0.0627
K	0.4682	0.2265	0.4881	0.2392
Ca	1.8983	0.4405	4.4711	0.4490
Fe	0.0226	0.1321	0.0721	0.0685
Pb	0.0011	0.0009	0.0012	0.0005

%	WB_{FG}	RC_{FG}	WB_{CBA}	RC_{CBA}
Na	0.7012	0.3360	1.2110	0.7270
Al	0.2460	0.2370	2.0020	0.2310
Si	0.0130	0.0080	0.1010	0.0094
P	0.0500	0.0621	0.1210	0.0320
K	0.1740	0.0700	0.3160	0.1150
Ca	0.1330	0.0800	0.2742	0.0600
Fe	0.0070	0.0240	0.0230	0.0120
Pb	0.4670	0.3820	0.6370	0.2640

In this analysis conditions, can be highlighted that $LWAS_{AP}$ with the addition of CBA easily releases P and K elements compared with FG aggregates. The chemical and mineralogical characteristics of the different clays used show a different degree of sintering, although the aggregates made with the Spanish clays show the lowest degree of sintering (1000°C), generating a more porous microstructure that favors the release of nutrients.

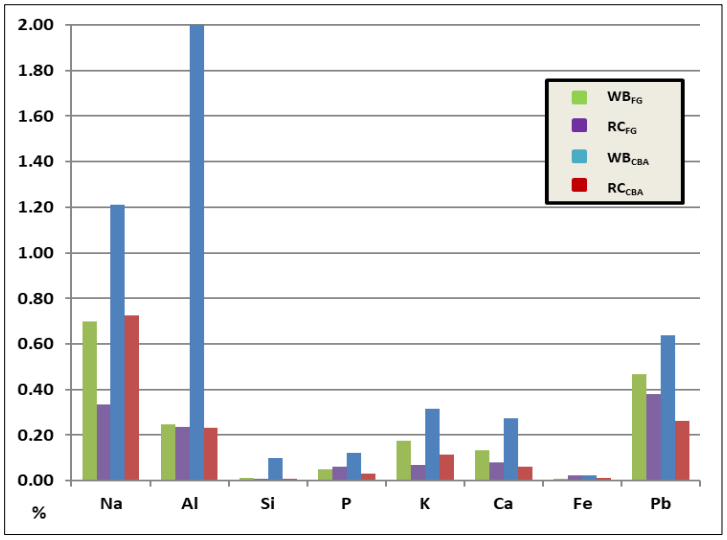

Figure D.5.2.6.1.1. ICP results (%) H_2O test for 30 min., WS.

The value of aluminum released turns out to be too high in all samples, due to the alumina (Al_2O_3) present in clay-material and by the probable contamination introduced by alumina silicate crucible, where the fertilizer glass (FG) was made. Lead (Pb) concentration lead yields a value between 0.26-0.63% and in any case within the reference standard (2003/33/CE, 2003).

D.5.2.6.2. CITRIC ACID TEST: 30 MINUTES.

In this section, powdered (PS) and whole samples (WS) were analyzed. The objective of this analysis was to characterize the nutrient release in citric acid, simulating vegetal growth substrate conditions, providing relevant information on the influence of the material microstructure.

Table D.5.2.6.2.1. ICP results (ppm/%) citric acid 2v/v% test for 30 min., PS.

ppm	WB_{FG}	RC_{FG}	WB_{CBA}	RC_{CBA}
Na	44.1175	6.4387	11.2232	2.0939
Al	153.3327	52.4916	134.2843	28.5304
Si	272.2907	81.0714	243.9727	46.7582
P	62.9494	41.5655	94.1352	96.1037
K	116.2715	14.8448	9.9677	1.9606
Ca	577.9388	221.7341	729.8387	238.2385
Fe	26.5957	9.2638	32.3143	6.5061
Pb	0.0387	0.0225	0.0108	0.0066

%	WB_{FG}	RC_{FG}	WB_{CBA}	RC_{CBA}
Na	72.4908	7.96	31.9191	3.8017
Al	40.62	8.3931	35.8796	4.585
Si	18.7713	4.5845	18.13	2.8115
P	96.2016	63.2319	63.8674	64.9052
K	57.5455	6.1161	8.6127	1.2567
Ca	53.9485	54.0036	59.6221	42.2461
Fe	11.4356	2.219	13.9392	1.561
Pb	22.1369	12.8393	7.6655	4.6972

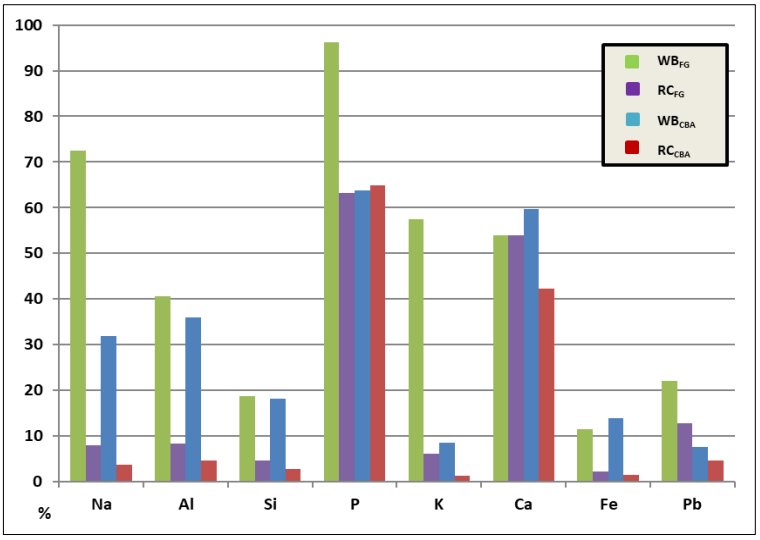

Figure D.5.2.6.2.2. ICP results (%) citric acid 2v/v% test for 30 min., PS.

This analysis shows the influence of the microstructure on the controlled release elements (Table D.5.2.6.2.1 and Figure D.5.2.6.2.2). As was expected, in the powder sample analysis the detection values are much higher than in the whole aggregate. The high values of phosphorus and potassium are related to the aggregates with the addition of FG (WB_{FG} and RC_{FG}).

Table D.5.2.6.2.2. ICP results (ppm/%) citric acid 2v/v% test for 30 min., WS.

ppm	WB_{FG}	RC_{FG}	WB_{CBA}	RC_{CBA}
Na	4.7824	0.9176	1.0571	0.0396
Al	12.1391	2.8031	11.4352	2.4352
Si	17.2763	0.5873	15.9967	0.1843
P	1.3661	0.7420	2.7951	6.3635
K	10.4649	0.0866	0.4607	0.2367
Ca	41.5859	11.4578	63.3332	24.9417
Fe	2.1456	0.4141	2.6503	0.7130
Pb	0.0062	0.0061	0.0020	0.0032

%	WB_{FG}	RC_{FG}	WB_{CBA}	RC_{CBA}
Na	7.8584	1.1348	3.0060	0.0726
Al	3.2161	0.4481	3.0555	0.3910
Si	1.1910	0.0330	1.1894	0.0116
P	2.0882	1.1290	1.8963	4.2980
K	5.1797	0.0361	0.3983	0.1529
Ca	3.8821	2.7910	5.1740	4.4237
Fe	0.9239	0.0991	1.1434	0.1710
Pb	3.5651	3.4978	1.4836	2.2697

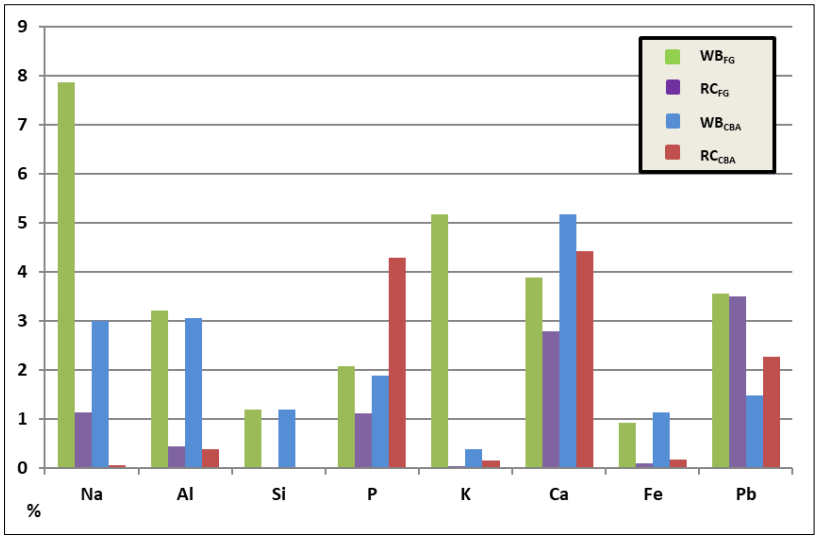

Figure D.5.2.6.2.3. ICP results (%) citric acid 2v/v% test for 30 min., WS.

In the case of the WBC mixtures, calcium and sodium followed by aluminum and silicon were the most released microelements, also there present the highest value release of potassium 5.17% for WB_{FG}. For RC mixtures, however, there is a significant percentage of phosphorus in the sample containing CBA (RC_{CBA} 4.29%), compared with 2.08% of WB_{CBA}. Lead (Pb) concentration lead yields a value between 0.002-0.006 ppm and in any case within the reference standard (2003/33/CE, 2003).

For the comparison of 30 minutes test in water and citric acid 2%, can be hightailed the following conclusions:

- The release of whole aggregates in a water medium is negligible compared to in citric acid at 30 min. The effect of grain size is important comparing the release data (ppm) obtained in citric acid, for whole and powdered samples.
- The nutrients values were much higher in the acid medium than in water due to the solubilization of the different elements analyzed.
- The WB_{FG} sample releases higher percentages of phosphorus (2.08%) and potassium (5.17%) in citric acid 2v/v% in comparison with RC_{FG} (P: 1.12% and K: 0.03%).
- In general, calcium and lead were the elements with higher values in acid solution and whole samples (WS), with the fundamental difference that calcium was found in the solution 105 times more than the lead. Regarding the lead content, Lead (Pb) concentration value is within the reference standard, 0.15 ppm (2003/33/CE, 2003).
- The trends are not linear between the two tests, implying a different reaction of the samples according to the environment in which the test was developed.

- RC_{CBA} powdered sample yields over 60% of the initial phosphorus and about 40% of calcium; behavior similar to the RC_{FG} glass sample.
- WB_{FG} samples release more amount of potassium respect to the similar composition made with red IT clay. This difference is due to the different microstructure (more porous in WB_{FG}). This fact implicates a high release at the short term.

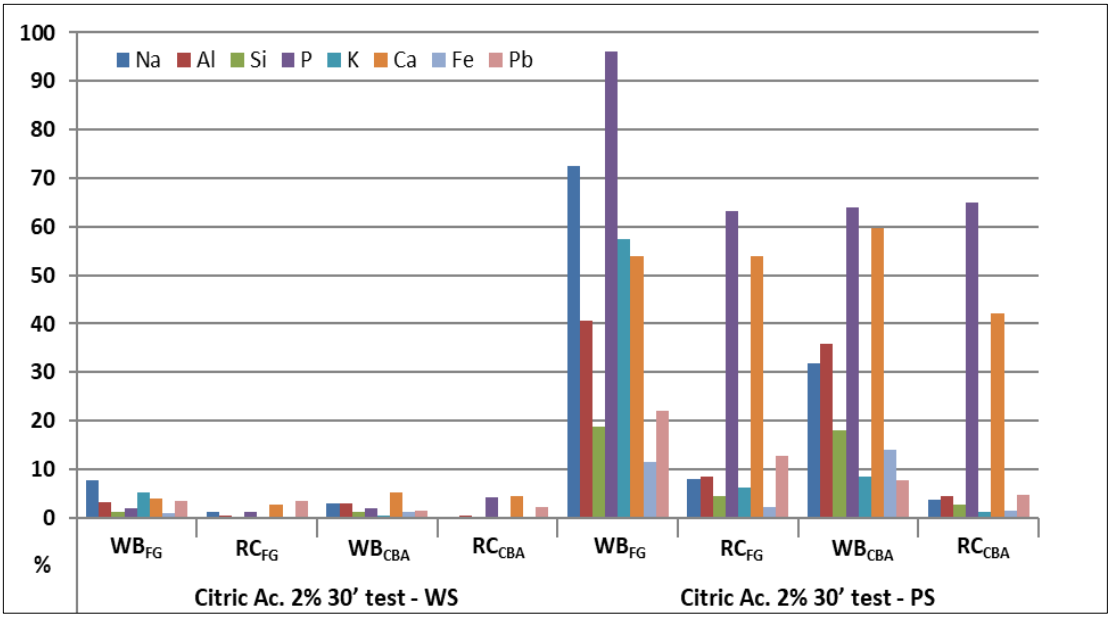

Figure D.5.2.6.2.4. ICP results (ppm/%) citric acid 2v/v% test for 30 min., comparison batwing WS and PS.

D.5.2.6.3. CITRIC ACID TEST: 21 DAYS.

The objective of this analysis, 21 days in acid-medium on whole samples (WS), were analyzed in order to evaluate the time-controlled release of micronutrients. This analysis was carried out under the same conditions as previous. During the test, a plastic cover on the top of the beaker was placed to prevent vapor released during magnetic stirring.

During the test, some aggregates made with WBC mixture, have broken. This is since being more porous ceramic has a higher reaction capacity with the acid medium and because of the stirring, aggregates hitting each other. This modifies the results due to exposure of a larger exchange surface to the medium.

Table D.5.2.6.2.3.1. ICP results (ppm/%) in citric acid 2v/v% test for 21 days, WS.

ppm	WB_{FG}	RC_{FG}	WB_{CBA}	RC_{CBA}
Na	51.5502	20.3491	24.1967	12.8741
Al	2238.1191	1706.5683	2606.5000	1461.6910
Si	152.6712	95.7813	141.4298	86.6326
P	69.6115	61.4462	100.5721	120.6847
K	81.4724	22.0811	24.4227	7.1864
Ca	653.0323	255.6554	772.8162	322.8712
Fe	45.5897	207.4586	240.9174	27.6854
Pb	0.0511	0.0239	0.0126	0.0167

%	WB_{FG}	RC_{FG}	WB_{CBA}	RC_{CBA}
Na	84.7042	25.1575	68.8141	23.3745
Al	100.0000	100.0000	100.0000	100.0000
Si	10.5250	5.4162	10.5105	5.2097
P	100.0000	93.4758	68.2346	81.5065
K	40.3224	9.0989	21.1073	4.6064
Ca	60.9585	62.2657	63.1334	57.2541
Fe	19.6036	49.6924	100.0000	6.6436
Pb	29.1614	13.0074	8.1944	12.1939

The higher values were related to aluminum, calcium, and silicon; phosphorus released in larger quantities by the two samples with CBA. Potassium (K) from is related to WB_{FG} 40.22% and WB_{CBA} 21.10%. The lead keeps quantities below 0.06 ppm for each sample analyzed.

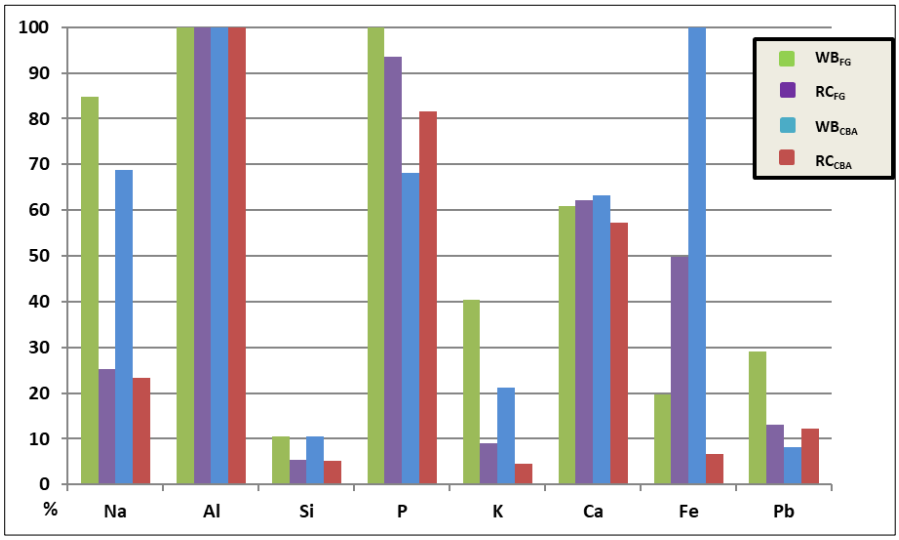

Figure D.5.2.6.2.3.1. ICP results (%) in citric acid 2v/v% test for 21 days, WS.

In particular, WB_{FG} and RC_{FG} show better phosphorus control release performance in 21-days period, meeting reference standard (CE-2003/2003, 2003). WB_{FG} released potassium in better proportions in almost all tests.

As previously was observed in section D.5.2.3. LWA_S X-ray powder diffraction (XRD), crystalline phase related to the content of P (hydroxyapatite) was detected.

The samples elaborated with RC clay-mix, as observed in SEM analysis, presenting a more compact structure allows a slower release of elements. The WB_{FG} and RC_{FG}, followed by WB_{CBA} have the best values of controlled release capacity in the 21-day for phosphorus and potassium.

The value of aluminum released turns out to be too high in all samples, due to the alumina (Al_2O_3) present in clay-material, probable contamination introduced by alumina silicate melting

pot, was the fertilizer glass was made. Regarding the lead content, Lead (Pb) concentration value is within the reference standard, 0.15 ppm (2003/33/CE, 2003).

D.5.2.7. INSULATION CAPACITY

The improvement of the insulation capacity for a crop soil, intel the improvement of water retention capacity during periods of drought (retain moisture in the soil), protects the soil from erosion and as well as isolation of roots during frost. To analyze the insulation capacity of the LWA_S, was perform a test using a thermal imaging camera Fluke Ti-32 (Fluke, Everett, USA) and a Thermal house 3.6.03-00 (Thermodynamics, PHYW, Germany).

The measurements were performed with the thermal camera, to take the images of infrared radiation emitted. The three $LWAS_{GR}$ BS_{15}, $BB_{15,}$ and DE_{15} (sintered at 1000°C) were compared with the aggregates without added waste (WBC and RC) with WB_{FG}-WB_{CBA} and RC_{FG}-RC_{CBA}. For the measurements, the LWA_S for each mix was placed in a metal tray and located over the thermal house, according to standards (UNE-EN-12667:2002, 2002).

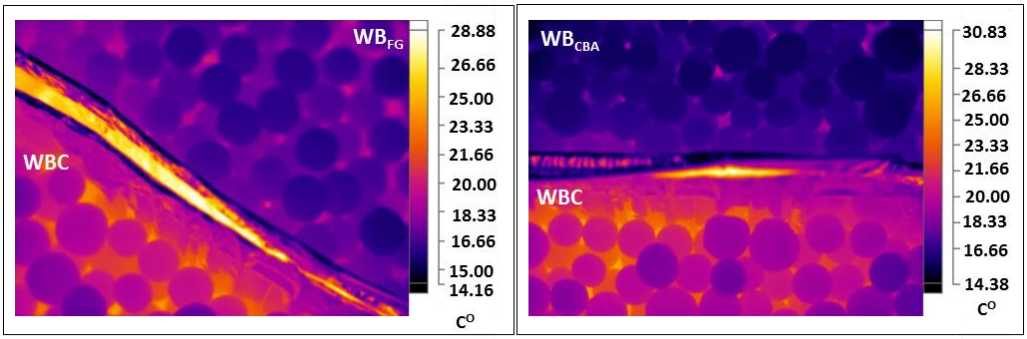

a). **b).**

Image D.5.2.7.1. Comparison of thermal imaging of WBC and WB_{FG}/WB_{CBA} (infrared imaging).

In image, D.5.2.7.1 were analyzed the results of the thermographic camera of WB_{FG}/WB_{CBA} in comparison with WBC. From the thermal image (a), can be highlighted that the strong violet color is more evident in the right upper side of the image, related to WB_{FG} by the temperature rate, the maximum temperature (28.88°C) is detected in WBC side, left-down from the image.

In image b), a more significant difference of colors is observed between the upper part of the image, corresponding to WB_{CBA} and the lower part, WBC. This is due to the higher porosity reflected in the results obtained.

In image, D.5.2.7.2 were analyzed the results of the thermographic camera of RC_{FG}/RC_{CBA} in comparison with RC. In the thermal image (a), can be seen that he strong violet color is more evident in the right upper side of the image, related to RC_{FG} by the temperature rate, the maximum temperature (25.11°C) is detected in RC side, left-down from the image.

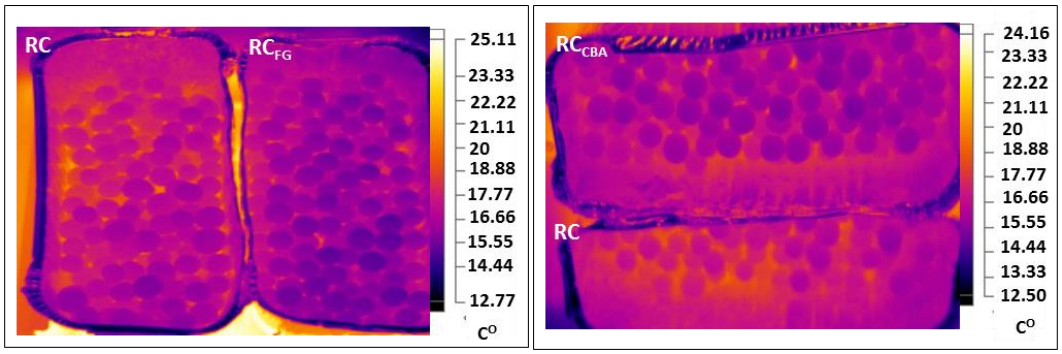

a). b).

Image D.5.2.7.1. Comparison of thermal imaging of RC and RC_{FG}/RC_{CBA} (infrared imaging).

In image b), can be seen that the strong violet colors are observed in the upper part of the image, corresponding to RC_{CBA} and the lower part, WBC. This is due to the higher porosity reflected in the results obtained.

The insulation capacity is related to the clause porosity (Elías, 2012b) and the water absorption capacity is related to open porosity. According to the weight loss and porosity percentages data in particular for WB_{CBA} reveal that higher organic content and high carbonates percentages content increased porosity and decreased bulk density, improving insulating properties.

D.5.2.8. Carbon Footprint calculation (CFP)

Based on the inventory analysis displayed in sections C.3.2 (Life Cycle Inventory), C.3.2.2 (LWA_S for agronomic porpoises) and C.3.3 (Assumption and Cutting); and the application of IPCC 2013 GWP 20y as impact assessment methodology for global warming and Carbon Footprint calculation, the CFP of $LWAS_{AP}$ in comparison with LWA_S without waste (WBC and RC). Based on the research results, the LWA_S suitable for agricultural use are the mixtures WBC_{FG}, WBC_{CBA}, $RC_{FG,}$ and RC_{CBA}.

Table D.5.2.8.1. CFP of $LWA_{S.}$ WBC/RC, WBC_{FG}, WBC_{CBA}, RC_{FG} and RC_{CBA}. IPCC 2013 GWP 20y.

Unit	WBC/RC	WB_{FG}/RC_{FG}	WB_{CBA}/RC_{CBA}
kg CO_2 eq.	4.78	5.33	3.82

The results show that 15% less extraction of virgin raw materials (clays) by replacing them with waste (BS 15wt%) that acts as alternative fuels inside the furnace, reduces the demand for non-removable resources (electric energy, diesel, pet-coke). This affects directly to the gas emissions, associated with the greenhouse effect and global warming.

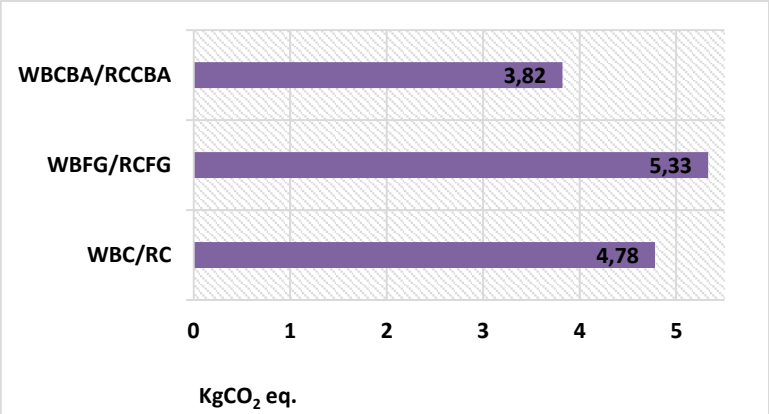

Figure D. 5.1.6.1. CFP of $LWA_{S.}$ WBC/RC, WBC_{FG}, WBC_{CBA}, RC_{FG} and RC_{CBA}. IPCC 2013 GWP 20y.

The use of 15wt% of BS reduces about 20.00% the emissions of GHG. The process to formulate de fertilizer glass increase the energy input due to the thermal cycle (11.00% increase the GHG emissions) from approximately 6.50 hours reaching maximum temperatures of 1450°C. In conclusion, the mix that less $KgCO_2$ eq. emits are WB_{CBA}/RC_{CBA}, being the mixtures with the more significant calorific contribution.

E. CONCLUSIONS

This study has shown that by selecting alternative raw materials for their use in the formulation of engineered sustainable LWA_S for green roof drainage layer and growing media, can be achieved, LWA_S with similar and improved properties comparable to commercially available LWA's.

The results indicate that the different clays and wide range of waste/by-products, raw materials innovation, have the potential for manufacturing high-quality, lightweight aggregates, using lower sintering temperature in comparison with traditional cycles with less environmental impact and economic savings, for the circular economy, with sustainable processing, reuse, recycling, and recovery.

Based on the results, the following general conclusions can be drawn:

- The innovation provided by this research is related to a wide range of waste/by-products, in combination with five different clays can be taken as a base study for the introduction of new technical and materials standards in the development of sustainable materials through the energy and raw materials savings. Therefore, it is considered that the research carried out, can be transposed to other geographic location. Furthermore, the functionalization of LWA_S with improved characteristics in comparison with commercial materials, developing materials with fertilizing and higher thermal insulation capacity. These improvements in the LWA_S technical features represent an environmentally sustainable innovation.
- The results achieved in this research can contribute to the interconnection of different production processes in the development of innovative and sustainable construction materials.
- The chemical composition of waste/by-products, studied by X-ray fluorescence, is appropriate for use in clay-based products formulation. The organic content of the technical nutrients (sludge (BS), bagasse (BB), diatomaceous earth (DE), meat-bone meal (MBM) and corn cob (CC) reduces bulk densities by increasing porosity (open and close), directly related to the increase of water absorption capacity.
- The results obtained from mercury intrusion porosimetry (MIP), scanning electron microscopy (SEM) and thermal imaging for the characterization of porosity confirmed that the addition of waste increases total porosity (open and closed porosity) so increases the thermal insulation by decreasing bulk density.

- Natural raw materials partial replacement and energy saving, due to the combustion of organic matter inside the furnace and low sintering temperature (ΔT=200-400ºC), reduces the environmental impact produced by the greenhouse gases (GHG) released into the atmosphere, resulting in the production of sustainable materials.
- The valorization of these residues, as alternative fuels, generates a reduction in the environmental impacts associated with the disposal in landfills.

Specifically, concerning lightweight aggregates developed for use as a drainage layer in green roofs ($LWAS_{GR}$), the following conclusions can be drawn:

- The residues produced by from the brewing industry have high potential as a pore-forming agent mixed with the clays (black, yellow and red ES) from Bailen, Spain, for the manufacturing of LWA_S as a drainage layer for green roofs.
- Brewery Sludge (BS), bagasse (BB) and diatomaceous earth (DE) in the percentages 10, 12.5 and 15wt%, mixed with clays and sintered at 1000ºC, show the best results of water absorption capacity (WA%), bulk density (BD) and total porosity (TP%) in agreement with similar materials and suitable for its use as $LWAS_{GR}$.
- The best performance according to these parameters was achieved by using bagasse in percentages between 10-15% sintered at 1000ºC. The addition of 15wt% BS it was considered the optimum amount of waste addition. For one hand, from an environmental point of view, more waste is valorized, and, in contrast, the addition of more organic matter (over 15wt% BB) could compromise the structure of the material and its durability.
- The addition of 15wt% BB, as was confirmed in the thermal test, improve insulating properties by reducing the thermal conductivity in 5.55ºC for BB_{15} samples.
- Micrographs (SEM) and MIP analysis results show very various pore sizes, with more prominent pores related to BB, followed by DE and BS. The addition of 15wt% BB generates the must porous structure, in quantity and size, associated with the total porosity values of 56.80%, total pore area of 5.13 m^3/g and a wide range of pore diameter of 0.10-100 µm.
- The leaching test results and the concentration values taken as a reference, concludes that measured elements (Cr, Ni, Cu, Zn, As, Se, Ag, Cd and Pb) are below the standards limits (2003/33/CE, 2003).
- It was noticed that the incorporation of waste/by-products led to a decrease of about 30% of global warming category in the case of BB_{15} (15wt% of Bagasse). The advantage

for the valorization of agro-industrial waste and by-product as additives in LWA_S was then confirmed from an environmental point of view.

Specifically, concerning lightweight aggregates developed for use as growing media ($LWAS_{AP}$), the following conclusions can be drawn:

- The wastes/by-product used, brewery sludge (BS), meat-bone meal (MBM) and corn cob (CC), present a great potential as ~~a~~ pore-forming agent mixed with clay minerals (black, white and red IT) from Bailen, Spain, and Modena, Italy, for the manufacturing of LWA_S for agronomic porpoises.
- $WBBS_{15}$ sintered at 1000°C for 1 hour, presents the best results as a pore-forming agent with values of water absorption of 51.02%, bulk density 1120.00 Kg/m^3 and total porosity of 60.15%, in comparison with similar commercial products suitable as growing media. Although the LWA_S developed with MBM and CC have shown better results (sintered at 1000°C), during the water absorption tests by boiling for 6 hours, some of them were partially or totally destroyed during the test, showing poor durability. Also, the pH values measured are resulted high (>8.00), not being suitable for their use as a growing media.
- Brewery sludge can be efficiently used as pore forming agent for LWA_S manufacturing, representing savings in virgin raw materials and energy consumption, as well as an alternative to landfill disposal. Also, BS was considered the waste with better adaptability as industrial raw material. After draining presents a clay-like consistency, which makes it more suitable as an input in the production of LAW_S. The strong odor produced during the drying and sintering process can be easily solved by situating a scrubber in the exhaust of the stove and oven.
- The red clay IT (RC) presents a higher degree of ceramization at 1000°C in contrast with Spanish clay mixture (WBC). This is related to the low content of carbonates and high content of K and Na, according to XRF analysis, generating the vitrification of the surface layer during thermal treatment, reducing the water absorption capacity and increasing its closed porosity. In turn, thanks to the low carbonates content, can be denominated an inter materials, i.e., present pH and electrical conductivity values in range for growing media.
- In X-ray powder diffraction (XRD), of the LWA_S samples after thermal treatment at 1000°C for one hour, was observed crystalline phase like hydroxyapatite related to the content of phosphorous (P), important contribution for the plants growth.
- The study of the material porosity carried out by mercury intrusion porosimetry (MIP), and SEM micrographs show that the WBC mixtures have higher porosity and larger pore

sizes, compared to RC samples. The porosity value of WBC mixture is double compared to RC mixture one (47.59% -22.15%).

- In EDS chemical analysis (surface material), elements like K and P were detected in the samples with the addition of FG and CBA. For WB_{FG} and WB_{CBA}, the K concentrations range between 0.61- 3.59 % and the highest concentrations of P were 9.14%. For RC_{FG} and RG_{CBA}, the K concentrations were 1.82 - 2.07% and for P 3.13%.
- The samples elaborated with RC clay-mix, as was observed in SEM analysis, present a more compact structure allowing a slower element release. The WB_{FG} and RC_{FG}, followed by WB_{CBA} have the best values of controlled release capacity in the 21-day for phosphorus and potassium, meeting reference standard (CE-2003/2003, 2003). WB_{FG} released potassium in better proportions in almost all tests. The addition of glass favours the long-term release of K and P, important for a continue fertilizing activity in soils.
- The LWA_S XRD analysis confirmed that during thermal treatment at 1000^{o}C the organic matter present in BS decomposed and the inorganic fraction present did not react with the clays, for that reason no new crystalline phases were observed.
- It was noticed that the incorporation of waste/by-products led to a decrease of about 20% of global warming category. The advantage for the valorization of agro-industrial waste and by-product as additives in LWA_S was then confirmed from an environmental point of view. These results show that the association of different industrial activities, within the same geographic location, can be very effective, generating a significant saving in logistics, extraction of natural raw materials, landfill disposal, energy inputs, for the development of green materials. Fertilizer glass increases the energy input due to the thermal cycle (11% increase the GHG emissions).

F. FUTURE RESEARCH LINES

Based on the results obtained and in order to enquire into more aspects of the sustainable materials developed, is intended to continue the postdoctoral studies on the following research lines:

Perform mechanical compression straight test. The addition of organic matter to the ceramic structure directly influences the structure and durability of the material. Although this aspect was studied through techniques such as Hg-MIP, SEM-EDS, physical and chemical tests, it is considered necessary to develop tests related to Compressive strength according to standards.

Replace the fertilizer glass (FG) with an input that promotes the same characteristics of the material but requiring less or non-energy for processing. In this case, the FG should be exchanged for another material that could provide the same characteristics, controlled release fertilizer (P and K), but through a sustainable process, continuing to prioritize the materials from an agro-industrial waste origin.

Deepen the LCA study including all stages of the LWA_S life cycle. In this research, a preliminary study has been carried out to highlight the most relevant aspects of the raw materials change. However, this preliminary study is biased by choice of the processes considered to be the most relevant in environmental terms. This leaves out the environmental analysis of others important stages in the LWA_S manufacturing, as well as other phases of the life cycle, like the use and end-of-life of the sustainable LWA_S, where it is considered that also have many environmental advantages in contrast with their commercial counterparts.

Testing with plants and compare their growth with different substrates. Although in this investigation is demonstrated, that the materials developed have potential as fertilizers (leaching test), lightening of structure and thermal insulation, as well as, water absorption capacity, to demonstrate in an empirical way and comparison with other commercial materials, its behaviour in green roofs and in the agronomic application.

Empirical evaluation of measuring emissions of greenhouse gases and particulate matter, during the sintering process. It is considered relevant to deepen the aspects related to gaseous and particulate matter emissions associated with changes in raw materials.

BIBLIOGRAPHY

2003/33/CE, 2003. Directiva Europea 2003/33 CE. Criterios y procedimientos de admisión de residuos en los vertederos.

A.Vieira, C. Gomes, F. Rocha, I.B., 1996. Emission and fixation of F and S in clay based ceramics. Adv. Clay Miner. 250–251.

Abajo, M.F., 2000. Manual sobre fabricación de baldosas, tejas y ladrillos. BERALMAR.

Agrawal, P., Misra, S.N., 2014. Irreversible Dilatometry as a Tool for Body Composition and Firing Schedule Design in Traditional Ceramics. Trans. Indian Ceram. Soc. 73, 14–21. https://doi.org/10.1080/0371750X.2013.870049

Aineto, M., 2006. Thermal expansion of slag and fly ash from coal gasification in IGCC power plant. Fuel 85, 2352–2358. https://doi.org/10.1016/j.fuel.2006.05.015

AINIA, (Intituto tecnologico Agroalimentario), 1996. Mejoras técnicas disponibles en el sector cervecero.

Allesina, G., Pedrazzi, S., Sgarbi, F., Pompeo, E., Roberti, C., Cristiano, V., Tartarini, P., 2015. Approaching sustainable development through energy management, the case of Fongo Tongo, Cameroon. Int. J. Energy Environ. Eng. 6, 121–127. https://doi.org/10.1007/s40095-014-0156-7

Alonso-Santurde, R., Coz, A., Quijorna, N., Viguri, J.R., Andrés, A., 2010. Valorization of Foundry Sand in Clay Bricks at Industrial Scale. J. Ind. Ecol. 14, 217–230. https://doi.org/10.1111/j.1530-9290.2010.00233.x

Alvarez, F.B., 2011. LECCION 20 .- CEMENTOS / HORNO ROTATORIO. TIPOS.

Andreola, F., Barbieri, L., Hreglich, S., Lancellotti, I., Morselli, L., Passarini, F., Vassura, I., 2008. Reuse of incinerator bottom and fly ashes to obtain glassy materials. J. Hazard. Mater. 153, 1270–1274. https://doi.org/10.1016/j.jhazmat.2007.09.103

Arancon, R.A.D., Lin, C.S.K., Chan, K.M., Kwan, T.H., Luque, R., 2013. Advances on waste valorization: New horizons for a more sustainable society, Energy Science and Engineering. https://doi.org/10.1002/ese3.9

Arioz, O., Kilinc, K., Karasu, B., Kaya, G., Arslan, G., Tuncan, M., Tuncan, A., Korkut, M., Kivrak, S., 2008. A preliminary research on the properties of lightweight expanded clay aggregate. J. Aust. Ceram. Soc. 44, 23–30.

Avnimelech, Y.C. and Y., 1986. The Role of Organic Matter in Modern Agriculture, Developments in Plant and Soil Sciences .

Azapagic, A., 2004. Developing a framework for sustainable development indicators for the mining and minerals industry. J. Clean. Prod. 2004662–639, 12 .

B. Fabbri, M.D., 1995. Caracteristiche e difetti del laterizio. Grup. Ed. Faenza.

Barbieri, L., Andreola, F., Bellucci, D., Cannillo, V., Lancellotti, I., Lugari, A., Rincon, J.M., Romero, M., Sola, A., 2014. Preliminary studies on the valorization of animal flour ash for the obtainment of active glasses. Ceram. Int. 40, 5619–5628. https://doi.org/10.1016/j.ceramint.2013.10.156

Barbieri, L., Andreola, F., Lancellotti, I., Taurino, R., 2013. Management of agricultural biomass wastes: Preliminary study on characterization and valorisation in clay matrix bricks. Waste Manag. 33, 2307–2315. https://doi.org/10.1016/j.wasman.2013.03.014

Barbieri, L., Bursi, E., Cramarossa, M.R., Ferroni, L., Forti, L., Lancellotti, I., Ponzoni, C., Vassura, I., 2016. Valorization of Glass Wastes As Support for Lipase Immobilization. Environ. Eng. Manag. J. 15, 1933–1940.

Barcelonactiva, 2013. Agro-food industry.

Baroni, E., n.d. http://www.escavazionibaroni.it/home [WWW Document].

Barrio, E.P. Del, 1998. Analysis of the green roofs cooling potential in buildings. Energy Build. 27, 179–193. https://doi.org/10.1016/S0378-7788(97)00029-7

Bates, A.J., Sadler, J.P., Greswell, R.B., Mackay, R., 2015. Effects of recycled aggregate growth substrate on green roof vegetation development: A six year experiment. Landsc. Urban Plan. 135, 22–31. https://doi.org/10.1016/j.landurbplan.2014.11.010

Bernard L. Cohen, 2008. The Nuclear Energy Option. Plenum Press.

Berndtsson, J.C., Bengtsson, L., Jinno, K., 2009. Runoff water quality from intensive and extensive vegetated roofs. Ecol. Eng. 35, 369–380. https://doi.org/10.1016/j.ecoleng.2008.09.020

Bernhardt, M., Tellesbø, H., Justnes, H., Wiik, K., 2013. Mechanical properties of lightweight aggregates. J. Eur. Ceram. Soc. 33, 2731–2743. https://doi.org/10.1016/j.jeurceramsoc.2013.05.013

Bettzieche, H., Schops, W., Hohmann, H., 2000. Pore-forming in brickmaking clay by means of expanded glass granules. Ziegelindustrie.

Biswas, W.K., 2014. Carbon footprint and embodied energy assessment of a civil works program in a residential estate of Western Australia. Int. J. Life Cycle Assess. 19, 732–744. https://doi.org/10.1007/s11367-013-0681-2

Bjorklund, A., Finnveden, G., 2005. Recycling revisited--life cycle comparisons of global warming impact and total energy use of waste management strategies. Resour. Conserv. Recycl. 44, 309–317.

Blengini, G.A., Garbarino, E., 2010. Resources and waste management in Turin (Italy): The role of recycled aggregates in the sustainable supply mix. J. Clean. Prod. 18, 1021–1030. https://doi.org/10.1016/j.jclepro.2010.01.027

Bories, C., Borredon, M.E., Vedrenne, E., Vilarem, G., 2014. Development of eco-friendly porous fired clay bricks using pore-forming agents: A review. J. Environ. Manage. 143, 186–196. https://doi.org/10.1016/j.jenvman.2014.05.006

Bories, C., Vedrenne, E., Paulhe-Massol, A., Vilarem, G., Sablayrolles, C., 2016. Development of porous fired clay bricks with bio-based additives: Study of the environmental impacts by Life Cycle Assessment (LCA). Constr. Build. Mater. 125, 1142–1151. https://doi.org/10.1016/j.conbuildmat.2016.08.042

Bouguerra, A., Ledhem, A., De Barquin, F., Dheilly, R.M., Quéneudec, M., 1998. Effect of microstructure on the mechanical and thermal properties of lightweight concrete prepared from clay, cement, and wood aggregates. Cem. Concr. Res. 28, 1179–1190. https://doi.org/10.1016/S0008-8846(98)00075-1

Bovea, M.D., Powell, J.C., 2016. Developments in life cycle assessment applied to evaluate the environmental performance of construction and demolition wastes. Waste Manag. 50, 151–172. https://doi.org/10.1016/j.wasman.2016.01.036

Brewers of Europe, 2016. http://www.brewersofeurope.org/uploads/mycms-files/documents/publications/2016/country-profiles/EU.pdf [WWW Document].

Bui, L.A., Lin, K., Young, M., 2013. Production of lightweight aggregate using sewage sludge and waste glass powder 47, 26–27.

Bursi, E., Barbieri, L., Lancellotti, I., Saccani, A., Bignozzi, M., 2017. Lead waste glasses management: Chemical pretreatment for use in cementitious composites. Waste Manag. Res. 35, 958–966. https://doi.org/10.1177/0734242X17715098

C. Mooney, 2017. https://www.washingtonpost.com/news/energy-environment/wp/2017/11/13/fossil-fuel-emissions-projected-to-reach-an-all-time-high-in-2017-dashing-hopes-of-progress/?utm_term=.b24cb2db9989 [WWW Document]. Washington Post.

Caffo, B., 2008. Building Materials Technology. Aalto Univ. Sch. Eng. 1–27.

Campani, M., 1999. Studio delle caretteristiche delle aegille rosse estratte nella cava di “Roncobotto”, polo N 20 (Comune di Zacca).

Carbone, M., Garofalo, G., Nigro, G., Piro, P., 2014. A conceptual model for predicting hydraulic behaviour of a green roof, in: Procedia Engineering. https://doi.org/10.1016/j.proeng.2014.02.030

Cargill, M., Ireland, J.S., Bolk, S., Roxbury, W., Us, M.A., Mccarthy, J.J., 2004. (12) United States Patent 1. https://doi.org/10.1016/j.(73)

Carter, G.W., Cannor, A.M., Mansell, D.S., 1982. Properties of bricks incorporating unground rice husks. Build. Environ. 17, 285–291. https://doi.org/10.1016/0360-1323(82)90021-X

CE-2003/2003, 2003. Relating to fertilisers. European Parliament.

Champion, E., 2013. Sintering of calcium phosphate bioceramics. Acta Biomater. 9, 5855–5875. https://doi.org/10.1016/j.actbio.2012.11.029

Chang, F.C., Lo, S.L., Lee, M.Y., Ko, C.H., Lin, J.D., Huang, S.C., Wang, C.F., 2007. Leachability of metals from sludge-based artificial lightweight aggregate. J. Hazard. Mater. https://doi.org/10.1016/j.jhazmat.2006.11.069

Cheeseman, C.R., Virdi, G.S., 2005. Properties and microstructure of lightweight aggregate produced from sintered sewage sludge ash. Resour. Conserv. Recycl. 45, 18–30. https://doi.org/10.1016/j.resconrec.2004.12.006

Chen, H.J., Yang, M. Der, Tang, C.W., Wang, S.Y., 2012. Producing synthetic lightweight aggregates from reservoir sediments. Constr. Build. Mater. 28, 387–394. https://doi.org/10.1016/j.conbuildmat.2011.08.051

Chiang, K.Y., Chou, P.H., Hua, C.R., Chien, K.L., Cheeseman, C., 2009. Lightweight bricks manufactured from water treatment sludge and rice husks. J. Hazard. Mater. 171, 76–82. https://doi.org/10.1016/j.jhazmat.2009.05.144

Chindaprasirt, P., Jaturapitakkul, C., Rattanasak, U., 2009. Influence of fineness of rice husk ash and additives on the properties of lightweight aggregate. Fuel 88, 158–162. https://doi.org/10.1016/j.fuel.2008.07.024

Chiou, I.J., Wang, K.S., Chen, C.H., Lin, Y.T., 2006. Lightweight aggregate made from sewage sludge and incinerated ash. Waste Manag. 26, 1453–1461. https://doi.org/10.1016/j.wasman.2005.11.024

Cicek, B., Tucci, A., Bernardo, E., Will, J., Boccaccini, A.R., 2014. Development of glass-ceramics from boron containing waste and meat bone ash combinations with addition of waste glass. Ceram. Int. 40, 6045–6051. https://doi.org/10.1016/j.ceramint.2013.11.054

Conesa, J.A., Fullana, A., Font, R., 2003. Thermal decomposition of meat and bone meal. J. Anal. Appl. Pyrolysis 70, 619–630. https://doi.org/10.1016/S0165-2370(03)00044-5

Cotes-Palomino, M.T.; Martínez-García, C.; Iglesias-Godino, F.J.; Eliche-Quesada, D.; Pérez-Latorre, F.J.; Calero de Hoces, F.M.; Corpas-Iglesias, F.A., 2016. Study of waste from two-phase olive oil extraction as an additive in ceramic material. Key Eng. Mater. 663, 86–93. https://doi.org/10.4028/www.scientific.net/KEM.663.86

Cotes-Palomino, M.T., Martínez-García, C., Iglesias-Godino, F.J., Eliche, D., Corpas-Iglesias, F.A., 2016. Study of the wet pomace as an additive in ceramic material. Desalin. Water Treat. 57, 2712–2718. https://doi.org/10.1080/19443994.2015.1035678

Cougny, G., 1990. Specifications for clayey raw materials used to produce expanded lightweight aggregates. Bull. Int. Assoc. Eng. Geol. 41, 47–55.

Couto D.M., Ringuedé A., Silva R.F., Labrincha J.A., R.C.M.S., 2003. Metallurgical Sludge in Clay-Based Fired Materials.

Cubaud, J.C., Murat, M., 1969. Fabricación industrial de arcilla expandida. Mater. construcción.

Cultrone, G., Sebastián, E., Elert, K., de la Torre, M.J., Cazalla, O., Rodriguez-Navarro, C., 2004. Influence of mineralogy and firing temperature on the porosity of bricks. J. Eur. Ceram. Soc. 24, 547–564. https://doi.org/10.1016/S0955-2219(03)00249-8

Cusidó, J.A., Cremades, L. V., 2012. Environmental effects of using clay bricks produced with sewage sludge: Leachability and toxicity studies. Waste Manag. 32, 1202–1208. https://doi.org/10.1016/j.wasman.2011.12.024

Cusidó, J.A., Cremades, L. V., González, M., 2003. Gaseous emissions from ceramics manufactured with urban sewage sludge during firing processes. Waste Manag. 23, 273–280. https://doi.org/10.1016/S0956-053X(02)00060-0

Cusidó, J.A., Soriano, C., 2011. Valorization of pellets from municipal WWTP sludge in lightweight clay ceramics. Waste Manag. 31, 1372–1380. https://doi.org/10.1016/j.wasman.2011.02.003

D. Pongkao, C. Lorprayoon, R. Conradt, 1999. Dissolution/precipitation behavior of hydroxyapatites prepared from cattle bone ash. Bioceramics 12, 43–46.

de Barros Filho, R.M., Mendes, L.M., Novack, K.M., Aprelini, L.O., Botaro, V.R., 2011. Hybrid chipboard panels based on sugarcane bagasse, urea formaldehyde and melamine formaldehyde resin. Ind. Crops Prod. 33, 369–373. https://doi.org/10.1016/j.indcrop.2010.11.007

de Gennaro, R., Langella, A., D'Amore, M., Dondi, M., Colella, A., Cappelletti, P., de' Gennaro, M., 2008. Use of zeolite-rich rocks and waste materials for the production of structural lightweight concretes. Appl. Clay Sci. 41, 61–72. https://doi.org/10.1016/j.clay.2007.09.008

de la Casa, J.A., Lorite, M., Jiménez, J., Castro, E., 2009. Valorisation of wastewater from two-phase olive oil extraction in fired clay brick production. J. Hazard. Mater. 169, 271–278. https://doi.org/10.1016/j.jhazmat.2009.03.095

Decree 75/2010, 2010. Italian Legislative Decree 75/2010. Reorganize and revise the discipline on fertilizers.

Deydier, E., Guilet, R., Sarda, S., Sharrock, P., 2005. Physical and chemical characterisation of crude meat and bone meal combustion residue: "Waste or raw material?" J. Hazard. Mater. 121, 141–148. https://doi.org/10.1016/j.jhazmat.2005.02.003

Díaz Rubio, R., Del Río Merino, M., 2014. Cuantificación de las variables que determinan la huella de carbono y energía embebida de los distintos productos de cerámica estructural (cuna a puerta con opciones). Bol. la Soc. Esp. Ceram. y Vidr. https://doi.org/10.3989/cyv.232014

DIN38414-2:1985-11, 1985. Methods for the Examination of Water and Sludge; Sludge and Sediments (Group S); Determination of Water Content, of Dry Residue and of Solids Content (S2).

Ditto Hangers, I., 2018. https://www.e-education.psu.edu/eme807/node/690 [WWW Document].

Donatello, S., Cheeseman, C.R., 2013. Recycling and recovery routes for incinerated sewage sludge ash (ISSA): A review. Waste Manag. 33, 2328–2340. https://doi.org/10.1016/j.wasman.2013.05.024

Dondi, M., 1999. Clay materials for ceramic tiles from the Sassuolo District (northern Apennines, Italy). Geology, composition and technological properties. Appl. Clay Sci. 15, 337–366. https://doi.org/10.1016/S0169-1317(99)00027-7

Dondi, M., Cappelletti, P., D'Amore, M., de Gennaro, R., Graziano, S.F., Langella, A., Raimondo, M., Zanelli, C., 2016. Lightweight aggregates from waste materials: Reappraisal of expansion behavior and prediction schemes for bloating. Constr. Build. Mater. https://doi.org/10.1016/j.conbuildmat.2016.09.111

Dondi, M., Marsigli, M., Fabbri, B., 1997. Recycling of Industrial and urban wastes in brick production : A review. Tile brick Int. 13, 218–225.

Dorado, M.P., Ballesteros, E., Arnal, J.M., Gómez, J., López, F.J., 2003. Exhaust emissions from a Diesel engine fueled with transesterified waste olive oil. Fuel 82, 1311–1315. https://doi.org/10.1016/S0016-2361(03)00034-6

Ducman, V., Mirtič, B., 2009. The applicability of different waste materials for the production of lightweight aggregates. Waste Manag. 29, 2361–2368. https://doi.org/10.1016/j.wasman.2009.02.013

Ducman, V., Mladenovic, A., 2002. Lightweight aggregate based on waste glass and its alkali – silica reactivity. Cem. Concr. Res. 32, 223–226.

Earthlok, n.d. http://www.earthlok.com/engineer/ [WWW Document].

EC, E.C., 2015. 2030 Framework for Climate and Energy Policies.

EC, E.C., 2008. Directive 2008/98/EC of the European Parliament and of the Council of 19 November 2008 on waste and repealing certain directives, Official Journal of the European Union. https://doi.org/2008/98/EC.; 32008L0098

EC, E.C., 1999. Directive 99/31/EC of 26 April 1999 on the landfill of waste, Official Journal of the European Communities.

EC, E.C., 1994. Directive 94/62/EC of 20 December 1994 on packaging and packaging waste, Official Journal of the European Communities. https://doi.org/10.1093/jel/7.2.323

Ecopneus, 2015. http://www.rinnovabili.it/greenbuilding/fattorie-verticali-agricoltura-areo-acqua-idroponica-confronto-876/ [WWW Document].

EIA, U.S.E.I.A., 2007. https://www.eia.gov/energyexplained/index.cfm?page=environment_how_ghg_affect_climate [WWW Document].

Eksi, M., Rowe, D.B., Fern??ndez-Ca??ero, R., Cregg, B.M., 2015. Effect of substrate compost percentage

on green roof vegetable production. Urban For. Urban Green. 14, 315–322. https://doi.org/10.1016/j.ufug.2015.03.006

Elías, X., 2012a. Tratamiento y valorización energética de residuos., Ediciones Díaz de Santos.

Elías, X., 2012b. Reciclaje de residuos industriales: Residuos solidos urbanos y fangos de depuradora, Ediciones Díaz de Santos.

Elias, X., Pleixats, R., Man, M.W.C., Moreau, J.J.E., 2007. Hybrid organic-inorganic materials derived from a monosilylated Hoveyda-type ligand as recyclable diene and enyne metathesis catalysts. Adv. Synth. Catal. 349, 1701–1713. https://doi.org/10.1002/adsc.200600627

Eliche-Quesada, D., Martínez-García, C., Martínez-Cartas, M.L., Cotes-Palomino, M.T., Pérez-Villarejo, L., Cruz-Pérez, N., Corpas-Iglesias, F.A., 2011. The use of different forms of waste in the manufacture of ceramic bricks. Appl. Clay Sci. 52, 270–276. https://doi.org/10.1016/j.clay.2011.03.003

Ellen MacArthur Foundation, 2015. Why the circular economy matters. Deliv. Circ. Econ. A Toolkit Policymakers 19–32.

Elsharief, A., Cohen, M.D., Olek, J., 2005. Influence of lightweight aggregate on the microstructure and durability of mortar. Cem. Concr. Res. 35, 1368–1376. https://doi.org/10.1016/j.cemconres.2004.07.011

Emilsson, T., Berndtsson, J.C., Mattsson, J.E., Rolf, K., 2007. Effect of using conventional and controlled release fertilizer on nutrient runoff from various vegetated roof systems. Ecol. Eng. 260–271.

Enzo, M., Gianquinto, G., Lazzarin, R., Pimpini, F., Sambo, P., 2001a. Principi tecnico-agronomici della fertirrigazione e del fuori suolo (Technical and agronomic principles of fertigation and soilless), Igarss 2014.

Enzo, M., Gianquinto, G., Lazzarin, R., Pimpini, F., Sambo, P., 2001b. Technical and agronomic principles of fertigation and soilless., Veneto Agricoltura.

ESCSI, 2007. Manufacturing of ESCS Lightweight Aggregate. Expand. Shale, Clay Slate Inst. 84117.

European Commission, 2014. Towards a circular economy: A zero waste programme for Europe.

European Commission, n.d. Sewage Sludge [WWW Document]. URL http://ec.europa.eu/environment/waste/sludge/

European Container Glass Federation., 2015. http://feve.org/glass-recycling-hits-73-eu/ [WWW Document].

European Insulation Manufacturers Association (EURIMA), 2011. The critical importance of building insulation for the environment.

Eurostat, n.d. http://ec.europa.eu/eurostat/statistics-explained/index.php/Material_flow_accounts_-_flows_in_raw_material_equivalents [WWW Document].

Export, H.U.S.C., 2017. Italy - Agricultural Sector [WWW Document]. URL https://www.export.gov/article?id=Italy-Agricultural-Sector

F. Rocha, A. Vieira, C.G., 1997. Fixation of F and S in bricks and roof tiles using carbonates as additives. Proc. 11th Int. Clay Conf.

Fallis, A.., 2013. Lightweight Aggregate Manufacturing. J. Chem. Inf. Model. 53, 1689–1699. https://doi.org/10.1017/CBO9781107415324.004

Farias, R.D., Martínez-García, C., Cotes-Palomino, M.T., Andreola, F., Lancellotti, I., Barbieri, L., 2017a. Valorization of agro-industrial wastes in lightweight aggregates for agronomic use: Preliminary study. Environ. Eng. Manag. J. 16, 1691–1700.

Farias, R.D., Martínez-García, C., Cotes-Palomino, M.T., Martínez-Arellano, M., 2017b. Effects of wastes from the brewing industry in lightweight aggregates manufactured with clay for green roofs. Materials (Basel). 10. https://doi.org/10.3390/ma10050527

Fillaudeau, L., Blanpain-Avet, P., Daufin, G., 2006. Water, wastewater and waste management in brewing industries. J. Clean. Prod. 14, 463–471. https://doi.org/10.1016/j.jclepro.2005.01.002

Franus, M., Barnat-Hunek, D., Wdowin, M., 2016. Utilization of sewage sludge in the manufacture of lightweight aggregate. Environ. Monit. Assess. 188, 1–13. https://doi.org/10.1007/s10661-015-5010-8

Galán-Arboledas, R.J., Cotes-Palomino, M.T., Bueno, S., Martínez-García, C., 2017. Evaluation of spent diatomite incorporation in clay based materials for lightweight bricks processing. Constr. Build. Mater. 144, 327–337. https://doi.org/10.1016/j.conbuildmat.2017.03.202

Galán-Arboledas, R.J., Merino, A., Bueno, S., 2013. Use of new raw materials and industrial wastes to improve the possibilities of using ceramic materials from Bailen, Jaen, southern Spain. Use new raw Mater. Ind. wastes to Improv. possibilities using Ceram. Mater. from Bailin (Jaen, South. Spain) 63, 553–568. https://doi.org/10.3989/mc.2012.03412

Galán-Arboledas, R.J., Merino, A., Bueno, S., 2013. Utilización de nuevas materias primas y residuos industriales para mejorar las posibilidades de uso de los materiales cerámicos del área de Bailén (Jaén). Mater. Construcción. https://doi.org/10.3989/mc.2012.03412

Galán, E., Aparicio, P., 2005. Materias primas para la industria cerámica, Utilización de Rocas y Minerales Industriales. John Wiley & Sons, Inc.

Galitsky, C., Worrell, E., Ruth, M., 2003. Energy Efficiency Improvement and Cost Saving Opportunities for the Corn Wet Milling Industry. An ENERGY STAR ® Guide for Energy and Plant Managers. Energy 1–90. https://doi.org/LBNL-4779E

Gallé, C., 2001. Effect of drying on cement-based materials pore structure as identified by mercury intrusion porosimetry - A comparative study between oven-, vacuum-, and freeze-drying. Cem. Concr. Res. 31, 1467–1477. https://doi.org/10.1016/S0008-8846(01)00594-4

Garc, C.A., Gonz, A., Vaca, M.L., 2013. Ceramic bricks made from municipal solid waste incineration-derived clay and ashes : a quality study 33, 36–41.

García-Ten, J., Silva, G., Cantavella, V., Lorente-Ayza, M.-M., 2005. Utilización de materiales aligerantes en la fabricación de bloques de Termoarcilla®. Influencia sobre la conductividad térmica y el comportamiento en el. Conarquitectura.

García Romero, E., Suárez Barrios, M., 2004. Las arcillas (propiedades y usos). Univ. Complut. (Madrid); Univ. Salamanca 25.

Getter, K.L., Bradley Rowe, D., Cregg, B.M., 2009. Solar radiation intensity influences extensive green roof plant communities. Urban For. Urban Green. https://doi.org/10.1016/j.ufug.2009.06.005

Getter, K.L., Rowe, D.B., Andresen, J.A., 2007. Quantifying the effect of slope on extensive green roof stormwater retention. Ecol. Eng. https://doi.org/10.1016/j.ecoleng.2007.06.004

Ghadiri, M., Chrzanowski, W., Rohanizadeh, R., 2015. Biomedical applications of cationic clay minerals. RSC Adv. 5, 29467–29481. https://doi.org/10.1039/C4RA16945J

Giraldo Cardenas, K.A., Garcia Escobar, J.O., 2006. Experimental Determination of the Aptitude To the Thermal Clay Expansion. Dyna 73, 69–80.

Goedkoop, M., Heijungs, R., Huijbregts, M., Schryver, A. De, Struijs, J., Zelm, R. Van, 2009. ReCiPe 2008. A life cycle impact assessment method which comprises harmonised category indicators at the midpoint and the endpoint level. Potentials 1–44.

Gonzalez-Corrochano, B.; Alonso-Azcarate, J.; Rodas, M., 2009. Characterization of lightweight aggregates manufactured from washing aggregate sludge and fly ash. Resour. Conserv. Recycl. 53, 571–581. https://doi.org/10.1016/j.resconrec.2009.04.008

González-Corrochano, B., Alonso-Azcárate, J., Rodas, M., 2014. Effect of prefiring and firing dwell times on the properties of artificial lightweight aggregates. Constr. Build. Mater. 53, 91–101. https://doi.org/10.1016/j.conbuildmat.2013.11.099

González-Corrochano, B., Alonso-Azcárate, J., Rodas, M., 2012. Chemical partitioning in lightweight aggregates manufactured from washing aggregate sludge, fly ash and used motor oil. J. Environ. Manage. 109, 43–53. https://doi.org/10.1016/j.jenvman.2012.05.007

González-Corrochano, B., Alonso-Azcárate, J., Rodas, M., 2009. Production of lightweight aggregates from mining and industrial wastes. J. Environ. Manage. 90, 2801–2812. https://doi.org/10.1016/j.jenvman.2009.03.009

González-Corrochano, B., Alonso-Azcárate, J., Rodas, M., Barrenechea, J.F., Luque, F.J., 2011. Microstructure and mineralogy of lightweight aggregates manufactured from mining and industrial wastes. Constr. Build. Mater. 25, 3591–3602. https://doi.org/10.1016/j.conbuildmat.2011.03.053

González, I., Galán, E., Fabbri, B., 1998. Problemática de las emisiones de flúor, cloro y azufre durante la cocción de materiales de la industria ladrillera. Boletín la Soc. Española Cerámica y Vidr. 37,nº4, 307–313.

Gonzalez, I., Galan, E., Miras, A., Aparicio, P., 1998. New Uses for Brick-Making Clay Materials from the Bailén Area (Southern Spain). Clay Miner. 33, 453–465.

Gunning, P.J., Hills, C.D., Carey, P.J., 2009. Production of lightweight aggregate from industrial waste and carbon dioxide. Waste Manag. 29, 2722–2728. https://doi.org/10.1016/j.wasman.2009.05.021

Haddad, A.N., de Moraes Sedrez, M., de Macedo Pires Condeixa, K., Evangelista, A.C.J., Boer, D.T., 2013. Life Cycle Assessment: A Comparison of Ceramic Brick Inventories to Subsidize the Development of Databases in Brazil. Appl. Mech. Mater. 431, 370–377. https://doi.org/10.4028/www.scientific.net/AMM.431.370

Hassanpour, M., Shafigh, P., Mahmud, H. Bin, 2012. Lightweight aggregate concrete fiber reinforcement – A review. Non Destr. Tech. Assess. Concr. 37, 452–461. https://doi.org/http://dx.doi.org/10.1016/j.conbuildmat.2012.07.071

Henkensiefken, R., Bentz, D., Nantung, T., Weiss, J., 2009. Volume change and cracking in internally cured mixtures made with saturated lightweight aggregate under sealed and unsealed conditions. Cem. Concr. Compos. 31, 427–437. https://doi.org/10.1016/j.cemconcomp.2009.04.003

Hortega-Huertas, M., 1996. Advances in clay minerals. Imprenta Artistica.

Hossain, M.U., Poon, C.S., Lo, I.M.C., Cheng, J.C.P., 2016. Comparative environmental evaluation of aggregate production from recycled waste materials and virgin sources by LCA. Resour. Conserv. Recycl. 109, 67–77. https://doi.org/10.1016/j.resconrec.2016.02.009

http://www.scai.uma.es/servicios/aqcm/spo/spo.html [WWW Document], n.d.

Huang, S.C., Chang, F.C., Lo, S.L., Lee, M.Y., Wang, C.F., Lin, J.D., 2007. Production of lightweight aggregates from mining residues, heavy metal sludge, and incinerator fly ash. J. Hazard. Mater. 144, 52–58. https://doi.org/10.1016/j.jhazmat.2006.09.094

Hung, M.-F.F., Hwang, C.-L.L., 2007. Study of fine sediments for making lightweight aggregate. Waste Manag. Res. 25, 449–456. https://doi.org/10.1177/0734242X07077615

Hwang, C.L., Bui, L.A.T., Lin, K.L., Lo, C.T., 2012. Manufacture and performance of lightweight aggregate from municipal solid waste incinerator fly ash and reservoir sediment for self-consolidating lightweight concrete. Cem. Concr. Compos. https://doi.org/10.1016/j.cemconcomp.2012.07.004

Hydroponics, P.H., n.d. http://www.powerhousehydroponics.com/use-clay-pebbles-hydroponic-gardening/ [WWW Document].

IndexMundi, 2016. http://www.indexmundi.com/agriculture/?commodity=corn [WWW Document].

Innova Europe, 2012. Guide to resource efficiency in manufacturing: Experiences from improving resource efficiency in manufacturing companies, Europe 30.

IPCC, 2007. IPCC Fourth Assessment Report (AR4), Working Group 1, Chapter 2, Changes in Atmospheric Constituents and in Radiative Forcing pp 234.

ISO-14021:2016, 2016. Environmental labels and declarations. Self-declared environmental claims (Type II environmental labelling).

ISO-14024:2018, 2018. Environmental labels and declarations. Type I environmental labelling. Principles and procedures.

ISO-14025:2006, 2006. Environmental labels and declarations. Type III environmental declarations. Principles and procedures.

ISO-21930:2017, 2017. Sustainability in buildings and civil engineering works. Core rules for environmental product declarations of construction products and services.

Italiana, S. ceramica, 1993. I materiali refrattari ed il loro impiego nell'industria ceramica.

Iwata, S., Chiba, K., Haraguchi, H., Fujimori, E., Minamoto, K., 2004. Enrichment of elements in industrial waste incineration bottom ashes obtained from three different types of incinerators, as studied by ICP-AES and ICP-MS. J Mater Cyclels Waste Manag 6, 73–79. https://doi.org/10.1007/s10163-003-0106-6

J. K. Mitchell, K.S., 1993. Fundamentals of Soil Behavior.

J. P. Ries, W.H.W.T.W.B., 1996. Environmentally friendly uses of Lightweight Aggregates. Nature 383, 781–781. https://doi.org/10.1038/383781a0

Jeng, A.S., Haraldsen, T.K., Grønlund, A., Pedersen, P.A., 2006. Meat and bone meal as nitrogen and phosphorus fertilizer to cereals and rye grass. Nutr. Cycl. Agroecosystems 76, 183–191. https://doi.org/10.1007/s10705-005-5170-y

Joschek, S., Nies, B., Krotz, R., Göpferich, A., 2000. Chemical and physicochemical characterization of porous hydroxyapatite ceramics made of natural bone. Biomaterials 21, 1645–1658. https://doi.org/10.1016/S0142-9612(00)00036-3

Kadir, A.A., Ariffin, N.M., 2013. Effects of Utilizing Rice Husk in Fired Clay Brick. Int. J. Zero Waste Gener.

1, 27–34.

Kavas, T., Christogerou, A., Pontikes, Y., Angelopoulos, G.N., 2011. Valorisation of different types of boron-containing wastes for the production of lightweight aggregates. J. Hazard. Mater. 185, 1381–1389. https://doi.org/10.1016/j.jhazmat.2010.10.059

Kaz'mina, O. V., 2010. Effect of the component composition and oxidation - reduction characteristics of mixes on foaming of pyroplastic silicate pastes. Glas. Ceram. (English Transl. Steklo i Keramika) 67, 1–5. https://doi.org/10.1007/s10717-010-9239-y

Khoo, W., Nor, F.M., Ardhyananta, H., Kurniawan, D., 2015. Preparation of Natural Hydroxyapatite from Bovine Femur Bones Using Calcination at Various Temperatures. Procedia Manuf. 2, 196–201. https://doi.org/10.1016/j.promfg.2015.07.034

Kim, Y., 2005. Recycling of dust wastes as lightweight aggregates. J. Ceram. Process. Res. 6, 91–94.

Kim, Y., Ryu, Y., Jeon, H., Lee, G.K., Kang, S., Kim, J., Jang, C.S., Lee, S.G., 2010. A study of the plasticity of lightweight aggregate green bodies including bottom ash. J. Ceram. Process. Res. 11, 225–232.

Kizinievič, O., Žurauskiene, R., Kizinievič, V., Žurauskas, R., 2013. Utilisation of sludge waste from water treatment for ceramic products. Constr. Build. Mater. 41, 464–473. https://doi.org/10.1016/j.conbuildmat.2012.12.041

Kochba, M., Gambash, S., Avnimelech, Y., 1990. Studies on Slow Release Fertilizers: 1. Effects of Temperature, Soil Moisture, and Water Vapor Pressure. Soil Sci. 149, 339–343.

Kockal, N.U., Ozturan, T., 2011. Characteristics of lightweight fly ash aggregates produced with different binders and heat treatments. Cem. Concr. Compos. 33, 61–67. https://doi.org/10.1016/j.cemconcomp.2010.09.007

Korat, L., Ducman, V., Legat, A., Mirtič, B., 2013. Characterisation of the pore-forming process in lightweight aggregate based on silica sludge by means of X-ray micro-tomography (micro-CT) and mercury intrusion porosimetry (MIP). Ceram. Int. 39, 6997–7005. https://doi.org/10.1016/j.ceramint.2013.02.037

Kumbhar, S., Kulkarni, N., Rao, A.B., Rao, B., 2014. Environmental life cycle assessment of traditional bricks in western Maharashtra, India. Energy Procedia 54, 260–269. https://doi.org/10.1016/j.egypro.2014.07.269

L. Aoubaa, C. Boriesc, M. Coutanda, B. Perrina, H.L., 2016. Properties of fired clay bricks with incorporated biomasses : Cases of Olive Stone Flour and Wheat Straw residues Properties of fired clay bricks with incorporated biomasses : cases of olive stone flour and wheat straw residues. Constr. Build. Mater. https://doi.org/10.1016/j.conbuildmat.2015.10.040

LCANZ, (Life Cycle Association of New Zealand), 2015. http://www.lcanz.org.nz/introduction-lca [WWW Document].

Lehtinen, H., Saarentaus, A., Rouhiainen, J., Pits, M., Azapagic, A., 2011. A review of LCA methods and tools and their suitability for SMEs. Eco- Innov. Biochem 24. https://doi.org/10.1017/CBO9781107415324.004

Liao, Y.C., Huang, C.Y., 2011. Effects of CaO addition on lightweight aggregates produced from water reservoir sediment. Constr. Build. Mater. 25, 2997–3002. https://doi.org/10.1016/j.conbuildmat.2010.12.034

Lubkowski, K., 2014. Coating fertilizer granules with biodegradable materials for controlled fertilizer release. Environ. Eng. Manag. J.

Lubkowski, K., Grzmil, B., 2007. Controlled release fertilizers. Pol. J. Chem. Tech. Polish J. Chem. Technol. 9, 81–81. https://doi.org/10.2478/v10026-007-0096-6

Lugari, A., 2011. Studi preliminari di valorizzazione di ceneri di farine animali nella progettazione di vetri attivi.

M. Goedkoop, M. Oele, J. Leijting, T. Ponsioen, E.M., 2013. Introduction to LCA with SimaPro 5.1, 1–80.

Magalhães, J.M., Silva, J.E., Castro, F.P., Labrincha, J.A., 2004. Effect of experimental variables on the inertization of galvanic sludges in clay-based ceramics. J. Hazard. Mater. 106, 139–147. https://doi.org/10.1016/j.jhazmat.2003.11.001

Mahzuz, H.M. a., Alam, R., Alam, M.N., Basak, R., Islam, M.S., 2009. Use of arsenic contaminated sludge in making ornamental bricks. Int. J. Environ. Sci. Technol. 6, 291–298.

MAPAMA-España, 2017. EVOLUCIÓN DE LOS BALANCES DE CEREALES EN ESPAÑA SUBDIRECCIÓN GENERAL DE CULTIVOS HERBÁCEOS E INDUSTRIALES DIRECCIÓN GENERAL DE PRODUCCIONES Y MERCADOS AGRARIOS.

Martínez-García, C., Cotes-Palomino, M.T., Corpas-Iglesias, F.A., 2015. Production of sintered lightweight aggregates using wastes of brewing industry.

Martínez-García, C., Cotes-Palomino, M.T., Iglesias-Godino, F.J., Corpas-Iglesias, F.A., 2014. Porosity of expanded clay manufactured with addition of sludge from the brewing industry. Int. J. Energy Environ. Eng. 5, 341–347. https://doi.org/10.1007/s40095-014-0112-6

Martínez-García, C., Eliche-Quesada, D., Pérez-Villarejo, L., Iglesias-Godino, F.J., Corpas-Iglesias, F.A., 2012. Sludge valorization from wastewater treatment plant to its application on the ceramic industry. J. Environ. Manage. 95. https://doi.org/10.1016/j.jenvman.2011.06.016

Martínez, M.L., Eliche, D., Cruz, N., Corpas, F.A., 2012. Utilization of bagasse from the beer industry in clay brick production for building. Mater. Construcción 62, 199–212. https://doi.org/10.3989/mc.2012.63410

Martínez, P.-F., Roca, D., 2011. Substrates for growing without soil. Materials, properties and handling. Sustratos, manejo del clima, Autom. y Control en Sist. Cultiv. sin suelo 37–77.

Mattone, I.L., Storia, N., n.d. I.I.S.S "E. Mattei" Rosignano Solvay.

Mentens, J., Raes, D., Hermy, M., 2006. Green roofs as a tool for solving the rainwater runoff problem in the urbanized 21st century? Landsc. Urban Plan. https://doi.org/10.1016/j.landurbplan.2005.02.010

Micromeritics, 1985. Mercury Intrusion Porosimetry. Appl. Catal. 13, 388. https://doi.org/10.1016/S0166-9834(00)81162-8

Mohan, D., Singh, K.P., 2002. Single- and multi-component adsorption of cadmium and zinc using activated carbon derived from bagasse—an agricultural waste. Water Res. 36, 2304–2318. https://doi.org/10.1016/S0043-1354(01)00447-X

Molineux, C.J., Fentiman, C.H., Gange, A.C., 2009. Characterising alternative recycled waste materials for use as green roof growing media in the U.K. Ecol. Eng. 35, 1507–1513. https://doi.org/10.1016/j.ecoleng.2009.06.010

Molineux, C.J., Gange, A.C., Connop, S.P., Newport, D.J., 2015. Using recycled aggregates in green roof substrates for plant diversity. Ecol. Eng. 82, 596–604. https://doi.org/10.1016/j.ecoleng.2015.05.036

Mondini, C., Cayuela, M.L., Sinicco, T., Sánchez-Monedero, M.A., Bertolone, E., Bardi, L., 2008. Soil application of meat and bone meal. Short-term effects on mineralization dynamics and soil biochemical and microbiological properties. Soil Biol. Biochem. 40, 462–474. https://doi.org/10.1016/j.soilbio.2007.09.010

Monteiro, S.N., Alexandre, J., Margem, J.I., Sánchez, R., Vieira, C.M.F., 2008. Incorporation of sludge waste from water treatment plant into red ceramic. Constr. Build. Mater. 22, 1281–1287. https://doi.org/10.1016/j.conbuildmat.2007.01.013

Monteiro, S.N., Vieira, C.M.F., 2014. On the production of fired clay bricks from waste materials: A critical update. Constr. Build. Mater. https://doi.org/10.1016/j.conbuildmat.2014.07.006

Moreno-Maroto, J.M., González-Corrochano, B., Alonso-Azcárate, J., Rodríguez, L., Acosta, A., 2017a. Development of lightweight aggregates from stone cutting sludge, plastic wastes and sepiolite rejections for agricultural and environmental purposes. J. Environ. Manage. 200, 229–242. https://doi.org/10.1016/j.jenvman.2017.05.085

Moreno-Maroto, J.M., González-Corrochano, B., Alonso-Azcárate, J., Rodríguez, L., Acosta, A., 2017b. Manufacturing of lightweight aggregates with carbon fiber and mineral wastes. Cem. Concr. Compos. 83, 335–348. https://doi.org/10.1016/j.cemconcomp.2017.08.001

Mueller, A., Sokolova, S.N., Vereshagin, V.I., 2008. Characteristics of lightweight aggregates from primary and recycled raw materials. Constr. Build. Mater. 22, 703–712. https://doi.org/10.1016/j.conbuildmat.2007.06.009

Mun, K.J., 2007. Development and tests of lightweight aggregate using sewage sludge for nonstructural concrete. Constr. Build. Mater. 21, 1583–1588. https://doi.org/10.1016/j.conbuildmat.2005.09.009

Muñoz Velasco, P., Mendívil, M.A., Morales, M.P., Muñoz, L., 2015. Eco-fired clay bricks made by adding spent coffee grounds: a sustainable way to improve buildings insulation. Mater. Struct. https://doi.org/10.1617/s11527-015-0525-6

Murray, H.H., 2007. Structure and composition of the clay minerals and their physical and chemical properties. Dev. Clay Sci. https://doi.org/10.1016/S1572-4352(06)02002-2

Nagase, A., Dunnett, N., 2011. The relationship between percentage of organic matter in substrate and plant growth in extensive green roofs. Landsc. Urban Plan. 103, 230–236. https://doi.org/10.1016/j.landurbplan.2011.07.012

Ng, K.S., Martinez Hernandez, E., 2016. A systematic framework for energetic, environmental and economic (3E) assessment and design of polygeneration systems. Chem. Eng. Res. Des. 106, 1–25. https://doi.org/10.1016/j.cherd.2015.11.017

Nguyen, L.H., Beaucour, A.L., Ortola, S., Noumowe, A., 2014. Influence of the volume fraction and the nature of fine lightweight aggregates on the thermal and mechanical properties of structural concrete. Constr. Build. Mater. 51, 121–132.

Njeumen Nkayem, D.E., Mbey, J.A., Kenne Diffo, B.B., Njopwouo, D., 2016. Preliminary study on the use of corn cob as pore forming agent in lightweight clay bricks: Physical and mechanical features. J. Build. Eng. 5, 254–259. https://doi.org/10.1016/j.jobe.2016.01.006

Nye, P., Greenland, D.J., 1960. The soil under shifting cultivation 156.

Nzihou, A., 2010. Waste and biomass valorization. Waste and Biomass Valorization 1, 1–2. https://doi.org/10.1007/s12649-010-9013-y

O'Connell, D.W., Birkinshaw, C., O'Dwyer, T.F., 2008. Heavy metal adsorbents prepared from the modification of cellulose: A review. Bioresour. Technol. 99, 6709–6724. https://doi.org/10.1016/j.biortech.2008.01.036

Oakton, n.d. http://www.oakton.edu/user/4/billtong/eas100/clays.htm [WWW Document].

P.A. Webb, C.O., 1997. Analytical Methods in Fine Particle Technology. Micrometrics Instrument Corporation, One Micrometritics Drive Norcross, GA 30093 U.S.A., U.S.A.

Papafotiou, M., Pergialioti, N., Tassoula, L., Massas, I., Kargas, G., 2013. Growth of native aromatic xerophytes in an extensive Mediterranean green roof as affected by substrate type and depth and irrigation frequency. HortScience 48, 1327–1333.

Pappu, A., Saxena, M., Asolekar, S.R., 2007. Solid wastes generation in India and their recycling potential in building materials. Build. Environ. 42, 2311–2320. https://doi.org/10.1016/j.buildenv.2006.04.015

Perez, N., 2014. http://www.unige.ch/sciences/terre/people/personal_pages/NoelPerez/NoelPerez.php [WWW Document].

Pinto, J., Paiva, A., Varum, H., Costa, A., Cruz, D., Pereira, S., Fernandes, L., Tavares, P., Agarwal, J., 2011. Corn's cob as a potential ecological thermal insulation material. Energy Build. 43, 1985–1990. https://doi.org/10.1016/j.enbuild.2011.04.004

Pinto, J., Vieira, B., Pereira, H., Jacinto, C., Vilela, P., Paiva, A., Pereira, S., Cunha, V.M.C.F., Varum, H., 2012. Corn cob lightweight concrete for non-structural applications. Constr. Build. Mater. 34, 346–351. https://doi.org/10.1016/j.conbuildmat.2012.02.043

Pinto, S., Rosenbom, K., Machado, L., Correia, A.M.S., Labrincha, J.A., Ferreira, V.M., 2005. Monitoring of exhaust gases from the production of lightweight aggregates containing industrial wastes. REWAS'04 - Glob. Symp. Recycl. Waste Treat. Clean Technol.

Procedures, G.C., Digestion, W.S., Digestion, S.S., Solids, T., Concentration, S., Verification, I.C., Standards, I.C., Verification, C.C., Blank, M., Range, L.A., Dilution, S., Analysis, D., 2006. STANDARD OPERATING PROCEDURES SOP : REV : DETERMINATION OF METALS BY INDUCTIVELY COUPLED PLASMA (ICP) STANDARD OPERATING PROCEDURES SOP : REV :

Proietti, S., Desideri, U., Sdringola, P., Zepparelli, F., 2013. Carbon footprint of a reflective foil and comparison with other solutions for thermal insulation in building envelope. Appl. Energy 112, 843–855. https://doi.org/10.1016/j.apenergy.2013.01.086

Quina, M.J., Almeida, M.A., Santos, R., Bordado, J.M., Quinta-Ferreira, R.M., 2014. Compatibility analysis of municipal solid waste incineration residues and clay for producing lightweight aggregates. Appl. Clay Sci. 102, 71–80. https://doi.org/10.1016/j.clay.2014.10.016

Rajput, D., Bhagade, S.S., Raut, S.P., Ralegaonkar, R. V., Mandavgane, S.A., 2012. Reuse of cotton and recycle paper mill waste as building material. Constr. Build. Mater. 34, 470–475. https://doi.org/10.1016/j.conbuildmat.2012.02.035

Ramezanianpour, A.A., Malhotra, V.M., 1995. Effect of curing on the compressive strength, resistance to chloride-ion penetration and porosity of concretes incorporating slag, fly ash or silica fume. Cem. Concr. Compos. 17, 125–133. https://doi.org/10.1016/0958-9465(95)00005-W

Raut, S., Ralegaonkar, R., Mandavgane, S., 2013. Utilization of recycle paper mill residue and rice husk ash in production of light weight bricks. Arch. Civ. Mech. Eng. 13, 269–275. https://doi.org/10.1016/j.acme.2012.12.006

Raut, S., Ralegaonkar, R., Mandavgane, S., 2011. Development of sustainable construction material using industrial and agricultural solid waste: A review of waste-create bricks. Constr. Build.

Raut, S.P., Ralegaonkar, R. V., Mandavgane, S.A.S., 2011. Development of sustainable construction material using industrial and agricultural solid waste: A review of waste-create bricks. Constr. Build. 25, 4037–4042. https://doi.org/10.1016/j.conbuildmat.2011.04.038

Regulation (EC) Nº 178/2002, 2002. Regulation (EC) Nº 178/2002, Official Journal of the EC. https://doi.org/2004R0726 - v.7 of 05.06.2013

Riley, C.M., 1951. Relation of Chemical Properties to the Bloating of Clays. J. Am. Ceram. Soc. 34, 121–128. https://doi.org/10.1111/j.1151-2916.1951.tb11619.x

Ronda, A., Blázquez, G., Martínez, C., Cotes, M.T., Martín-Lara, M.Á., Calero, M., 2015. Physic-Chemical Characterization of a Waste from Olive Industry. Key Eng. Mater. 663, 140–147. https://doi.org/10.4028/www.scientific.net/KEM.663.140

Rouquerol, J., Avnir, D., Fairbridge, C.W., Everett, D.H., Haynes, J.H., Pernicone, N., Ramsay, J.D.F., Sing, K.S.W., Unger, K.K., 1994. Recommendations for the characterization of porous solids. Pure Appl. Chem. 66, 1739–1758. https://doi.org/doi:10.1351/pac199466081739

Rowe, D.B., 2011. Green roofs as a means of pollution abatement. Environ. Pollut. https://doi.org/10.1016/j.envpol.2010.10.029

Rowe, D.B., Monterusso, M.A., Rugh, C.L., 2006. Assessment of heat-expanded slate and fertility requirements in green roof substrates. Horttechnology 16, 471–477.

Saccani, A., Bignozzi, M.C., Barbieri, L., Lancellotti, I., Bursi, E., 2017. Effect of the chemical composition of different types of recycled glass used as aggregates on the ASR performance of cement mortars. Constr. Build. Mater. 154, 804–809. https://doi.org/10.1016/j.conbuildmat.2017.08.011

Sadineni, S.B., Madala, S., Boehm, R.F., 2011. Passive building energy savings: A review of building envelope components. Renew. Sustain. Energy Rev. https://doi.org/10.1016/j.rser.2011.07.014

Salvo, M., Rizzo, S., Caldirola, M., Novajra, G., Canonico, F., Bianchi, M., Ferraris, M., 2015. Biomass ash as supplementary cementitious material (SCM). Adv. Appl. Ceram. 114, S3–S10. https://doi.org/10.1179/1743676115Y.0000000043

Sánchez, C., 2010. Cultivation of Pleurotus ostreatus and other edible mushrooms. Appl. Microbiol. Biotechnol. 85, 1321–1337. https://doi.org/10.1007/s00253-009-2343-7

Shaviv, A., Mikkelsen, R.L., 1993. Controlled-release fertilizers to increase efficiency of nutrient use and minimize environmental degradation - A review. Fertil. Res. 35, 1–12. https://doi.org/10.1007/BF00750215

Shaviv, A., Raban, S., Zaidel, E., 2003. Modeling controlled nutrient release from polymer coated fertilizers: Diffusion release from single granules. Environ. Sci. Technol. 37, 2251–2256. https://doi.org/10.1021/es011462v

Shelby, J.E., 2005. Introduction to glass science and technology. RS.C.

Silva, C.F., Azevedo, R.S., Braga, C., da Silva, R., Dias, E.S., Schwan, R.F., 2009. Microbial diversity in a bagasse-based compost prepared for the production of Agaricus brasiliensis. Brazilian J. Microbiol. [publication Brazilian Soc. Microbiol. 40, 590–600. https://doi.org/10.1590/S1517-838220090003000023

Simion, I.M., Ghinea, C., Maxineasa, S.G., Taranu, N., Bonoli, A., Gavrilescu, M., 2013. Ecological

footprint applied in the assessment of construction and demolition waste integrated management. Environ. Eng. Manag. J. 12, 779–788.

Soto, P.J.S., Pérez Rodríguez, J.L., 1998. Cerámica y Vidrio Características generales, propiedades, yacimientos y aplicaciones de pirofilita. II. Yacimientos, aplicaciones y utilización como materia prima cerámica. Cerámica y Vidr.

Styron, R.W., 1988. Process for forming a light-weight aggregate (US 4741782 A).

Sud, D., Mahajan, G., Kaur, M.P.M., 2008. Agricultural waste material as potential adsorbent for sequestering heavy metal ions from aqueous solutions–A review. Bioresour. Technol. 99, 6017–6027. https://doi.org/10.1016/j.biortech.2007.11.064

Sutcu, M., Akkurt, S., 2009. The use of recycled paper processing residues in making porous brick with reduced thermal conductivity. Ceram. Int. 35, 2625–2631. https://doi.org/10.1016/j.ceramint.2009.02.027

Sutcu, M., del Coz Díaz, J.J., Álvarez Rabanal, F.P., Gencel, O., Akkurt, S., 2014. Thermal performance optimization of hollow clay bricks made up of paper waste. Energy Build. 75, 96–108. https://doi.org/10.1016/j.enbuild.2014.02.006

Tadic, D., Epple, M., 2004. A thorough physicochemical characterisation of 14 calcium phosphate-based bone substitution materials in comparison to natural bone. Biomaterials 25, 987–994. https://doi.org/10.1016/S0142-9612(03)00621-5

Tang, C.W., Chen, H.J., Wang, S.Y., Spaulding, J., 2011. Production of synthetic lightweight aggregate using reservoir sediments for concrete and masonry. Cem. Concr. Compos. 33, 292–300. https://doi.org/10.1016/j.cemconcomp.2010.10.008

The Ellen MacArthur Foundation, 2012. Towards a Circular Economy - Economic and Business Rationale for an Accelerated Transition. Greener Manag. Int. 97. https://doi.org/2012-04-03

Tortosa Masiá, A.A., Buhre, B.J.P., Gupta, R.P., Wall, T.F., 2007. Characterising ash of biomass and waste. Fuel Process. Technol. 88, 1071–1081. https://doi.org/10.1016/j.fuproc.2007.06.011

Toth, M.N., Csaky, I.B., 1989. Role of the smectite group in the bloating process. ZI, Ziegelindustrie Int. Tile Ind. Int. 42, 246–250.

Tsai, W.T., Hsien, K.J., Chang, Y.M., Lo, C.C., 2005. Removal of herbicide paraquat from an aqueous solution by adsorption onto spent and treated diatomaceous earth. Bioresour. Technol. 96, 657–663. https://doi.org/10.1016/j.biortech.2004.06.023

Tsai, W.T., Hsien, K.J., Yang, J.M., 2004. Silica adsorbent prepared from spent diatomaceous earth and its application to removal of dye from aqueous solution. J. Colloid Interface Sci. 275, 428–433. https://doi.org/10.1016/j.jcis.2004.02.093

Tuan, B.L.A., Hwang, C.-L., Lin, K.-L., Chen, Y.-Y., Young, M.-P., 2013. Development of lightweight aggregate from sewage sludge and waste glass powder for concrete. Constr. Build. Mater. 47, 334–339. https://doi.org/10.1016/j.conbuildmat.2013.05.039

Turner, D.A., Williams, I.D., Kemp, S., 2016. Combined material flow analysis and life cycle assessment as a support tool for solid waste management decision making. J. Clean. Prod. 129, 234–248. https://doi.org/10.1016/j.jclepro.2016.04.077

U.C. Cubaud, M.M., 1968. Fabricacion Industrial De Arcilla Expandida. Silic. Ind. 5, 145–152.

UNE-32-006, 1995. Solid mineral fuels. Determination of gross calorific value by automatic calorimeter.

UNE-EN-1097-3, 1999. Determination of loose bulk density and voids.

UNE-EN-1097-6, 2014. Determination of particle density and water absorption.

UNE-EN-12667:2002, 2002. Thermal performance of building materials and products. Determination of thermal resistance by means of guarded hot plate and heat flow meter methods. Products of high and medium thermal resistance.

UNE-EN-13037, 2012. Soil improvers and growing substrates. pH determination. AENOR.

UNE-EN-13038, 2012. Soil improvers and growing substrates. Electrical conductivity determination. AENOR.

UNE-EN-772-21:2011, 2011. Métodos de ensayo de piezas para fábricas de albañilería. Parte 21: Determinación de la absorción de agua de piezas para fábrica de albañilería de arcilla cocida y silicocalcáreas por absorción de agua fría. AENOR.

UNE-EN-772-7:1999, 1999. Métodos de ensayo de piezas para fábrica de albañilería. Parte 7: Determinación de la absorción de agua por inmersión en agua hirviendo de piezas de arcilla cocida para fábrica de albañilería que sirven de barrera al agua por capilaridad. AENOR.

UNE-EN-ISO-14040, 2006. Gestión ambiental. Análisis del ciclo de vida. Principios y marco de referencia. AENOR.

UNE-EN-ISO-14044, 2006. Gestion ambiental. Analisis de ciclo de vida. Requisitos y directrices., AENOR.

UNE-EN-ISO-14064-1:2006, 2015. Parte 1: Especificación con orientación, a nivel de las organizaciones, para la cuantificación y el informe de las emisiones y remociones de gases de efecto invernadero. AENOR.

UNE-EN-ISO-14064-2:2006, 2015. Parte 2: Especificación con orientación, a nivel de proyecto, para la cuantificación, el seguimiento y el informe de la reducción de emisiones o el aumento en las remociones de gases de efecto invernadero. AENOR.

UNE-EN-ISO-14064-3:2006, 2015. Parte 3: Especificación con orientación para la validación y verificación de declaraciones sobre gases de efecto invernadero. AENOR.

UNE-EN13055-1, 2003. Lightweight aggregates. Part 1: Lightweight aggregates for concrete, mortar and grout.

Valderrivas, G.C.P., n.d. http://www.valderrivas.es/es/portal.do?TR=C&IDR=127 [WWW Document].

Vašina, M., Hughes, D.C., Horoshenkov, K. V., Lapčík, L., 2006. The acoustical properties of consolidated expanded clay granulates. Appl. Acoust. 67, 787–796. https://doi.org/10.1016/j.apacoust.2005.08.003

Vázquez, M.; J.J.-M., 2004. Materias primas ricas en arciila de las Capas Rojas Triássicas (Norte de Jáen, España) para fabricar materiales céramicos de construcción. Mater. construcción 54, 5–20.

Vázquez, M., Jiménez-Millán, J., Sánchez-Jiménez, C., Parras, J., 2003. Composición y propiedades cerámicas de las pizarras de la Zona Centro Ibérica del Macizo Ibérico Meridional (Norte de Jaén, España). Bol. la Soc. Esp. Ceram. y Vidr.

Velasco, P.M., Ortiz, M.P.M., Gir??, M.A.M., Melia, D.M., Rehbein, J.H., 2015. Development of sustainable fired clay bricks by adding kindling from vine shoot: Study of thermal and mechanical properties. Appl. Clay Sci. 107, 156–164. https://doi.org/10.1016/j.clay.2015.01.017

Vicente, D., Juan, C., Cintas, M., Mart, L., 2012. Herramientas para la Optimización Energética en la fabricación de materiales cerámicos, FUNDACIÓN. ed. FUNDACIÓN INNOVARCILLA.

Vijayaraghavan, K., Joshi, U.M., Balasubramanian, R., 2012. A field study to evaluate runoff quality from green roofs. Water Res. https://doi.org/10.1016/j.watres.2011.12.050

Vijayaraghavan, K., Raja, F.D., 2015. Pilot-scale evaluation of green roofs with Sargassum biomass as an additive to improve runoff quality. Ecol. Eng. 75, 70–78. https://doi.org/10.1016/j.ecoleng.2014.11.029

Villarreal, E.L., Bengtsson, L., 2005. Response of a Sedum green-roof to individual rain events. Ecol. Eng. 25, 1–7. https://doi.org/10.1016/j.ecoleng.2004.11.008

Wang, X., Jin, Y., Wang, Z., Nie, Y., Huang, Q., Wang, Q., 2009. Development of lightweight aggregate from dry sewage sludge and coal ash. Waste Manag. 29, 1330–1335. https://doi.org/10.1016/j.wasman.2008.09.006

Weber Saint-Gobain, n.d. http://www.weber.es/soluciones-ligeras-con-arlitareg-lecareg/ayuda-y-consejos/que-es-arlitareg-lecareg.html [WWW Document].

Wei, Y.L., Lin, C.Y., Ko, K.W., Wang, H.P., 2011. Preparation of low water-sorption lightweight aggregates from harbor sediment added with waste glass. Mar. Pollut. Bull. 63, 135–140. https://doi.org/10.1016/j.marpolbul.2011.01.037

Whittinghill, L.J., Bradley Rowe, D., Cregg, B.M., 2013. Evaluation of vegetable production on extensive green roofs. Agroecol. Sustain. Food Syst. 37. https://doi.org/10.1080/21683565.2012.756847

Whittinghill, L.J., Rowe, D.B., 2012. The role of green roof technology in urban agriculture. Renew. Agric. Food Syst. 27. https://doi.org/10.1017/S174217051100038X

William D. Callister, J., 2007. Materials Science and Engineering. John Wiley & Sons, Inc.

Wimmer W., Züst R., L.K., 2004. Environmental Communication. In: ECODESIGN Implementation. Springer. https://doi.org/https://doi.org/10.1007/978-1-4020-3071-0_5

Wong, N.H., Chen, Y., Ong, C.L., Sia, A., 2003. Investigation of thermal benefits of rooftop garden in the tropical environment. Build. Environ. 38, 261–270. https://doi.org/10.1016/S0360-1323(02)00066-5

Ylivainio, K., Uusitalo, R., Turtola, E., 2008. Meat bone meal and fox manure as P sources for ryegrass (Lolium multiflorum) grown on a limed soil. Nutr. Cycl. Agroecosystems 81, 267–278. https://doi.org/10.1007/s10705-007-9162-y

Young, T., Cameron, D.D., Sorrill, J., Edwards, T., Phoenix, G.K., 2014. Importance of different components of green roof substrate on plant growth and physiological performance. Urban For. Urban Green. 13, 507–516. https://doi.org/10.1016/j.ufug.2014.04.007

Zabalza Bribián, I., Valero Capilla, A., Aranda Usón, A., 2011. Life cycle assessment of building materials: Comparative analysis of energy and environmental impacts and evaluation of the eco-efficiency improvement potential. Build. Environ. 46, 1133–1140. https://doi.org/10.1016/j.buildenv.2010.12.002

Zanzucchi, G., 1975. Introduzione alla geologia dell'Emilia-Romagna.

Zhang, L., 2013. Production of bricks from waste materials - A review. Constr. Build. Mater. https://doi.org/10.1016/j.conbuildmat.2013.05.043

Zorić, D., Lazar, D., Rudić, O., Radeka, M., Ranogajec, J., Hiršenberger, H., 2012. Thermal conductivity of lightweight aggregate based on coal fly ash. J. Therm. Anal. Calorim. 110, 489–495. https://doi.org/10.1007/s10973-012-2339-x